Chemical Constituents from *Boesenbergia pandurata*, *Caesalpinia crista* and *Suregada multiflora* and Search for Novel Terpenes in *Erythropodium caribaeorum* and Study for Carotenoids from a Coral-Derived *Micrococcus* strain PAH83

Sarot Cheenpracha

A Thesis Submitted in Fulfillment of the Requirements for the Degree of

Doctor of Philosophy in Organic Chemistry

Prince of Songkla University

2007

Thesis Title	Chemical Constituents from *Boesenbergia pandurata*, *Caesalpinia crista* and *Suregada multiflora* and Search for Novel Terpenes in *Erythropodium caribaeorum* and Study for Carotenoids from a Coral-Derived *Micrococcus* strain PAH83
Author	Mr. Sarot Cheenpracha
Major Program	Organic Chemistry

Advisory Committee :

.....Chairman
(Assoc. Prof. Dr. Chatchanok Karalai)

.....Committee
(Assoc. Prof. Dr. Sanan Subhadhirasakul)

Examining Committee :

.....Chairman
(Assoc. Prof. Dr. Kan Chantrapromma)

.....Committee
(Assoc. Prof. Dr. Chatchanok Karalai)

.....Committee
(Assoc. Prof. Dr. Sanan Subhadhirasakul)

.....Committee
(Assoc. Prof. Chanita Ponglimanont)

.....Committee
(Assoc. Prof. Dr. Supinya Tewtrakul)

The Graduate School, Prince of Songkla University, has approved this thesis as fulfillment of the requirements for the Doctor of Philosophy Degree in Organic Chemistry.

.....
(Assoc. Prof. Dr. Krerkchai Thongnoo)
Dean of Graduate School

ชื่อวิทยานิพนธ์	องค์ประกอบทางเคมีจากกระชาย เทพี และ ขันทองพยาบาท และการค้นหาเทอร์พีนตัวใหม่ในอีริโทรโพเดียม คาริเบโอรัม และการศึกษาแคโรทีนอยด์จากเชื้อไมโครคอคคัส พีเอเอช 83
ผู้เขียน	นายสาโรจน์ จีนประชา
สาขาวิชา	เคมีอินทรีย์
ปีการศึกษา	2550

บทคัดย่อ

ส่วนที่ 1 องค์ประกอบทางเคมีจาก กระชาย เทพี และ ขันทองพยาบาท

จากการศึกษาพืชสมุนไพรไทย คือ กระชาย, เทพี และ ขันทองพยาบาท สามารถแยกสารใหม่ได้ 17 สาร คือ สารประกอบชาลโคน 1 สาร (BP1), สารประกอบไดเทอร์พีนชนิดคาสเซน 14 สาร (SC1-SC7, SC9, RH1, RH3, RH4 และ SD3-SD5) และสารประกอบไดเทอร์พีนชนิด เอ็นเคาเรน 2 สาร (BMC1 และ BMC2) นอกจากนี้ยังสามารถแยกสารประกอบที่มีการรายงานแล้ว 23 สาร (BP2-BP11, SC8, SC10, RH2, RH5, RH6, SD1, SD2, SD6 และ BMC3-BMC7) สารประกอบ BP1-BP11 แยกได้จากเหง้ากระชาย ส่วนสารประกอบ SC1-SC10, RH1-RH6 และ SD1-SD6 แยกได้จากลำต้น ราก และ เมล็ด จากเทพี ตามลำดับ สำหรับเปลือกลำต้นของขันทองพยาบาทสามารถแยกสารประกอบ BMC1-BMC7 ได้ จากการศึกษาฤทธิ์ทางชีวภาพพบว่า สารประกอบ BP3 มีฤทธิ์ต่อต้าน HIV-1 PR ที่ค่า IC_{50} = 5.6 μM และตามด้วยสารประกอบ BP2 (IC_{50} = 18.7 μM) สารประกอบ SC10 เพียงสารเดียวที่มีฤทธิ์ต้านมาลาเรีย ที่ค่า IC_{50} 4.1 μg/ml ขณะที่สารประกอบที่แยกได้จากขันทองพยาบาท (BMC1-BMC7) แสดงฤทธิ์ทางชีวภาพต้านโรคภูมิแพ้ใน RBL-2H3 เซลล์โมเดล ด้วยค่า IC_{50} ในช่วง 22.5 ถึง 42.2 μM โครงสร้างของสารประกอบเหล่านี้วิเคราะห์โดยใช้ข้อมูลทางสเปกโทรสโกปี สำหรับสารประกอบ SC1 มีข้อมูลทางเอกซ์เรย์ในการพิสูจน์โครงสร้างด้วย

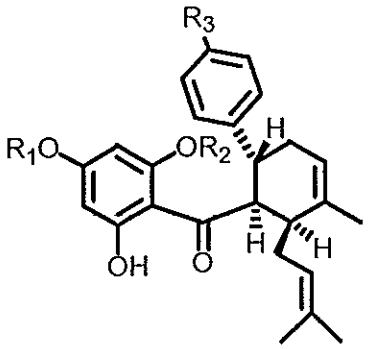

BP1: R_1 = H, R_2 = Me, R_3 = OH Panduratin C

BP2: R_1 = Me, R_2 = R_3 = H; Pandurarin A

BP3: R_1 = R_2 = R_3 = H; Hydroxypanduratin A

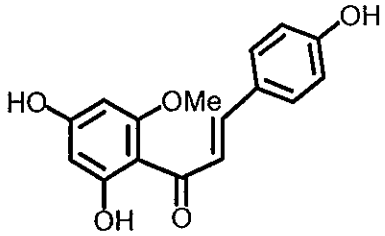

BP4: Helichrysetin

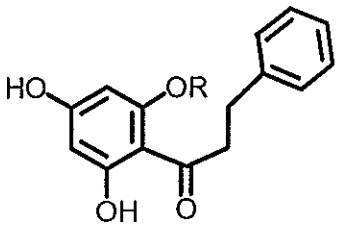

BP5: R = H; 2′,4′,6′-Trihydroxyhydrochalcone

BP6: R = Me; Uvangoletin

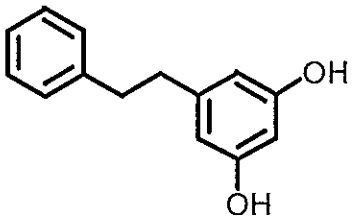

BP7: Dihydropinosylvin

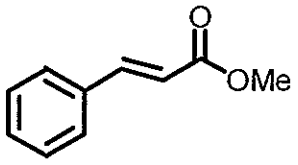

BP8: Methyl *trans*-cinnamate

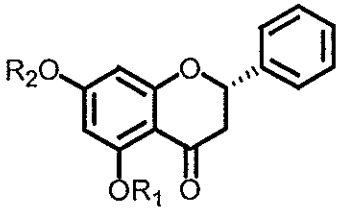

BP9: R_1 = R_2 = H; Pinocembrin

BP10: R_1 = H, R_2 = Me; Pinostrobin

BP11: R_1 = Me, R_2 = H; Alpinetin

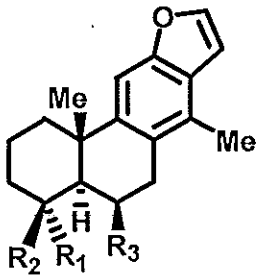

SC1: $R_1 = CO_2Me$, $R_2 = Me$, $R_3 = H$; Taepeenin A

SC2: $R_1 = CO_2H$, $R_2 = Me$, $R_3 = H$; Taepeenin B

SC3: $R_1 = CO_2Me$, $R_2 = Me$, $R_3 = OH$; Taepeenin C

SC4: $R_1 = CO_2Me$, $R_2 = Me$, $R_3 = OCOMe$; Taepeenin D

RH1: $R_1 = CO_2Me$, $R_2 = CHO$, $R_3 = H$; Taepeenin E

SD1: $R_1 = R_2 = Me$, $R_3 = H$; 17-Methylvouacapane-8(14),9(11)-diene

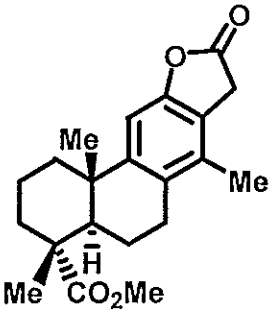

SC5: Taepeenin F

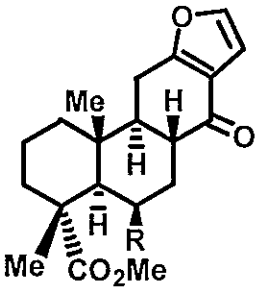

SC6: R = H; Nortaepeenin A

SC7: R = OH; Nortaepeenin B

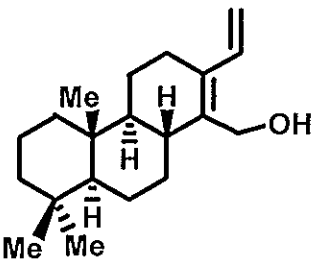

SC9: Taepeenin G

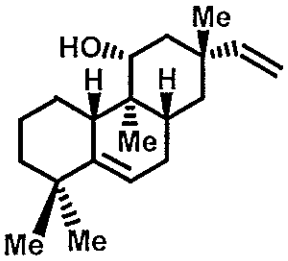

SC10: *ent*-11β-Hydroxy-rosa-5,15-diene

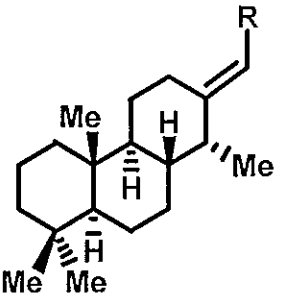

SD4: R = CHO; Taepeenin K

SD5: R = CH_2OH; Taepeenin L

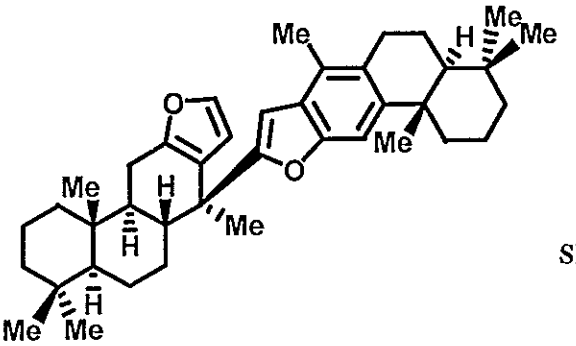

SD3: Taepeenin J

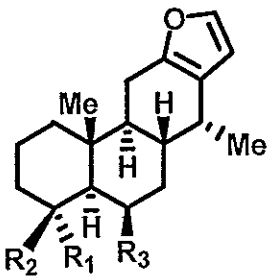

SC8: R_1 = CO_2Me, R_2 = Me, R_3 = H; Methyl vinhaticoate

RH2: R_1 = CO_2H, R_2 = Me, R_3 = H; Vinhaticoic acid

RH3: R_1 = CO_2Me, R_2 = CHO, R_3 = H; Taepeenin H

RH4: R_1 = CO_2Me, R_2 = CH_2OH, R_3 = H; Taepeenin I

SD2: R_1 = R_2 = Me, R_3 = H; Vouacapane

SD6: R_1 = R_2 = Me, R_3 = OH; 6β-Hydroxyvouacapane

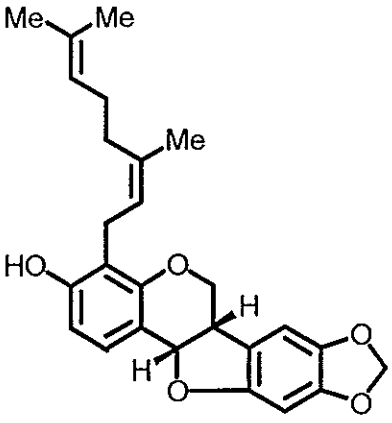

RH5: Nutiducol

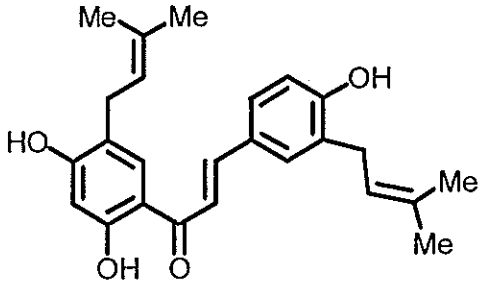

RH6: Stipulin

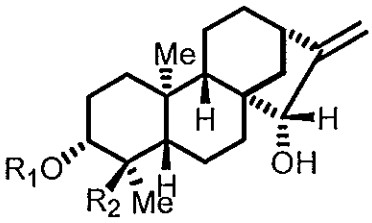

BMC1: R_1 = OH, R_2 = CH_2OH; *ent*-16-Kaurene-3β,15β,18-triol

BMC2: R_1 = =O, R_2 = CH_2OH; *ent*-3-Oxo-16-kaurene-15β,18-diol

BMC3: R_1 = OH, R_2 = Me; *ent*-16-Kaurene-3β,15β-diol

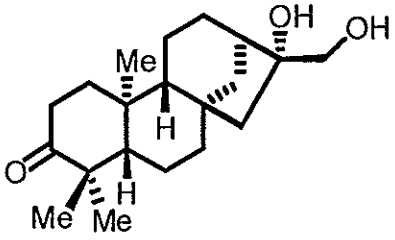

BMC4: Abbeokutone

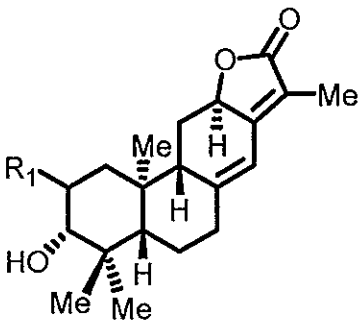

BMC5: R_1 = H_2; Helioscopinolide A

BMC6: R_1 = =O; Helioscopinolide C

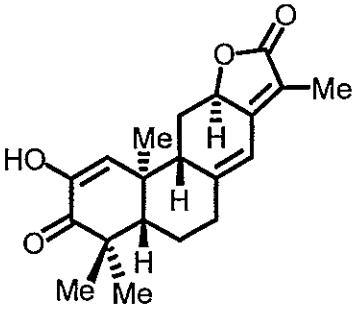

BMC7: Helioscopinolide I

ส่วนที่ 2 การค้นหาเทอร์พีนตัวใหม่ในอีริโทรโพเดียม คาริเบโอรัม และการศึกษาแคโรทีนอยด์จากเชื้อไมโครคอคคัส พีเอเอช 83

สารประกอบ 5 สาร คือ eleutherobin, desacetyleleutherobin, erythrolide A และ B และ erythrodiene แยกได้จากปะการังอ่อน อีริโทรโพเดียม คาริเบโอรัม ในส่วนย่อย EC1H พบไอออนโมเลกุล 303 ที่เวลา 24.72 นาที เป็นข้อมูลที่น่าสนใจ ซึ่งสอดคล้องกับสารมัธยันต์ที่ได้เสนอไว้ ดังนั้นข้อมูลนี้น่าจะต้องมีการศึกษาต่อในอนาคต

สำหรับการศึกษาการผลิตแคโรทีนอยด์ของเชื้อไมโครคอคคัส พีเอเอช 83 โดยศึกษาผลของความเป็นกรด-เบส อุณหภูมิ อัตราการให้ออกซิเจน เวลา ปริมาณเชื้อตอนเริ่มต้น อาหารเลี้ยงเชื้อ และน้ำตาล แคโรทีนอยด์หลัก 3 สาร คือ sarcinaxanthin, sarcinaxanthin monoglucoside และ sarcinaxanthin diglucoside แยกได้จากเชื้อชนิดนี้ การวิเคราะห์โครงสร้างของสารประกอบเหล่านี้อาศัยข้อมูลของ อัตราไวโอเลต และ แมสสเปกตรัม

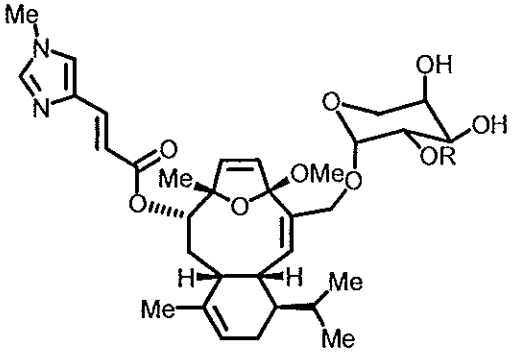

R = Ac; Eleutherobin

R = H; Desacetyleleutherobin

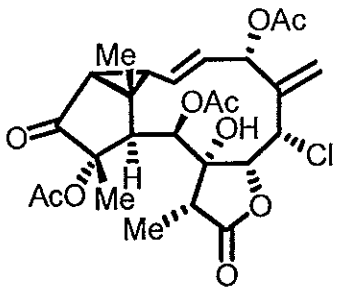

Erythrolide A

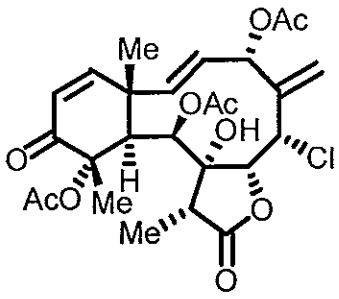

Erythrolide B

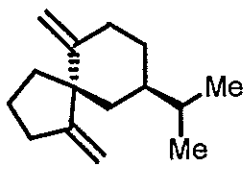

Erythrodiene

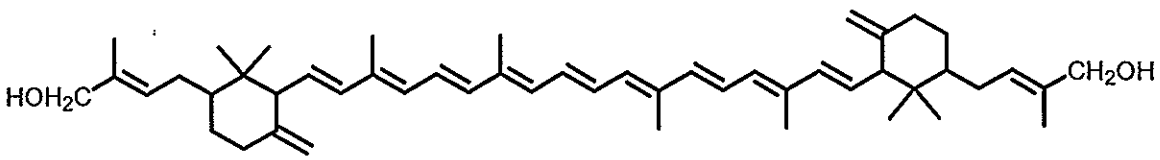

Sarcinaxanthin

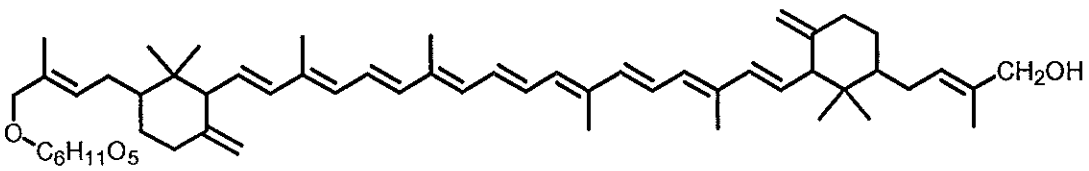

Sarcinaxanthin monoglucoside

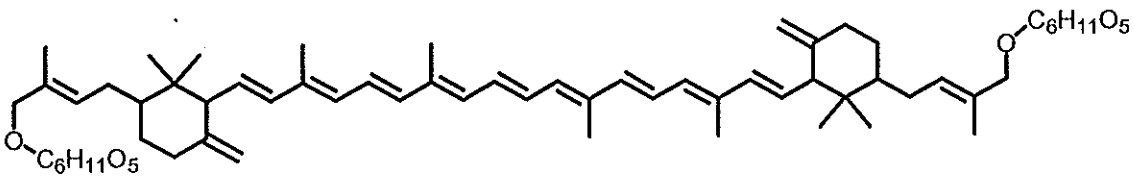

Sarcinaxanthin diglucoside

Thesis Title	Chemical Constituents from *Boesenbergia pandurata*, *Caesalpinia crista* and *Suregada multiflora* and Search for Novel Terpenes in *Erythropodium caribaeorum* and Study for Carotenoids from a Coral-Derived *Micrococcus* strain PAH83
Author	Mr. Sarot Cheenpracha
Major Program	Organic Chemistry
Academic Year	2007

ABSTRACT

PART I Chemical constituent from *Boesenbergia pandurata*, *Caesalpinia crista* and *Suregada multiflora*

The investigation of Thai medicinal plants of *B. pandurata*, *C. crista* and *S. multiflora* has led to the isolation of seventeen new compounds: one cyclohexenylchalcone (**BP1**), fourteen cassane-type diterpenes (**SC1-SC7, SC9, RH1, RH3, RH4** and **SD3-SD5**) and two *ent*-kaurene diterpenes (**BMC1** and **BMC2**) together with twenty-three known compounds (**BP2-BP11, SC8, SC10, RH2, RH5, RH6, SD1, SD2, SD6** and **BMC3-BMC7**). Compounds **BP1-BP11** were isolated from the rhizomes of *B. pandurata* while compounds **SC1-SC10, RH1-RH6** and **SD1-SD6** were obtained from the stems, roots and seeds of *C. crista*, respectively. The bark of *S. multiflora* yielded compounds **BMC1-BMC7.** It was found that **BP3** possessed the most potent anti-HIV-1 PR activity with an IC_{50} value of 5.6 μM, followed by **BP2** (IC_{50} = 18.7 μM). Only one compound (**SC10**) exhibited significant anti-malarial activity with IC_{50} 4.1 μg/ml whereas compounds **BMC1-BMC7** possessed appreciable anti-allergic activities in RBL-2H3 cells model with IC_{50} values ranging from 22.5 to 42.2 μM. The structures of all compounds were elucidated on the basis of chemical and spectroscopic methods. Structure of **SC1** was also confirmed by X-ray diffraction data.

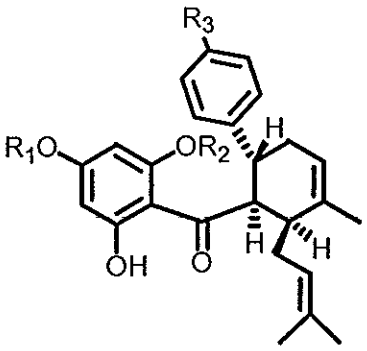

BP1: R_1 = H, R_2 = Me, R_3 = OH Panduratin C

BP2: R_1 = Me, R_2 = R_3 = H; Pandurarin A

BP3: R_1 = R_2 = R_3 = H; Hydroxypanduratin A

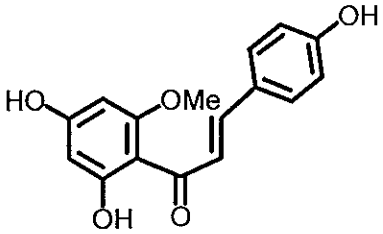

BP4: Helichrysetin

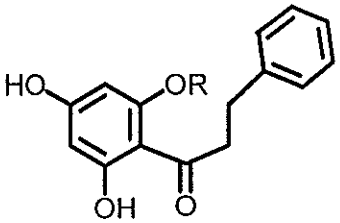

BP5: R = H; 2′,4′,6′-Trihydroxyhydrochalcone

BP6: R = Me; Uvangoletin

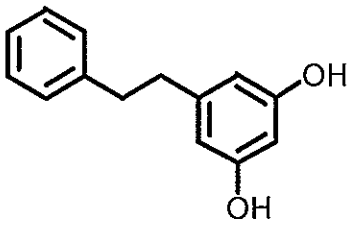

BP7: Dihydropinosylvin

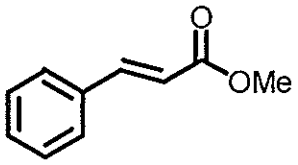

BP8: Methyl *trans*-cinnamate

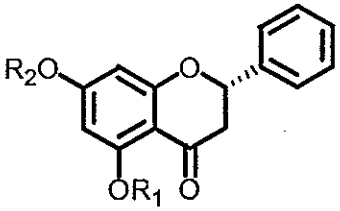

BP9: R_1 = R_2 = H; Pinocembrin

BP10: R_1 = H, R_2 = Me; Pinostrobin

BP11: R_1 = Me, R_2 = H; Alpinetin

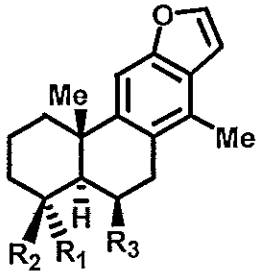

SC1: R_1 = CO_2Me, R_2 = Me, R_3 = H; Taepeenin A

SC2: R_1 = CO_2H, R_2 = Me, R_3 = H; Taepeenin B

SC3: R_1 = CO_2Me, R_2 = Me, R_3 = OH; Taepeenin C

SC4: R_1 = CO_2Me, R_2 = Me, R_3 = OCOMe; Taepeenin D

RH1: R_1 = CO_2Me, R_2 = CHO, R_3 = H; Taepeenin E

SD1: R_1 = R_2 = Me, R_3 = H; 17-Methylvouacapane-8(14),9(11)-diene

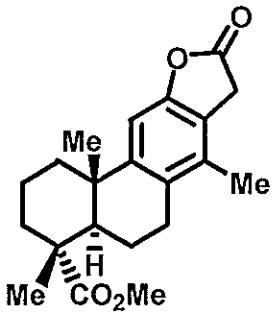

SC5: Taepeenin F

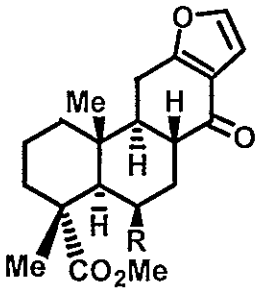

SC6: R = H; Nortaepeenin A

SC7: R = OH; Nortaepeenin B

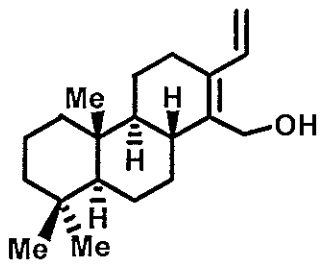

SC9: Taepeenin G

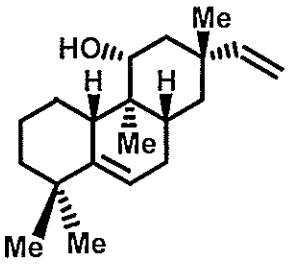

SC10: *ent*-11β-Hydroxy-rosa-5,15-diene

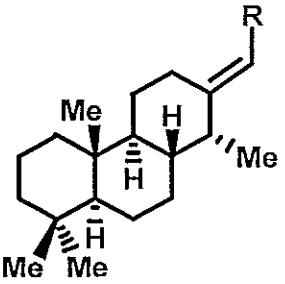

SD4: R = CHO; Taepeenin K

SD5: R = CH_2OH; Taepeenin L

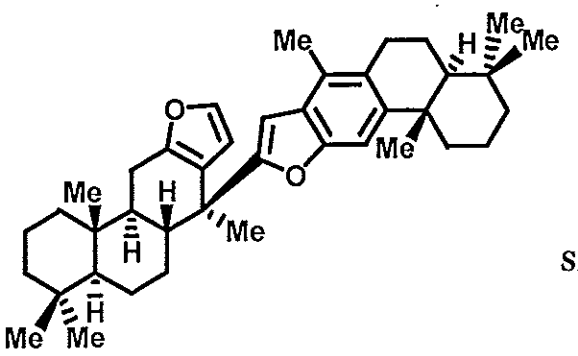

SD3: Taepeenin J

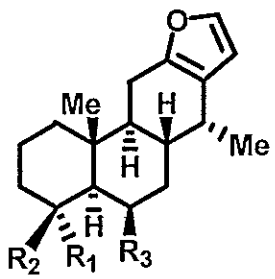

SC8: R_1 = CO_2Me, R_2 = Me, R_3 = H; Methyl vinhaticoate

RH2: R_1 = CO_2H, R_2 = Me, R_3 = H; Vinhaticoic acid

RH3: R_1 = CO_2Me, R_2 = CHO, R_3 = H; Taepeenin H

RH4: R_1 = CO_2Me, R_2 = CH_2OH, R_3 = H; Taepeenin I

SD2: R_1 = R_2 = Me, R_3 = H; Vouacapane

SD6: R_1 = R_2 = Me, R_3 = OH; 6β-Hydroxyvouacapane

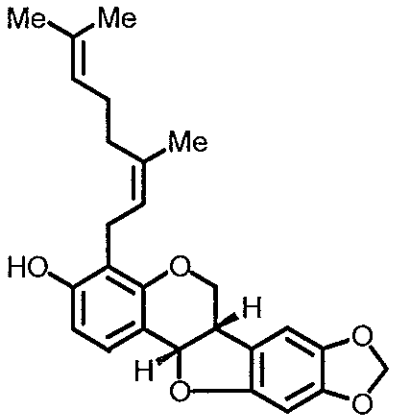

RH5: Nutiducol

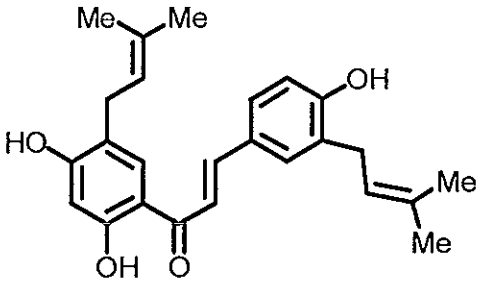

RH6: Stipulin

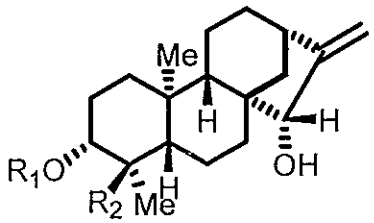

BMC1: R_1 = OH, R_2 = CH_2OH; *ent*-16-Kaurene-3β,15β,18-triol

BMC2: R_1 = =O, R_2 = CH_2OH; *ent*-3-Oxo-16-kaurene-15β,18-diol

BMC3: R_1 = OH, R_2 = Me; *ent*-16-Kaurene-3β,15β-diol

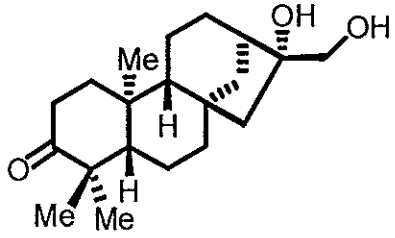

BMC4: Abbeokutone

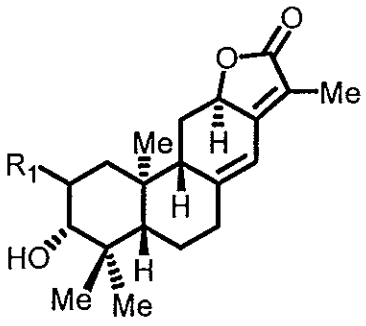

BMC5: R_1 = H_2; Helioscopinolide A

BMC6: R_1 = =O; Helioscopinolide C

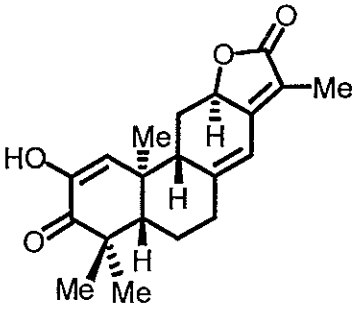

BMC7: Helioscopinolide I

PART II Search for novel terpenes in *Erythropodium caribaeorum* and study for carotenoids from a coral-derived *Micrococcus* strain PAH83

Five compounds: eleutherobin, desacetyleleutherobin, erythrolide A and B, and erythrodiene were isolated from *E. caribaeorum*. The retention time 24.72 min of fraction EC1H showed the molecular ion at *m/z* 303 corresponding with the molecular ion of terpene synthase product which should be further investigated.

The effects of pH, temperature, aeration, different incubation periods, inoculation, media and sugar on the growth and carotenoids biosynthesis of *Micrococcus* strain PAH83 were investigated. Three major carotenoids: sarcinaxanthin, sarcinaxanthin monoglucoside and sarcinaxanthin diglucoside, were identified from this culture. Their structures were elucidated on the basis of UV and MS spectra.

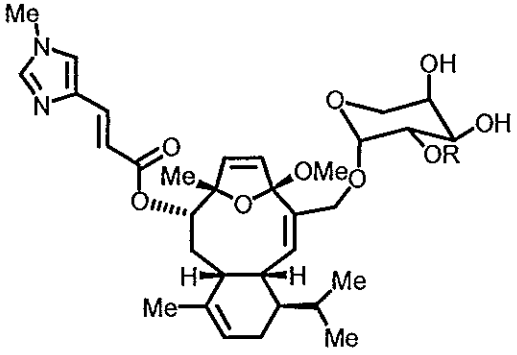

R = Ac; Eleutherobin

R = H; Desacetyleleutherobin

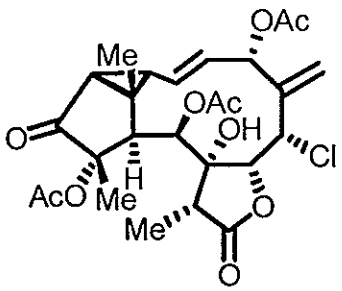

Erythrolide A

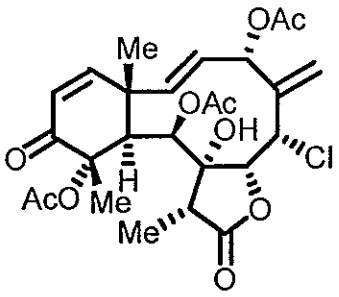

Erythrolide B

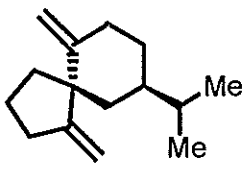

Erythrodiene

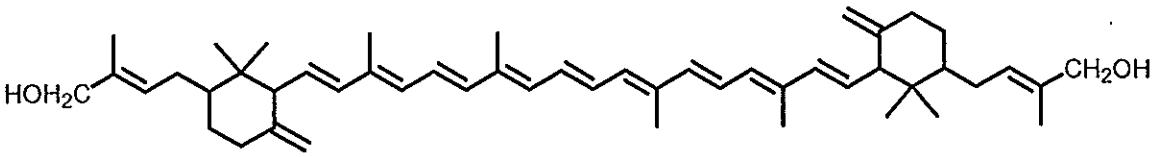

Sarcinaxanthin

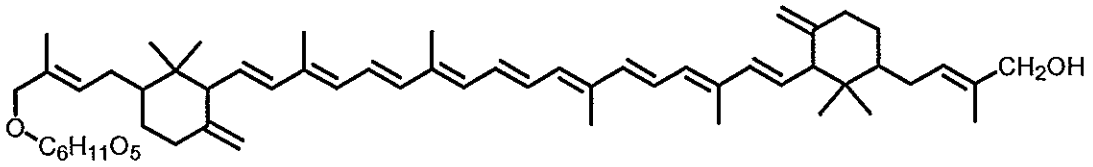

Sarcinaxanthin monoglucoside

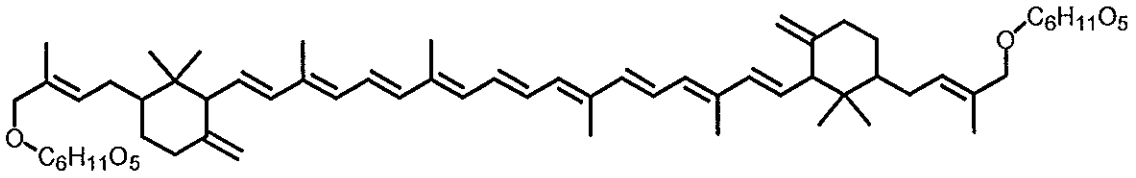

Sarcinaxanthin diglucoside

ACKNOWLEDGEMENTS

I wish to express my deepest and sincere gratitude to my supervisor, Associate Professor Dr. Chatchanok Karalai, for his valuable instructions, expert guidance, excellent suggestions and kindness which are more than I can describe here. Everything will always be in my mind.

My sincere thanks are expressed to Associate Professor Dr. Sanan Subpharathirasakul my co-advisor for his kindness and valuable advices, and also to Associate Professor Chanita Ponglimanont for her kindness and valuable advices. Special thanks are addressed to Professor Dr. Russell G. Kerr, Department of Chemistry, University of Prince Edward Island, Canada for marine biosynthesis training and to Associate Professor Dr. Kan Chantrapromma, the Institute of Research and Development, Walailak University, Thasala, Nakhon Si Thummarat for valuable advices. In addition, I am also very grateful to Professor Dr. Hoong-Kun Fun, X-ray Crystallography Unit, School of Physics, Universiti Sains Malaysia, Malaysia, Dr. Shazia Anjum, H.E.J. Research Institute of Chemistry, International Center for Chemical Sciences, University of Karachi and Associate Professor Dr. Suchada Chantrapromma for the structure determination by single X-ray diffraction and Professor Puangpen Sirirugsa for plant identification.

I would like to express my appreciation to the staffs of the Department of Chemistry, Faculty of Science, Prince of Songkla University for making this thesis possible.

This research was made possible by a scholarship from Thailand Research Fund through the Royal Golden Jubilee Ph.D. Program, Center for Innovation in Chemistry: Postgraduate Education and Research Program in Chemistry, funded by The Royal Thai Government and Prince of Songkla University through Natural Products from Mangrove Plants and Synthetic Materials Research Unit and the Graduate School for financial support. I am also indebted to the Biodiversity Research and Training Program (BRT) for partial financial support and to BIOTEC for bioactivity testing.

Sarot Cheenpracha

THE RELEVANCE OF THE RESEARCH WORK TO THAILAND

The purpose of this research is to investigate the chemical constituents of *B. pandurata*, *C. crista* and *S. multiflora*. They are parts of the basic research on the utilization of the Thai medicinal plants. Chemical investigation of constituents from the rhizomes of *B. pandurata*, the stems, roots and seeds of *C. crista* and the bark of *S. multiflora* led to isolation of seventeen new compounds together with twenty-three known compounds. Some of the compounds exhibited anti-HIV-1 PR, anti-malarial and anti-allergic activities. These results have demonstrated that *B. pandurata*, *C. crista* and *S. multiflora* are among the potential sources of anti-HIV-1 PR, anti-malarial and anti-allergic activities, respectively, so they have potential to be developed into drugs.

Marine natural products offer great potential as a source of novel therapeutic agents, however, the development of many of these compounds has been hampered by the lack of an available supply. Thus, the second part of this research is to search for novel terpenes in *E. caribaeorum* to complete the pathway elucidation studies and study for carotenoids from a coral-derived *Micrococcus* strain PAH83, into a more easily fermented bacterium for the efficient production of marine natural products.

CONTENTS

CONTENTS (Continued)

CONTENTS (Continued)

CONTENTS (Continued)

CONTENTS (Continued)

LIST OF TABLES

LIST OF TABLES (Continued)

LIST OF TABLES (Continued)

LIST OF ILLUSTRATIONS

LIST OF ILLUSTRATIONS (Continued)

LIST OF ILLUSTRATIONS (Continued)

LIST OF ILLUSTRATIONS (Continued)

LIST OF ILLUSTRATIONS (Continued)

LIST OF SCHEMES

LIST OF ABBREVIATIONS AND SYMBOLS

s	=	*singlet*
d	=	*doublet*
t	=	*triplet*
q	=	*quartet*
m	=	*multiplet*
dd	=	*doublet of doublet*
dt	=	*doublet of triplet*
br s	=	*broad singlet*
R_f	=	Rate of flow
g	=	gram
nm	=	nanometer
mp	=	melting point
cm^{-1}	=	reciprocol centimeter (wave number)
δ	=	chemical shift relative to TMS
J	=	coupling constant
$[\alpha]_D$	=	specific rotation
λ_{max}	=	maximum wavelength
ν	=	absorption frequencies
ε	=	molar extinction coefficient
m/z	=	a value of mass divided by charge
^oC	=	degree celcius
MHz	=	Megahertz
ppm	=	part per million
c	=	concentration

LISTS OF ABBREVIATIONS AND SYMBOLS (continued)

IR	=	Infrared
UV-VIS	=	Ultraviolet-Visible
MS	=	Mass Spectroscopy
NMR	=	Nuclear Magnetic Resonance
2D NMR	=	Two Dimensional Nuclear Magnetic Resonance
COSY	=	Correlation Spectroscopy
DEPT	=	Distortionless Enhancement by Polarization Transfer
HMBC	=	Heteronuclear Multiple Bond Correlation
HMQC	=	Heteronuclear Multiple Quantum Coherence
NOE	=	Nuclear Overhauser Effect Spectroscopy
CC	=	Column Chromatography
QCC	=	Quick Column Chromatography
PLC	=	Preparative Thin Layer Chromatography
TMS	=	Tetramethylsilane
$CDCl_3$	=	Deuterochloroform
CD_3OD	=	Deuteromethanol
C_6D_6	=	Deuterobenzene

PART I

Chemical Constituents from *Boesenbergia pandurata*, *Caesalpinia crista* and *Suregada multiflora*

CHAPTER 1.1
INTRODUCTION

1.1.1 Chemical constituents from *Boesenbergia pandurata*

1.1.1.1 Introduction

Boesenbergia pandurata Holtt., locally known in Thai as Kra-chai (กระชาย), is a perennial herb belonging to the Zingiberaceae family. *B. pandurata* is an erect terrertrial small herb, almost stemless, with subterranean, thickened, yellow to brown aromatic rhizome, 30-60 cm high. *Leaf* is simple, alternate distichous, ovate-oblong, 4.5-10 cm wide, 15-30 cm long; petioles canaliculate. Inflorescence spiciform, is enclosed between sheaths of 2 uppermost leaves; *flowers* are pale pink, faintly fragrant; bracteole lanceolate, reddish purple. *Fruit* is capsule.

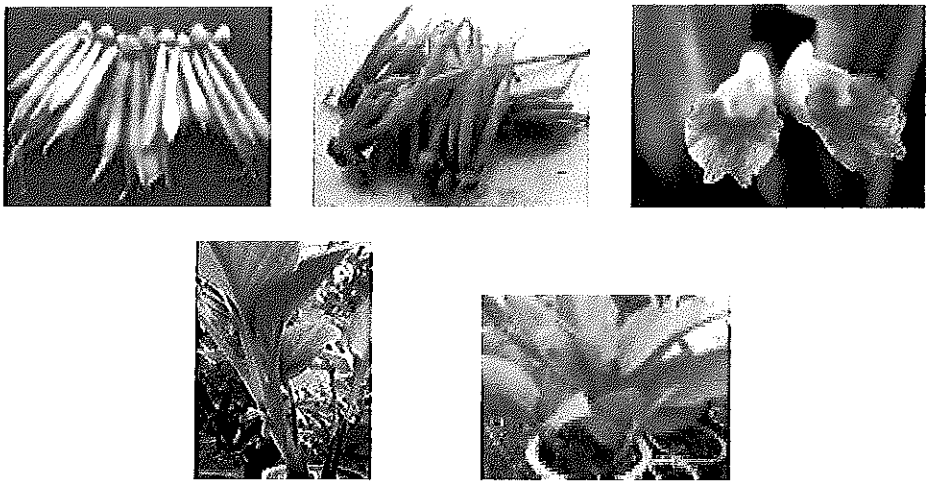

Figure 1 ***Boesenbergia pandurata***

1.1.1.2 Review of literatures

Plants in the *Boesenbergia* genus (Zingiberaceae) are well known to be rich in a variety of compounds. Information from NAPRALERT database developed by University of Illinois at Chicago revealed several types of compounds present in plants of *Boesenbergia* genus and they can be classified into groups as follows: alicyclics, diterpene, flavanones, flavones, flavonols, flavonoids and monoterpenes. These compounds are presented in Table 1.

Table 1 Compounds from plants of *Boesenbergia* genus

a : alicyclics b : diterpene c : flavanones
d : flavones e : flavonols f : flavonoids
g : monoterpenes

Plant	Part	Compound	Bibliography
B. pandurata	Entire plants	Alpinetin, 5c	Suphat, 1964
		Boesenbergin A, 22f	Tuntiwachwuttikul et al., 1980
		Cardamonin, 24f	
		4-Hydroxypanduratin A, 30f	
		Pinostrobin, 7c	Suphat, 1964
	Rhizomes	Alpinetin, 5c	Suphat, 1964; Pandji et al., 1993
		Boesenbergin A, 22f	Jaipetch et al., 1982 Tuntiwachwuttikul et al., 1980
		Boesenbergin B, 23f	Mahidol et al., 1984
		Chrysin dimethyl ether, 11d	Pathong et al., 1989
		Geranial, 32g	Pandji et al., 1993
		Neral, 33g	
		4-Hydroxypanduratin A, 30f	Trakoontiyakorn et al. 2001

Table 1 (Continued)

Plant	Part	Compound	Bibliography
B. pandurata	Rhizomes	Cardamonin, 24f	Murakami et al., 1993; Trakoontiyakorn et al., 2001; Nakahara, 2001
		Panduratin A, 29f	Tuntiwachwuttikul et al., 1984; Mahidol et al., 1984; Trakoontiyakorn et al. 2001
		Pinocembrin, 6c	Nakahara, 2001;
		Pinocembrin chalcone, 26f	Trakoontiyakorn et al., 2001
		Pinostrobin, 7c	Suphat, 1961; Tuntiwachwuttikul et al., 1984
		Pinostrobin chalcone, 25f	Jaipetch et al., 1982
		Rubranine, 31f	Tuntiwachwuttikul et al., 1984
B. pandurata black type	Rhizomes	2′-Hydroxy-4′,6′-dimethoxychalcone, 27f	Herunsalee et al., 1987
		2′-Hydroxy-4,4′,6′-trimethoxy chalcone, 28f	
		3,3′,4′,5,7-Pentamethoxyflavone, 16e	
		3,4′,5,7-Tetramethoxyflavone, 18e	
		Tsugafolin, 8c	

Table 1 (Continued)

Plant	Part	Compound	Bibliography
B. pandurata cv. black	Rhizomes	Chrysin dimethyl ether, 11d 5,7-Dimethoxyflavanone, 9c 3′,4′,5,7-Tetramethoxyflavone, 12d 3,5,7-Trimethoxyflavone, 17e 4′,5,7-Trimethoxyflavone, 13d 5-Hydroxy-3,3′,4′,7-tetramethoxyflavone, 19e 5-Hydroxy-3,4′,7-trimethoxy-flavone, 20e 5-Hydroxy-3,7-dimethoxy-flavone, 21e 5-Hydroxy-4′,7-dimethoxy-flavone, 14d Tectochrysin, 15d	Jaipetch et al., 1983
B. pandurata cv. flava	Rhizomes	Boesenbergin B, 23f	Mahidol et al., 1982
B. pandurata cv. yellow	Rhizomes	Boesenbergin A, 22f Boesenbergin B, 23f Cardamonin, 24f Panduratin A, 29f Pinocembrin, 6c Pinostrobin, 7c Rubranine, 31f	Mahidol et al., 1985
B. pandurata red type	Rhizomes	Panduratin A, 29f	Tuchinda et al., 2002

Table 1 (Continued)

Plant	Part	Compound	Bibliography
B. pandurata red type	Rhizomes	4-Hydroxypanduratin A, 30f Pinocembrin, 6c Pinostrobin, 7c Sakuranetin, 10c	Tuchinda et al., 2002
B. species	Rhizomes	Boesenboxide, 1a 2′-Hydroxy-4,4′,6′-trimethoxychalcone, 28f Crotepoxide, 2a Isopimaric acid, 4b (+)-Zeylenol, 3a	Tuntiwachwuttikul et al., 1987

Structures

a : alicyclics

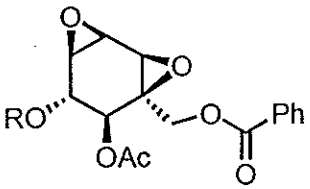

1a : R = COPh; Boesenboxide

2a : R = Ac; Crotepoxide

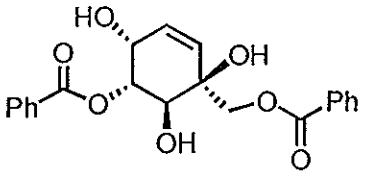

3a : (+)-Zeylenol

b : diterpene

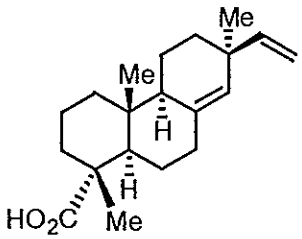

4b : Isopimaric acid

c : flavanones

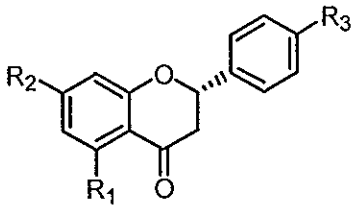

5c : R_1 = OMe, R_2 = OH, R_3 = H; Alpinetin

6c : R_1 = OH, R_2 = OH, R_3 = H; Pinocembrin

7c : R_1 = OH, R_2 = OMe, R_3 = H; Pinostrobin

8c : R_1 = OMe, R_2 = OH, R_3 = OMe; Tsugafolin

9c : R_1 = OMe, R_2 = OMe, R_3 = H;
5,7-Dimethoxyflavanone

10c : R_1 = OH, R_2 = OMe, R_3 = OH; Sakuranetin

d : flavones

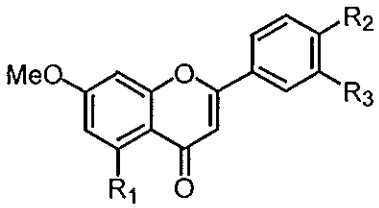

11d : R_1 = OMe, R_2 = H, R_3 = H; Chrysin dimethyl ether

12d : R_1 = OMe, R_2 = OMe, R_3 = OMe;
3′,4′,5,7-Tetramethoxyflavone

13d : R_1 = OMe, R_2 = OMe, R_3 = H;
4′,5,7-Trimethoxyflavone

14d : R_1 = OH, R_2 = OMe, R_3 = H;
5-Hydroxy-4′,7-dimethoxyflavone

15d : R_1 = OH, R_2 = H, R_3 = H; Tectochrysin

e : flavonols

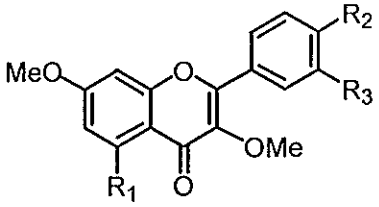

16e : R_1 = OMe, R_2 = OMe, R_3 = OMe;
3,3′,4′,5,7-Pentamethoxyflavone

17e : R_1 = OMe, R_2 = H, R_3 = H;
3,5,7-Trimethoxyflavone

18e : R_1 = OMe, R_2 = OMe, R_3 = H;
3,4′,5,7-Tetramethoxyflavone

19e : R_1 = OH, R_2 = OMe, R_3 = OMe;
5-Hydroxy-3,3′,4′,7-tetramethoxyflavone

20e : R_1 = OH, R_2 = OMe, R_3 = H;
5-Hydroxy-3,4′,7-trimethoxyflavone

21e : R_1 = OH, R_2 = H, R_3 = H;
5-Hydroxy-3,7-dimethoxyflavone

f : flavonoids

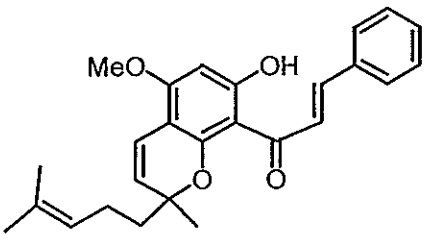

22f : Boesenbergin A

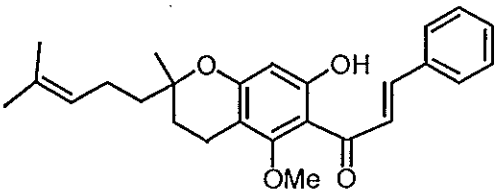

23f : Boesenbergin B

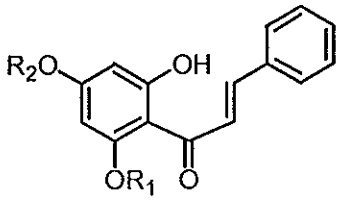

24f : R_1 = Me, R_2 = H; Cardamonin

25f : R_1 = H, R_2 = Me; Pinostrobin chalcone

26f : R_1 = H, R_2 = H; Pinocembrin chalcone

27f : R_1 = Me, R_2 =Me;

2′-Hydroxy-4′,6′-dimethoxychalcone

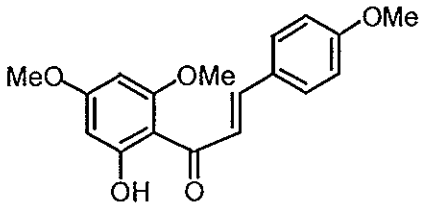

28f : 2′-Hydroxy-4,4′,6′-trimethoxychalcone

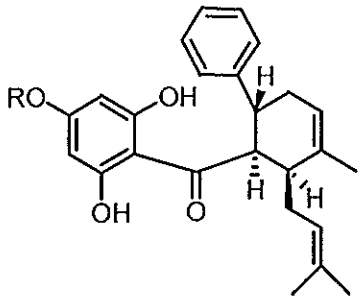

29f : R = Me; Panduratin A

30f : R = H; 4-Hydroxypanduratin A

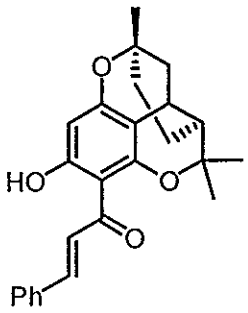

31f : Rubranine

g : monoterpenes

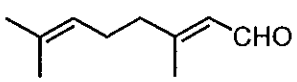

32g : Geranial

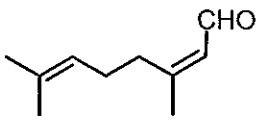

33g : Neral

1.1.2 Chemical constituents from *Caesalpinia crista*

1.1.2.1 Introduction

Caesalpinia crista L., known locally as "Taepee (เทพี)" in Thai, is a climber distributed from India and Ceylon through most of Southeast Asia to the Ryu-Kyu Islands, Queensland and Caledonia. The Leguminosae-Caesalpioideae family contains about 150 genera with 2,200 species. In Thailand only 20 genera with 113 species are found, from *Caesalpinia* genus only 18 species are found. *C. crista* was found in Chiang Mai, Bangkok, Chumphon, Ranong, Surat Thani and Phuket.

C. crista is a climber, glabrous on all vegetative parts, armed with recurved prickles. *Stipules* awl-shaped, ca 1 mm, caducous. *Leaves* : rhachis 10-20 cm; pinnae 2-4 pairs; leaf-lets 2-4 pairs, opposite, petiolulate (2-4 mm), elliptic-ovate or lanceolate, 2-6 by 1-3 cm, obtuse or shortly acuminate at the tip, rounded or cuneate and subequal at the base. *Racemes* axillary and combined into terminal panicles. *Bracts* ca 1 mm, caducous. *Pedicels* are 10-15 mm, glabrous, jointed near the top. *Sepals* are glabrous, the lowest one hood-shaped. *Petals* are yellow, the standard red or red-striped, constricted, and hairy inside towards the middle with hairly *Filaments*. Ovary is shortly stalked, glabrous or pubescent, 1-2 ovulate. *Pods* stalked above the receptacle (2-5 mm), subelliptic or rhombic in outline, 4-7 by 2.5-3.5 cm, obtuse to acute at the top and at the base. *Seeds* 1 (rarely 2) flattened, subreniform, 12 by 20 mm.

Figure 2 ***Caesalpinia crista***

1.1.2.2 Review of literatures

Plants in the *Caesalpinia* genus (Leguminosae-Caesalpioideae) are well known to be rich in diterpenes. Information from NAPRALERT database developed by University of Illinois in Chicago revealed several types of compounds present in plants of *Caesalpinia* genus and they can be classified into groups as follows: alkanes, alkanols, alkaloids, benzenoids, carbohydrates, carotenoids, coumarins, diterpenes, flavonoids, flavonols, flavones, flavonones, iridoids, lipids, phenylpropanoid, quinolizidine alkaloids, quinoids, sesquiterpenes, steroids, triterpenes and vitamin. These compounds are presented in **Table 2.**

Table 2 Compounds from plants of *Caesalpinia* genus

a : Alkanes b: Alkanols c : Alkaloids d : Benzenoids
e : Carbohydrates f : Carotenoids g : Coumarins h : Diterpenes
i : Flavonoids j : Iridoids k : Lipids l : Phenylpropanoids
m : Quinoids n : Sesquiterpene o : Steroids p : Triterpenes
q : Vitamin

Plant	Part	Compound	Bibliography
C. bonducella	Part not specified	α-Amyrin, 192p	Lai et al., 1997
		β-Amyrin, 193p	
		Lupeol, 198p	
		Lupeol acetate, 199p	
		β-Sitosterol, 191o	
	Seeds	α-Amyrin, 192p	Asif Saeed and Sabir, 2003
		β-Amyrin, 193p	Ahmad et al., 1997
		Bondenolide, 33h	Simin et al., 2001; Ahmad et al., 1997
		α-Caesalpin, 50h	Pelizzoni, 1968;
		β-Caesalpin, 51h	Qudrat-I-Khuda and Erfan Ali, 1963
		γ-Caesalpin, 59h	Canonica et al., 1963 and 1966
		ε-Caesalpin, 52h	Balmain et al., 1967
		Caesalpin D, 61h	Kinoshita, 2000
		n-Heptacosane, 1a	Katti and Puntambekar, 1930
		Hexadeca-7,10-dienoic acid, 176k	Shameel et al., 1997

Table 2 (Continued)

Plant	Part	Compound	Bibliography
C. bonducella	Seeds	Lignoceric acid, 175k	Ahmad et al., 1997
		Lupeol, 198p	Saeed and Sabir, 2001; Asif Saeed and Sabir, 2003
		Lupeol acetate, 199p	Kinoshita et al., 1996
		Neocaesalpin B, 100h	
		Neocaesalpin C, 101h	
		Neocaesalpin D, 102h	
		Neocaesalpin H, 104h	
		Oleanolic acid, 194p	Ahmad et al., 1997
		Sucrose, 25e	Ghatak, 1934
		β-Sitosterol, 191o	Katti and Puntambekar, 1930
	Roots	Bonducellpin A, 34h	Peter et al., 1997a
		Bonducellpin B, 36h	
		Bonducellpin C, 35h	
		Bonducellipin D, 37h	
		Caesaldekarin A, 38h	Lyder et al., 1998a
		Caesaldekarin B, 39h	
		Caesaldekarin C, 40h	Peter et al., 1998a
		Caesaldekarin G, 44h	
		Caesaldekarin H, 45h	Lyder et al., 1998a
		Caesaldekarin F, 43h	Peter et al., 1998a
		Caesaldekarin I, 46h	Lyder et al., 1998a
		Caesaldekarin J, 47h	
		Caesaldekarin K, 48h	
		Caesaldekarin L, 49h	

Table 2 (Continued)

Plant	Part	Compound	Bibliography
C. bonducella	Roots	Caesalpin, 86h	Peter et al., 1998b
		Caesalpinin B, 75h	Lyder et al., 1998b
		Caesalpin F, 53h	Peter et al., 1998b
		Caesalpin G, 58h	
		Caesalpin H, 62h	
		Demethylcaesaldekarin C, 41h	Lyder et al., 1998a
		Neocaesalpin I, 107h	
		2-Acetoxycaesaldekarin E, 32h	Peter et al., 1997b
	Kernels	Bonducellin, 155i	Purushothaman et al., 1982
		Caesalpinin J, 76h	Katti, 1930
		Caesalpin F, 53h	Pascoe et al., 1986
		α-Caesalpin, 50h	Ali and Qudrat-I-Khuda, 1960
		β-Caesalpin, 51h	
		γ-Caesalpin, 59h	
		Glucose, 19e	Katti, 1930
		Lignoceric acid, 175k	
		Octadec-4-enoic acid, 178k	Rastogi et al., 1996
		Octadeca-2,4-dienoic acid, 181k	
		Palmitic acid, 174k	Rastogi et al., 1996;
		Stearic acid, 173k	Katti, 1930
		Sucrose, 25e	Katti, 1930
	Entire plants	β-Caesalpin, 51h	Goyal et al., 1981
	Leaves	Glucose, 19e	Khuda et al., 1961

Table 2 (Continued)

Plant	Part	Compound	Bibliography
C. bonducella	Leaves	Palmitic acid, 174k (+)-*D*-Pinitol, 23e	Khuda et al., 1961
C. brevifolia	Fruits	Algarobin, 7d Brevifolin carboxylic acid, 28g Brevilagin 1, 8d Brevilagin 2, 10d	Schmidt et al., 1967a-c
C. cacalaco	Seeds	Arachidic acid, 170k Linoleic acid, 177k Linolenic acid, 182k Oleic acid, 179k Palmitic acid, 174k Palmitoleic acid, 180k Stearic acid, 173k	Contreras et al., 1995
	Bark	Ascorbic acid, 201p	Giral and Aguilar, 1953
C. coriaria	Entire plants	Aucubin, 169j	Nageshwar et al., 1984
C. crista	Kernels	2-Acetoxy-3-deacetoxy-caesaldekarin E, 30h 7-Acetoxybonducellpin C, 70h Caesaldekarin E, 31h Caesalmin B, 55h Caesalpinin C, 63h Caesalpinin D, 57h Caesalpinin E, 69h Caesalpinin F, 71h	Banskota et al., 2003

Table 2 (Continued)

Plant	Part	Compound	Bibliography
C. crista	Kernels	Caesalpinin MA, 77h	Banskota et al.,
		Caesalpinin MB, 79h	2003
		Caesalpinin MC, 81h	
		Caesalpinin MD, 82h	
		Caesalpinin ME, 78h	
		Caesalpinin MF, 80h	
		Caesalpinin MG, 83h	
		Caesalpinin MH, 84h	
		Caesalpinin MI, 85h	
		Caesalpinin MJ, 87h	
		Caesalpinin MK, 88h	
		Caesalpinin ML, 90h	
		Caesalpinin MM, 91h	
		Caesalpinin MN, 92h	
		Caesalpinin MO, 93h	
		Caesalpinin MP, 94h	
		14(17)-Dehydrocaesalpin F, 68h	
		Norcaesalpinin A, 66h	
		Norcaesalpinin B, 67h	
		Norcaesalpinin C, 96h	
		Norcaesalpinin D, 64h	
		Norcaesalpinin E, 65h	
		Norcaesalpinin MA, 97h	
		Norcaesalpinin MB, 98h	
		Norcaesalpinin MC, 89h	

Table 2 (Continued)

Plant	Part	Compound	Bibliography
C. crista	Entire plants	(+)-Ononitol, 22e	Shi et al., 1988
	Fruit hulls	(+)-*D*-Pinitol, 23e	Mondai et al., 1993
C. decapetala	Seeds	Linoleic acid, 177k Malvalic acid, 184k Myristic acid, 172k Oleic acid, 179k Palmitic acid, 174k Ricinoleic acid, 183k Stearic acid, 173k Sterculic acid, 185k	Hosamani, 1995
C. decapetala var. *japonica*	Roots	Betulinic acid, 200p Caesaljapin, 95h (+)-Catechin, 159i Gallic acid methyl ester, 14d Lupeol, 198p Sappanchalcone, 133i	Ogawa et al., 1992
C. digyna	Roots	Bergenin, 27g	Chaudhry, 1957 and 1954
	Leaves	Bergenin, 27g Caesalpimine A, 5c Celallocinnine, 6c Ellagic acid, 29g Gallic acid, 12d	Mahato et al., 1983 Mahato et al., 1985 Mahato et al., 1983 Chaudhry et al., 1954
C. ferrea	Fruits	Ellagic acid, 29g Gallic acid, 12d	Ueda et al., 2001 Nakamura et al., 2002

Table 2 (Continued)

Plant	Part	Compound	Bibliography
C. ferrea	Fruits	3-Hydroxy-1-(4-hydroxy-3-methoxyphenyl)propan-1-one, **187l** Gallic acid methyl ester, **14d**	Ueda et al., 2001 Nakamura et al., 2002
C. gilliesii	Flowers	Arabinose, **17e** Glucose, **19e** Kaempferol, **140i** Luteolin, **136i** Nicotiflorin, **146i** Quercetin, **141i** Isoquercitrin, **150i** Isorhamnetin, **142i** Isorhamnetin-3-O-rutinoside, **147i**	Suarez et al., 1984
	Leaves	Kaempferol, **140i** Luteolin, **136i** Nicotiflorin, **146i** Quercetin, **141i** Isoquercitrin, **150i** Isorhamnetin, **142i** Isorhamnetin-3-O-rutinoside, **147i**	Suarez et al., 1984
C. hintonii	Seeds	Arachidic acid, **170k** Linoleic acid, **177k** Linolenic acid, **182k** Oleic acid, **179k**	Contreras et al., 1995

Table 2 (Continued)

Plant	Part	Compound	Bibliography
C. hintonii	Seeds	Palmitic acid, 174k Palmitoleic acid, 180k Stearic acid, 173k	Contreras et al., 1995
C. japonica	Stems	Apigenin, 137i (+)-Catechin, 159i 3′,4′,7-Trihydroxyflavone, 138i 4′,7-Dihydroxyflavone, 139i Palmitic acid, 174k (+)-Pinitol, 23e Resokaempferol, 143i β-Sitosterol, 191o	Imamura et al., 1980 Sohn et al., 2000 Sohn et al., 2000; Imamura et al., 1980 Imamura et al., 1980 Sohn et al., 2000 Imamura et al., 1980
	Flowers	Arachic acid, 170k β-Carotene, 26f *n*-Heptacosane, 1a Hyperoside, 149i n-Nonacosane, 2a n-Triacotane, 3a	Imamura et al., 1980
	Wood	Butein, 134i 3′-Deoxy-4-O-methylsappanol, 161i Episappanol, 165i	Namikoshi et al., 1987a,b

Table 2 (Continued)

Plant	Part	Compound	Bibliography
C. japonica	Wood	Isoliquiritigenin, **135i** 4-*O*-Methylsappanol, **163i** Sappanol, **160i** Sappanchalcone, **133i** Sappanone A, **158i** Sappanone B, **167i**	Namikoshi et al., 1987a,b
C. major	Roots	Caesaldekarin A, **38h** Caesaldekarin B, **39h** Caesaldekarin C, **40h** Caesaldekarin D, **42h**	Kitagawa et al., 1994; Shibuya and Kitagawa, 1996 Kitagawa et al., 1996 and 1994 Kitagawa et al., 1996
	Kernel	Caesaldekarin B, **39h** Caesaldekarin E, **31h** 14-Deoxy-ε-caesalpin, **108h**	Roengsumran et al., 2000; Kitagawa et al., 1994 Kitagawa et al., 1996 and 1994 Roengsumran et al., 2000
C. mexicana	Entire plants	Linoleic acid, **177k** Oleic acid, **179k**	Saeedi-Ghomi and Garcia, 1982
C. minax	Seeds	Bonducellpin D, **37h** Caesalmin A, **54h** Caesalmin B, **55h** Caesalmin C, **60h**	Jiang et al., 2002a-c and 2002a-c

Table 2 (Continued)

Plant	Part	Compound	Bibliography
C. minax	Seeds	Caesalmin D, 72h Caesalmin F, 73h Caesalmin G, 56h Caesalmin H, 74h Macrocaesalmin, 109h Spirocaesialmin, 110h	Jiang et al., 2002a-c
	Stems	Friedelin, 195p Epifriedelinol, 196p	
C. pulcherrima	Stems	Bonducellin, 155i 2,6-Dimethoxy-1,4-benzo-quinone, 188m 8-Methoxybonducellin, 156i Bilobetin, 153i Pulcherralpin, 111h Pulcherrimin, 168i	Jiang et al., 2002a Parmar et al., 1987; McPherson et al., 1983 McPherson et al., 1982 Che et al., 1985 and 1986 McPherson et al., 1983
	Leaves	Benzyl-2,6-dimethoxy-benzoate, 9d Caesaldekarin A, 38h Gentisic acid, 15d Isovouacapenol A, 112h Isovouacapenol B, 113h Isovouacapenol C, 114h	Ragasa et al., 2002 Ragasa et al., 2003 Griffiths, 1959 Ragasa et al., 2002

Table 2 (Continued)

Plant	Part	Compound	Bibliography
C. pulcherrima	Leaves	Isovouacapenol D, **115h**	Ragasa et al., 2002
		Myricetin, **151i**	Paris and Delaveau, 1965 and 1967
		Phytol, **126h**	Ragasa et al., 2003
		β-Sitosterol, **191o**	
		Spathulenol, **190n**	
	Entire plants	Benzyl-2,6-dimethoxy-benzoate, **9d**	Srinivas et al., 2003
		5,7-Dimethoxyflavanone, **127i**	
		5,7-Dimethoxy-3′,4′-methylenedioxyflavanone, **128i**	
		2′,3,4′,5,6,7-Hexahydroxy-flavone, **129i**	
		Isobonducellin, **157i**	
	Roots	6β-Cinnamoyl-7β-hydroxy vouacapen-5α-ol, **123h**	Roach et al., 2003
		8,9,11,14-Didehydrovoua-capen-5α-ol, **124h**	McPherson et al., 1985
		7-Ketoisovouacapenol C, **125h**	Roach et al., 2003
		Neocaesalpin E, **105h**	
		Neocaesalpin F, **106h**	
		Neocaesalpin G, **103h**	
		Pulcherrimin A, **116h**	Patil et al., 1997
		Pulcherrimin B, **121h**	

Table 2 (Continued)

Plant	Part	Compound	Bibliography
C. pulcherrima	Roots	Pulcherrimin C, 117h	Patil et al., 1997
		Pulcherrimin D, 118h	
		Pulcherrimin E, 119h	Roach et al., 2003
		Pulcherrimin F, 120h	
		β-Sitosterol, 191o	McPherson et al., 1986
		Vouacapen-5α-ol, 122h	McPherson et al., 1986 and 1985
	Barks	Caesalpin, 86h	Sengupta et al., 1970
		Leucodelphinidin, 130i	
		Quercimeritrin, 152i	Awasthi and Misra, 1977
		β-Sitosterol, 191o	
	Flowers	Lupeol, 198p	Varshney and Pal, 1978
		β-Sitosterol, 191o	
		Sucrose, 25e	
	Stem barks	Ellagic acid, 29g	Awasthi and Misra, 1978 and 1980
		Gallic acid, 12d	
		Gallic acid ethyl ester, 13d	
		Leucodelphinidin, 130i	Awasthi and Misra, 1978
		Leucoefdin, 131i	
		Sebacic acid, 186k	Awasthi et al., 1980
		β-Sitosterol, 191o	
C. pulcherrima var. *flava*	Flowers	Gallic acid, 12d	Rao and Prasad, 1978
		Lupeol acetate, 199p	
		Myricetin, 151i	

Table 2 (Continued)

Plant	Part	Compound	Bibliography
C. pulcherrima var. *flava*	Flowers	Quercetin, 141i β-Sitosterol, 191o	Rao and Prasad, 1978
C. pulcherrima var. *rubra*	Flowers	Gallic acid, 12d Lupeol, 198p Quercetin, 141i Rutin, 148i β-Sitosterol, 191o	Rao and Prasad, 1978
C. pyramidalis	Leaves	Agathisflavone, 154i Lupeol, 198p	Mendes et al., 2000
C. sappan	Seeds	β-Amyrin, 193p Arachidic acid, 170k Capric acid, 171k	Oswal and Garg, 1993 Oswal and Garg, 1984
	Heartwoods	3′-Deoxysappanol, 162i 3′-Deoxysappanone B, 166i 4,4′-Dihydroxy-2′-methoxy chalcone, 132i Galactose, 128e Gallic acid, 12d Glucose, 19e Juglone, 189m Lactose, 20e 8-Methoxy bonducellin, 156i 4-*O*-Methylgalactose, 21e	Namikoshi et al., 1987 Morota et al., 1990 Namikoshi et al., 1987 Nigam et al., 1977 Steinmetz, 1960 Nigam et al., 1977 Nageshwar et al., 1984 Nigam et al., 1977 Namikoshi et al., 1987 Nigam et al., 1977

Table 2 (Continued)

Plant	Part	Compound	Bibliography
C. sappan	Heartwoods	3′-*O*-Methylsappanol, **164i**	Namikoshi et al., 1987
		4-*O*-Methylsappanol, **163i**	Reddy et al., 2003
		Octacosan-1-ol, **4b**	Yadava and Nigam, 1987
		Ombuin, **145i**	Namikoshi et al., 1987
		Palmitic acid, **174k**	Nigam et al., 1978; Yadava et al., 1978
		Quercetin, **141i**	Namikoshi et al., 1987
		Rhamnetin, **144i**	
		Sappanchalcone, **133i**	Nagai et al., 1984
		β-Sitosterol, **191o**	Morota et al., 1990
		Sorbose, **24e**	Nigam et al., 1977
		Stearic acid, **173k**	Nigam et al., 1978
		Taraxerol, **197p**	Yadava and Nigam, 1987
C. spinosa	Seeds	Digallic acid, **11d**	Delahaye and Verzele, 1983
		Gallic acid, **12d**	
		Trigallic acid, **16d**	
C. velutina	Seeds	Arachidic acid, **170k**	Contreras et al., 1995
		Linoleic acid, **177k**	
		Linolenic acid, **182k**	
		Oleic acid, **179k**	

Structures

a : Alkanes

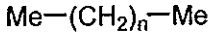

1a : n = 25; *n*-Heptacosane
2a : n = 27; *n*-Nonacosane
3a : n = 28; *n*-Triacotane

b: Alkanols

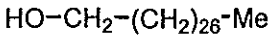

4b : Octacosan-1-ol

c : Alkaloids

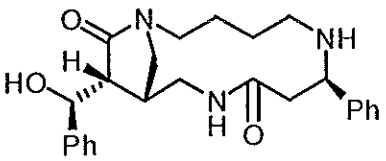

5c : Caesalpimine A

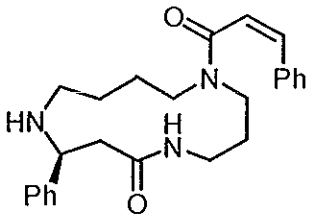

6c : Celallocinnine

d : Benzenoids

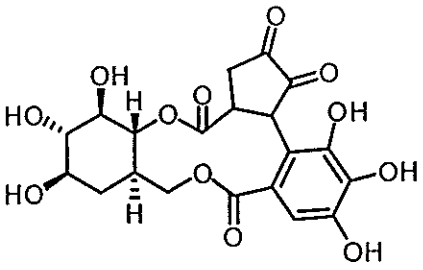

7d : Algarobin

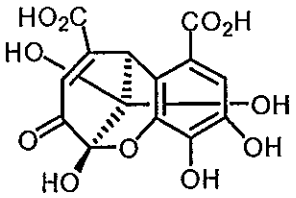

8d : Brevilagin 1

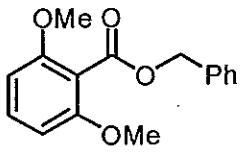

9d : Benzyl-2,6-dimethoxybenzoate

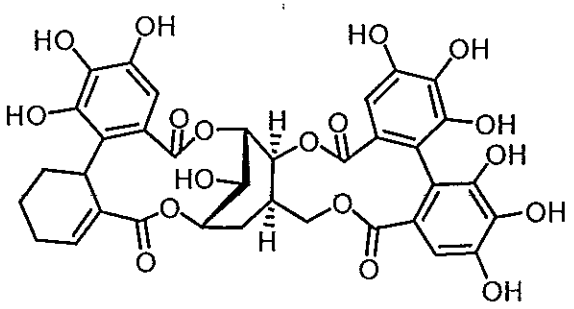

10d : Brevilagin 2

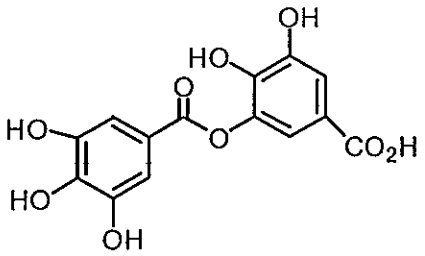

11d : Digallic acid

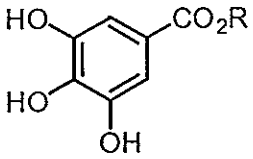

12d : R = H; Gallic acid

13d : R = Et; Gallic acid ethyl ester

14d : R = Me; Gallic acid methyl ester

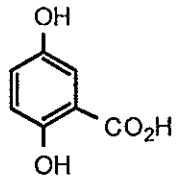

15d : Gentisic acid

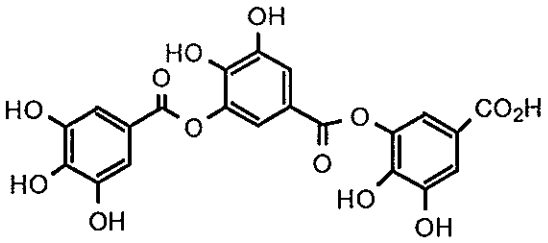

16d : Trigallic acid

e : Carbohydrates

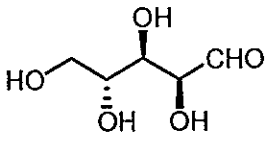

17e : Arabinose

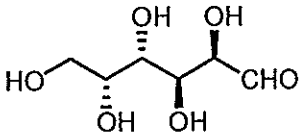

18e : Galactose

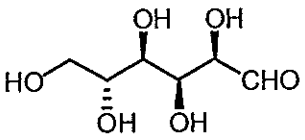

19e : Glucose

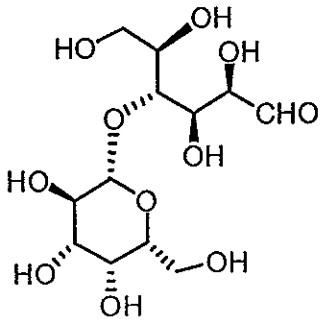

20e : Lactose

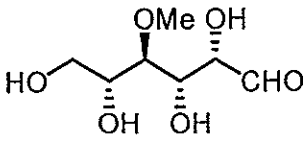

21e : 4-*O*-Methylgalactose

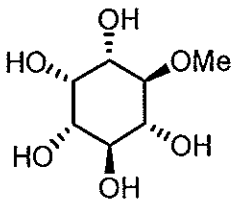

22e : (+)-Ononitol

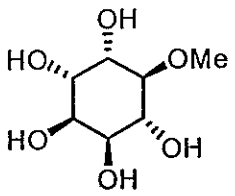

23e : (+)-*D*-Pinitol

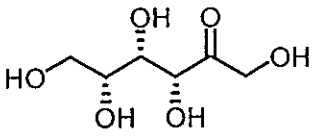

24e : Sorbose

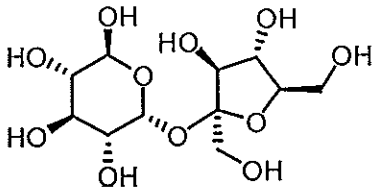

25e : Sucrose

f : Carotenoids

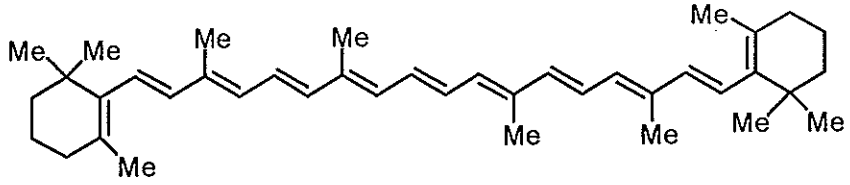

26f : β-Carotene

g : Coumarins

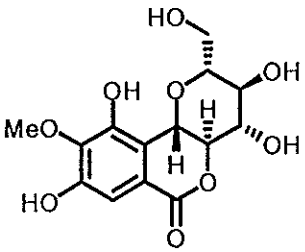

27g : Bergenin

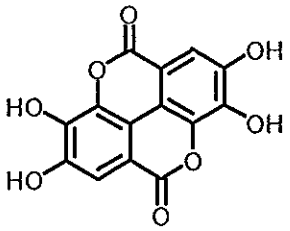

28g : Brevifolin carboxylic acid

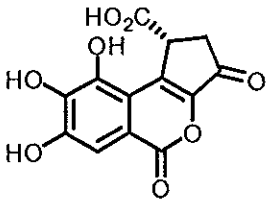

29g : Ellagic acid

h : Diterpenes

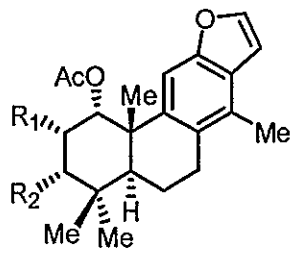

30h : R_1 = OAc, R_2 = H;
2-Acetoxy-3-deacetoxycaesaldekarin E

31h : R_1 = H, R_2 = OAc; Caesaldekarin E

32h : R_1 = R_2 = OAc; 2-Acetoxycaesaldekarin E

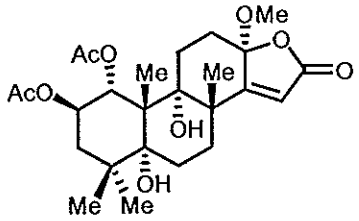

33h : Bondenolide

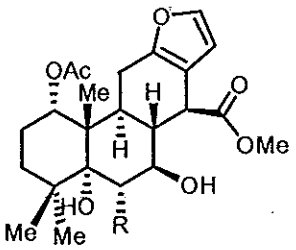

34h : R = OAc; Bonducellpin A

35h : R = H; Bonducellpin C

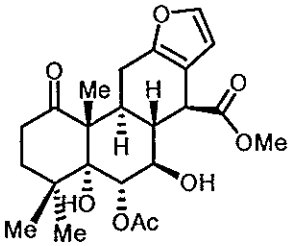

36h : Bonducellpin B

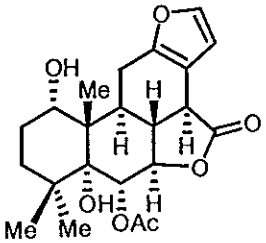

37h : Bonducellpin D

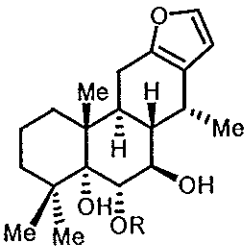

38h : R = Ac; Caesaldekarin A

39h : R = H; Caesaldekarin B

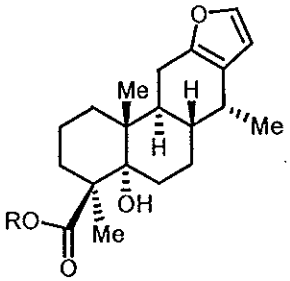

40h : R = Me; Caesaldekarin C

41h : R = H; Demethylcaesaldekarin C

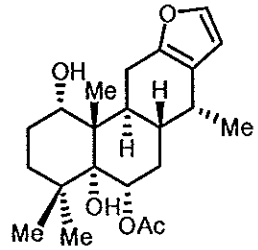

42h : Caesaldekarin D

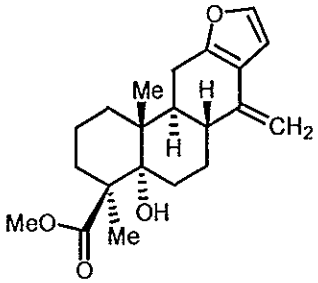

43h : Caesaldekarin F

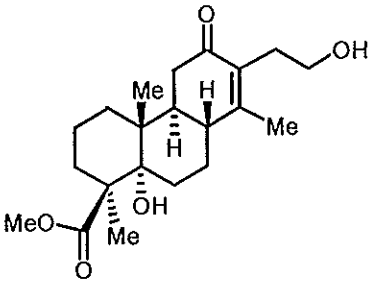

44h : Caesaldekarin G

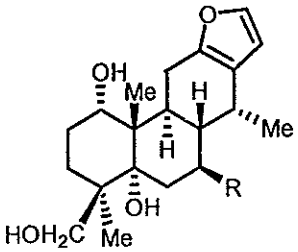

45h : R = H; Caesaldekarin H

46h : R = OH; Caesaldekarin I

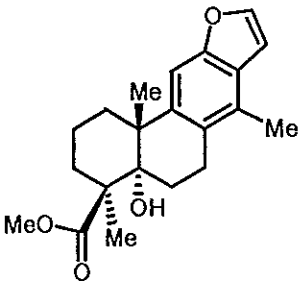

47h : Caesaldekarin J

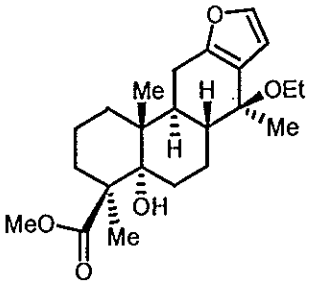

48h : Caesaldekarin K

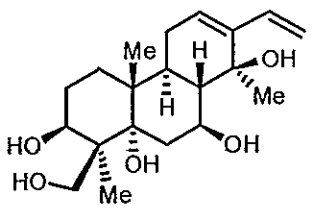

49h : Caesaldekarin L

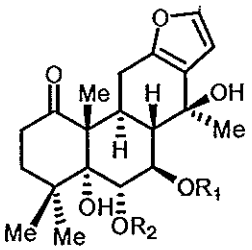

50h : R = Ac; α-Caesalpin

51h : R = H; β-Caesalpin

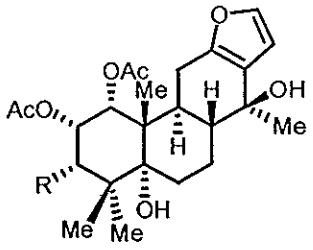

52h : R = H; ε-Caesalpin

53h : R = OAc; Caesalpin F

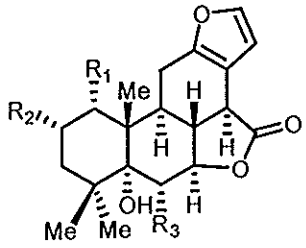

54h : $R_1 = R_2 = OH$, $R_3 = OAc$; Caesalmin A

55h : $R_1 = OAc$, $R_2 = R_3 = H$; Caesalmin B

56h : $R_1 = OH$, $R_2 = R_3 = H$; Caesalmin G

57h : $R_1 = R_3 = OAc$, $R_2 = H$; Caesalpinin D

58h : $R_1 = R_2 = OAc$, $R_3 = H$; Caesalpinin G

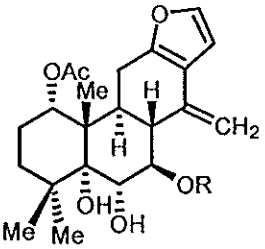

59h : R = H; γ-Caesalpin

60h : R = Ac; Caesalmin C

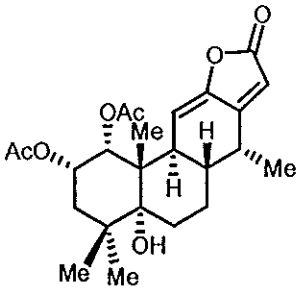

61h : Caesalpin D

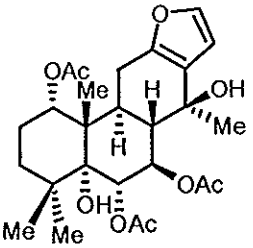

62h : Caesalpin H

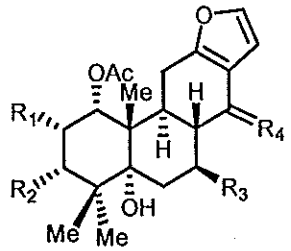

63h : $R_1 = R_3 = OH$, $R_2 = OAc$, $R_4 = CH_2$; Caesalpinin C

64h : $R_1 = R_2 = OAc$, $R_3 = H$, $R_4 = O$; Norcaesalpinin D

65h : $R_1 = R_2 = H$, $R_3 = OH$, $R_4 = O$; Norcaesalpinin E

66h : $R_1 = OAc$, $R_2 = R_3 = H$, $R_4 = O$; Norcaesalpinin A

67h : $R_1 = R_3 = H$, $R_2 = OAc$, $R_4 = O$; Norcaesalpinin B

68h : $R_1 = R_2 = OAc$, $R_3 = H$, $R_4 = CH_2$;
14(17)-Dehydrocaesalpin F

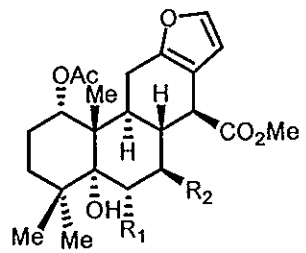

69h : $R_1 = OAc$, $R_2 = H$; Caesalpinin E

70h : $R_1 = H$, $R_2 = OAc$; 7-Acetoxybonducellpin C

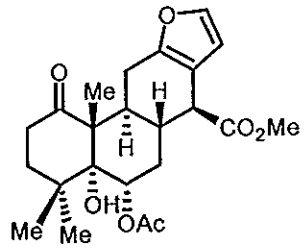

71h : Caesalpinin F

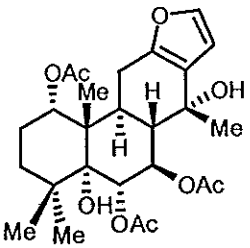

72h : Caesalmin D

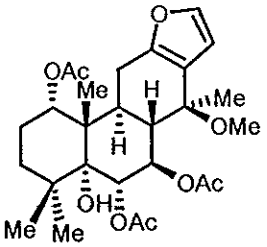

73h : Caesalmin F

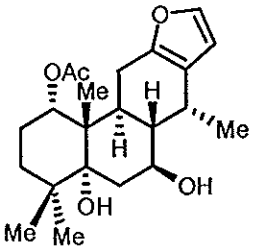

74h : Caesalmin H

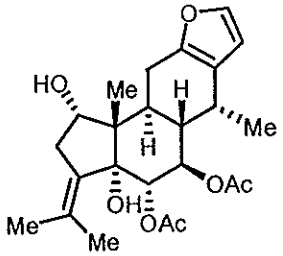

75h : Caesalpinin B

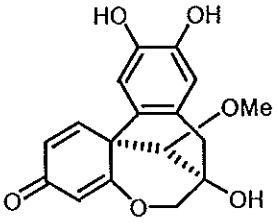

76h : Caesalpinin J

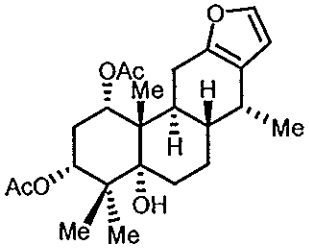

77h : Caesalpinin MA

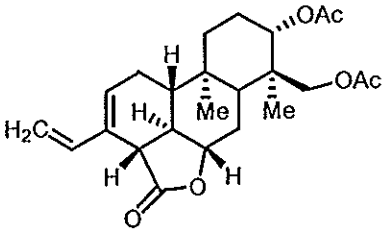

78h : Caesalpinin ME

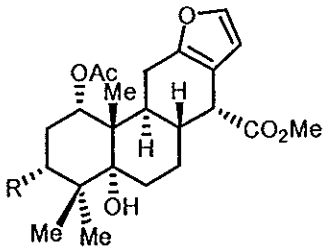

79h : R = H; Caesalpinin MB

80h : R = OAc; Caesalpinin MF

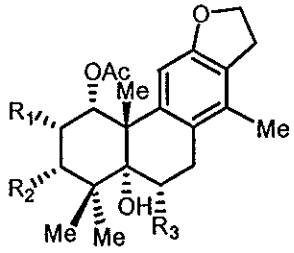

81h : R_1 = H, R_2 = OAc, R_3 = H; Caesalpinin MC

82h : R_1 = OAc, R_2 = H, R_3 = OAc; Caesalpinin MD

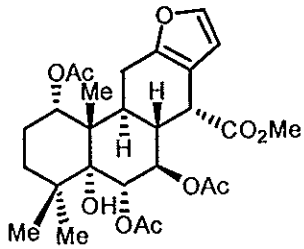

83h : Caesalpinin MG

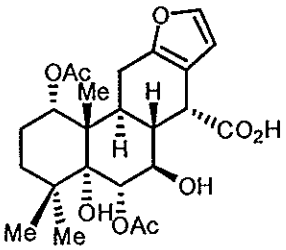

84h : Caesalpinin MH

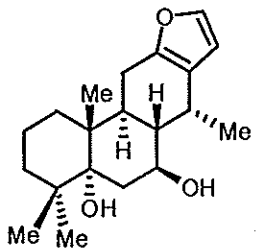

85h : Caesalpinin MI

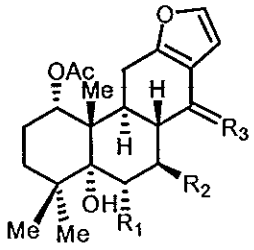

86h : R_1 = OH, R_2 = OAc, R_3 = CH_2; Caesalpin

87h : R_1 = H; R_2 = OAc, R_3 = CH_2; Caesalpinin MJ

88h : R_1 = OAc, R_2 = H, R_3 = CH_2; Caesalpinin MK

89h : R_1 = OAc, R_2 = OAc, R_3 = O; Norcaesalpinin MC

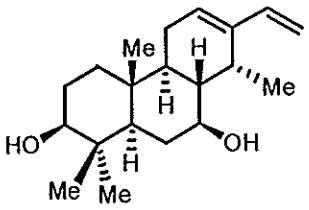

90h : Caesalpinin ML

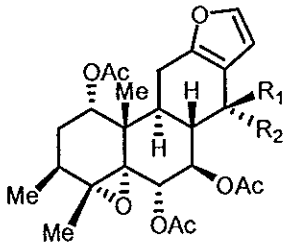

91h : R_1 = Me, R_2 = OH; Caesalpinin MM

92h : R_1 = OH, R_2 = Me; Caesalpinin MN

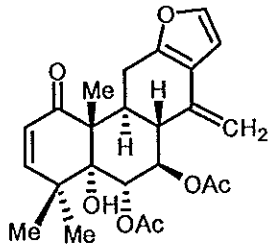

93h : Caesalpinin MO

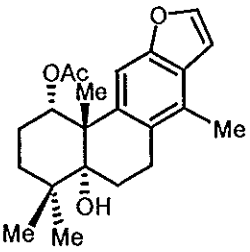

94h : Caesalpinin MP

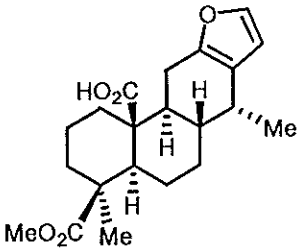

95h : Caesaljapin

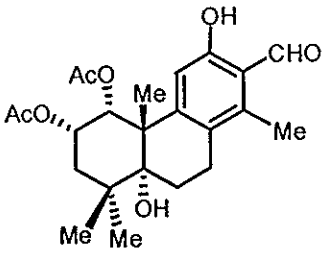

96h : R_1 = OAc; R_2 = H; Norcaesalpinin C

97h : R_1 = H, R_2 = OAc; Norcaesalpinin MA

98h : R_1 = OAc, R_2 = OAc; Norcaesalpinin MB

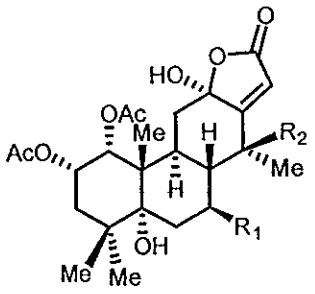

99h : R_1 = H, R_2 = OH; Neocaesalpin A

100h : R_1 = H, R_2 = H; Neocaesalpin B

101h : R_1 = OH, R_2 = H; Neocaesalpin C

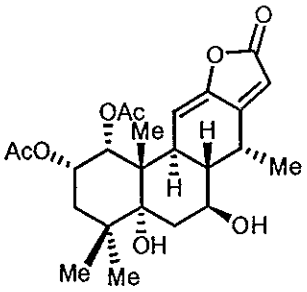

102h : Neocaesalpin D

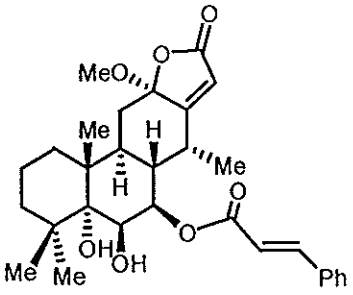

103h : Neocaesalpin G

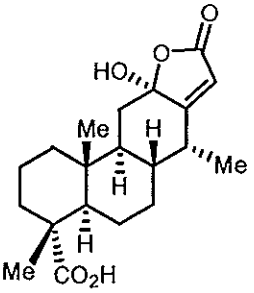

104h : Neocaesalpin H

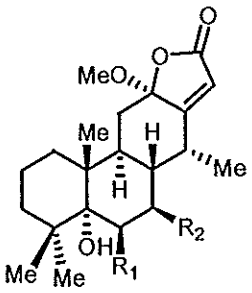

105h : R_1 = R_2 = H; Neocaesalpin E

106h : R_1 = OH, R_2 = OCOPh; Neocaesalpin F

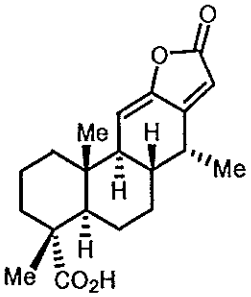

107h : Neocaesalpin I

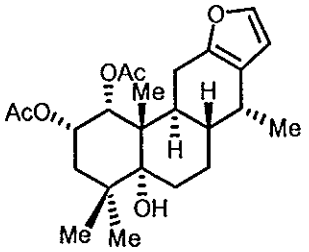

108h : 14-Deoxy-ε-caesalpin

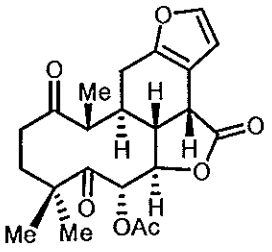

109h : Macrocaesalmin

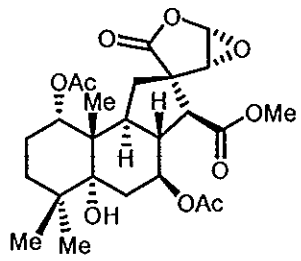

110h : Spirocaesalmin

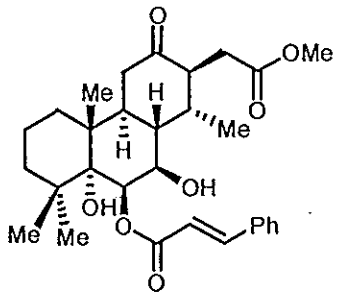

111h : Pulcherralpin

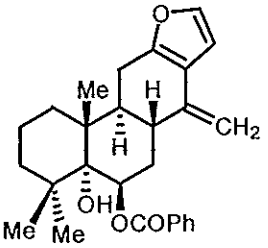

112h : Isovouacapenol A

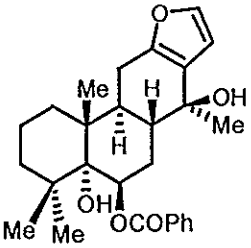

113h : Isovouacapenol B

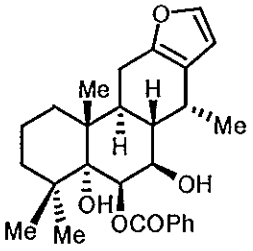

114h : Isovouacapenol C

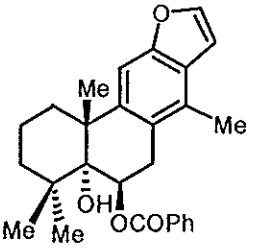

115h : Isovouacapenol D

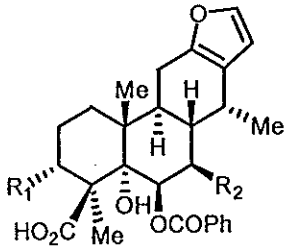

116h : R_1 = OH, R_2 = OCOPh; Pulcherrimin A

117h : R_1 = H, R_2 = OCOPh; Pulcherrimin C

118h : R_1 = OAc, R_2 = OCOPh; Pulcherrimin D

119h : R_1 = OCOPh, R_2 = OAc; Pulcherrimin E

120h : R_1 = OH, R_2 = OAc; Pulcherrimin F

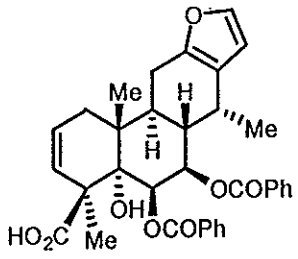

121h : Pulcherrimin B

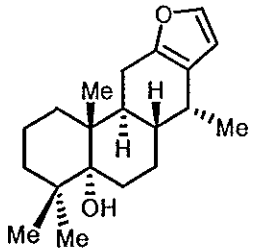

122h : Vouacapen-5α-ol

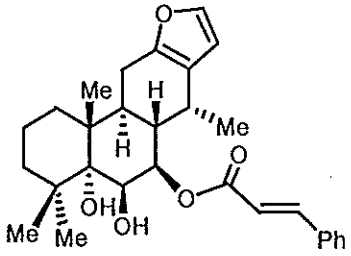

123h : 6β-Cinnamoyl-7β-hydroxyvouacapen-5α-ol

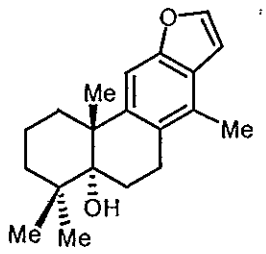

124h : 8,9,11,14-Didehydrovouacapen-5α-ol

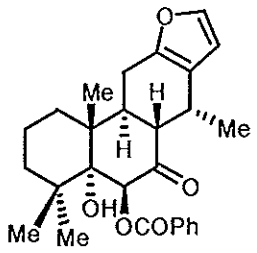

125h : 7-Ketoisovouacapenol C

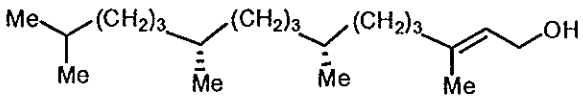

126h : Phytol

i : Flavonoids

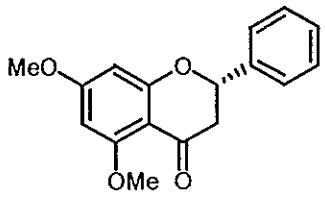

127i : 5,7-Dimethoxyflavanone

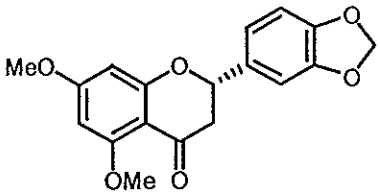

128i : 5,7-Dimethoxy-3′,4′-methyllenedioxyflavanone

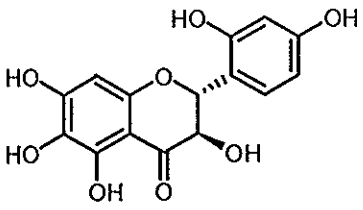

129i : 2′,3,4′,5,6,7-Hexahydroxyflavone

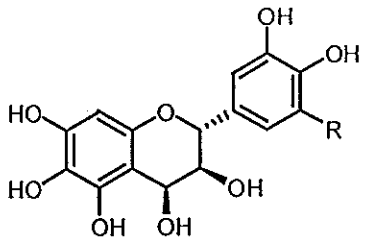

130i : R = H; Leucodelphinidin

131i : R = OH; Leucoefdin

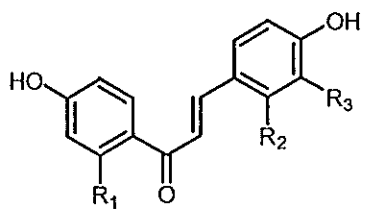

132i : $R_1 = R_3 = H$, $R_2 = OMe$;
4,4′-Dihydroxy-2′-methoxychalcone

133i : $R_1 = OMe$, $R_2 = H$, $R_3 = OH$; Sappanchalcone

134i : $R_1 = OH$, $R_2 = H$, $R_3 = OH$; Betein

135i : $R_1 = OMe$, $R_2 = R_3 = H$; Isoliquiritigenin

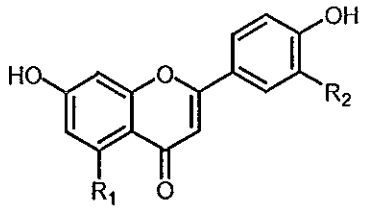

136i : $R_1 = R_2 = OH$; Luteolin

137i : $R_1 = OH$, $R_2 = H$; Apigenin

138i : $R_1 = H$, $R_2 = OH$; 3′,4′,7-Trihydroxyflavone

139i : $R_1 = R_2 = H$; 4′,7-Dihydroxyflavone

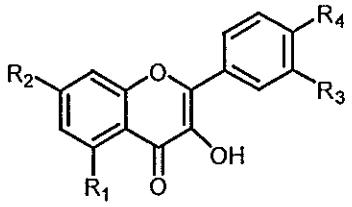

140i : $R_1 = R_2 = R_4 = OH$, $R_3 = H$; Kaempferol

141i : $R_1 = R_2 = R_3 = R_4 = OH$; Quercetin

142i : $R_1 = R_2 = R_4 = OH$, $R_3 = OMe$; Isorhamnetin

143i : $R_1 = R_3 = H$, $R_2 = R_4 = OH$; Resokaempferol

144i : $R_1 = R_3 = R_4 = OH$, $R_2 = OMe$; Rhamnetin

145i : $R_1 = R_3 = OH$, $R_2 = R_4 = OMe$; Ombuin

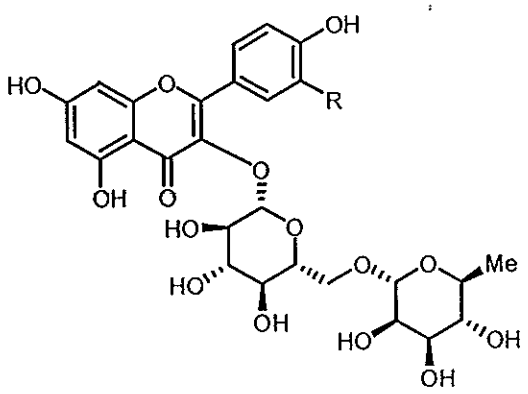

146i : R = H; Nicotiflorin

147i : R = OMe; Isorhamnetin-3-*O*-rutinoside

148i : R = OH; Rutin

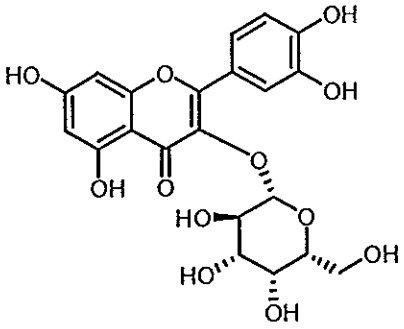

149i : Hyperoside

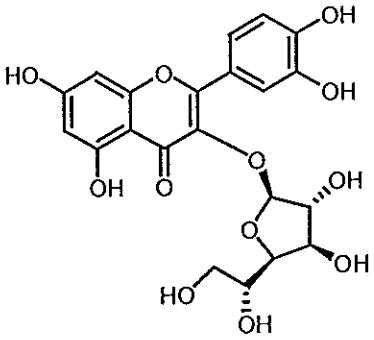

150i : Isoquercitrin

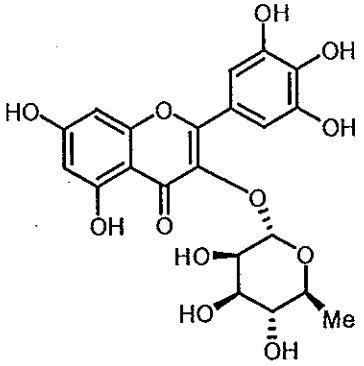

151i : Myricetin

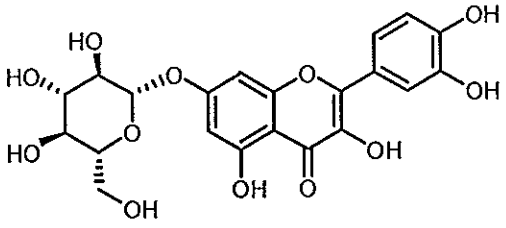

152i : Quercimeritrin

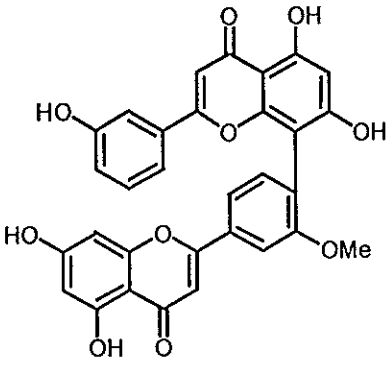

153i : Bilobetin

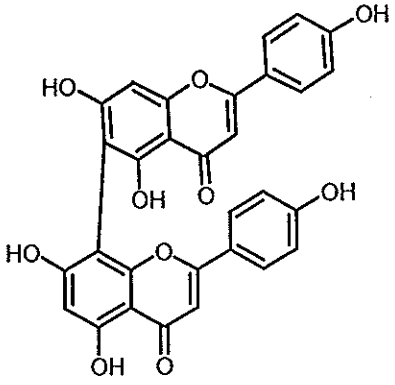

154i : Agathisflavone

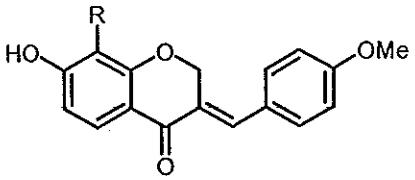

155i : R = H; Bonducellin

156i : R = OMe; 8-Methoxybonducellin

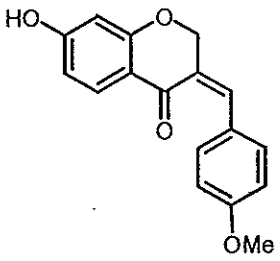

157i : Isobonducellin

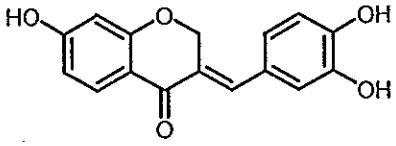

158i : Sappanone A

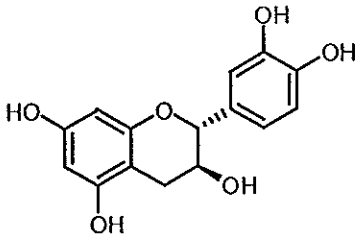

159i : (+)-Catechin

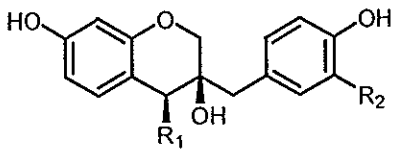

160i : $R_1 = R_2$ = OH; Sappanol

161i : R_1 = OMe, R_2 = H; 3′-Deoxy-4-*O*-methylsappanol

162i : R_1 = OH, R_2 = H; 3′-Deoxysappanol

163i : R_1 = OMe, R_2 = OH; 4-*O*-Methylsappanol

164i : R_1 = OH, R_2 = OMe; 3′-*O*-Methylsappanol

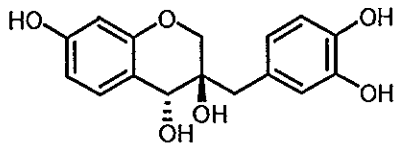

165i : Episappanol

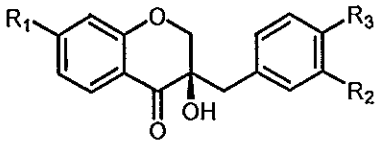

166i : $R_1 = R_3$ = OMe, R_2 = H; 3′-Deoxysappanone B

167i : $R_1 = R_2 = R_3$ =OH; Sappanone B

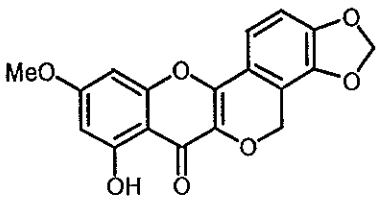

168i : Pulcherrimin

j : Iridoids

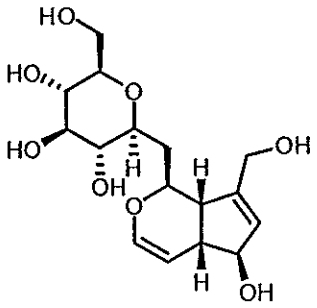

169j : Aucubin

k : Lipids

170k : n = 18; Arachidic acid

171k : n = 8; Capric acid

172k : n = 12; Myristic acid

173k : n = 16; Stearic acid

174k : n = 14; Palmitic acid

175k : n = 22; Lignoceric acid

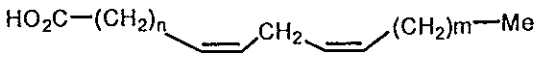

176k : n = 5, m = 4; Hexadeca-7,10-dienoic acid

177k : n = 7, m = 4; Linoleic acid

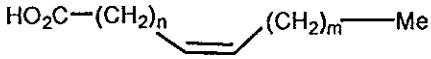

178k : n = 2, m = 12; Octadec-4-enoic acid

179k : n = 7, m = 7; Oleic acid

180k : n = 7, m = 5; Palmitoleic acid

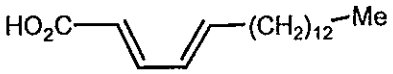

181k : Octadec-2,4-dienoic acid

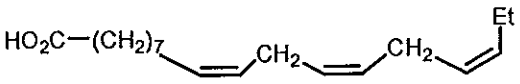

182k : Linolenic acid

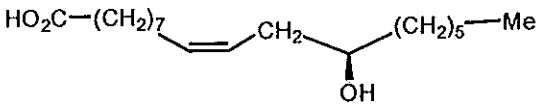

183k : Ricinoleic acid

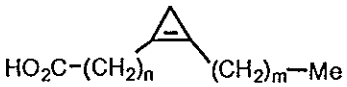

184k : n = 6, m = 7; Malvalic acid

185k : n = 7, m = 7; Sterculic acid

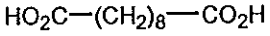

186k : Sebacic acid

l : Phenylpropanoids

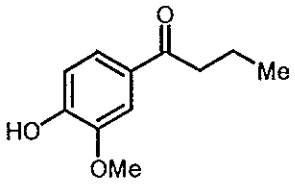

187l : 3-Hydroxy-1-(4-hydroxy-3-methoxyphenyl) propan-1-one

m : Quinoids

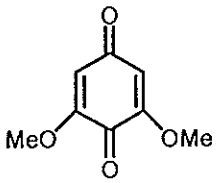

188m : 2,6-Dimethoxy-1,4-benzoquinone

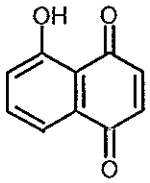

189m : Juglone

n : Sesquiterpene

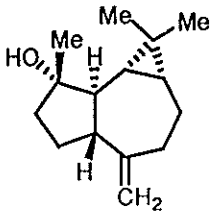

190n : Spathulenol

o : Steroids

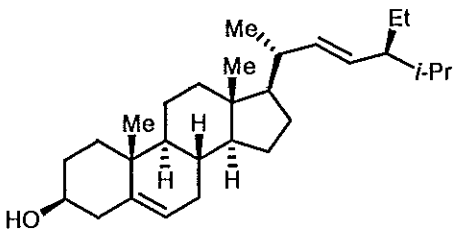

191o : β-Sitosterol

p: Triterpenes

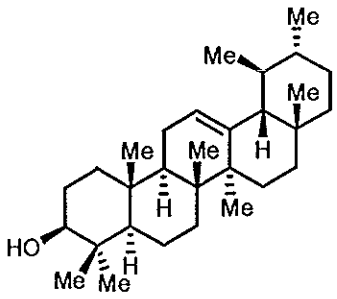

192p : α-Amyrin

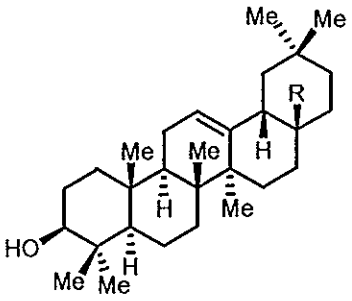

193p : R = Me; β-Amyrin

194p : R = CO_2H; Oleanolic acid

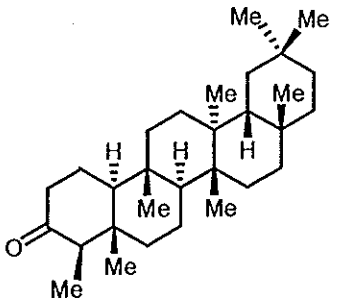

195p : Friedelin

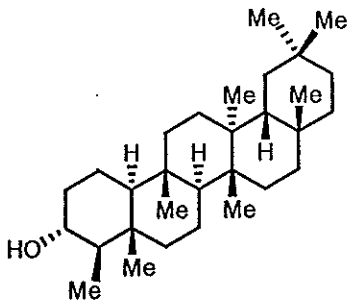

196p: Epifriedelinol

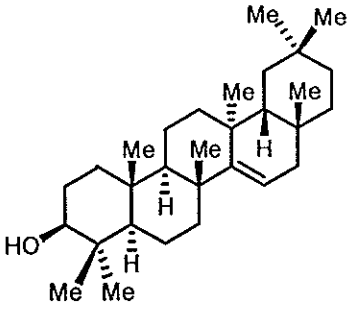

197p : Taraxerol

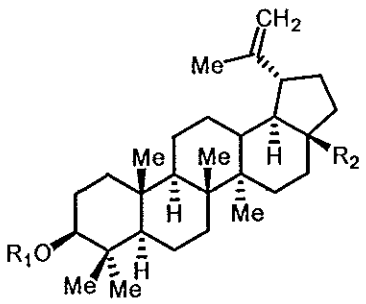

198p : R_1 = H, R_2 = Me; Lupeol

199p : R_1 = Ac, R_2 = Me; Lupeol acetate

200p : R_1 = H, R_2 = CO_2H; Betulinic acid

q : Vitamin

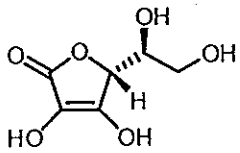

201p : Ascorbic acid

1.1.3 Chemical constituents from *Suregada multiflora*

1.1.3.1 Introduction

Suregada multiflora Baill. is a plant distributed in India, Burma, Indo-china and Malay Peninsula belonging to the Euphorbiaceae family. locally known in Thai as Khop nang nang (ขอบนางนั่ง); khanthotsakon (ขัณฑสกร), chong ram phan (ช้องรำพัน), salot nam (สลอดน้ำ) (Chantaburi); khan thong phaya bat (ขันทองพยาบาท); duk sai (ดูกไทร), muat rot (เหมือดโรด); duk hin (ดูกหิน), thong phan chang (ทองพันชั่ง); takhop nok (ตะขบนก); thurian pa (ทุเรียนป่า), fai (ไฟ), ma duk lueam (มะดูกเลื่อม); yai pluak (ยายปลวก).

S. multiflora is a shrub or small tree, 3-15 m high, glabrous. *Stipules* minute, caducous. *Leaves*: blade elliptic, 12-15 by 5-7 cm, length/width ratio 2.1-2.4, base cuneate, margin entire, apex acute, dark green, secondary veins 5-7 pairs. *Inflorescences* fascicles or short cymes on 0.3-1 cm long peduncle. *Flowers* are unisexual, 0.8-1.2 cm in diameter; pedicel 4-6 mm long, covered with short hair; sepals 5, round, flower fragrant; sepals 3-4 by 2.5-3.5 mm, the receptacle with numerous small disc glands among the filaments; pistillode minute. *Pistillate flowers*: sepals are longer than the staminate ones, disc with papery margin, concave, sometime with tiny staminodes; ovary 3-locular, stigmas shortly bifid, spreading. *Fruits* subglobular or shallowly 3-lobed, 2.5-

3.5 by 2–2.5 cm, mostly smooth, tardily dehiscent, red-orange when ripe. *Seeds* are subglobose, sarcotesta fleshy and white when fresh.

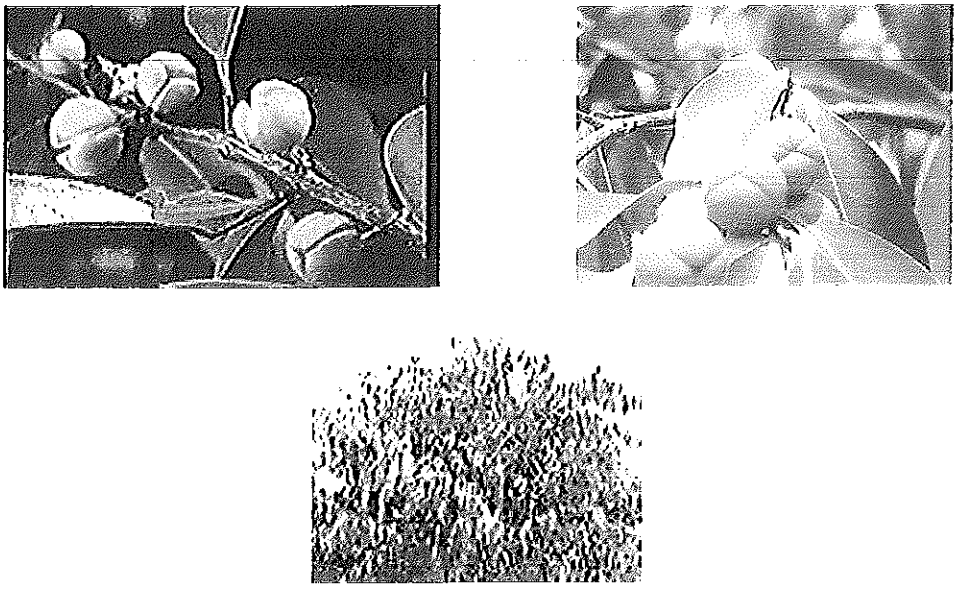

Figure 3 ***Suregada multiflora***

1.1.3.2 Review of literatures

Plants in the *Suregada* genus (Euphorbiaceae) are well known to be rich in diterpenes. Information from NAPRALERT database developed by University of Illinois at Chicago revealed several types of compounds present in plants of *Suregada* genus and they can be classified into groups as follows: diterpenes, flavonoids, lipids and steroids. These compounds are presented in **Table 3.**

Table 3 Compounds from plants of *Suregada* genus

a : diterpenes b : flavonoids c : lipids

d : steroids

Plant	Part	Compound	Bibliography
S. multiflora	Seeds	Caprylic acid, **39c** Gelomuloside A, **36b** Gelomuloside B, **37b** Myristic acid, **40c** Oleic acid, **42c** Palmitic acid, **41c**	Ghosh, 1979 Das and Chakravarty, 1993 Ghosh, 1979
	Leaves	3β-Acetoxy-1-one-8β,14β-epoxy-13,15-abiatene-6,12-olide, **5a** 6β-Acetoxy-2-ene-8β,14α-dihydroxy-1-one-13,15-abiatene-16,12-olide, **27a** 6β-Acetoxy-2-ene-1-one-8β, 14β-epoxy-13,15-abiatene-16,12-olide, **29a** 3β-Acetoxy-8β,14α-dihydroxy-13,15-abiatene-16,12-olide, **25a** 3β-Acetoxy-8β,14α-dihydroxy-1-one-13,15-abiatene-16,12-olide, **26a** 3β,6β-Diacetoxy-1-one-8β,14β-epoxy-13,15-abiatene-16,12-olide, **3a**	Choudhary et al., 2004

Table 3 (Continued)

Plant	Part	Compound	Bibliography
S. multiflora	Leaves	2-Ene-1-one-8β,14β-epoxy-13,15-abiatene-16,12-olide, 28a	Choudhary et al., 2004
		3β-Hydroxy-1-one-8β,14β-epoxy-13,15-abiatene-6,12-olide, 4a	
		Dihydrogelomulide A, 6a	
		Gelomulide A, 1a	Talapatra et al., 1989
		Gelomulide B, 7a	
		Gelomulide C, 9a	
		Gelomulide D, 11a	
		Gelomulide E, 12a	
		Gelomulide F, 10a	
		Gelomulide G, 2a	
		Gelomulide H, 13a	
		Gelomulide I, 14a	
		Gelomulide J, 8a	
		Jolkinolide B, 15a	
		Luteolin-4′-7-dimethyl ether 3′-*O*-β-*D*-glucoside, 38b	Parveen and Khan, 1987
		β-Sitosterol, 43c	Talapatra et al., 1989
	Roots	Angeflorin, 35b	Das et al., 1994
		Demethoxykanugin, 33b	

Table 3 (Continued)

Plant	Part	Compound	Bibliography
S. multiflora	Roots	Kanugin, 32b	Das et al., 1994
		Ladanine, 30b	
		Pinnatin, 34b	
		Salvigenin, 31b	
	Bark	Bannaringaolide A, 21a	Jahan et al., 2003
		Euphorangin B, 24a	
		Suregedolide A, 16a	Jahan et al., 2002
		Suregadolide B, 18a	
		Suregedolide C, 17a	
		Suregedolide D, 19a	
		Suremulol A, 22a	Jahan et al., 2003
		Suremulol B, 23a	
		Suremulide A, 20a	

Structures

a : Diterpenes

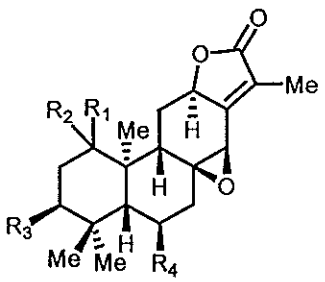

1a : $R_1 = R_2 = R_4 = H$, $R_3 = OAc$; Gelomulide A

2a : $R_1 = R_2 = H$, $R_3 = R_4 = OAc$; Gelomulide G

3a : $R_1 = R_2 = O$, $R_3 = R_4 = OAc$; 3β,6β-Diacetoxy-1-one-8β,14β-epoxy-13,15-abiatene-16,12-olide

4a : $R_1 = R_2 = O$, $R_3 = OH$, $R_4 = H$; 3β-Hydroxy-1-one-8β,14β-epoxy-13,15-abiatene-16,12-olide

5a : $R_1 = R_2 = O$, $R_3 = OAc$, $R_4 = H$; 3β-Acetoxy-1-one-8β,14β-epoxy-13,15-abiatene-16,12-olide

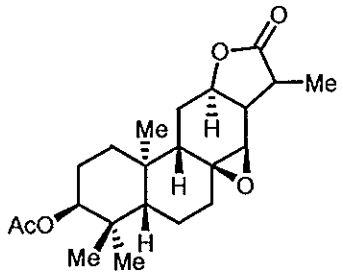

6a : Dihydrogelomulide A

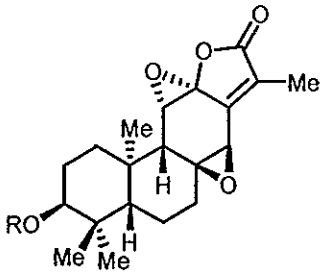

7a : R = H; Gelomulide B

8a : R = Ac; Gelomulide J

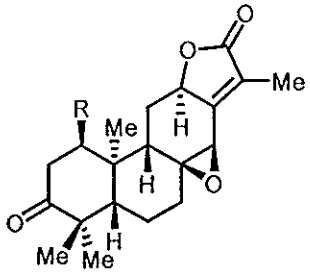

9a : R = H; Gelomulide C

10a : R = OAc; Gelomulide F

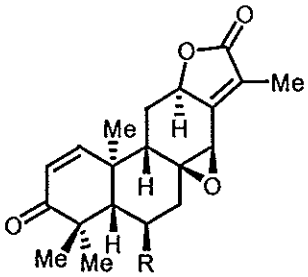

11a : R = H; Gelomulide D

12a : R = OAc; Gelomulide E

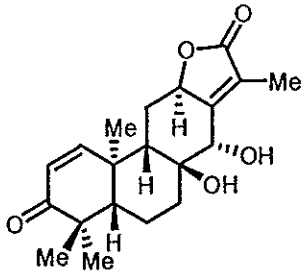

13a : Gelomulide H

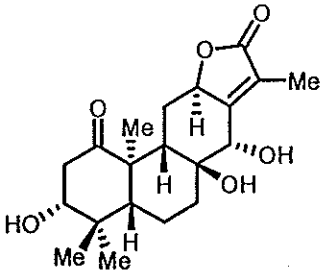

14a : Gelomulide I

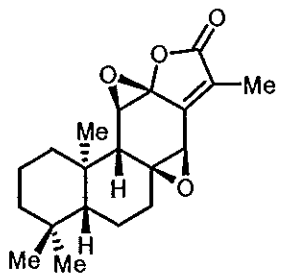

15a : Jolkinolide B

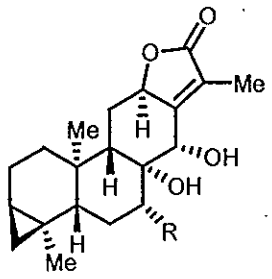

16a : R = H; Suregadolide A

17a : R = OH; Suregadolide C

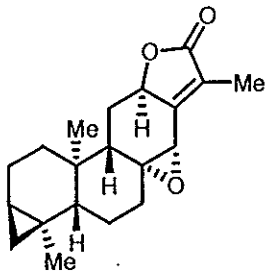

18a : Suregadolide B

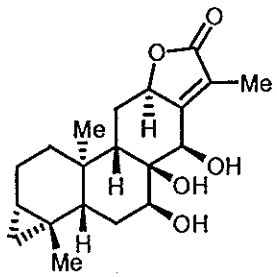

19a : Suregadolide D

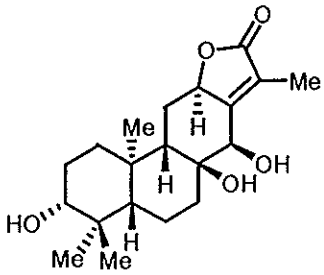

20a : Suremulide A

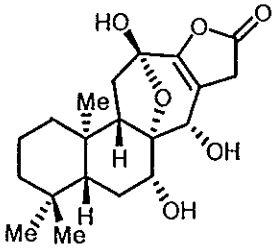

21a : Bannaringaolide A

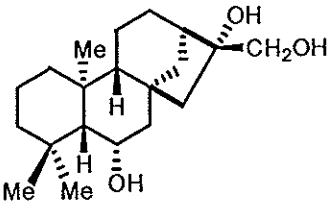

22a : Suremulol A

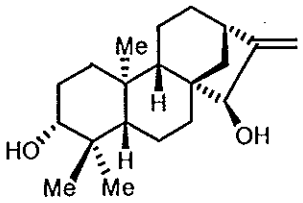

23a : Suremulol B

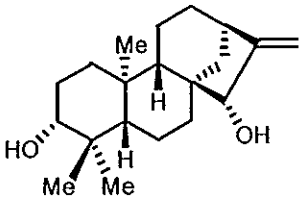

24a : Euphorangin B

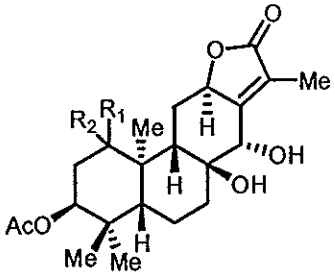

25a : R_1 = R_2 = H; 3β-Acetoxy-8β,14α-dihydroxy-13,15-abiatene-16,12-olide

26a : R_1 = R_2 = O; 3β-Acetoxy-8β,14α-dihydroxy-1-one-13,15-abiatene-16,12-olide

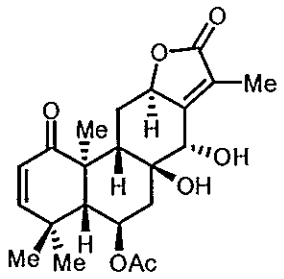

27a : 6β-Acetoxy-2-ene-8β,14α-dihydroxy-1-one-13,15-abiatene-16,12-olide

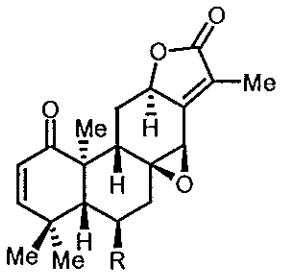

28a : R = H; 2-Ene-1-one-8β,14β-epoxy-13,15-abiatene-16,12-olide

29a : R = OAc; 6β-Acetoxy-2-ene-1one-8β,14β-epoxy-13,15-abiatene-16,12-olide

b : Flavonoids

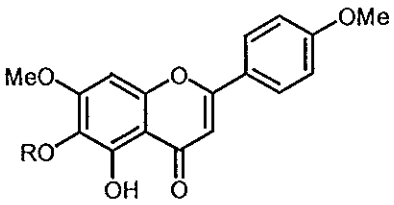

30b : R = H; Ladanine

31b : R = Me; Salvigenin

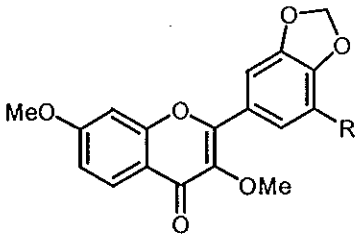

32b : R = OMe; Kanugin

33b : R = H; Demethoxykanugin

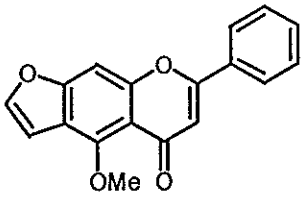

34b : Pinnatin

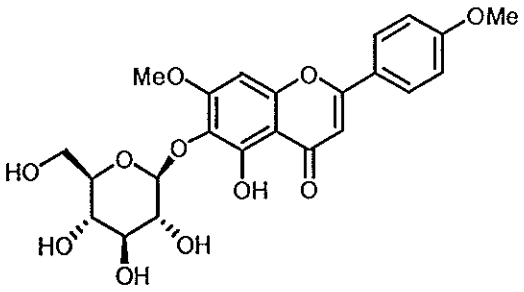

35b : Angeflorin

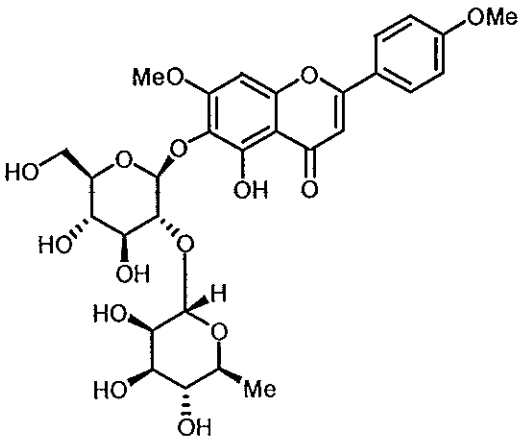

36b : Gelomuloside A

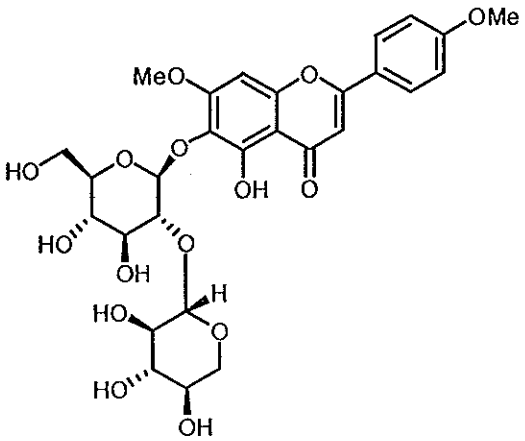

37b : Gelomuloside B

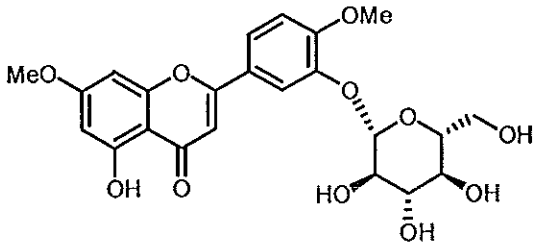

38b : Luteolin-4′-7-dimethyl ether 3′-*O*-β-D-glucoside

c : Lipids

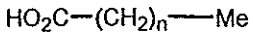

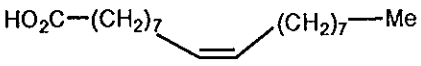

39c : n = 6; Caprylic acid

40c : n = 12; Myristic acid

41c : n = 14; Palmitic acid

42c : Oleic acid

d : Steroid

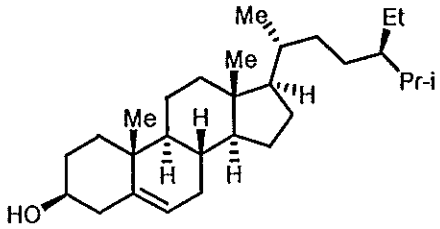

43c : β-Sitosterol

1.1.4 Objective

Up to the present, the chemical constituents and biological activities of these plants are interested. This research part involved isolation, purification and structure elucidation of chemical constituents isolated from the rhizomes of *B. pandurata*; the seeds, roots and stems of *C. crista*; and the bark of *S. multiflora* and also evaluation of pure compounds for anti-HIV PR-1 for *B. pandurata*, anti-malarial activity for *C. crista* and anti-allergic activity for *S. multiflora*.

CHAPTER 1.2

EXPERIMENTAL

1.2.1 Instruments and Chemicals

Melting point was recorded in $^{\circ}C$ and was measured on an Electrothermal Melting Point Apparatus. Infrared spectra were recorded using FTS FT-IR spectrophotometer and major bands (ν) were recorded in wave number (cm^{-1}). Ultraviolet (UV) absorption spectra were recorded using a SPECORD S 100 (Analytikjena) and UV-160A spectrophotometer (SHIMADZU) and principle bands (λ_{max}) were recorded as wavelengths (nm) and log ε in chloroform and methanol solution. Nuclear magnetic resonance spectra were recorded on 500 MHz Varian UNITY INOVA spectrometer and FTNMR Bruker Ultra Shield™ 300 MHz. Spectra were recorded in chloroform-d and methanol-d_4 solution and were recorded as δ value in ppm downfield from TMS (internal standard δ 0.00). Single-crystal X-ray diffraction measurements were collected using SMART 1-K CCD diffractometer with monochromated Mo-Kα radiation (λ = 0.71073 A°) using ω-scan mode and SHELXTL for structure solution and refinement. Optical rotation was measured in chloroform solution with sodium D line (590 nm) on a JASCO P-1020 polarimeter. Solvent for extraction and chromatography were distilled at their boiling point ranges prior to use except diethyl ether was analytical grade reagent. Quick column chromatography (QCC) was performed on silica gel 60 GF_{254} (Merck). Column chromatography was performed on silica gel (Merck) type 100 (0.063 * 0.200). Precoated plates of silica gel 60 GF_{254} or reversed-phase C_{18} were used for analytical purposes.

1.2.2 Plant materials

The fresh rhizomes of *B. pandurata* Holtt. were bought from Hat Yai Market, Hat Yai, Thailand in 2003. The voucher specimen (number : SN 4412015) was identified by Assoc. Prof. Dr. Sanan Subhadhirasakul, and kept in the Herbarium of the Faculty of Pharmaceutical Sciences, Prince of Songkla University, Thailand.

Roots, stems and seeds of *Caesalpinia crista* L. were collected from Trang province, Thailand in May 2004. Identification was made by Prof. Puangpen Sirirugsa, Department of Biology, Faculty of Science, Prince of Songkla University and a specimen (No. SC03) deposited at Prince of Songkla University Herbarium.

Bark of *S. multiflora* were collected from Songkhla province, Thailand in November 2004. Identification was made by Prof. Puangpen Sirirugsa, Department of Biology, Faculty of Science, Prince of Songkla University and a specimen (No. SC04) deposited at Prince of Songkla University Herbarium.

1.2.3 Extractions and Isolations

1.2.3.1 Isolation and Chemical Investigation of B. pandurata

Chopped-dried rhizomes (10.00 kg) of *B. pandurata* were extracted with $CHCl_3$ and MeOH (30 l x 3, 7 days each) successively at room temperature and the solvent was evaporated under reduced pressure to afford the $CHCl_3$ (608.40 g) and MeOH (211.70 g) extracts, respectively. A part of the MeOH extract (140 g) was further subjected to QCC on silica gel (200 g) eluting with hexane-CH_2Cl_2-MeOH (9:1:0, 1:1:0, 0:100:0, 0:19:1, 0:17:1, 0:1:1, 0:0:100, each 1500 ml) to yield seven fractions (F1-F7, Scheme 1).

Fraction F2 (hexane-CH_2Cl_2, 1:1, 18.7 g) was chromatographed by QCC on silica gel (180 g) eluting with hexane-CH_2Cl_2 (1:1, 2000 ml) to give three subfractions (F2a-F2c). Subfraction F2c (10.03 g) was recrystallized from CH_2Cl_2 to give **BP2** (715.2 mg, R_f = 0.32 (4:1, CH_2Cl_2-hexane)) and **BP10** (2.30 g, R_f = 0.21 (4:1, CH_2Cl_2-hexane)).

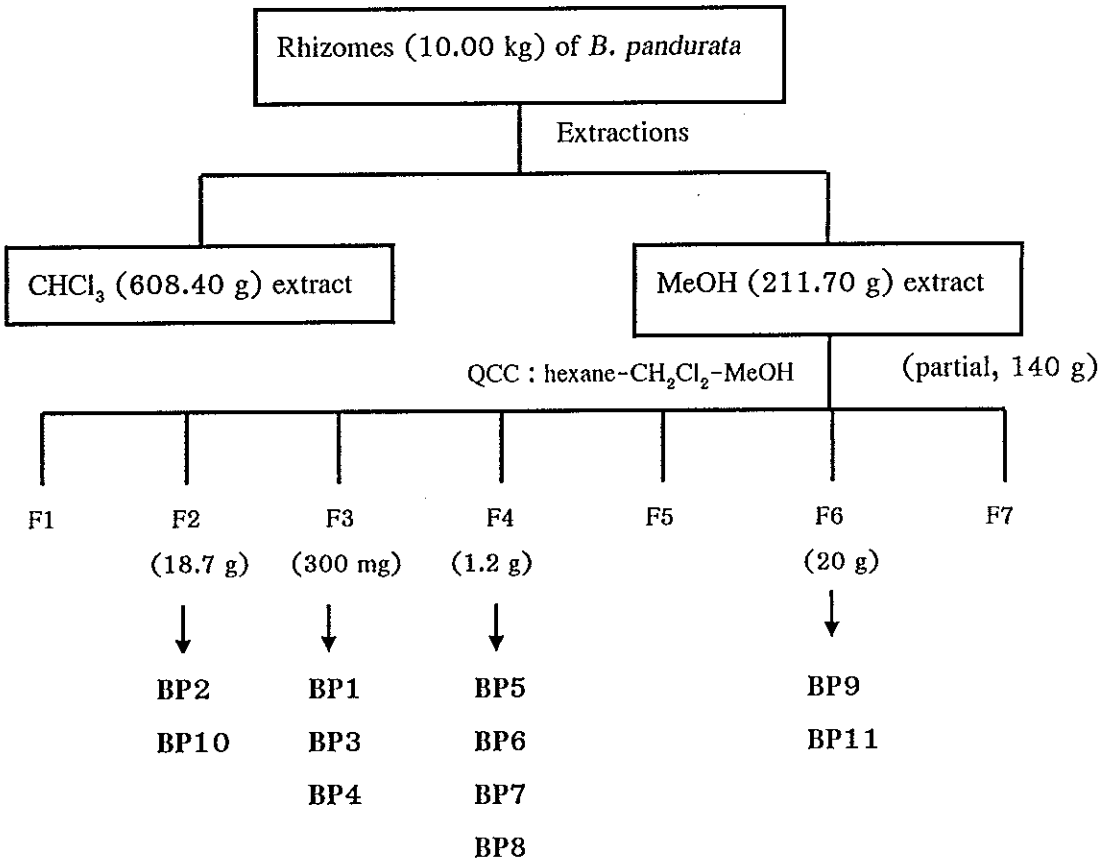

Scheme 1 Extraction and isolation of compounds **BP1-BP11** from the rhizomes of *B. pandurata*

Fraction F3 (CH_2Cl_2-MeOH, 19:1, 300 mg) was separated by CC on silica gel (18 g) with CH_2Cl_2-MeOH (19:1, 1000 ml) to afford four subfractions (F3a-F3d). Subfraction F3b (10.3 mg) was purified by preparative TLC with hexane-EtOAc (3:2) to obtain **BP4** (8.3 mg, R_f = 0.40 (19:1, CH_2Cl_2-MeOH)). Subfraction F3c (130.0 mg) was separated by CC on silica gel (8 g) with hexane-EtOAc (13:7, 400 ml) to give **BP1** (6.2 mg, R_f = 0.36 (3:97, CH_2Cl_2- MeOH)) and **BP3** (36.6 mg, R_f = 0.18 (7:3, hexane-EtOAc)).

Fraction F4 (CH_2Cl_2-MeOH, 17:1, 1.2 g) was purified by CC on silica gel (60 g) and eluted with hexane-EtOAc (13:7, 1500 ml) to give four subfractions (F4a-F4d). Subfraction F4c (49.3 mg) was purified by reversed-phase preparative TLC with MeOH-H_2O (3:1) to afford **BP5** (25.2 mg, R_f = 0.21 (19:1, CH_2Cl_2-MeOH)) and **BP8** (20.2 mg, R_f = 0.42 (9:1, hexane-EtOAc)). Subfraction F4d (898.0 mg) was

subjected to CC on silica gel (60 g) with hexane-EtOAc (13:7, 1000 ml) to give **BP6** (21.0 mg, R_f = 0.11 (97:3, CH_2Cl_2- MeOH)) and **BP7** (15.9 mg, R_f = 0.13 (17:3, hexane-EtOAc)).

Fraction F6 (CH_2Cl_2-MeOH, 9:1, 20 g) was separated by CC on silica gel (800 g) with CH_2Cl_2-MeOH (9:1, 3000 ml) to afford **BP9** (41.2 mg, R_f = 0.38 (9:1, CH_2Cl_2-MeOH)) and **BP11** (100 mg, R_f = 0.49 (9:1, CH_2Cl_2-MeOH)).

Compound BP1 : Yellow viscous oil; $[\alpha]_D^{27}$: -24.0° (*c* 0.13, MeOH); UV λ_{max} (MeOH) (log ε): 292 (3.71), 220 (3.95) nm; IR (neat): 3438, 1624 cm^{-1}; EI-MS: *m/z* = 422 [M^+] (2), 421 [M^+-1) (5), 406 (6), 286 (11), 166 (100), 106 (9); HRMS: *m/z* = 422.2044 (calcd. for $C_{26}H_{30}O_5$: 422.2088); ^{1}H-NMR ($CDCl_3$, 300 MHz), see Table 4; ^{13}C-NMR ($CDCl_3$, 75 MHz), see Table 4.

Compound BP2 : Yellow solid, mp : 155-156 °C; $[\alpha]_D^{27}$: -23.0° (*c* 0.38, MeOH); UV λ_{max} (MeOH)(log ε): 224 (4.24), 290 (4.33) nm; IR (KBr): 3435 (OH), 1628 (C=O), 1586 (C=C) cm^{-1}; ^{1}H-NMR ($CDCl_3$, 300 MHz), see Table 5; ^{13}C-NMR ($CDCl_3$, 75 MHz), see Table 5.

Compound BP3 : Yellow solid, mp : 214-215 °C; $[\alpha]_D^{27}$: -24.4° (*c* 0.38, MeOH); UV λ_{max} (MeOH)(log ε): 224 (3.93), 292 (4.02) nm; IR (KBr): 3438, (OH), 1628 (C=O) cm^{-1}; ^{1}H-NMR ($CDCl_3$+MeOD, 300 MHz), see Table 7; ^{13}C-NMR ($CDCl_3$+MeOD, 75 MHz), see Table 7.

Compound BP4 : Yellow solid, mp 240-241 °C; UV λ_{max} (MeOH)(log ε): 220 (4.10), 227 (3.94), 277 (4.02), 370 (3.41) nm; IR (KBr): 3439, (OH), 1627 (C=O) cm^{-1}; ^{1}H-NMR ($CDCl_3$+MeOD, 300 MHz), see Table 10; ^{13}C-NMR ($CDCl_3$+MeOD, 75 MHz), see Table 10.

Compound BP5 : Yellow solid, mp 134-135 °C; UV λ_{max} (MeOH)(log ε): 222 (4.16), 286 (4.18), 327 (3.51) nm; IR (KBr): 3297 (OH), 1627 (C=O), 1595 (C=C) cm^{-1}; ^{1}H-NMR ($CDCl_3$+MeOD, 300 MHz), see Table 11; ^{13}C-NMR ($CDCl_3$+MeOD, 75 MHz), see Table 11.

Compound BP6 : Yellow solid, mp 188-189 °C; UV λ_{max} (MeOH)(log ε): 221 (4.05), 287 (4.05) nm; IR (KBr): 3439, (OH), 1623 (C=O) cm^{-1}; ^{1}H-NMR ($CDCl_3$+MeOD, 300 MHz), see Table 12; ^{13}C-NMR ($CDCl_3$+MeOD, 75 MHz), see Table 12.

Compound BP7 : Yellow viscous oil; UV λ_{max} (MeOH)(log ε): 224 (3.92), 279 (3.23) nm; IR (neat): 3372 (OH), 1602 (ArH) cm^{-1}; ^{1}H-NMR ($CDCl_3$+MeOD, 300 MHz), see Table 15; ^{13}C-NMR ($CDCl_3$+MeOD, 75 MHz), see Table 15.

Compound BP8 : Colorless oil; UV λ_{max} ($CHCl_3$)(log ε): 214 (3.85), 220 (3.77), 270 (4.00) nm; IR (neat): 1709 (C=O), 1634 (C=C) cm^{-1}; ^{1}H-NMR ($CDCl_3$, 300 MHz), see Table 16; ^{13}C-NMR ($CDCl_3$, 75 MHz), see Table 16.

Compound BP9 : White solid; mp.: 218-219 °C, $[\alpha]_D^{26}$: -51.2° (c 0.23, MeOH). UV λ_{max} (MeOH)(log ε): 207 (4.00), 284 (4.12), 320 (3.74) nm; IR (KBr): 3392 (OH), 1693 (C=O), 1612 (C=C) cm^{-1}; ^{1}H-NMR ($CDCl_3$+DMSO-d_6, 300 MHz), see Table 17; ^{13}C-NMR ($CDCl_3$+DMSO-d_6, 75 MHz), see Table 17.

Compound BP10 : White solid; mp.: 220-221 °C, $[\alpha]_D^{26}$: -49.9° (c 0.54, MeOH); UV λ_{max} (MeOH)(log ε): 204 (3.73), 280 (3.99), 322 (3.71) nm; IR (KBr): 3393 (OH), 1682 (C=O), 1610 (C=C) cm^{-1}; ^{1}H-NMR ($CDCl_3$+DMSO-d_6, 300 MHz), see Table 18; ^{13}C-NMR ($CDCl_3$+DMSO-d_6, 75 MHz), see Table 18.

Compound BP11 : White solid; mp.: 217-218 °C, $[\alpha]_D^{26}$: -57.5° (c 0.38, MeOH); UV λ_{max} (MeOH)(log ε): 202 (3.83), 289 (4.01), 318 (3.93) nm; IR (KBr): 3401 (OH), 1697 (C=O), 1621 (C=C) cm^{-1}; ^{1}H-NMR ($CDCl_3$+DMSO-d_6, 300 MHz), see Table 19; ^{13}C-NMR ($CDCl_3$+DMSO-d_6, 75 MHz), see Table 19.

1.2.3.2 Isolation and Chemical Investigation of C. crista

Ground-dried stems (7.5 kg) of *C. crista* were extracted with hexane and CH_2Cl_2 (each 2 x 7.5 l, for 5 days) successively at room temp. The crude extracts were evaporated under reduced pressure to afford a brownish crude hexane (29.4 g) and crude CH_2Cl_2 (70.2 g) extracts (scheme 2).

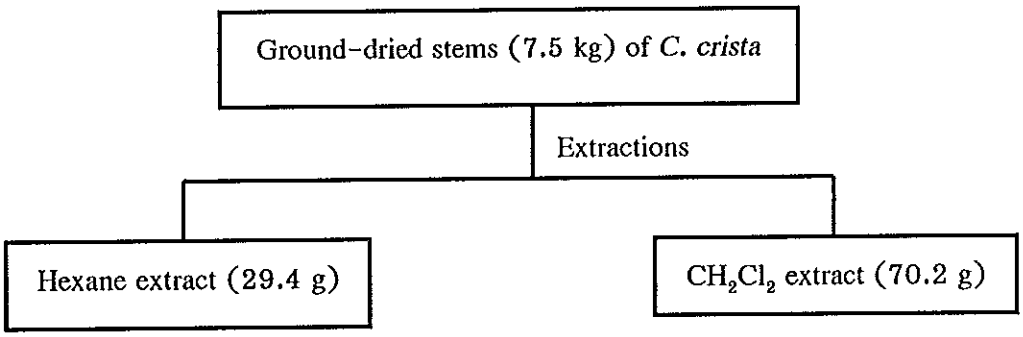

Scheme 2 Extraction of the stems of *C. crista*

The crude hexane extract was further purified by QCC using hexane as eluent and increasing polarity with EtOAc to give six fractions (H1-H6, scheme 3).

Fraction H2 (4.2 g) was recrystallized from CH_2Cl_2 to give SC1 (692.8 mg, R_f = 0.16 (3:17, EtOAc-hexane)) and mother liquor (3.5 g). This mother liquor was further subjected to CC with $CHCl_3$-hexane (1:9, v/v) to afford four subfractions (H2a-H2d). Subfraction H2a (1.1 g) was separated by CC with acetone-hexane (1:1, v/v) and followed by prep. TLC with CH_2Cl_2-hexane (9:11, v/v) to give SC4 (3.3 mg R_f = 0.25 (7:93, EtOAc-hexane)) and SC9 (9.5 mg, R_f = 0.19 (7:93, EtOAc-hexane)). Subfraction H2b (100 mg) was purified by prep TLC with $CHCl_3$-hexane (1:9, v/v) to afford SC8 (10.1 mg, R_f = 0.10 (1:9, $CHCl_3$-hexane)). Subfraction H2c (148.0 mg) was purified by CC with acetone-hexane (1:19, v/v) and followed by prep TLC with EtOAc-hexane (1:19, v/v) to give SC10 (31.8 mg, R_f = 0.29 (1:19, acetone-hexane)).

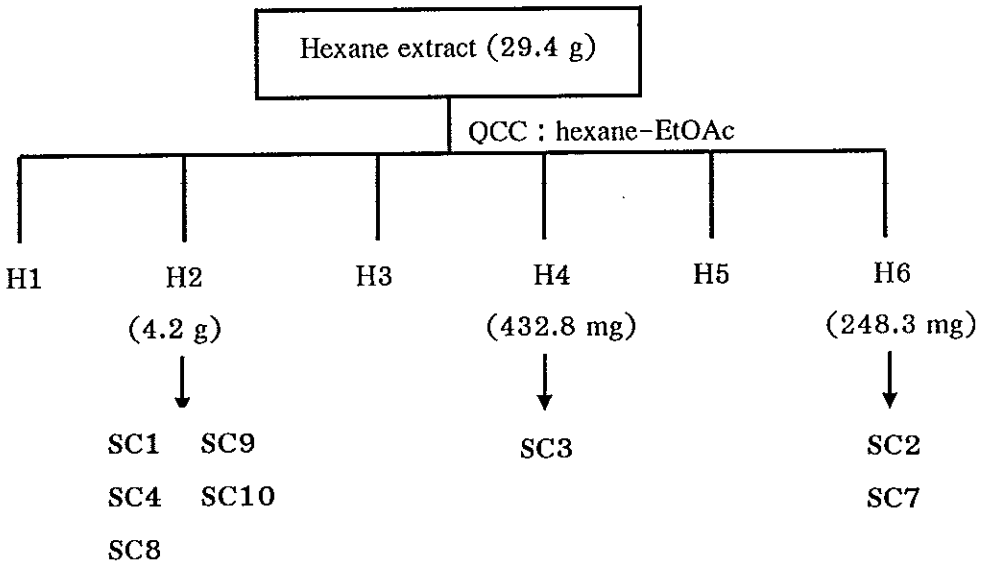

Scheme 3 Isolation of compounds SC1-SC4, SC7-SC10 of *C. crista*

Fraction H4 (432.8 mg) was separated by Sephadex LH-20 with CH_2Cl_2 to afford SC3 (72.5 mg, R_f = 0.21 (3:17, EtOAc-hexane)).

Fraction H6 (248.3 mg) was subjected to CC with acetone-$CHCl_3$ (3:97, v/v) and followed by prep TLC with acetone-hexane (1:5, v/v) to give SC2 (5.9 mg, R_f = 0.15 (1:3, EtOAc-hexane)) and SC7 (4.1 mg, R_f = 0.10 (1:3, EtOAc-hexane)).

Compound SC1 : White solid, mp 156-157°C; $[\alpha]_D^{27}$: +56.6° (c 0.05, $CHCl_3$); UV ($CHCl_3$) λ_{max} (log ε): 212 (3.56), 260 (3.00), 282 (2.62), 292 (2.61) nm; IR (KBr) ν_{max} : 1723, 771 cm^{-1}; HREIMS *m/z* $[M]^+$ 326.1887 (calcd for $C_{21}H_{26}O_3$, 326.1882); ^1H NMR ($CDCl_3$, 300 MHz), see Table 20; ^{13}C NMR ($CDCl_3$, 75 MHz), see Table 20.

Compound SC2 : White solid, mp 221-222°C; $[\alpha]_D^{27}$: +11.8° (c 0.02, $CHCl_3$); UV ($CHCl_3$) λ_{max} (log ε): 212 (3.34), 263 (2.94), 282 (2.42), 292 (2.41) nm; IR (KBr) ν_{max}: 3418, 1691, 761 cm^{-1}; HRFABMS *m/z* $[M]^+$ 312.1733 (calcd for $C_{20}H_{24}O_3$, 312.1725); ^1H NMR ($CDCl_3$, 300 MHz), see Table 21; ^{13}C NMR ($CDCl_3$, 75 MHz), see Table 21.

Compound SC3 : White solid, mp 154-155°C; $[\alpha]_D^{27}$: -2.6° (c 0.08, $CHCl_3$); UV ($CHCl_3$) λ_{max} (log ε): 212 (3.42), 260 (2.89), 281 (2.29), 291 (2.26) nm; IR (KBr) ν_{max}: 3419, 1719, 769 cm^{-1}; HREIMS *m/z* $[M]^+$ 342.1825 (calcd for $C_{21}H_{26}O_4$, 342.1831); ^1H NMR ($CDCl_3$, 300 MHz), see Table 22; ^{13}C NMR ($CDCl_3$, 75 MHz), see Table 22.

Compound SC4 : White solid, mp 118.5-119°C; $[\alpha]_D^{27}$: -29.4° (c 0.03, $CHCl_3$); UV ($CHCl_3$) λ_{max} (log ε): 212 (3.32), 263 (2.80), 281 (2.43), 291 (2.42) nm; IR (KBr) ν_{max}: 1736, 764 cm^{-1}; HREIMS *m/z* $[M]^+$ 384.1936 (calcd for $C_{23}H_{28}O_5$, 384.1937); ^1H NMR ($CDCl_3$, 300 MHz), see Table 23; ^{13}C NMR ($CDCl_3$, 125 MHz), see Table 23.

Compound SC7 : White solid, mp 145-146°C; $[\alpha]_D^{27}$: -4.2° (c 0.02, $CHCl_3$); UV ($CHCl_3$) λ_{max} (log ε): 211 (3.69), 257 (3.67) nm; IR (KBr) ν_{max}: 3415, 1721, 751 cm^{-1}; HREIMS *m/z* $[M]^+$ 346.1787 (calcd for $C_{20}H_{26}O_5$, 346.1780); ^1H NMR ($CDCl_3$, 300 MHz), see Table 26; ^{13}C NMR ($CDCl_3$, 125 MHz), see Table 26.

Compound SC8 : Viscous oil; $[\alpha]_D^{27}$:+6.7° (c 0.01, $CHCl_3$); UV ($CHCl_3$) λ_{max} (log Ɛ): 220 (3.46) nm; IR (neat) ν_{max}: 2927, 1725, 752 cm^{-1}; ^1H NMR ($CDCl_3$, 300 MHz), see Table 27; ^{13}C NMR ($CDCl_3$, 75 MHz), see Table 27.

Compound SC9 : Viscous oil; $[\alpha]_D^{27}$: +4.7° (c 0.02, $CHCl_3$); UV ($CHCl_3$) λ_{max} (log Ɛ): 205 (3.67), 239 (4.09) nm; IR (neat) ν_{max}: 3396, 758 cm^{-1}; HREIMS *m/z* $[M]^+$ 288.2455 (calcd for $C_{20}H_{32}O$, 288.2453); ^1H NMR ($CDCl_3$, 300 MHz), see Table 28; ^{13}C NMR ($CDCl_3$, 75 MHz), see Table 28.

Compound SC10 : White solid, mp 90-91°C; $[\alpha]_D^{27}$: +20.3° (c 0.04, $CHCl_3$); UV ($CHCl_3$) λ_{max} (log ε): 208 (3.19) nm; IR (KBr) ν_{max}: 3412, 2924, 1636, cm^{-1}; ^1H NMR ($CDCl_3$, 300 MHz), see Table 30; ^{13}C NMR ($CDCl_3$, 75 MHz), see Table 30.

The crude CH_2Cl_2 extract was fractionated by QCC with hexane and increasing polarity with EtOAc to give six fractions (C1-C6, scheme 4).

Fraction C2 (1.59 g) was subjected to CC with EtOAc-hexane (1:9, v/v) to afford SC5 (3.7 mg, R_f = 0.30 (1:9, EtOAc- hexane)).

Fraction C3 (1.28 g) was purified by CC with acetone-hexane (1:9, v/v) and followed by recrystallization from CH_2Cl_2 to give SC6 (19.5 mg, R_f = 0.14 (4:1, CH_2Cl_2-hexane)).

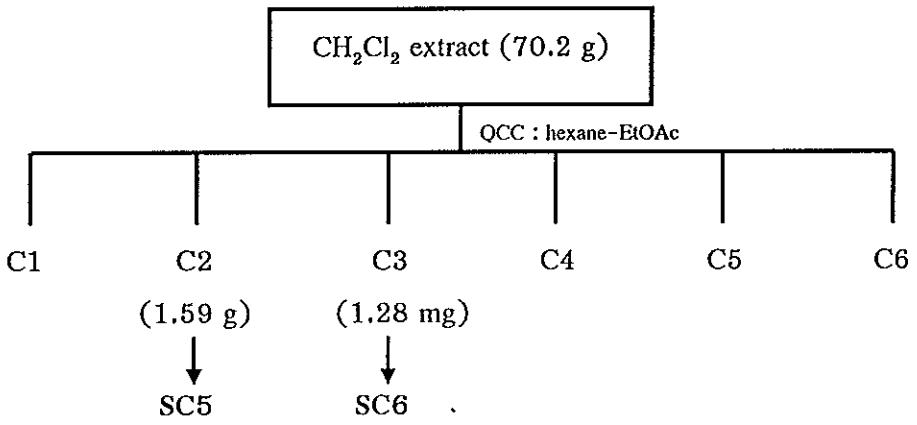

Scheme 4 Isolation of compounds SC5 and SC6 of *C. crista*

Compound SC5 : White solid, mp 194-195°C; $[\alpha]_D^{27}$:+23.3° (c 0.003, $CHCl_3$); UV ($CHCl_3$) λ_{max} (log ε): 203 (3.13), 235 (2.55), 280 (2.18) nm; IR (KBr) ν_{max}: 1811, 1727 cm^{-1}; HREIMS *m/z* $[M]^+$ 342.1836 (calcd for $C_{21}H_{26}O_4$, 342.1831); ^1H NMR ($CDCl_3$, 300 MHz), see Table 24; ^{13}C NMR ($CDCl_3$, 125 MHz), see Table 24.

Compound SC6 : White solid, mp 157-158°C; $[\alpha]_D^{27}$: -5.7° (c 0.003, $CHCl_3$); UV ($CHCl_3$) λ_{max} (log ε): 217 (3.59), 258 (3.67) nm; IR (KBr) ν_{max}: 1724, 1668, 762 cm^{-1}; HREIMS *m/z* $[M]^+$ 330.1832 (calcd for $C_{20}H_{26}O_4$, 330.1831); ^1H NMR ($CDCl_3$, 300 MHz), see Table 25; ^{13}C NMR ($CDCl_3$, 75 MHz), see Table 25.

Chopped-dried roots of *C. crista* (4.2 kg) were extracted with hexane (2 x 5 l, for 5 days) at room temp. The mixture was filtered and the filtrate was evaporated under reduced pressure to give brownish crude hexane extract. This crude extract (47.5 g) was subjected to QCC with hexane and increasing polarity with EtOAc to afford five fractions (R1-R5, scheme 5).

Fraction R1 (25.4 mg) was purified by prep. TLC with EtOAc-hexane (1:19, v/v) to give **RH1** (3.4 mg, R_f = 0.35 (1:19, EtOAc-hexane)) and **RH3** (8.2 mg, R_f = 0.41 (1:15, EtOAc-hexane)).

Fraction R3 (966.1 mg) was separated by flash CC with CH_2Cl_2-hexane (2:3, v/v) and followed by prep. TLC with CH_2Cl_2-hexane (9:11, v/v) to afford **RH2** (16.4 mg, R_f = 0.31 (3:2, CH_2Cl_2-hexane)) and **RH5** (20.0 mg, R_f = 0.21 (1:9, EtOAc-hexane)).

Fraction R5 (778.0 mg) was subjected to CC with EtOAc-hexane (3:17, v/v) and followed by reversed-phase prep. TLC with MeOH-H_2O (17:3, v/v) to give **RH4** (31.2 mg, R_f = 0.19 (3:17, EtOAc-hexane)) and **RH6** (12.4 mg, R_f = 0.10 (1:3, EtOAc-hexane)).

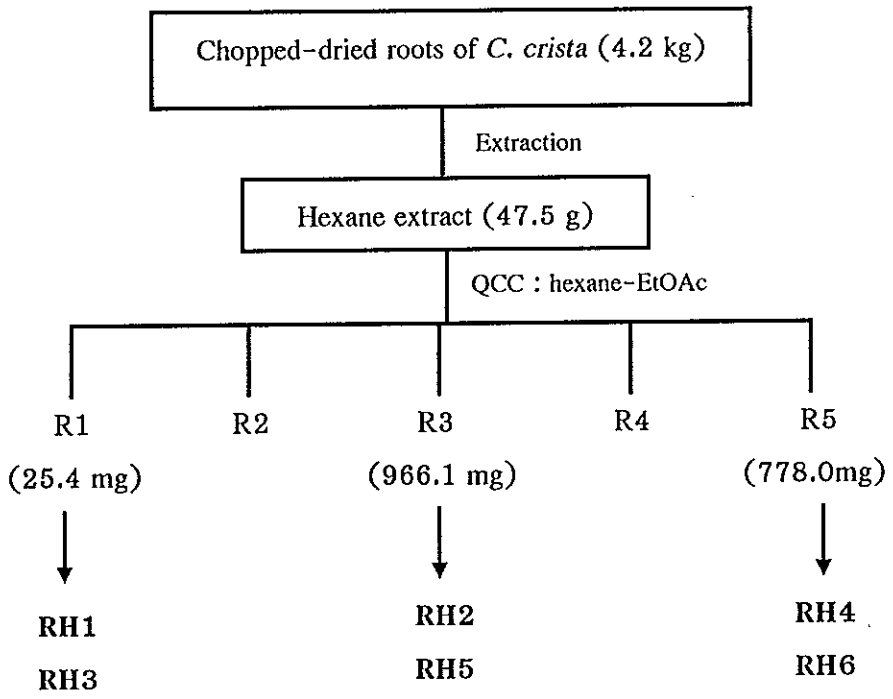

Scheme 5 Isolation of compounds **RH1-RH6** of *C. crista*

Compound RH1 : White solid, mp 57-58°C; $[\alpha]_D^{27}$:+22.7° (c 0.004, $CHCl_3$); UV ($CHCl_3$) λ_{max} (log ε): 211 (3.64), 260 (2.96), 281 (2.52), 293 (2.48) nm; IR (KBr) ν_{max}: 2880, 1718, 766 cm^{-1}; HREIMS *m/z* $[M]^+$ 340.1671 (calcd for $C_{21}H_{24}O_4$, 340.1675); ^1H NMR ($CDCl_3$, 300 MHz), see Table 31; ^{13}C NMR ($CDCl_3$, 75 MHz), see Table 31.

Compound RH2 : White solid, mp 118.5-119 °C; $[\alpha]_D^{27}$:+29.4° (c 0.03, $CHCl_3$); UV ($CHCl_3$) λ_{max} (log ε): 236 (3.43) nm; IR (KBr) ν_{max}: 3414, 2927, 1718, 756 cm^{-1}; ^1H NMR ($CDCl_3$, 300 MHz), see Table 33; ^{13}C NMR ($CDCl_3$, 75 MHz), see Table 33.

Compound RH3 : White solid, mp 164.5-165°C; $[\alpha]_D^{27}$:+20.8° (c 0.005, $CHCl_3$); UV ($CHCl_3$) λ_{max} (log ε): 222 (3.40) nm; IR (KBr) ν_{max}: 2870, 1748, 1714, 734 cm^{-1}; HREIMS *m/z* $[M]^+$ 344.1942 (calcd for $C_{21}H_{28}O_4$, 344.1988); ^1H NMR ($CDCl_3$, 300 MHz), see Table 34; ^{13}C NMR ($CDCl_3$, 75 MHz), see Table 34.

Compound RH4 : White solid, mp 83-84°C; $[\alpha]_D^{27}$:+90.1° (c 0.011, $CHCl_3$); UV ($CHCl_3$) λ_{max} (log ε): 225 (2.84) nm; IR (KBr) ν_{max}: 3451, 1715, 755 cm^{-1}; HREIMS *m/z* $[M]^+$ 346.2111 (calcd for $C_{21}H_{30}O_4$, 346.2144); ^1H NMR ($CDCl_3$, 300 MHz), see Table 35; ^{13}C NMR ($CDCl_3$, 75 MHz), see Table 35.

Compound RH5 : Orange viscous oil; $[\alpha]_D^{27}$:+60.4° (c 0.02, MeOH); UV ($CHCl_3$) λ_{max} (log ε): 206 (4.94), 234 (4.42), 283 (3.95), 311 (4.23) nm; IR (KBr) ν_{max}: 3415, 1615 cm^{-1}; ^1H NMR ($CDCl_3$, 300 MHz), see Table 37; ^{13}C NMR ($CDCl_3$, 75 MHz), see Table 37.

Compound RH6 : Yellow solid, mp 178-179 °C; UV (MeOH) λ_{max} (log ε): 206 (4.26), 242 (3.90), 264 (3.77), 377 (4.15) nm; IR (KBr) ν_{max}: 3418, 1635, 1562 cm^{-1}; ^1H NMR ($CDCl_3$, 300 MHz), see Table 38; ^{13}C NMR ($CDCl_3$, 75 MHz), see Table 38.

The seeds (110.7 g) of *C. crista* were extracted with acetone at room temperature (5 days) and evaporated under reduced pressure to afford acetone extract. The acetone extract (16.3 g) was further chromatographed on normal phase silica gel and eluted with hexane-EtOAc mixtures to give five fractions (S1-S5).

Fraction S2 (677.9 mg) was purified by CC with CH_2Cl_2-hexane (1:19, v/v) to yield **SD3** (17.3 mg, R_f = 0.30 (100%, hexane)) and **SD6** (11.8 mg, R_f = 0.48 (100%, hexane)).

Fraction S3 (150.0 mg) was separated by CC with EtOAc-hexane (1:19, v/v) to afford **SD1** (4.8 mg, R_f = 0.28 (100%, hexane)) and **SD2** (6.9 mg, R_f = 0.25 (1:19, EtOAc-hexane)).

Fraction S4 (118.5 mg) was purified by CC with EtOAc-hexane (1:9, v/v) and followed by prep. TLC with EtOAc-hexane (1:9, v/v) to give **SD4** (7.3 mg, R_f = 0.40 (1:9, EtOAc-hexane)) and **SD5** (12.4 mg, R_f = 0.31 (3:7, EtOAc-hexane)).

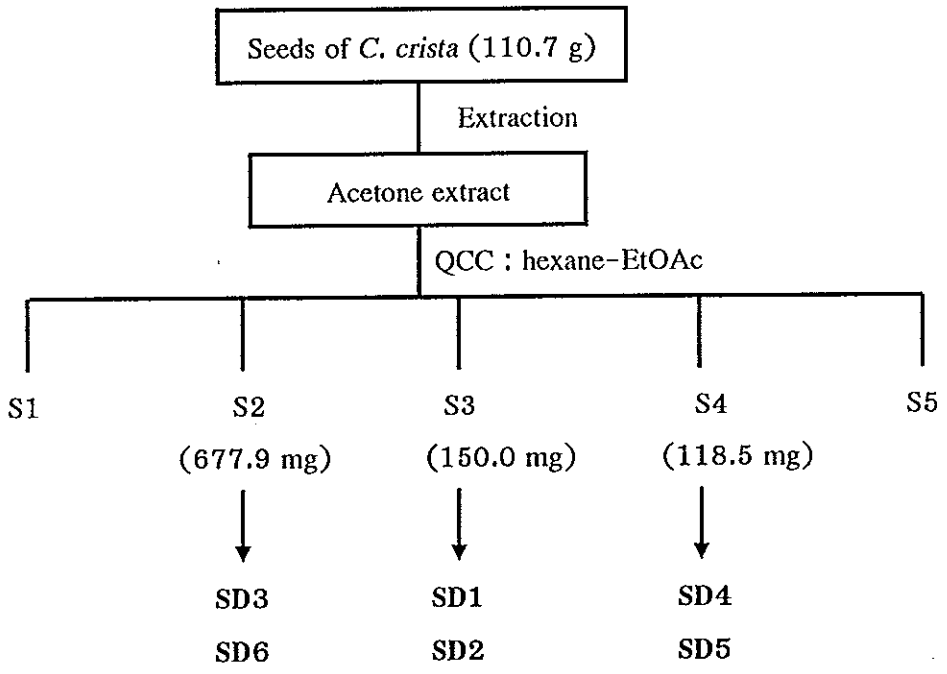

Scheme 6 Extraction and isolation of compounds **SD1-SD6** of *C. crista*

Compound SD1 : Yellow solid, mp. 70-71 °C, $[\alpha]_D^{27}$: +42.1° (c 0.11, $CHCl_3$); UV λ_{max} ($CHCl_3$)(log ε): 212 (4.40), 260 (4.00), 282 (3.62), 292 (3.59) nm; IR (neat) ν_{max}: 1458, 761 cm^{-1}; ^1H NMR ($CDCl_3$, 300 MHz), see Table 39; ^{13}C NMR ($CDCl_3$, 75 MHz), see Table 39.

Compound SD2 : Colorless viscous oil, $[\alpha]_D^{27}$: +19.4° (c 0.09, $CHCl_3$); UV λ_{max} ($CHCl_3$)(log ε): 227 (3.80) nm; IR (neat) ν_{max}: 1458, 761 cm^{-1}; HREIMS *m/z* 302.2265 (calcd for $C_{20}H_{30}O_2$, 302.2246); ^1H NMR ($CDCl_3$, 300 MHz), see Table 40; ^{13}C NMR ($CDCl_3$, 75 MHz), see Table 40.

Compound SD3 : Colorless viscous oil, $[\alpha]_D^{27}$: +36.6° (c 0.27, $CHCl_3$); UV λ_{max} ($CHCl_3$)(log ε): 217 (4.10), 255 (3.79), 283 (3.24), 293 (3.21) nm; IR (neat) ν_{max}: 1612, 755 cm^{-1}; HREIMS *m/z* 566.4109 (calcd for $C_{40}H_{54}O_2$, 566.4124); ^1H NMR ($CDCl_3$, 300 MHz), see Tables 41 and 42; ^{13}C NMR ($CDCl_3$, 75 MHz), see Tables 41 and 42.

Compound SD4 : Amorphous solid, mp 189-190 °C, $[\alpha]_D^{27}$: +28.3° (c 0.07, $CHCl_3$); UV λ_{max} ($CHCl_3$)(log ε): 224 (3.24), 240 (3.11) nm; IR (neat) ν_{max} : 1682, 731 cm^{-1}; HREIMS *m/z* 288.2466 (calcd for $C_{20}H_{32}O$, 288.2453); ^1H NMR ($CDCl_3$, 300 MHz), saa Table 43; ^{13}C NMR ($CDCl_3$, 75 MHz), see Table 43.

Compound SD5 : Colorless viscous oil, $[\alpha]_D^{27}$: +23.0° (c 0.06, $CHCl_3$); UV λ_{max} ($CHCl_3$)(log ε): 222 (3.40) nm; IR (neat) ν_{max}: 3409, 1642 cm^{-1}; HREIMS *m/z* 290.2603 (calcd for $C_{20}H_{34}O$, 290.2610); ^1H NMR ($CDCl_3$, 300 MHz), see Table 44; ^{13}C NMR ($CDCl_3$, 75 MHz), see Table 44.

Compound SD6 : Colorless viscous oil, $[\alpha]_D^{27}$: +11.7° (c 0.03, $CHCl_3$); UV λ_{max} ($CHCl_3$)(log ε): 222 (3.79) nm; IR (neat) ν_{max}: 3484, 730 cm^{-1}; ^1H NMR ($CDCl_3$, 300 MHz), see Table 45; ^{13}C NMR ($CDCl_3$, 75 MHz), see Table 45.

1.2.3.3 Isolation and Chemical Investigation of S. multiflora

Ground-dried barks (5.9 kg) of *S. multiflora* were extracted with CH_2Cl_2 (2 x 7.5 l, for 5 days) at room temp. The crude extract was evaporated under reduced pressure to afford a brownish CH_2Cl_2 extract (27.3 g).

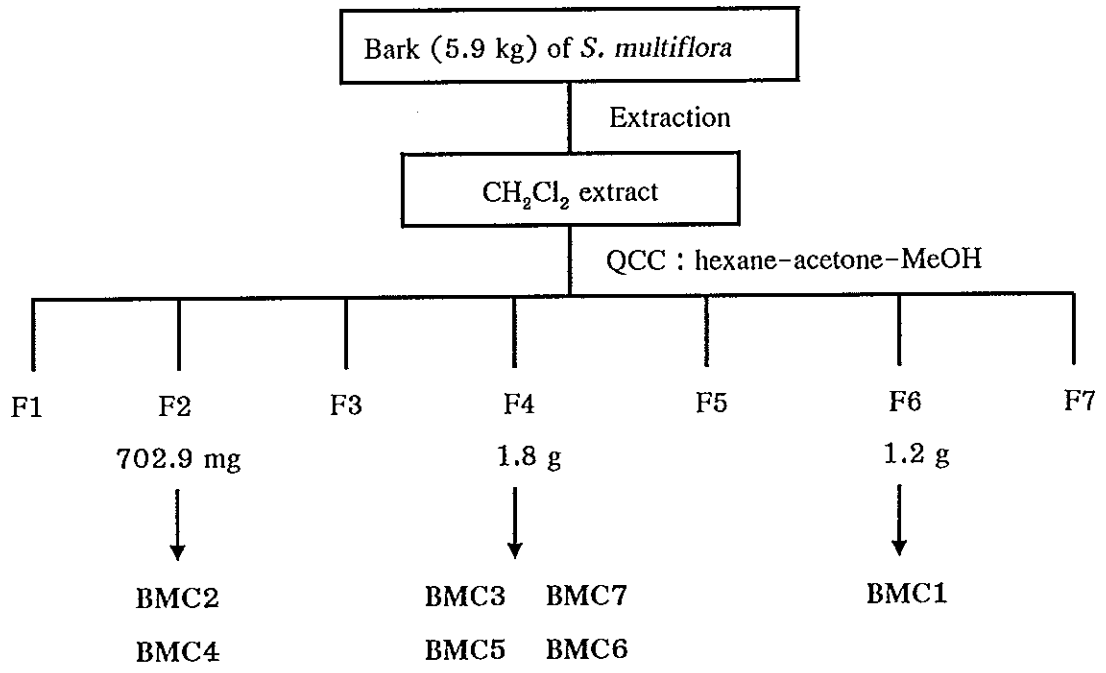

Scheme 7 Extraction and isolation of compounds **BMC1-BMC7** of *S. multiflora*

The CH_2Cl_2 extract was further purified by QCC using hexane as eluent and increasing polarity with acetone and MeOH to give seven fractions (F1-F7).

Fraction F2 (702.9 mg) was subjected to CC with EtOAc-hexane (1:3, v/v) and followed by prep TLC with MeOH-CH_2Cl_2 (1:49, v/v) to give **BMC2** (3.3 mg, R_f = 0.15 (7:3, EtOAc-hexane)) and **BMC4** (7.2 mg, R_f = 0.08 (1:49, MeOH-CH_2Cl_2)).

Fraction F4 (1.8 g) was purified by CC with acetone-CH_2Cl_2 (1:49, v/v) to afford four subfractions. Subfraction F4b (67.4 mg) was separated by CC with EtOAc-hexane (3:7, v/v) to afford **BMC5** (12.6 mg, R_f = 0.14 (3:7, EtOAc-hexane)). Subfraction F4d (370.2 mg) was purified by CC with EtOAc-hexane (3:7, v/v) and followed by prep TLC with EtOAc-hexane (3:7, v/v) to give **BMC3** (6.2 mg, R_f = 0.16

(3:97, acetone-hexane)), BMC6 (9.1 mg, R_f = 0.19 (3:7, EtOAc-hexane)) and BMC7 (8.3 mg, R_f = 0.11 (3:7, EtOAc-hexane)).

Fraction F6 (1.2 g) was subjected to CC with MeOH-CH_2Cl_2 (1:19, v/v) to afford three subfractions (F6a-F6c). Subfraction F6c (327.7 mg) was further purified by CC with acetone-CH_2Cl_2 (1:9, v/v) to give **BMC1** (22.5 mg, R_f = 0.18 (1:19, MeOH-CH_2Cl_2)).

Compound BMC1 : White solid, mp 205-206 °C; $[\alpha]_D^{27}$: -2.5° (c 0.04, MeOH); UV (MeOH) λ_{max} (log ε): 206 (3.30) nm; IR (KBr) ν_{max}: 3337 cm^{-1}; HREIMS: *m/z* $[M]^+$ 320.2351 (calcd for $C_{20}H_{32}O_3$, 320.2351); EIMS: *m/z* 320 (23)(M^+), 302 (63), 287 (85), 271 (100); ^1H NMR ($CDCl_3$+MeOD, 300 MHz), see Table 47; ^{13}C NMR ($CDCl_3$+MeOD, 75 MHz), see Table 47.

Compound BMC2 : Colorless viscous oil; $[\alpha]_D^{27}$: +35.7° (c 0.06, MeOH); UV (MeOH) λ_{max} (log ε): 205 (2.87) nm; IR (KBr) ν_{max}: 3407, 1694 cm^{-1}; HREIMS: *m/z* $[M]^+$ 318.2195 (calcd for $C_{20}H_{30}O_3$, 318.2195); EIMS: *m/z* 318 (23)(M^+), 288 (100), 273 (25), 159 (33), 84 (40); ^1H NMR ($CDCl_3$, 300 MHz), see Table 48; ^{13}C NMR ($CDCl_3$, 75 MHz), see Table 48.

Compound BMC3 : Colorless viscous oil; $[\alpha]_D^{27}$: -20.8° (c 0.03, MeOH); UV (MeOH) λ_{max} (log ε): 206 (3.53), 225 (3.17) nm; IR (KBr) ν_{max}: 3358, 2919, 1717 cm^{-1}; ^1H NMR ($CDCl_3$, 300 MHz), see Table 49; ^{13}C NMR ($CDCl_3$, 75 MHz), see Table 49.

Compound BMC4 : Colorless viscous oil; $[\alpha]_D^{27}$: -7.5° (c 0.04, MeOH); UV (MeOH) λ_{max} (log ε): 207 (3.04), 221 (2.96), 276 (2.69) nm; IR (KBr) ν_{max}: 3407, 2926, 1698 cm^{-1}; ^1H NMR ($CDCl_3$, 300 MHz), see Table 50; ^{13}C NMR ($CDCl_3$, 75 MHz), see Table 50.

Compound BMC5 : White solid, mp 175-176 °C; $[\alpha]_D^{27}$:+187.0° (c 0.10, MeOH); UV (MeOH) λ_{max} (log ε): 205 (3.49), 275 (3.93) nm; IR (KBr) ν_{max}:

3463, 2926, 1739, 1663, 1087 cm^{-1}; ^1H NMR ($CDCl_3$, 300 MHz), see Table 51; ^{13}C NMR ($CDCl_3$, 75 MHz), see Table 51.

Compound BMC6 : White solid, mp 197-198 °C; $[\alpha]_D^{27}$:+101.5° (c 0.28, MeOH); UV (MeOH) λ_{max} (log ε): 207 (3.42), 274 (3.81) nm; IR (KBr) ν_{max}: 3470, 2926, 1743, 1670 cm^{-1}; ^1H NMR ($CDCl_3$, 300 MHz), see Table 52; ^{13}C NMR ($CDCl_3$, 75 MHz), see Table 52.

Compound BMC7 : White solid, mp 211-212.5 °C; $[\alpha]_D^{27}$:-28.1° (c 0.11, MeOH); UV (MeOH) λ_{max} (log ε): 204 (3.28), 275 (3.86) nm; IR (KBr) ν_{max}: 3420, 2913, 1743, 1666 cm^{-1}; ^1H NMR ($CDCl_3$, 300 MHz), see Table 53; ^{13}C NMR ($CDCl_3$, 75 MHz), see Table 53.

1.2.4 Bioassays

1.2.4.1 Anti-HIV-1 protease activity

This assay was modified from the previously reported method (Min et al., 1999). Briefly, the recombinant HIV-1 PR solution was diluted with a buffer composed of a solution containing 50 mM of sodium acetate (pH 5.0), 1 mM ethylenediamine disodium (EDTA.2Na) and 2 mM 2-mercaptoethanol (2-ME) and mixed with glycerol in the ratio of 3:1. The substrate peptides, Arg-Val-Nle-(*p*NO_2-Phe)-Glu-Ala-Nle-NH_2, was diluted with a buffer solution of 50 mM sodium acetate (pH 5.0). Two microliters of plant extract and 4 µl of HIV-1 PR solution (0.025 mg/ml) were added to a solution containing 2 µl of 50 mM buffer solution (pH 5.0) and 2 µl of substrate solution (2 mg/ml), and the reaction mixture 10 µl was incubated at 37°C for 1 hr. A control reaction was performed under the same condition but without the plant extract. The reaction was stopped by heating the reaction mixture at 90 °C for 1 min. Subsequently, 20 µl of sterile water was added and an aliquot of 10 µl was analyzed by HPLC using RP-18 column (4.6 x 150 mm I.D., Supelco 516 C-18-DB 5 µm, USA). Ten microlitres of the reaction mixture was injected to the column and gradiently eluted with acetonitrile (15-40%) and 0.2% trifluoroacetic acid (TFA) in water, at a flow rate of 1.0 ml/min. The elution profile was monitored at 280 nm. The retention times of the substrate and *p*-NO_2-

Phe-bearing hydrolysate were 11.356 and 9.457 min, respectively. The inhibitory activity on HIV-1 PR was calculated as follows : % inhibition = ($A_{control}$-A_{sample}) x 100/ $A_{control}$; whereas A is a relative peak area of the product hydrolysate. Acetyl pepstatin was used as a positive control. For statistical analysis, the results of anti-HIV-1 PR activity were expressed as mean ± SD of three determinations. The IC_{50} values were calculated using the Microsoft Excel program. Statistical significance was calculated by Dunnett's test.

1.2.4.2 Antimalarial activity

The parasite *P. falciparum* (K1, multidrug resistant strain) was cultured continuously according to the method of Trager and Jensen, 1976. Quantitative assessment of antimalarial activity in vitro was determined by means of the microculture radioisotope technique based upon the method described by Desjardins et al., 1979. Briefly, a mixture of 200 μl of 1.5% of erythrocytes with 1% parasitemia at the early ring stage was pre-exposed to 25 μl of the medium containing a test sample dissolved in DMSO (0.1% final concentration) for 24 h employing the incubation conditions described above. Subsequently, 25 μl of [3H]hypoxanthine (Amersham, USA) in culture medium (10 μCi) was added to each well and plates were incubated for an additional 24 h. Levels of incorporated radioactively labeled hypoxanthine indicating parasite growth were determined using the Top Count microplate scintillation counter (Packard, USA). An IC_{50} value of 1.2 ± 0.02 μg/ml (n = 3) was observed for the standard compound, dihydroartemisinin.

1.2.4.3 Anti-allergic activity

1.2.4.3.1 Inhibitory effects on the release of β-hexosaminidase from RBL-2H3 cells

Inhibitory effects on the release of β-hexosaminidase from RBL-2H3 were evaluated by the following method (Matsuda et al., 2002). Briefly, RBL-2H3 cells were dispensed in 24-well plates at a concentration of 2×10^5 cells/well using Minimum Essential Medium Eagle (MEM) containing 10% fetal calf serum (FCS), penicillin (100

units/ml), streptomycin (100 units/ml) and anti-DNP IgE (0.45 μg/ml), then incubated overnight at 37 °C in 5% CO_2 for sensitization of the cells. The cells were washed twice with 500 μL of Siraganian buffer [119 mM NaCl, 5 mM KCl, 5.6 mM glucose, 0.4 mM $MgCl_2$, 1 mM $CaCl_2$, 25 mM piperazine-*N*,*N'*-bis(2-ethanesulfonic acid) (PIPES), 0.1 % BSA and 40 mM NaOH, pH 7.2] and then incubated in 160 μl of Siraganian buffer for an additional 10 min at 37 °C. After that, 20 μl of test sample solution were added to each well and incubated for 10 min, followed by addition of 20 μl of antigen (DNP-BSA, final concentration 10 μg/ml) at 37 °C for 20 min to stimulate the cells to degranulate. The supernatant was transferred into 96-well plate and incubated with 50 μl of substrate (1mM *p*-nitrophenyl-*N*-acetyl-β-D-glucosaminide) in 0.1 M citrate buffer (pH 4.5) at 37 °C for 1 hr. The reaction was stopped by addition of 200 μl of stop solution (0.1 M Na_2CO_3/$NaHCO_3$, pH 10.0). Measurement of absorbance was performed with a microplate reader at 405 nm. The test sample was dissolved in dimethylsulfoxide (DMSO), and the solution added to Siraganian buffer (final DMSO concentration 0.1 %). The inhibition (%) of the release of β-hexosaminidase by the test samples was calculated by the following equation, and IC_{50} values were determined graphically:

$$\text{Inhibition } \% = [1 - (T-B-N)/(C-N)] \times 100$$

Control (C): DNP-BSA (+), Test sample (-); Test (T) : DNP-BSA (+), Test sample (+); Blank (B) : DNP-BSA (-), Test sample (+); Normal (N) : DNP-BSA (-), Test sample (-)

1.2.4.3.2 β-Hexosaminidase inhibitory activity

In order to clarify that the anti-allergic effects of samples were due to the inhibition on β-hexosaminidase release, but not from the inhibition of β-hexosaminidase activity. The following assay was then carried out. The cell suspension (5×10^7 cells) in 6 ml of PBS was sonicated. The solution was then centrifuged; and the supernatant diluted with Siraganian buffer and adjusted to equalize the enzyme activity of the degranulation tested above. The enzyme solution (45 μl) and test sample solution (5 μl) were transferred into a 96-well microplate and incubated with 50 μl of the substrate solution at 37 °C for 1 hr. The reaction was stopped by adding 200 μl of the stop solution. The

absorbance was measured using a microplate reader at 405 nm and the results were expressed as mean ± S.E.M of four determinations. The IC_{50} values were calculated using the Microsoft Excel program. The statistical significance was calculated by one-way analysis of variance (ANOVA), followed by Dunnett's test.

1.2.5 X-ray crystallographic analysis of taepeenin A (SC1)

The data were collected using a 4 K SMART CCD diffractometer with a graphite monochromated Mo Kα radiation (λ = 0.71073 Å). The data were collected at a temperature of 293(2) K to a maximum 2θ value of 56.44°. The collected data were reduced using SAINT program (Siemens, 1997), and the empirical absorption corrections were performed using SADABS program (Sheldrick, 1996). Crystal data: Orthorhombic, $C_{21}H_{26}O_3$ (M_r = 326.42), space group $P2_12_12_1$ with a = 13.135(5) Å, b = 7.293(3) Å, c = 18.296(7) Å, α = β = γ = 90.0°, V = 1752.6(1) Å^3, Z = 4, and D_{calcd} = 1.237 g/cm^3. The structure was solved by direct method and was refined by least-squares using the SHELXTL software package (Sheldrick, 1997). All non-hydrogen atoms were located and refined anisotropically with SHELXTL using full-matrix least-squares procedure, whereas the hydrogen atom positions were geometrically idealized and allowed to ride on their parent atoms and refined isotropically with fixed displacement parameters. The final cycle of full matrix least-squares refinement was based on 3088 observed reflections ($I > 2\sigma(I)$, $2\theta \leq 50.0°$) and 222 variable parameters and converged with unweighted and weighted agreement factors of R = 0.0693 and R_w = 0.1897.

The crystallographic-information file for **SC1** has been deposited with the Cambridge Crystallographic Data Centre, CCDC deposition number 262744. The supplementary crystallographic data for SC1 can be obtained free of charge from CCDC, 12 Union Road, Cambridge CB2 1EZ, UK (fax: +44 1233 336033; e-mail: deposit@ccdc.cam.ac.uk or http://www.ccdc.cam.ac.uk/).

CHAPTER 1.3
RESULTS AND DISCUSSION

1.3.1 Structural elucidation of compounds from the rhizomes of *B. pandurata*

Chopped-dried rhizomes of *B. pandurata* were extracted with $CHCl_3$ and MeOH, successively at room temperature and the solvent was evaporated under reduced pressure to afford the $CHCl_3$ and MeOH extracts, respectively. The MeOH extract was subjected to chromatography and/or crystallization to give three cyclohexylchalcones (**BP1-BP3**), three chalcones (**BP4-BP6**) and two aromatic compounds (**BP7-BP8**). Their structures were elucidated by 1D and 2D spectroscopic data. All carbons were assigned by ^{13}C NMR, DEPT 135°, DEPT 90°, HMQC and HMBC data.

1.3.1.1 Compound BP1

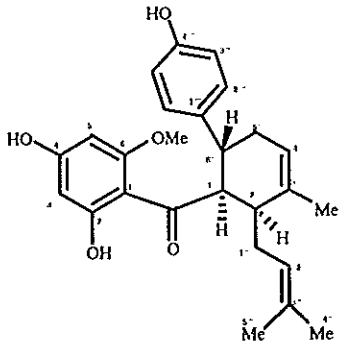

Compound **BP1**, $[\alpha]_D^{27}$: -24.0° (*c* 0.13, MeOH), was obtained as a yellow viscous oil and analyzed as $C_{26}H_{30}O_5$ ($[M]^+$ *m/z* 422.2044). The IR spectrum displayed absorption bands at 3438 (hydroxyl) and 1624 (conjugated carbonyl) cm^{-1} and UV absorption bands at λ_{max} 220 and 292 nm supporting the presence of a conjugated carbonyl in the structure. The ^{13}C-NMR and DEPT spectrum (Table 4, Figure 20) indicated the presence of 26 carbons as 12 aliphatic carbons (3Me, $2CH_2$, 3CH and 2C=CH-), 12 aromatic carbons (6CH, 2C and 4C-O), one carbonyl and one methoxyl carbon.

The ^{1}H NMR spectral data (Table 4, Figure 19) displayed a downfield resonance at δ 13.90, attributable to a chelated hydroxyl group, while two doublets in the aromatic region (at δ 7.04 and 6.85, each 2H, J = 8.1 Hz) suggested the presence of a *para*-disubstituted aromatic ring. Two aromatic protons as two doublets at δ 5.89 and 5.92 (each J = 2.4 Hz) and one singlet at δ 3.90 were assigned to H-3, H-5 and OMe, respectively. The proton signals at δ 4.85 (1H, t, J = 6.6 Hz), 2.47 (1H, m), 2.26 (1H, m) and 1.50 (6H, s) indicated the presence of an isoprenyl moiety. Additionally, four methine proton signals at δ 5.42 (1H, br s, H-4′), 4.41 (1H, dd, J = 11.4, 4.5 Hz, H-1′), 3.35 (1H, td, J = 11.4, 6.6 Hz, H-6′), and 2.47 (1H, m, H-2′) and a vinylic methyl protons at δ 1.78 (3H, s) indicated that **BP1** had a cyclohexenyl chalcone skeleton. The cross peaks of H-4′/H-5′, H-5′/H-6′, H-6′/H-1′, H-1′/H-2′, H-2′/H-1″ and H-1″/H-2″ in COSY spectrum confirmed that the isoprenyl group was connected to C-2′.

In the HMBC spectrum, the methine proton at δ 4.41 (H-1′) correlated with carbons at δ 206.5 (C=O), 42.5 (C-2′), 35.8 (C-5′), 36.3 (C-6′) and 28.9 (C-1″), a methine proton at δ 2.47 (H-2′) with carbons at δ 124.2 (C-2″), 121.0 (C-4′) and 36.3 (C-6′), a methine proton at δ 3.35 (H-6′) with carbons at δ 139.2 (C-1‴), 128.1 (C-2‴/6‴) and 54.4 (C-1′), and methyl protons at δ 1.78 (3′-Me) with carbons at δ 137.2 (C-3′), 121.0 (C-4′) and 42.5 (C-2′). These evidences confirmed that the *para*-disubstituted aromatic ring, isoprenyl moiety and vinylic methyl were attached to carbons C-6′, C-2′ and C-3′, respectively. The chelated hydroxyl group at δ 13.90 correlated with carbons at δ 167.5 (C-2), 106.8 (C-1) and 96.7 (C-3). The methoxyl protons at δ 3.90 was assigned at C-6 from its HMBC correlation with carbon at δ 162.8 (C-6) and a NOESY cross-peak with H-5 (δ 5.92).

The relative stereochemistry of **BP1** was identified on the basis of coupling constants and NOESY experiments. The large J value of proton H-1′ (J = 11.4 Hz) indicated that H-1′ should be α-axial oriented. In the NOESY, a methine proton at δ 4.41 (H-1′) showed cross-peaks with protons δ 2.47 (H-2′) and 7.04 (H-2‴/H-6‴) but none with proton at δ 3.35 (H-6′), suggesting that H-2′ and H-6′ should be α-equatorial and β-axial oriented, respectively. Thus, compound **BP1** was determined to be panduratin C, a new compound (Cheenpracha et al., 2006).

Table 4 ^{1}H, ^{13}C NMR, DEPT and HMBC spectral data of compound **BP1**

Position	δ_H (mult, *J*, Hz)	δ_C	DEPT	HMBC
1		106.8	C	
2		167.5	C	
3	5.89 (d, *J* = 2.4)	96.7	CH	1,2, 5
4		162.1	C	
5	5.92 (d, *J* = 2.4)	90.8	CH	1, 3, 6
6		162.8	C	
1′	4.41 (dd, *J* = 11.4, 4.5)	54.4	CH	C=O, 2′, 5′, 6′, 1″
2′	2.47 (m)	42.5	CH	4′, 6′, 2″
3′		137.2	C	
4′	5.42 (br s)	121.0	CH	
5′	2.45 (m)	35.8	CH_2	3′
	2.40 (m)			
6′	3.35 (td, *J* = 11.4, 6.6)	36.3	CH	1′, 1‴, 2‴, 6‴
1″	2.47 (m)	28.9	CH_2	2′, 3′
	2.26 (m)			
2″	4.85 (t, *J* = 6.6)	124.2	CH	
3″		131.8	C	
4″	1.50 (s)	17.9	CH_3	2″, 3″, 5″
5″	1.50 (s)	25.6	CH_3	2″, 3″, 4″
1‴		139.2	C	
2‴	7.04 (d, *J* = 8.1)	128.1	CH	6′, 3‴, 5‴, 6‴
3‴	6.85 (d, *J* = 8.1)	115.2	CH	1‴, 2‴, 4‴, 6‴
4‴		153.3	C	
5‴	6.85 (d, *J* = 8.1)	115.2	CH	1‴, 2‴, 4‴, 6‴
6‴	7.04 (d, *J* = 8.1)	128.1	CH	6′, 2‴, 3‴, 5‴
C=O		206.5	C	
OMe	3.90 (s)	55.8	CH_3	6
2-OH	13.90 (s)			1, 2, 3
3′-Me	1.78 (s)	22.9	CH_3	2′, 3′, 4′

1.3.1.2 Compound BP2

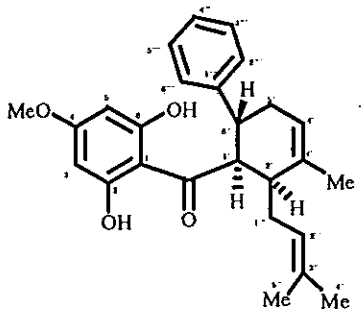

Compound **BP2** was obtained as a yellow solid, mp. 155-156 °C, $[\alpha]_D^{27}$: -23.0° (*c* 0.38, MeOH). The IR and UV spectrum showed absorption bands similar to those of **BP1**.

The ^{1}H and ^{13}C NMR spectral data (Tables 5 and 6, Figures 21 and 22) were closely related to those of **BP1**, except that the *meta*-coupled protons at δ 5.89 and 5.92 (each d, *J* = 2.4 Hz) in **BP1** were replaced by a *singlet* signal at δ 5.92 and aromatic proton signals at δ 7.04 and 6.85 (each d, *J* = 8.1 Hz) replaced by *multiplet* signals at δ 7.03-7.23 in **BP2**. This data indicated that compound **BP2** had a monosubstituted benzene and two magnetically equivalent aromatic protons, respectively. Thus on the basis of its spectroscopic data and comparison with previously reported compound (Tuntiwachwuttikul et al., 1984), compound **BP2** was assigned as panduratin A.

Table 5 ^{1}H, ^{13}C NMR, DEPT and HMBC spectral data of compound **BP2**

Position	δ_H (mult, *J*, Hz)	δ_C	DEPT	HMBC
1		106.0	C	
2		165.6	C	
3	5.92 (s)	94.5	CH	1, 2, 5
4		165.6	C	
5	5.92 (s)	94.5	CH	1, 3, 6
6		165.6	C	
1′	4.76 (dd, *J* = 11.4, 4.8)	53.8	CH	C=O, 2′, 3′, 5′, 6′, 1″, 1‴
2′	2.69 (m)	43.0	CH	3′, 4′, 5′, 6′, 1″, 2″, 3′-Me
3′		137.2	C	

Table 5 (Continued)

Position	δ_H (mult, *J*, Hz)	δ_C	DEPT	HMBC
4′	5.42 (br s)	121.2	CH	5′, 6′, 3′-Me
5′	2.43 (m)	36.2	CH_2	3′, 2″, 3″
	2.05 (m)			
6′	3.43 (ddd, *J* = 11.4, 10.8, 6.0)	37.2	CH	1′, 2′, 5′, 1‴, 2‴, 6‴
1″	2.30 (m)	29.0	CH_2	1′, 2′, 3″, 4″
	2.10 (m)			
2″	4.90 (br t, *J* = 6.9)	124.4	CH	1″, 4″, 5″
3″		132.0	C	
4″	1.55 (s)	18.0	CH_3	2″, 3″, 5″
5″	1.55 (s)	25.7	CH_3	2″, 3″, 4″
1‴		147.0	C	
2‴	7.03-7.23 (m)	127.1	CH	6′, 1‴
3‴		128.5	CH	
4‴		125.7	CH	
5‴		128.5	CH	
6‴		127.1	CH	6′, 1‴
C=O		207.6	C	
OMe	3.70 (s)	55.4	CH_3	6
3′-Me	1.80 (s)	22.8	CH_3	2′, 3′, 4′

Table 6 Comparison of ^{1}H NMR spectral data of compounds **BP1**, **BP2** and panduratin A (recorded in $CDCl_3$)

Position	Compound BP1 δ_H (mult, *J*, Hz)	Compound BP2 δ_H (mult, *J*, Hz)	Panduratin A δ_H (mult, *J*, Hz)
3	5.89 (d, *J* = 2.4)	5.92 (s)	5.86 (s)
5	5.92 (d, *J* = 2.4)	5.92 (s)	5.86 (s)
1′	4.41 (dd, *J* = 11.4, 4.5)	4.76 (dd, *J* = 11.4, 4.8)	4.78 (dd, *J* = 11.0, 4.4)

Table 6 (Continued)

Position	Compound BP1 δ_H (mult, *J*, Hz)	Compound BP2 δ_H (mult, *J*, Hz)	Panduratin A δ_H (mult, *J*, Hz)
2′	2.47 (m)	2.69 (m)	2.67 (ddd, *J* = 7.7, 7.5, 4.4)
4′	5.42 (br s)	5.42 (br s)	5.43 (dd, *J* = 5.0, 3.0)
5′	2.45 (m)	2.43 (m)	2.40 (ddd, *J* = 18.0, 6.3, 5.0)
	2.40 (m)	2.05 (m)	2.05 (ddd, *J* = 18.0, 11.0, 3.0)
6′	3.35 (td, *J* = 11.4, 6.6)	3.43 (ddd, *J* = 11.4, 10.8, 6.0)	3.45 (ddd, *J* = 11.0, 11.0, 6.3)
1″	2.47 (m)	2.30 (m)	2.30 (ddd, *J* = 15.0, 7.5, 7.0)
	2.26 (m)	2.10 (m)	2.15 (ddd, *J* = 15.0, 7.5, 7.0)
2″	4.85 (t, *J* = 6.6)	4.90 (br t, *J* = 6.9)	4.89 (t, *J* = 7.0)
4″	1.50 (s)	1.55 (s)	1.52 (s)
5″	1.50 (s)	1.55 (s)	1.52 (s)
2‴	7.04 (d, *J* = 8.1)	7.03-7.23 (m)	7.09-7.21 (m)
3‴	6.85 (d, *J* = 8.1)		
5‴	6.85 (d, *J* = 8.1)		
6‴	7.04 (d, *J* = 8.1)		
OMe	3.90 (s)	3.70 (s)	3.67 (s)
2-OH	13.90 (s)		10.30 (br s)
3′-Me	1.78 (s)	1.80 (s)	1.73 (s)

1.3.1.3 Compound BP3

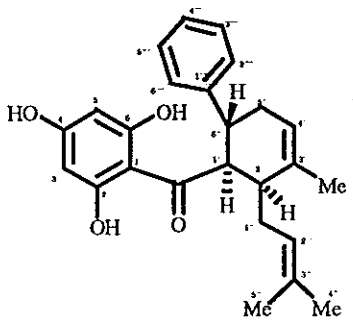

Compound **BP3** was obtained as a yellow solid, mp. 214-215 °C, $[\alpha]_D^{27}$: -24.4° (*c* 0.38, MeOH). The IR and UV spectrum showed absorption bands similar to those of **BP2**.

The ^1H and ^{13}C NMR spectral data (Tables 7, 8 and 9, Figures 23 and 24) of **BP3** and **BP2** exhibited the same pattern. The difference was shown in the ^1H NMR spectra of substituent group in which compound **BP2** displayed a methoxyl group at δ 3.70 but not observed in **BP3**. Thus on the basis of its spectroscopic data and comparison of the NMR spectral data with previous reported data (Tuchinda et al., 2002), compound **BP3** was assigned as hydroxypanduratin A.

Table 7 ^1H, ^{13}C NMR, DEPT and HMBC spectral data of compound **BP3**

Position	δ_H (mult, *J*, Hz)	δ_C	DEPT	HMBC
1		105.4	C	
2		163.5	C	
3	5.75 (s)	94.8	CH	1, 2, 4, 5
4		163.5	C	
5	5.75 (s)	94.8	CH	1, 3, 4, 6
6		163.5	C	
1′	4.69 (dd, *J* = 11.1, 4.5)	53.4	CH	C=O, 2′, 3′, 5′, 6′, 1″, 1‴
2′	2.58 (m)	42.3	CH	3′, 4′, 6′, 1″, 2″, 3′-Me
3′		137.4	C	
4′	5.38 (br s)	120.7	CH	5′, 6′, 3′-Me

Table 7 (Continued)

Position	δ_H (mult, *J*, Hz)	δ_C	DEPT	HMBC
5′	1.96 (m)			
6′	3.37 (ddd, *J* = 11.1, 10.8, 6.1)	37.0	CH	C=O, 1′, 2′, 5′, 1‴, 2‴, 6‴
1″	2.26 (m)	28.8	CH_2	1′, 2′, 3′, 2″, 3″
	2.07 (m)			
2″	4.86 (br t, *J* = 6.9)	124.3	CH	1″, 4″, 5″
3″		131.4	C	
4″	1.47 (s)	17.4	CH_3	2″, 3″, 5″
5″	1.47 (s)	25.4	CH_3	2″, 3″, 4″
1‴		147.3	C	
2‴	7.02-7.18 (m)	127.0	CH	6′, 1‴
3‴		128.1	CH	
4‴		125.3	CH	
5‴		128.1	CH	
6‴		127.0	CH	6′, 1‴
C=O		206.7	C	
3′-Me	1.73 (s)	22.5	CH_3	2′, 3′, 4′

Table 8 Comparison of ^{1}H NMR spectral data of BP2, BP3 and hydroxypanduratin A (recorded in $CDCl_3$)

Position	Compound BP2 δ_H (mult, *J*, Hz)	Compound BP3 δ_H (mult, *J*, Hz)	Hydroxypanduratin A* δ_H (mult, *J*, Hz)
3	5.92 (s)	5.75 (s)	5.88 (br s)
5	5.92 (s)	5.75 (s)	5.88 (br s)
1′	4.76 (dd, *J* = 11.4, 4.8)	4.69 (dd, *J* = 11.1, 4.5)	4.82 (dd, *J* = 11.6, 4.6)
2′	2.69 (m)	2.58 (m)	2.69 (m)
4′	5.42 (br s)	5.38 (br s)	5.41 (m)

Table 8 (Continued)

Position	Compound BP2 δ_H (mult, *J*, Hz)	Compound BP3 δ_H (mult, *J*, Hz)	Hydroxypanduratin A* δ_H (mult, *J*, Hz)
5′	2.43 (m)	1.96 (m)	2.35 (m)
	2.05 (m)		1.95 (m)
6′	3.43 (ddd, *J* = 11.4, 10.8, 6.0)	3.37 (ddd, *J* = 11.1, 10.8, 6.1)	3.45 (br ddd, *J* = 11.6, 10.7, 6.3)
1″	2.30 (m)	2.26 (m)	2.26 (m)
	2.10 (m)	2.07 (m)	2.10 (m)
2″	4.90 (br t, *J* = 6.9)	4.86 (br t, *J* = 6.9)	4.92 (m)
4″	1.55 (s)	1.47 (s)	1.51 (m)
5″	1.55 (s)	1.47 (s)	1.51 (m)
2‴	7.03-7.23 (m)	7.02-7.18 (m)	7.19 (m)
3‴			7.17 (m)
4‴			7.04 (m)
5‴			7.17 (m)
6‴			7.19 (m)
OMe	3.70 (s)		
2-OH			11.74 (br s)
3′-Me	1.80 (s)	1.73, s	1.76 (d, *J* = 1.8)

*Recorded in CD_3COCD_3.

Table 9 Comparison of ^{13}C NMR spectral data of BP1, BP2, BP3, panduratins A and hydroxypanduratin A (recorded in $CDCl_3$)

Position	BP1	BP2	BP3	Panduratin A	R*
1	106.8	106.0	105.4	106.4	106.2
2	167.5	165.6	163.5	163.2	164.8
3	96.7	94.5	94.8	94.6	95.9
4	162.1	165.6	163.5	165.3	164.8
5	90.8	94.5	94.8	94.6	95.9
6	162.8	165.6	163.5	163.2	164.8

Table 9 (Continued)

Position	BP1	BP2	BP3	Panduratin A	R*
1′	54.4	53.8	53.4	54.1	54.5
2′	42.5	43.0	42.3	42.8	43.4
3′	137.2	137.2	137.4	137.3	137.9
4′	121.0	121.2	120.7	121.3	121.7
5′	35.8	36.2	35.8	35.9	36.8
6′	36.3	37.2	37.0	37.2	37.8
1″	28.9	29.0	28.8	28.9	29.5
2″	124.2	124.4	124.3	124.4	125.4
3″	131.8	132.0	131.4	132.0	131.7
4″	17.9	18.0	17.4	17.9	18.0
5″	25.6	25.7	25.4	25.7	25.9
1‴	139.2	147.0	147.3	147.2	148.3
2‴	128.1	127.1	127.0	127.3	128.0
3‴	115.2	128.5	128.1	128.0	128.9
4‴	153.3	125.7	125.3	125.7	126.2
5‴	115.2	128.5	128.1	128.0	128.9
6‴	128.1	127.1	127.0	127.3	128.0
C=O	206.5	207.6	206.7	206.6	207.0
OMe	55.8	55.4		55.5	
3′-Me	22.9	22.8	22.5	22.8	23.0

*Recorded in CD_3COCD_3., R = Hydroxypanduratin A

1.3.1.4 Compound BP4

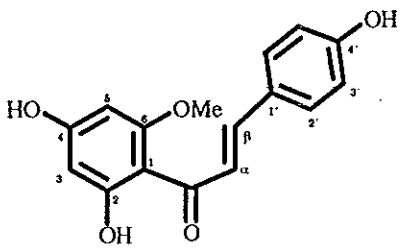

Compound **BP4** was isolated as yellow solid, mp 240-241 °C. The UV spectrum displayed maximum absorptions at λ_{max} 220, 227, 277, and 370 nm, suggesting the presence of conjugatation in the molecule. The IR spectrum suggested hydroxyl (3439 cm^{-1}) and carbonyl (1627 cm^{-1}) functionalities.

The ^{13}C NMR spectral data (Table 10, Figure 26) exhibited 16 carbons, including one methyl (δ 55.7), eight methines (δ 142.7, 130.3 (2C), 124.5, 115.8 (2C), 96.2, 91.6) and seven quarternary carbons (δ 192.6, 164.0, 163.5, 163.0, 159.1, 115.5, 106.0).

The ^{1}H NMR spectral data (Table 10, Figure 25) displayed the presence of 1,4-disubstituted benzene ring at δ 7.49 and 6.85 (each 2H, d, J = 8.7 Hz), and *meta*-coupled aromatic protons at δ 6.00 and 5.98 (each 1H, d, J = 1.8 Hz) which were assigned as H-3, and H-5, respectively. The proton signal at δ 3.92 (s) was assigned as a methoxyl group at C-6. In addition, the proton signals at δ 7.75 and 7.73 (each 1H, d, J = 15.3 Hz) were deduced as *trans* double bond at C-α and C-β, respectively.

The structure of **BP4** was confirmed by HMBC correlations. The proton signal at δ 7.49 (H-2′/H-6′) showed correlation with carbons at δ 159.1 (C-4′), 142.7 (C-β) and 115.8 (C-3′/C-5′), suggesting that 1,4-disubstituted benzene ring was connected at C-β. The correlations of proton signals at δ 6.00 (H-3) with carbons at δ 164.0 (C-2), 163.5 (C-4), 106.0 (C-1) and 91.6 (C-5), of proton at δ 5.98 (H-5) with carbons at δ 163.5 (C-4), 163.0 (C-6), 106.0 (C-1) and 96.2 (C-3), and of methoxyl group at δ 3.92 with carbon at δ 163.0 (C-6) confirmed the location of methoxyl group at C-6. Therefore, compound **BP4** was identified as helichrysetin which was previously isolated from *Helichrysum odoratissimum* (Puyvelde et al., 1989).

Table 10 ^{1}H, ^{13}C NMR, DEPT and HMBC spectral data of compound BP4

Position	δ_H (mult, *J*, Hz)	δ_C	DEPT	HMBC
α	7.75 (d, *J* = 15.3)	124.5	CH	β, C=O
β	7.73 (d, *J* = 15.3)	142.7	CH	α, C=O, 2′, 6′
1		106.0	C	
2		164.0	C	
3	6.00 (d, *J* = 1.8)	96.2	CH	1, 2, 4, 5
4		163.5	C	
5	5.98 (d, *J* = 1.8)	91.6	CH	1, 3, 4, 6
6		163.0	C	
1′		115.5	C	
2′	7.49 (d, *J* = 8.7)	130.3	CH	β, 3′, 4′, 5′
3′	6.85 (d, *J* = 8.7)	115.8	CH	1′, 2′, 4′, 6′
4′		159.1	C	
5′	6.85 (d, *J* = 8.7)	115.8	CH	1′, 2′, 4′, 6′
6′	7.49 (d, *J* = 8.7)	130.3	CH	β, 3′, 4′, 5′
C=O		192.6	C	
OMe	3.92 (s)	55.7	CH_3	6

1.3.1.5 Compound BP5

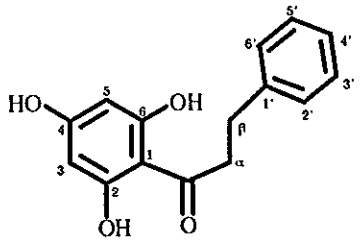

Compound **BP5** was isolated as yellow solid, mp 134-135 °C. Its UV (λ_{max} 222, 286, 327 nm) and IR (3297 and 1627 cm^{-1}) spectra displayed absorptions bands of hydroxyl and conjugated carbonyl group.

The ^{13}C NMR spectral data (Table 11, Figure 28) showed a total of 15 carbons with one carbonyl carbon at δ 205.1. The assignments of all carbons were

achieved by ^{13}C, DEPT, HMQC and HMBC experiments. The carbon chemical shift values suggested two methylene carbons (δ 45.5 and 30.8) and two aromatic rings with twelve aromatic carbons identified as seven protonated, (δ 128.4 (2C), 128.3 (2C), 126.2, 95.2 (2C)), five non-protonated, of which three oxygenated (δ 164.1 and 163.6 (2C)) and two non-oxygenated (δ 141.8 and 104.6) carbons were observed. The ^{1}H NMR spectral data (Table 11, Figure 27) exhibited the presence of a magnetically equivalent aromatic proton signal at δ 5.85 (2H, s, H-3 and H-5), a monosubstituted benzene ring at δ 7.15-7.31 (m), and two methylene proton signals at 3.38 and 2.99 (each t, J = 8.1 Hz). The HMBC correlations of proton at δ 2.99 (H-β) with carbons at δ 205.1 (C=O), 141.8 (C-1′) and 128.4 (C-2′/C-6′) confirmed the location of monosubstituted benzene ring at C-β. Thus compound **BP5** was determined as 2,4,6-trihydroxydihydrochalcone which was previously isolated from *Lindera unbellata* (Tanaka et al., 1984)

Table 11 ^{1}H, ^{13}C NMR, DEPT and HMBC spectral data of compound **BP5**

Position	δ_H (mult, J, Hz)	δ_C	DEPT	HMBC
α	3.38 (t, J = 8.1)	45.5	CH_2	β, C=O, 1′
β	2.99 (t, J = 8.1)	30.8	CH_2	α, C=O, 1′, 2′, 6′
1		104.6	C	
2		163.6	C	
3	5.85 (s)	95.2	CH	1, 2, 4, 5, 6
4		164.1	C	
5	5.85 (s)	95.2	CH	1, 2, 3, 4, 6
6		163.6	C	
1′		141.8	C	
2′	7.15-7.31 (m)	128.4*	CH	β, 1′, 3′, 4′, 5′
3′		128.3*	CH	1′, 2′, 4′, 6′
4′		126.2	CH	
5′		128.3*	CH	1′, 2′, 4′, 6′
6′		128.4*	CH	β, 1′, 3′, 4′, 5′
C=O		205.1	C	

*May be interchangeable.

1.3.1.6 Compound BP6

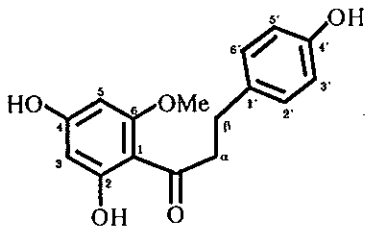

Compound **BP6** was isolated as yellow solid, mp 188-189 °C. The absorption bands for UV and IR spectrum were similar to compound **BP5**.

The ^{1}H NMR spectral data of compound **BP6** and **BP4** (Tables 12-14, Figures 29 and 30) showed structural similarity, except that the olefinic proton signals at δ 7.75 and 7.73 in compound **BP4** were not observed in compound **BP6**. The additional proton signals at δ 3.25 and 2.90 (each t, J = 8.1 Hz) were assigned to H-α and H-β, respectively. The assignment was confirmed by COSY spectrum. The connectivity of 1,4-disubstituted benzene ring was assigned by HMBC experiment in which the methylene protons at δ 2.90 (H-β) were connected at C-1′ of 1,4-disubstituted benzene ring by correlation with carbons at δ 204.8 (C=O), 132.7 (C-1′), 129.3 (C-2′/C-6′) and 46.0 (C-α). Thus compound **BP6** was postulated as 2,4,4′-trihydroxy-6-methoxydihydrochalcone which was previously isolated from *Goniothalamus gardneri* and *Goniothalamus thwaitesii* (Seidel et al., 2000).

Table 12 ^{1}H, ^{13}C NMR, DEPT and HMBC spectral data of compound **BP6**

Position	δ_H (mult, J, Hz)	δ_C	DEPT	HMBC
α	3.25 (t, J = 8.1)	46.0	CH_2	β, C=O, 1′
β	2.90 (t, J = 8.1)	30.0	CH_2	α, C=O, 1′, 2′, 6′
1		105.0	C	
2		166.7	C	
3	5.97 (br s)	96.0	CH	1, 4, 5, 6
4		164.6	C	
5	5.93 (br s)	91.2	CH	1, 2, 3, 4
6		163.4	C	
1′		132.7	C	

Table 12 (Continued)

Position	δ_H (mult, *J*, Hz)	δ_C	DEPT	HMBC
2′	7.08 (d, *J* = 8.1)	129.3	CH	β, 3′, 4′, 5′, 6′
3′	6.77 (d, *J* = 8.1)	115.2	CH	2′, 4′, 5′, 6′
4′		154.7	C	
5′	6.77 (d, *J* = 8.1)	115.2	CH	2′, 4′, 5′, 6′
6′	7.08 (d, *J* = 8.1)	129.3	CH	β, 3′, 4′, 5′, 6′
C=O		204.8	C	
OMe	3.85 (s)	55.4	CH_3	6

*May be interchangeable.

Table 13 Comparison of ^{1}H NMR spectral data of **BP4**, **BP5** and **BP6** (recorded in $CDCl_3$)

Position	BP4	BP5	BP6
	δ_H (mult, *J*, Hz)	δ_H (mult, *J*, Hz)	δ_H (mult, *J*, Hz)
α	7.75 (d, *J* = 15.3)	3.38 (t, *J* = 8.1)	3.25 (t, *J* = 8.1)
β	7.73 (d, *J* = 15.3)	2.99 (t, *J* = 8.1)	2.90 (t, *J* = 8.1)
3	6.00 (d, *J* = 1.8)	5.85 (s)	5.97 (br s)
5	5.98 (d, *J* = 1.8)	5.85 (s)	5.93 (br s)
2′	7.49 (d, *J* = 8.7)	7.15-7.31 (m)	7.08 (d, *J* = 8.1)
3′	6.85 (d, *J* = 8.7)		6.77 (d, *J* = 8.1)
4′			
5′	6.85 (d, *J* = 8.7)		6.77 (d, *J* = 8.1)
6′	7.49 (d, *J* = 8.7)		7.08 (d, *J* = 8.1)
OMe	3.92 (s)		3.85 (s)

Table 14 Comparison of ^{1}H NMR spectral data of **BP4, BP5, BP6**, helichrysetin, 2,4,6-trihydroxydihydrochalcone and 2,4,4′-trihydroxy-6-methoxydihydrochalcone (recorded in $CDCl_3$)

Position	BP4	BP5	BP6	A[a]	B[a]	C[b]
α	124.5	45.5	46.0	125.2	46.1	47.2
β	142.7	30.8	30.0	143.3	31.4	31.0
1	106.0	104.6	105.0	106.3	105.3	106.0
2	164.0	163.6	166.7	165.7	165.1	168.8
3	96.2	95.2	96.0	97.0	96.0	97.6
4	163.5	164.1	164.6	164.2	165.3	167.2
5	91.6	95.2	91.2	92.2	96.0	92.8
6	163.0	163.6	163.4	168.9	165.3	164.6
1′	115.5	141.8	132.7	128.0	133.6	133.2
2′	130.3	128.4*	129.3	131.2	130.1	130.6
3′	115.8	128.3*	115.2	116.8	116.0	106.0
4′	159.1	126.2	154.7	160.6	126.7	157.7
5′	115.8	128.3*	115.2	116.8	116.0	106.0
6′	130.3	128.4*	129.3	131.2	130.1	130.6
C=O	192.6	205.1	204.8	193.1	205.6	205.3
OMe	55.7		55.4	56.3		56.1

A = helichrysetin, B = 2,4,6-trihydroxydihydrochalcone,

C = 2,4,4′-trihydroxy-6-methoxydihydrochalcone

[a]Recorded in Me_2CO-d_6 (20 MHz)

[b]Recorded in C_5D_5N (100 MHz)

*May be interchangeable.

1.3.1.7 Compound BP7

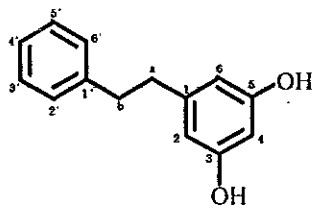

Compound **BP7** was obtained as a yellow viscous oil. The UV absorption bands at λ_{max} 224 and 279 nm supported the presence of an aromatic chromophore in the structure. The IR spectrum showed absorption bands of hydroxyl group (3372 cm^{-1}) and aromatic stretching (1602 cm^{-1}).

The ^{13}C NMR and DEPT spectral data (Table 15, Figure 32) indicated the presence of 14 carbons including 12 aromatic carbons and 2 aliphatic carbons. The ^{1}H NMR spectral data (Table 15, Figure 31) displayed the highfield resonances at δ 2.74 and 2.85 (each 2H, m) which were assigned as H-a and H-b, respectively. The aromatic proton signals at δ 6.23 (2H, d, J = 2.1 Hz) and 6.20 (1H, t, J = 2.1 Hz) suggested the presence of a 1,3,5-trisubstituted benzene ring whereas the other proton signals at δ 7.14-7.29 (m) confirmed a monosubstituted benzene ring.

The locations of 1,3,5-trisubstituted and monosubstituted benzene rings were confirmed by HMBC correlations of methylene protons at δ 2.74 (H-a) with carbons at δ 145.0 (C-1), 141.6 (C-1′), 108.2 (C-2/C-6) and 37.4 (C-b), and methylene protons at δ 2.85 (H-b) with carbons at δ 145.0 (C-1), 141.6 (C-1′), 128.5 (C-2′/C-6′) and 37.7 (C-a). Thus compound **BP7** was identified as dihydropinosylvin which was previously isolated from *Dioscorea rotundata* (Fagboun et al., 1987).

Table 15 ^{1}H, ^{13}C NMR, DEPT and HMBC spectral data of compound **BP7**

Position	δ_H (mult, J, Hz)	δ_C	DEPT	HMBC
a	2.74 (m)	37.7	CH_2	b, 1, 1′, 2, 6
1		145.0	C	
2	6.23 (d, J = 2.1)	108.2	CH	a, 3, 4, 6
3		156.6	C	
4	6.20 (t, J = 2.1)	100.6	CH	2, 3, 5, 6

Table 15 (Continued)

Position	δ_H (mult, *J*, Hz)	δ_C	DEPT	HMBC
5		156.6	C	
6	6.23 (d, *J* = 2.1)	108.2	CH	a, 2, 3, 4
b	2.85 (m)	37.4	CH_2	a, 1, 1′, 2′, 6′
1′		141.6	C	
2′		128.5	CH	
3′		128.4	CH	
4′	7.14-7.29 (m)	126.0	CH	
5′		128.4	CH	
6′		128.5	CH	

1.3.1.8 Compound BP8

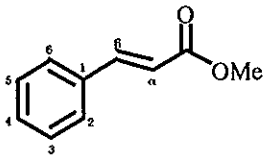

Compound BP8 was obtained as a colorless oil. The UV (λ_{max} 214, 220 and 270 nm) and IR (1709 cm^{-1}) absorption bands supported the presence of conjugated carbonyl ester in the structure.

The ^{13}C NMR and DEPT spectral data (Table 16, Figure 34) indicated the presence of 10 carbons including 6 aromatic, one carbonyl and one methoxyl carbons. The ^{1}H NMR spectral data (Table 16, Figure 33) displayed two olefinic protons at δ 6.43 and 7.69 (each 1H, d, *J* = 15.9 Hz) which were identified as *trans*-double bond at C-α and C-β, respectively. The aromatic proton signals at δ 7.35-7.52 (m) were assigned as a monosubstituted benzene ring. In addition, the ^{1}H NMR spectrum displayed the presence of a methoxyl group at δ 3.78 which showed correlation with carbon at δ 167.4 (C=O) from HMBC experiments. Therefore, compound BP8 was determined as methyl *trans*-cinnamate which was previously isolated from *Alpinia speciosa* (Itokawa et al., 1981).

Table 16 ^{1}H, ^{13}C NMR, DEPT and HMBC spectral data of compound BP8

Position	δ_H (mult, *J*, Hz)	δ_C	DEPT	HMBC
α	6.43 (d, *J* = 15.9)	117.8	CH	β, C=O, 1
β	7.69 (d, *J* = 15.9)	144.9	CH	α, C=O, 1, 2, 6
1		134.4	C	
2	7.49-7.52 (m)	128.1	CH	β, 3, 5, 6
3	7.35-7.37 (m)	128.9	CH	1, 2, 5, 6
4		130.2	CH	2, 3, 5, 6
5		128.9	CH	1, 2, 3, 6
6	7.49-7.52 (m)	128.1	CH	β, 3, 5, 6
C=O		167.4	C	
OMe	3.78 (s)	51.6	CH_3	C=O

1.3.1.9 Compound BP9

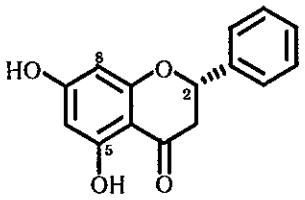

Compound **BP9** was isolated as a white solid, mp: 218-219 °C, $[\alpha]_D^{26}$: -51.2° (c 0.23, MeOH). The UV absorption bands (207, 284 and 320 nm) suggested that conjugated-carbonyl chromophore was in the molecule. Its IR spectrum showed hydroxyl (3392 cm^{-1}) and carbonyl (1693 cm^{-1}) functionalities. The ^{1}H NMR spectral data (Table 17, Figure 35) displayed ABX system at δ 5.36 (dd, *J* = 12.9, 3.3 Hz, H-2), 3.03 (dd, *J* = 17.4, 12.9 Hz, H-3ax) and 2.75 (dd, *J* = 17.4, 3.3 Hz, H-3eq) and monosubstituted benzene ring at δ 7.45-7.32. The *singlet* signal at δ 6.02 (2H, s) was deduced to be H-6 and H-8. In addition, ^{1}H NMR spectral data displayed a *singlet* signal of chelated hydroxyl group at δ 12.10 and a broad *singlet* at δ 10.11 whose signals suggested the locations of hydroxyl at C-5 and C-7, respectively. ^{1}H NMR spectral data of **BP9** were similar to pinocembrin (Lui et al.,1992 and Su et al., 2003). The optical rotation of compound **BP9** is a levorotatory ($[\alpha]_D$ = -51.2°), the same as pinocembrin

(lit. $[\alpha]_D^{23}$ = -58.5°) (Su et al., 2003) suggesting the same configuration at C-2. Thus compound **BP9** was assigned as pinocembrin.

Table 17 ^{1}H and ^{13}C NMR ($CDCl_3$+DMSO-d_6) spectral data of compound **BP9** and pinocembrin

Position	BP9		Pinocembrin (DMSO-d_6)	
	δ_H (mult, *J*, Hz)	δ_C	δ_H (mult, *J*, Hz)	δ_C
2	5.36 (dd, *J* = 12.9, 3.3)	78.9	5.58 (dd, *J* = 13.0, 3.0)	78.2
3	2.75 (dd, *J* = 17.4, 3.3)	43.2	2.72 (dd, *J* = 18.0, 3.0)	42.0
	3.03 (dd, *J* = 17.4, 12.9)		3.23 (dd, *J* = 18.0, 13.0)	
4		195.4		195.5
4a		102.4		101.6
5		164.2		163.5
6	6.02 (s)	96.8	5.90 (d, *J* = 2.1)	95.8
7		167.0		166.6
8	6.02 (s)	95.7	5.93 (d, *J* =2.1)	94.9
8a		163.0		162.6
1′		138.6		138.6
2′/6′	7.45-7.32 (m)	126.2	7.55-7.41 (m)	126.4
3′/5′		128.7		128.7
4′		128.7		128.7
5-OH	12.10 (s)		12.13 (s)	
7-OH	10.11 (brs)			

1.3.1.10 Compound BP10

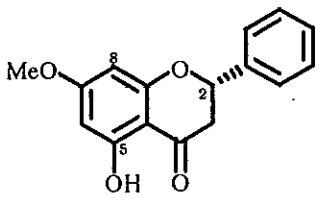

Compound **BP10** was isolated as a white solid, mp: 220-221 °C, $[\alpha]_D^{26}$: -49.9° (c 0.54, MeOH). The absorption bands for UV and IR spectrum were similar to **BP10**. The ^{1}H NMR spectral data (Table 18, Figure 37) of **BP10** and **BP9** showed structural similarity, except for the appearance of a methoxyl signal at δ 3.76 whose location was assigned at C-7. Therefore, compound **BP10** was identified as pinostrobin (Su et al., 2003).

Table 18 ^{1}H and ^{13}C NMR ($CDCl_3$+DMSO-d_6) spectral data of **BP9** and **BP10**

Position	BP10		BP9	
	δ_H (mult, *J*, Hz)	δ_C	δ_H (mult, *J*, Hz)	δ_C
2	5.35 (dd, *J* = 12.9, 3.0)	79.2	5.36 (dd, *J* = 12.9, 3.3)	78.9
3	2.77 (dd, *J* = 17.4, 3.0)	43.3	2.75 (dd, *J* = 17.4, 3.3)	43.2
	3.03 (dd, *J* = 17.4, 12.9)		3.03 (dd, *J* = 17.4, 12.9)	
4		195.8		195.4
4a		103.1		102.4
5		164.2		164.2
6	6.02 (d, *J* = 2.1)	95.2	6.02 (s)	96.8
7		168.0		167.0
8	6.05 (d, *J* = 2.1)	94.3	6.02 (s)	95.7
8a		162.8		163.0
1′		138.4		138.6
2′/6′	7.44-7.36 (m)	126.2	7.45-7.32 (m)	126.2
3′/5′		128.9		128.7
4′		128.9		128.7
5-OH	12.00 (s)		12.10 (s)	
7-OMe	3.76 (br s)	56.3		

1.3.1.11 Compound BP11

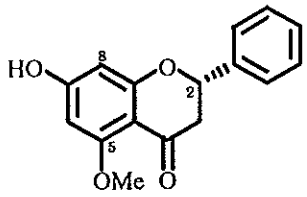

Compound **BP11** was isolated as a white solid, mp.: 217-218 °C, $[\alpha]_D^{26}$: -57.5° (c 0.38, MeOH). The absorption bands for UV and IR spectrum were similar to **BP10**. The ^{1}H NMR spectral data (Table 19, Figure 39) of **BP11** and **BP10** showed structural similarity, except for the absence of a chelated-hydroxyl signal at δ 12.00. In addition, the broad *singlet* at δ 9.98 was deduced to OH at C-7. Thus, compound **BP11** was identified as alpinetin (Itokawa et al., 1981).

Table 19 ^{1}H and ^{13}C NMR spectral data* of compounds **BP10** and **BP11**

Position	BP10		BP11	
	δ_H (mult, *J*, Hz)	δ_C	δ_H (mult, *J*, Hz)	δ_C
2	5.35 (dd, *J* = 12.9, 3.0)	79.2	5.37 (dd, *J* = 12.9, 3.0)	78.8
3	2.77 (dd, *J* = 17.4, 3.0)	43.3	2.76 (dd, *J* = 16.5, 3.0)	45.6
	3.03 (dd, *J* = 17.4, 12.9)		2.98 (dd, *J* = 16.5, 12.9)	
4		195.8		189.1
4a		103.1		105.0
5		164.2		164.7
6	6.02 (d, *J* = 2.1)	95.2	6.09 (d, *J* = 2.1)	96.4
7		168.0		164.9
8	6.05 (d, *J* = 2.1)	94.3	6.13 (d, *J* = 2.1)	93.6
8a		162.8		162.7
1′		138.4		139.0
2′/6′	7.44-7.36 (m)	126.2	7.47-7.35 (m)	126.1
3′/5′		128.9		128.6
4′		128.9		128.5
5-OR	12.00 (s) (R = H)		3.87 (s) (R = Me)	56.0
7-OR	3.76 (s) (R = Me)	56.3	9.98 (s) (R = H)	

*Recorded in $CDCl_3$+DMSO-d_6

1.3.2 Structural elucidation of compounds from *C. crista*

1.3.2.1 *Determination of isolated compounds from the stems of C. crista*

Eight new cassane-type diterpenes, (SC1-SC7 and SC9), and two known compounds, (SC8 and SC10), were isolated from the stems of *C. crista*. Their structures were elucidated on the basis of spectral analysis. In addition, the structure of compound SC1 was confirmed by X-ray diffraction analysis.

1.3.2.1.1 Compound SC1

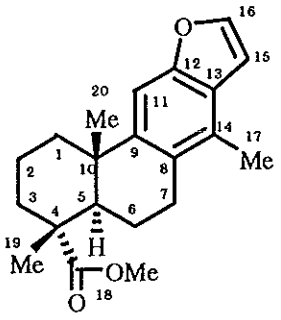

Compound SC1 was found to have the molecular formula $C_{21}H_{26}O_3$ ($[M]^+$ *m/z* 326.1887) by HREIMS. The IR (1723 and 771 cm^{-1}) and UV (λ_{max} 212, 260, 282 and 292 nm) absorption bands were characteristic of ester carbonyl and benzofuran moieties, respectively.

The ^1H NMR spectrum (Table 20, Figure 41) displayed the presence of two tertiary methyl groups at δ 1.27 (Me-20) and 1.31 (Me-19), and one aromatic methyl group at δ 2.35 (Me-17). In addition, there was a singlet at δ 3.70 (OMe) due to the presence of a methyl ester group. The presence of a 1,2-disubstituted furan was evident in the ^1H NMR spectrum from the downfield signals at δ 6.72 (dd, *J* = 2.1, 0.9 Hz, H-15) and 7.53 (d, *J* = 2.1 Hz, H-16). An aromatic proton at δ 7.32 (br s, H-11) along with the aromatic methyl group at δ 2.35 confirmed the presence of trisubstituted benzofuran moiety in SC1. The methine proton at δ 2.27 (dd, *J* = 12.9, 2.4 Hz, H-5) was shown to be connected to a methine carbon at δ 44.4 (C-5) from the HMQC experiment. The ^{13}C NMR spectral data (Table 20, Figure 42) with the analysis of DEPT experiments exhibited signal of an ester carbonyl carbon at δ 179.2 (C-18) and of the

benzofuran ring moiety at δ 104.3 (C-11), 105.0 (C-15), 125.4 (C-13), 127.5 (C-8), 128.3 (C-14), 144.2 (C-16), 147.2 (C-9) and 153.6 (C-12). Except for a methoxyl group the carbon framework of **SC1** had 20 carbon signals indicating it to be a cassane-type diterpene.

In the HMBC spectrum, the methyl proton at δ 1.31 (Me-19) correlated with the carbons at δ 36.6 (C-3), 44.4 (C-5), 47.7 (C-4) and 179.2 (C-18), and methyl proton at δ 1.27 (Me-20) with carbons at δ 37.8 (C-10), 38.9 (C-1), 44.4 (C-5) and 147.2 (C-9). These evidences indicated that the protons Me-19 and Me-20 were attached to carbons C-4 and C-10, respectively. In addition, the methyl ester at δ 3.70 showed long-range correlation with ester carbonyl carbon at δ 179.2, confirming that carbonyl carbon was C-18. The relative stereochemistry of **SC1** was determined on the basis of coupling constants and NOESY experiments. The large *J* value of proton H-5 (*J* = 12.9 Hz) indicated that H-5 should be α-axial oriented. In the NOESY, methyl protons at δ 1.27 (Me-20) showed cross-peak with δ 1.31 (Me-19), 1.55 (H-6β) and 1.74 (H-2β), suggesting that Me-20 and Me-19 should be β-axial oriented. From these data, compound **SC1** was deduced to be taepeenin A, a new compound (Cheenpracha et al., 2005) and its structure was additionally confirmed by X-ray diffraction analysis (Figure 4).

Table 20 ^{1}H, ^{13}C NMR, DEPT and HMBC spectral data of compound **SC1**

Position	δ_H (mult, *J*, Hz)	δ_C	DEPT	HMBC
1	2.38 (m), 1.55 (m)	38.9	CH_2	3, 5, 10
2	1.81 (m), 1.74 (m)	18.8	CH_2	4, 10
3	1.80 (m), 1.68 (m)	36.6	CH_2	1, 2, 4, 5, 18, 19
4		47.7	C	
5	2.27 (dd, *J* = 12.9, 2.4)	44.4	CH	4, 6, 7, 9, 10, 18, 19, 20
6	1.92 (m), 1.55 (m)	21.8	CH_2	5, 7
7	2.83 (m)	27.6	CH_2	5, 6, 8, 9
8		127.5	C	
9		147.2	C	
10		37.8	C	
11	7.32 (br s)	104.3	CH	8, 9, 10, 12, 13

Table 20 (Continued)

Position	δ_H (mult, *J*, Hz)	δ_C	DEPT	HMBC
12		153.6	C	
13		125.4	C	
14		128.3	C	
15	6.72 (dd, *J* = 2.1, 0.9)	105.0	CH	12, 13, 16
16	7.53 (d, *J* = 2.1)	144.2	CH	12, 13, 15
17	2.35 (s)	15.9	CH_3	8, 13, 14
18		179.2	C	
19	1.31 (s)	16.6	CH_3	3, 4, 5, 18
20	1.27 (s)	25.6	CH_3	1, 5, 9, 10
18-O*Me*	3.70 (s)	52.0	CH_3	18

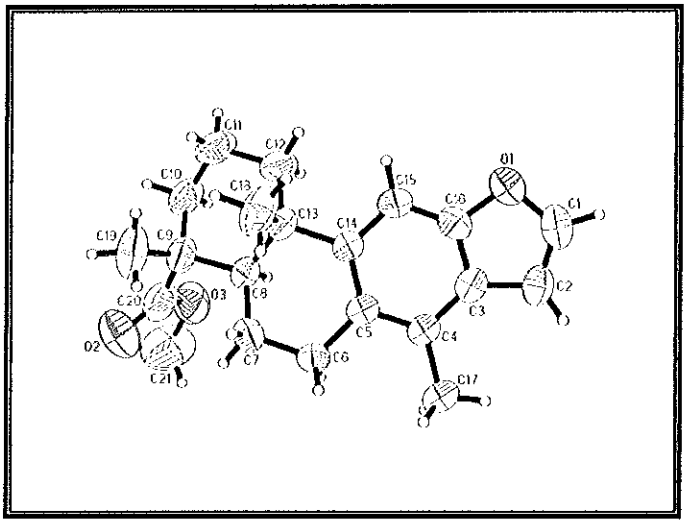

Figure 4 ORTEP drawing of compound **SC1**

1.3.2.1.2 Compound SC2

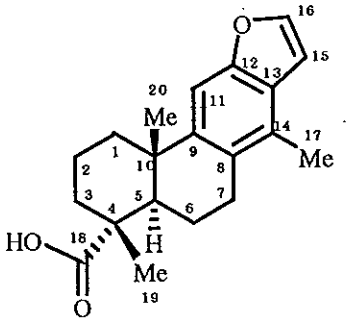

Compound SC2 showed the molecular ion $[M]^+$ at *m/z* 312.1733 in HRFABMS spectrum in agreement with the formula $C_{20}H_{24}O_3$. The presence of carboxyl (3418 and 1691 cm^{-1}) functionality was evident from IR absorptions.

The ^1H and ^{13}C NMR spectra (Table 21, Figures 43 and 44) of SC2 showed characteristics similar to those of SC1 except for the disappearance of the OMe signal at δ 3.70, thus indicating a presence of a free carboxylic acid instead of the methyl ester at C-18. This finding was supported by HMBC spectrum of SC2, in which the methyl protons at δ 1.31 (Me-19) were correlated with the carbons at δ 36.7 (C-3), 44.1 (C-5), 47.4 (C-4) and 184.2 (C-18). Therefore, compound SC2 was determined to be taepeenin B, a new compound (Cheenpracha et al., 2005).

Table 21 ^1H, ^{13}C NMR, DEPT and HMBC spectral data of compound SC2

Position	δ_H (mult, *J*, Hz)	δ_C	DEPT	HMBC
1	2.38 (m), 1.60 (m)	38.8	CH_2	2, 5
2	1.84 (m)	18.7	CH_2	4
3	1.87 (m), 1.77 (m)	36.7	CH_2	4
4		47.4	C	
5	2.27 (dd, *J* = 12.6, 2.1)	44.1	CH	1, 4, 6 ,7, 18, 19, 20
6	1.95 (m), 1.70 (m)	21.8	CH_2	8
7	2.94 (m), 2.84 (m)	27.5	CH_2	5, 6, 8 , 9, 14
8		128.3	C	
9		147.0	C	
10		37.8	C	
11	7.31 (br s)	104.3	CH	8, 10, 12, 13

Table 21 (Continued)

Position	δ_H (mult, *J*, Hz)	δ_C	DEPT	HMBC
12		153.5	C	
13		125.4	C	
14		127.4	C	
15	6.71 (dd, *J* = 2.1, 0.9)	105.0	CH	12, 13, 16
16	7.52 (d, *J* = 2.1)	144.2	CH	12, 13, 15
17	2.34 (s)	15.9	CH_3	8, 13, 14
18		184.2	C	
19	1.31 (s)	16.3	CH_3	3, 5, 4, 18
20	1.27 (s)	25.6	CH_3	1, 5, 9

1.3.2.1.3 Compound SC3

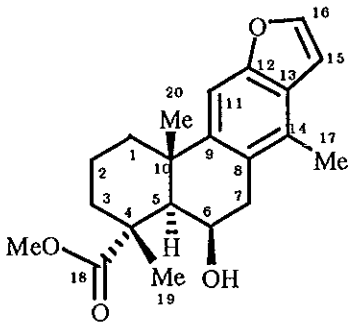

Compound SC3 with the molecular formula $C_{21}H_{26}O_4$ ($[M]^+$ *m/z* 342.1825) as determined by HREIMS showed IR and UV absorption bands similar to those of SC1 with additional hydroxyl (3419 cm^{-1}) stretching.

The ^1H and ^{13}C NMR spectral data (Table 22, Figures 45 and 46) revealed that compound SC3 had the same cassane-type skeleton as SC1. The ^1H NMR spectral data (Table 22) exhibited a signal due to an oxymethine proton at δ 4.26 (br dt, *J* = 5.4, 1.8 Hz) for H-6 which was connected to oxymethine carbon at δ 68.7 (C-6) in the HMQC spectrum. This proton signal showed HMBC correlations with carbons at δ 37.8 (C-10), 48.5 (C-4) and 124.2 (C-8), confirming the location of the hydroxyl group at C-6. The α-orientation of both protons at C-5 and C-6 was determined from the results of small coupling constants of protons H-5 (δ 2.33, br s) and H-6 (δ 4.26, dd, *J* = 5.4, 1.8 Hz) and the observed cross-peaks between these protons and H-7α (δ 3.10)

from NOESY experiments. This result suggested that H-5 and H-6 should be α-axial and α-equatorial oriented, respectively. Therefore, compound SC3 was deduced to be taepeenin C, a new compound (Cheenpracha et al., 2005).

Table 22 ^{1}H, ^{13}C NMR, DEPT and HMBC spectral data of compound SC3

Position	δ_H (mult, *J*, Hz)	δ_C	DEPT	HMBC
1	2.26 (m), 1.53 (m)	42.2	CH_2	2, 5, 10, 20
2	1.91 (m)	19.1	CH_2	4
3	1.85 (m), 1.70 (m)	38.1	CH_2	2, 5, 10, 18
4		48.5	C	
5	2.33 (br s)	47.5	CH	1, 4, 6 ,7, 9, 18, 19, 20
6	4.26 (br dt, *J* = 5.4, 1.8)	68.7	CH	4, 8, 10
7	3.10 (dd, *J* = 17.4, 5.4) 2.87 (br d, *J* = 17.4)	38.8	CH_2	5, 6, 8 , 9, 14
8		124.2	C	
9		146.1	C	
10		37.8	C	
11	7.35 (br s)	105.1	CH	8, 9, 10, 12, 13
12		153.8	C	
13		125.7	C	
14		128.7	C	
15	6.71 (dd, *J* = 2.4, 0.6)	105.0	CH	12, 13, 16
16	7.52 (d, *J* = 2.4)	144.3	CH	12, 13, 15
17	2.34 (s)	16.1	CH_3	8, 13, 14
18		179.3	C	
19	1.64 (s)	18.6	CH_3	3, 5, 18
20	1.64 (s)	27.5	CH_3	1, 5, 9
18-O*Me*	3.70 (s)	52.1	CH_3	18

1.3.2.1.4 Compound SC4

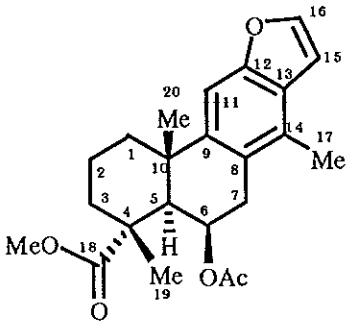

Compound SC4 had the molecular formula $C_{23}H_{28}O_5$ ($[M]^+$ at *m/z* 384.1936), based on HREIMS. The ^1H and ^{13}C NMR spectral data (Table 23, Figures 47 and 48) of SC4 were closely related to those of SC3, except for the presence of an additional acetyl group (δ_H 2.00 and δ_C 170.7, 21.7). The oxymethine proton H-6 of SC4 appeared at δ 5.30 (dt, *J* = 5.7, 1.5 Hz), more downfield than that of SC3 (δ 4.26, br dt, *J* = 5.4, 1.8 Hz) as a result of the deshielding effect of the OAc group and showed HMBC correlations with the carbons at δ 38.0 (C-10), 46.1 (C-5), 48.0 (C-4), 123.8 (C-8) and 170.7 (*OCO*Me) confirming the location of the OAc group at C-6. Thus, compound SC4 was characterized as taepeenin D, a new compound (Cheenpracha et al., 2005).

Table 23 ^1H, ^{13}C NMR, DEPT and HMBC spectral data of compound SC4

Position	δ_H (mult, *J*, Hz)	δ_C	DEPT	HMBC
1	2.31 (m), 1.58 (m)	42.1	CH_2	5, 10
2	1.92 (m), 1.76 (m)	19.0	CH_2	4, 10
3	1.79 (m), 1.67 (m)	38.4	CH_2	18
4		48.0	C	
5	2.50 (br s)	46.1	CH	1, 3, 4, 9, 10, 18, 19, 20
6	5.30 (dt, *J* = 5.7, 1.5)	70.7	CH	4, 5, 10, 6-*CO*
7	3.12 (dd, *J* = 18.3, 5.4)	34.8	CH_2	8 , 9, 14
	2.96 (br d, *J* = 18.3)			
8		123.8	C	
9		145.5	C	
10		38.0	C	

Table 23 (Continued)

Position	δ_H (mult, *J*, Hz)	δ_C	DEPT	HMBC
11	7.38 (s)	105.0	CH	8, 12, 13, 10
12		153.7	C	
13		125.8	C	
14		128.7	C	
15	6.73 (dd, *J* = 2.4, 0.9)	105.0	CH	12, 13, 16
16	7.54 (d, *J* = 2.4)	144.5	CH	12, 13, 15
17	2.33 (s)	16.1	CH_3	8, 13, 14
18		178.6	C	
19	1.45 (s)	18.1	CH_3	3, 4, 5, 18
20	1.64 (s)	27.6	CH_3	1, 5, 9, 10
6-*CO*		170.7	C	
6-CO*Me*	2.00 (s)	21.7	CH_3	6-*CO*
18-O*Me*	3.71 (s)	52.3	CH_3	18

1.3.2.1.5 Compound SC5

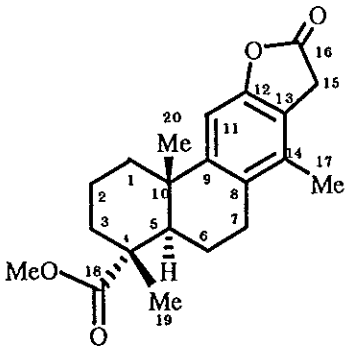

Compound SC5, $C_{21}H_{26}O_4$ ([M]$^+$ *m/z* 342.1836 by HREIMS), exhibited additional IR absorption band at 1811 (lactone carbonyl) cm^{-1}. The ^{1}H and ^{13}C NMR spectral data (Table 24, Figures 49 and 50) of SC5 were comparable to those of SC1, except for the presence of a singlet signal of methylene protons (δ 3.61) instead of the two proton signals of a 1,2-disubstituted furan. These methylene protons showed the HMBC correlations with the carbons at δ 119.8 (C-13), 132.9 (C-14), 152.7 (C-12) and lactone carbonyl at δ 174.7 (C-16), indicating them (2H-15) to be connected to the

lactone carbonyl and aromatic carbons at C-16 and C-13, respectively. Thus, compound SC5 was assigned to be taepeenin F, a new compound (Cheenpracha et al., 2005).

Table 24 ^{1}H, ^{13}C NMR, DEPT and HMBC spectral data of compound SC5

Position	δ_H (mult, *J*, Hz)	δ_C	DEPT	HMBC
1	2.27 (m), 1.47 (m)	38.4	CH_2	2, 5
2	1.79 (m)	18.5	CH_2	1, 5
3	1.78 (m), 1.65 (m)	36.5	CH_2	1, 2, 5
4		47.6	C	
5	2.19 (dd, *J* = 12.6, 2.1)	44.2	CH	1, 4, 7, 9, 18, 20
6	1.54 (m)	21.4	CH_2	4
7	2.74 (m), 2.64 (m)	27.4	CH_2	5, 6, 8, 9, 14
8		129.2	C	
9		150.7	C	
10		37.8	C	
11	6.90 (s)	104.1	CH	8, 10, 12, 13
12		152.7	C	
13		119.8	C	
14		132.9	C	
15	3.61 (s)	32.5	CH_2	12, 13, 14, 16
16		174.7	C	
17	2.10 (s)	16.4	CH_3	8, 13, 14
18		179.0	C	
19	1.25 (s)	16.5	CH_3	3, 4, 5, 18
20	1.28 (s)	25.1	CH_3	1, 5, 9, 10
18-O*Me*	3.68 (s)	52.0	CH_3	18

1.3.2.1.6 Compound SC6

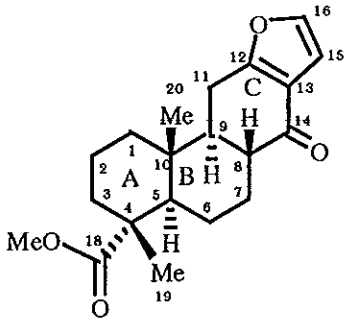

Compound SC6 had the molecular formula $C_{20}H_{26}O_4$ ($[M]^+$ *m/z* 330.1832) as determined by HREIMS. The ^{13}C NMR and DEPT spectra (Table 25) exhibited 20 carbons, two of these were a conjugated carbonyl (δ 195.7) and an ester carbonyl (δ 178.9). Excluding the signal due to the methoxy substituent, SC6 contained only 19 carbons in the main carbon framework, suggesting it to be a norditerpene. The ^1H and ^{13}C NMR spectral data (Table 25, Figures 51 and 52) of SC6 revealed that this compound had the same A and B rings as SC1. The difference was found in ring C which was aliphatic in SC6. This was supported by the absence of one aromatic proton at δ 7.32 (H-11) in the ^1H NMR spectrum and the presence of methylene protons at δ 2.66 (dd, *J* =17.1, 12.0 Hz, H-11β), 2.90 (dd, *J* = 17.1, 5.1 Hz, H-11α) and two methine protons at δ 1.88 (td, *J* = 12.0, 5.1 Hz, H-9) and 2.31 (td, *J* = 12.0, 4.2 Hz, H-8). The observed HMBC correlations between a methine proton at δ 1.88 (H-9) with carbons at δ 14.8 (C-20), 36.9 (C-10) 49.0 (C-5), 166.3 (C-12) and 195.7 (C-14), of a methine proton at δ 2.31 (H-8) with carbons at δ 22.8 (C-11), 23.5 (C-6), 52.9 (C-9) and 195.7 (C-14) and of a methine proton at δ 6.63 (H-15) with carbons at δ 166.3 (C-12) and 195.7 (C-14), indicated that the conjugated carbonyl should be C-14. The relative stereochemistry of SC6 was determined on the basis of coupling constants and the results of NOESY experiments. The large *J* values for H-8 and H-9 (*J* = 12.0 Hz) indicated that H-8 and H-9 should be axial protons. From the NOESY correlations, the methyl group at δ 1.01 (Me-20) showed a cross-peak with the methyl protons at δ 1.21 (Me-19) and a methine proton at δ 2.31 (H-8), suggesting that Me-19, Me-20 and H-8 should be in β-axial orientation. From these data, the new compound SC6 was characterized as nortaepeenin A (Cheenpracha et al., 2005).

Table 25 ^{1}H, ^{13}C NMR, DEPT and HMBC spectral data of compound SC6

Position	δ_H (mult, *J*, Hz)	δ_C	DEPT	HMBC
1	1.74 (m)	37.9	CH_2	3, 5, 9, 20
	1.14 (m)			
2	1.69 (m)	17.9	CH_2	4, 10
3	1.62 (m)	36.7	CH_2	1, 5, 18, 19
4		47.3	C	
5	1.78 (dd, *J* = 12.3, 2.4)	49.0	CH	3, 4, 6, 7, 9, 10, 18, 19, 20
6	1.49 (m)	23.5	CH_2	7, 8, 10
	1.29 (m)			
7	2.46 (m)	26.8	CH_2	5, 8, 9, 14
	1.31 (m)			
8	2.31 (td, *J* = 12.0, 4.2)	45.0	CH	6, 7, 9, 11, 14
9	1.88 (td, *J* = 12.0, 5.1)	52.9	CH	5, 7, 8, 10, 11, 12, 14, 20
10		36.9	C	
11	2.90 (dd, *J* = 17.1, 5.1)	22.8	CH_2	8, 9, 10, 12, 13, 14
	2.66 (dd, *J* = 17.1, 12.0)			
12		166.3	C	
13		119.8	C	
14		195.7	C	
15	6.63 (d, *J* = 1.8)	106.5	CH	12, 13, 16
16	7.30 (d, *J* = 1.8)	142.8	CH	12, 13, 15
18		178.9	C	
19	1.21 (s)	16.8	CH_3	3, 4, 5, 18
20	1.01 (s)	14.8	CH_3	1, 5, 9, 10
18-O*Me*	3.65 (s)	52.0	CH_3	18

1.3.2.1.7 Compound SC7

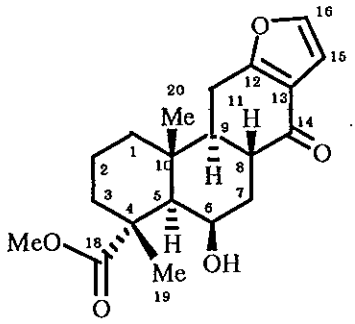

Compound SC7 showed the $[M]^+$ at *m/z* 346.1787 ($C_{20}H_{26}O_5$) in HREIMS. Its IR spectrum displayed a hydroxyl stretching at 3415 cm^{-1}. The ^1H and ^{13}C NMR spectral data (Table 26, Figures 53 and 54) revealed that SC7 had the same norcassane-type diterpene as SC6. The minor difference was found on replacement of a multiplet signal of methylene protons at δ 1.49 and 1.29 (2H-6) with an oxymethine proton at δ 4.03 which gave the HMQC cross-peak to the carbon at δ 69.3. This proton showed HMBC correlations with the carbons at δ 37.1 (C-7), 37.5 (C-10), 40.8 (C-8) and 48.2 (C-4). The configuration at C-6 was determined as β-OH by the cross-peak between H-5 (δ 1.80), H-6 (δ 4.03) and H-7α (δ 2.48) in NOESY experiments and the small coupling constant of H-5 (br s) and H-6 (m). Thus, compound SC7 was identified as nortaepeenin B, a new compound (Cheenpracha et al., 2005).

Table 26 ^1H, ^{13}C NMR, DEPT and HMBC spectral data of compound SC7

Position	δ_H (mult, *J*, Hz)	δ_C	DEPT	HMBC
1	1.72 (m), 1.19 (m)	40.6	CH_2	3, 5, 9, 20
2	1.78 (m)	18.1	CH_2	3
3	1.78 (m), 1.56 (m)	38.6	CH_2	5, 19
4		48.2	C	
5	1.80 (br s)	51.0	CH	4, 6, 7, 9, 18, 19, 20
6	4.03 (m)	69.3	CH	7, 8, 10
7	2.48 (dt, *J* = 14.4, 3.6)	37.1	CH_2	6, 9, 14
	1.50 (m)			
8	2.76 (td, *J* = 12.0, 3.6)	40.8	CH	7, 9, 10, 13, 14

Table 26 (Continued)

Position	δ_H (mult, *J*, Hz)	δ_C	DEPT	HMBC
9	1.91 (td, *J* = 12.0, 5.4)	53.3	CH	1, 5, 7, 8, 12, 14
10		37.5	C	
11	2.93 (dd, *J* = 17.1, 5.4)	22.6	CH_2	8, 9, 12, 13, 14
	2.76 (dd, *J* = 17.1, 12.0)			
12		166.6	C	
13		119.9	C	
14		196.1	C	
15	6.64 (d, *J* = 1.8)	106.5	CH	12, 13, 16
16	7.31 (d, *J* = 1.8)	142.8	CH	12, 13, 15
18		179.0	C	
19	1.59 (s)	19.0	CH_3	3, 4, 5
20	1.35 (s)	17.8	CH_3	1, 5, 9, 10
18-O*Me*	3.68 (s)	52.1	CH_3	18

1.3.2.1.8 Compound SC8

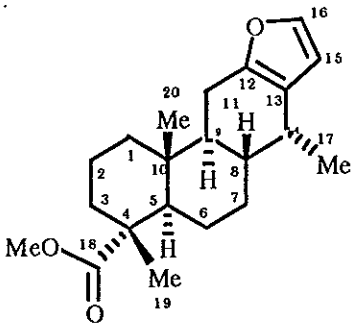

Compound SC8 was isolated as a colorless viscous oil and showed absorption band of carbonyl group at 1725 cm^{-1} by IR spectrum. The ^1H and ^{13}C NMR spectral data (Table 27, Figures 55 and 56) were similar to those of SC6, except for the replacement of the carbonyl carbon signal by that of a methine proton at δ 2.62 (m) and a methyl group at δ 0.99 (d, *J* = 7.2 Hz), whose location was deduced to be on C-14 on the basis of the HMBC correlations of H-11, H-16 and H-17 with the quaternary carbon

at C-13. Thus, compound SC8 was assigned as methyl vinhaticoate which was previously isolated from *Plathymenia* genus (Matos et al., 1984).

Table 27 ^{1}H, ^{13}C NMR, DEPT and HMBC spectral data of compound SC8

Position	δ_H (mult, *J*, Hz)	δ_C	DEPT	HMBC
1	1.74 (m), 1.16 (m)	38.6	CH_2	3, 5, 20
2	1.58 (m)	17.9	CH_2	
3	1.79 (m), 1.59 (m)	36.8	CH_2	4, 5, 18, 19
4		47.5	C	
5	1.79 (m)	49.7	CH	1, 3, 4, 6, 7, 20
6	1.50 (m), 1.19 (m)	24.1	CH_2	
7	1.69 (m), 1.44 (m)	30.8	CH_2	5
8	2.33 (m)	35.7	CH	6, 9, 10, 13
9	1.59 (m)	45.7	CH	5, 8, 12, 13
10		36.9	C	
11	2.58 (dd, *J* = 16.8, 7.2)	22.0	CH_2	8, 9, 10, 12, 13
	2.38 (dd, *J* = 16.8, 9.9)			
12		149.4	C	
13		122.5	C	
14	2.62 (m)	31.5	CH	7, 8, 9, 12, 13
15	6.19 (d, *J* = 1.8)	109.5	CH	12, 16
16	7.23 (d, *J* = 1.8)	140.4	CH	12, 13, 15
17	0.99 (d, *J* = 7.2)	17.6	CH_3	8, 13, 14
18		179.4	C	
19	1.23 (s)	17.0	CH_3	3, 4, 5, 18
20	0.94 (s)	14.6	CH_3	1, 5, 9, 10
18-O*Me*	3.69 (s)	51.9	CH_3	18

1.3.2.1.9 Compound SC9

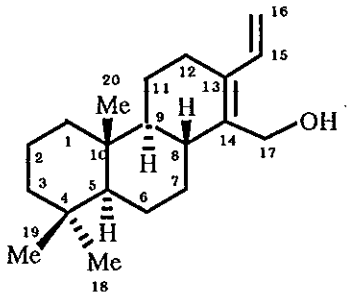

Compound SC9 was deduced as $C_{20}H_{32}O$ ($[M]^+$ *m/z* 288.2455 by HREIMS). The hydroxyl functionality was shown in IR absorption at 3396 cm^{-1}.

The ^1H NMR spectral data (Table 28, Figure 57) showed three singlets of three methyl groups at δ 0.83 (Me-18), 0.84 (Me-20) and 0.85 (Me-19), a typical pattern of vinyl protons at δ 6.86 (dd, *J* = 17.1, 10.8 Hz, H-15), 5.23 (d, *J* = 17.1 Hz, H-16a) and 5.07 (d, *J* = 10.8 Hz, H-16b). The presence of oxymethylene protons were revealed by ^1H NMR signals at δ 4.26 and 4.33 (each d, *J* = 11.7 Hz, 2H-17) connecting to carbon at δ 59.1. The ^{13}C NMR spectrum (Tables 28 and 29, Figure 58) with analysis of DEPT experiments displayed 20 carbons; four of these were sp^2 carbons: attributable to two quaternary carbons (δ 133.5, 139.3), one methine carbon (δ 134.4) and a methylene carbon (δ 113.4).

From the HMBC experiments, the oxymethylene protons at δ 4.33 and 4.26 (2H-17) showed long-range correlations to the carbons at δ 38.8 (C-8), 133.5 (C-13) and 139.3 (C-14). The olefinic proton at δ 6.86 (H-15) also showed long-range correlations to the carbons at δ 26.9 (C-12), 133.5 (C-13) and 139.3 (C-14). Methylene olefinic protons at δ 5.23 and 5.07 (2H-16) gave a cross-peak with the carbon at δ 133.5 (C-13). This result suggested that the vinyl substituent was at sp^2 carbon C-13.

The relative stereochemistry of SC9 was determined from the results of NOESY experiments and compared with cassa-13(14),15-dien-19-oic acid (Kido et al., 2003) in which the methyl group at δ 0.84 (Me-20) showed cross-peak with a methine proton at δ 2.26 (H-8). Thus, the relative stereostructure of SC9 was confirmed and assigned for taepeenin G, a new compound (Cheenpracha et al., 2005).

Table 28 ^{1}H, ^{13}C NMR, DEPT and HMBC spectral data of compound SC9

Position	δ_H (mult, *J*, Hz)	δ_C	DEPT	HMBC
1	1.43 (m),1.18 (m)	42.2	CH_2	3, 5, 10
2	1.63 (m), 1.45 (m)	19.0	CH_2	1
3	1.78 (m), 0.94 (m)	38.7	CH_2	
4		36.7	C	
5	0.91 (m)	55.3	CH	3, 4, 10, 18, 19, 20
6	1.29 (m), 0.93 (m)	21.6	CH_2	
7	2.30 (m), 1.08 (m)	31.8	CH_2	
8	2.26 (m)	38.8	CH	6, 13, 14
9	0.96 (m)	53.8	CH	6, 8
10		33.2	C	
11	1.75 (m), 1.39 (m)	21.0	CH_2	8
12	2.39 (m), 2.10 (m)	26.9	CH_2	5, 9, 13, 14
13		133.5	C	
14		139.3	C	
15	6.86 (dd, *J* = 17.1, 10.8)	134.4	CH	12, 13, 14
16	5.23 (d, *J* = 17.1)	113.4	CH_2	13
	5.07 (d, *J* = 10.8)			
17	4.33 (d, *J* = 11.7)	59.1	CH_2	8, 13, 14
	4.26 (d, J = 11.7)			
18	0.83 (s)	22.2	CH_3	3, 4, 5, 19
19	0.85 (s)	33.4	CH_3	3, 4, 5, 18
20	0.84 (s)	14.2	CH_3	1, 5, 9, 10

Table 29 Comparison of ^{13}C NMR (75 MHz) spectral data of compounds SC1-SC9*

Position	SC1	SC2	SC3	SC4[a]	SC5[a]	SC6	SC7[a]	SC8	SC9
1	38.9	38.8	42.2	42.1	38.4	37.9	40.6	38.6	42.2
2	18.8	18.7	19.1	19.0	18.5	17.9	18.1	17.9	19.0
3	36.6	36.7	38.1	38.4	36.5	36.7	38.6	36.8	38.7
4	47.7	47.4	48.5	48.0	47.6	47.3	48.2	47.5	36.7
5	44.4	44.1	47.5	46.1	44.2	49.0	51.0	49.7	55.3
6	21.8	21.8	68.7	70.7	21.4	23.5	69.3	24.1	21.6
7	27.6	27.5	38.8	34.8	27.4	26.8	37.1	30.8	31.8
8	127.5	128.3	124.2	123.8	129.2	45.0	40.8	35.7	38.8
9	147.2	147.0	146.1	145.5	150.7	52.9	53.3	45.7	53.8
10	37.8	37.8	37.8	38.0	37.8	36.9	37.5	36.9	33.2
11	104.3	104.3	105.1	105.0	104.1	22.8	22.6	22.0	21.0
12	153.6	153.5	153.8	153.7	152.7	166.3	166.6	149.4	26.9
13	125.4	125.4	125.7	125.8	119.8	119.8	119.9	122.5	133.5
14	128.3	127.4	128.7	128.7	132.9	195.7	196.1	31.5	139.3
15	105.0	105.0	105.0	105.0	32.5	106.5	106.5	109.5	134.4
16	144.2	144.2	144.3	144.5	174.7	142.8	142.8	140.4	113.4
17	15.9	15.9	16.1	16.1	16.4			17.6	59.1
18	179.2	184.2	179.3	178.6	179.0	178.9	179.0	179.4	22.2
19	16.6	16.3	18.6	18.1	16.5	16.8	19.0	17.0	33.4
20	25.6	25.6	27.5	27.6	25.1	14.8	17.8	14.6	14.2
OMe	52.0		52.1	52.3	52.0	52.0	52.1	51.9	
OCOMe				21.7					
OCOMe				170.7					

* Recorded in $CDCl_3$.

[a]The ^{13}C NMR spectra were measured at 125 MHz

1.3.2.1.10 Compound SC10

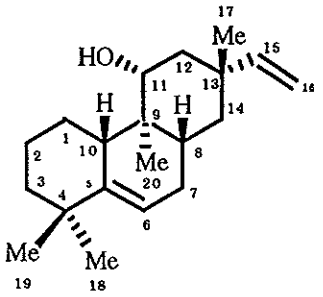

Compound SC10 was isolated as a white solid, mp 90-91 °C. The IR spectrum displayed absorption band of hydroxyl group at 3412 cm^{-1}. The ^{13}C NMR spectral data (Table 30, Figure 60) showed the existence of 20 signals for 20 carbon atoms in the molecule. Analysis of DEPT 90° and 135° spectra of this compound suggested the presence of four methyl, seven methylene, five methine and four quaternary carbons.

The ^{1}H NMR spectral data (Table 30, Figure 59) displayed four methyl singlets at δ 1.06 (Me-17), 1.02 (Me-18), 1.05 (Me-19) and 0.69 (Me-20). Three olefinic proton signals including monosubstituted alkene group at δ 5.78 (dd, J = 17.4, 10.8 Hz), 5.07 (dd, J = 10.8, 1.2 Hz) and 4.92 (dd, J = 17.4, 1.2 Hz), and trisubstituted alkene group at δ 5.48 (dt, J = 6.0, 1.8 Hz) were characterized as a rosane-type diterpene. In addition, an oxymethine proton signal at δ 3.72 (dd, J = 11.4, 4.5 Hz) was assigned as H-11 on the basis of HMBC correlations. The correlations of olefinic proton at δ 5.48 (H-6) with carbons at δ 47.1 (C-10), 36.4 (C-4), 36.3 (C-8) and 29.4 (C-7) confirmed the location of olefinic carbon at C-6. The correlations of a methyl group at δ 0.69 (Me-20) with carbons at δ 78.0 (C-11), 47.1 (C-10), 40.6 (C-9) and 36.3 (C-8), and an oxymethine proton signal at δ 3.72 (H-11) with carbons at δ 47.1 (C-10), 42.5 (C-12), 40.6 (C-9) and 5.9 (Me-20) confirmed the position of Me-20 and oxymethine proton at C-9 and C-11, respectively. The connectivities of Me-17 and monosubstituted alkene were assigned by HMBC experiment in which Me-17 (δ 1.06) and monosustituted alkene were located at C-13 by correlations of Me-17 (δ 1.06) with carbons at δ 150.0 (C-15), 42.5 (C-12) and 38.6 (C-14). The relative stereochemistry of SC10 was assigned by comparison with ent-11β-hydroxy-rosa-5,15-

diene (Alvarez et al., 1981). Thus compound **SC10** was identified as ent-11β-hydroxy-rosa-5,15-diene.

Table 30 ^{1}H, ^{13}C NMR, DEPT and HMBC spectral data of compound **SC10**

Position	δ_H (mult, *J*, Hz)	δ_C	DEPT	HMBC
1	2.45 (m)	30.9	CH_2	2, 10
	1.07 (m)			
2	1.58 (m)	22.4	CH_2	
3	1.42 (m)	40.9	CH_2	4
	1.19 (m)			
4		36.4	C	
5		146.8	C	
6	5.48 (dt, *J* = 6.0, 1.8)	115.7	CH	4, 7, 8, 10
7	1.76 (m)	29.4	CH_2	5, 6, 8, 9
8	1.42 (m)	36.3	CH	9, 13
9		40.6	C	
10	2.20 (m)	47.1	CH	1
11	3.72 (dd, *J* = 11.4, 4.5)	78.0	CH	9, 10, 12, 20
12	1.52 (m)	42.5	CH_2	9, 13, 15, 17
	1.41 (m)			
13		37.3	C	
14	1.34 (m)	38.6	CH_2	8, 12, 15
	1.08 (m)			
15	5.78 (dd, *J* = 17.4, 10.8)	150.0	CH	12, 13, 14, 17
16	4.92 (dd, *J* = 17.4, 1.2)	109.1	CH_2	13, 15
	5.07 (dd, *J* = 10.8, 1.2)			
17	1.06 (s)	23.8	CH_3	12, 14, 15
18	1.02 (s)*	28.6*	CH_3	3, 4, 5, 19
19	1.05 (s)*	30.0*	CH_3	3, 4, 5, 18
20	0.69 (s)	5.9	CH_3	8, 9, 10, 11

* May be interchangeable

1.3.2.2 *Determination of isolated pure compounds from the roots of C. crista*

Investigation of the hexane extract of the roots of *C. crista* resulted in three new diterpenoids (**RH1**, **RH3** and **RH4**), together with three known compounds (**RH2**, **RH5** and **RH6**). Their structures were elucidated by spectroscopic methods.

1.3.2.2.1 Compound RH1

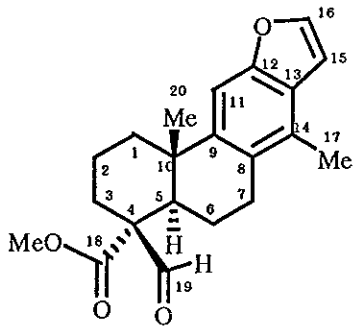

Compound **RH1** was deduced as $C_{21}H_{24}O_4$ from an exact mass measurement ($[M]^+$ *m/z* 340.1671 by HREIMS). The UV and IR spectrum showed absorption band similarities with compound **SC1**. Its ^1H NMR and ^{13}C NMR spectral data (Tables 31 and 32, Figures 61 and 62) of **RH1** were closely related to those of **SC1**. The major difference was the replacement of the ^1H NMR signal of Me-19 at δ 1.31 with an aldehydic proton at δ 9.95 (s). The latter was connected to an aldehydic carbon at δ 199.8 from the HMQC experiment and showed HMBC correlations to carbons at δ 29.4 (C-3), 61.1 (C-4) and 173.5 (C-18). Therefore, the structure of **RH1** was assigned as taepeenin E, a new compound (Cheenpracha et al., 2005).

Table 31 ^1H, ^{13}C NMR, DEPT and HMBC spectral data of compound **RH1**

Position	δ_H (mult, *J*, Hz)	δ_C	DEPT	HMBC
1	2.32 (m)	38.6	CH_2	3, 5, 9, 10
	1.55 (m)			
2	1.75 (m)	18.9	CH_2	3, 10

Table 31 (Continued)

Position	δ_H (mult, *J*, Hz)	δ_C	DEPT	HMBC
3	2.47 (m)	29.4	CH_2	5, 18, 19
4		61.1	C	
5	2.48 (dd, *J* = 12.9, 1.8)	46.8	CH	3, 4, 7, 9, 10, 18, 19, 20
6	2.01 (br dd, *J* = 12.9, 7.2)	21.8	CH_2	5, 7, 8, 10
7	2.99 (br dd, *J* = 16.5, 5.4) 2.86 (m)	28.4	CH_2	5, 8 , 9, 14
8		126.9	C	
9		144.7	C	
10		37.9	C	
11	7.30 (br s)	105.0*	CH	8, 10, 12, 13
12		153.5	C	
13		125.8	C	
14		128.5	C	
15	6.72 (d, *J* = 2.1)	104.9*	CH	12, 13
16	7.53 (d, *J* = 2.1)	144.5	CH	12, 13
17	2.36 (s)	15.9	CH_3	8, 13, 14
18		173.5	C	
19	9.95 (s)	199.8	CH	3, 4
20	1.11 (s)	24.5	CH_3	1, 5, 9, 10
18-O*Me*	3.76 (s)	52.6	CH_3	18

* May be interchangeable

Table 32 Comparison of ^{1}H and ^{13}C NMR spectral data of compounds **SC1** and **RH1**

Position	Compound SC1		Compound RH1	
	δ_H (mult, *J*, Hz)	δ_C	δ_H (mult, *J*, Hz)	δ_C
1	2.38 (m)	38.9	2.32 (m)	38.6
	1.55 (m)		1.55 (m)	
2	1.81 (m)	18.8	1.75 (m)	18.9
	1.74 (m)			
3	1.80 (m)	36.6	2.47 (m)	29.4
	1.68 (m)			
4		47.7		61.1
5	2.27 (dd, *J* = 12.9, 2.4)	44.4	2.48 (dd, *J* = 12.9, 1.8)	46.8
6	1.92 (m)	21.8	2.01 (br dd, *J* = 12.9, 7.2)	21.8
	1.55 (m)			
7	2.83 (m)	27.6	2.99 (br dd, *J* = 16.5, 5.4)	28.4
			2.86 (m)	
8		127.5		126.9
9		147.2		144.7
10		37.8		37.9
11	7.32 (br s)	104.3	7.30 (br s)	105.0*
12		153.6		153.5
13		125.4		125.8
14		128.3		128.5
15	6.72 (dd, *J* = 2.1, 0.9)	105.0	6.72 (d, *J* = 2.1)	104.9*
16	7.53 (d, *J* = 2.1)	144.2	7.53 (d, *J* = 2.1)	144.5
17	2.35 (s)	15.9	2.36 (s)	15.9
18		179.2		173.5
19	1.31 (s)	16.6	9.95 (s)	199.8
20	1.27 (s)	25.6	1.11 (s)	24.5
18-O*Me*	3.70 (s)	52.0	3.76 (s)	52.6

* May be interchangeable

1.3.2.2.2 Compound RH2

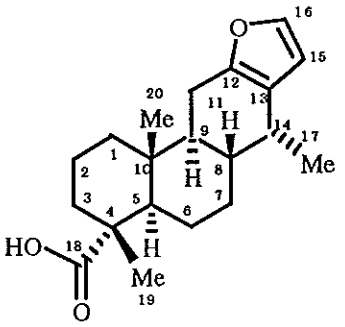

Compound **RH2** was isolated as a white solid, mp 118.5-119 °C, $[\alpha]_D^{27}$: +29.4° (c 0.03, $CHCl_3$). The presence of carboxyl (3414 and 1718 cm^{-1}) functionality was evident from IR absorptions.

The ^1H and ^{13}C NMR (Table 33, Figures 63 and 64) of compound **RH2** showed characteristics similar to those of compound **SC8** except for the disappearance of the OMe signal at δ 3.69, thus indicating a presence of a free carboxylic acid instead of the methyl ester at C-18. This finding was supported by HMBC spectrum of compound **RH2**, in which the methyl proton at δ 1.23 (Me-19) were correlated with carbons at δ 185.2 (C-18), 49.2 (C-5), 47.2 (C-4) and 36.9 (C-3). Therefore, compound **RH2** was determined to be vinhaticoic acid (Narayanan et al., 1965).

Table 33 ^1H, ^{13}C NMR, DEPT and HMBC spectral data of compound **RH2**

Position	δ_H (mult, *J*, Hz)	δ_C	DEPT	HMBC
1	1.76 (m)	38.5	CH_2	3, 10, 20
	1.15 (m)			
2	1.60 (m)	17.8	CH_2	4, 10
3	1.66 (m)	36.9	CH_2	5, 19
	1.34 (m)			
4		47.2	C	
5	1.79 (m)	49.2	CH	3, 4, 10, 18, 19, 20
6	1.54 (m)	24.1	CH_2	4, 5
	1.33 (m)			

Table 33 (Continued)

Position	δ_H (mult, *J*, Hz)	δ_C	DEPT	HMBC
7	1.70 (m)	30.8	CH_2	5
	1.50 (m)			
8		35.7	CH	
9	1.59 (m)	45.8	CH	8, 11, 20
10		36.8	C	
11	2.57 (dd, *J* = 17.4, 6.9)	22.0	CH_2	9, 10, 12, 13
	2.37 (dd, *J* = 17.4, 10.5)			
12		149.4	C	
13		122.5	C	
14	2.62 (m)	31.5	CH	8, 9, 12, 13, 17
15	6.17 (d, *J* = 1.8)	109.5	CH	12, 13, 14
16	7.21 (d, *J* = 1.8)	140.4	CH	12, 13, 15
17	0.97 (d, *J* = 6.9)	17.6	CH_3	8, 13, 14
18		185.2	C	
19	1.23 (s)	16.8	CH_3	3, 4, 5, 18
20	0.93 (s)	14.6	CH_3	1, 5, 9, 10

1.3.2.2.3 Compound RH3

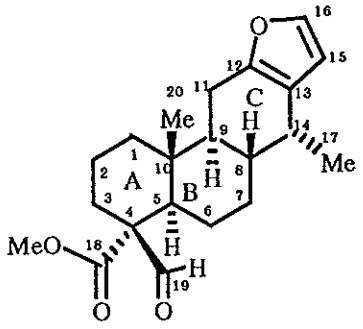

Compound **RH3** showed the molecular formula $C_{21}H_{28}O_4$ ($[M]^+$ *m/z* 344.1942) by HREIMS. Its ^1H and ^{13}C NMR spectral data (Table 34, Figures 65 and 66) revealed that taepeenin H had the same A and B rings as **RH1**. The ring C was comparable to that of SC6 with additional ^1H NMR signals of one methine and one methyl

doublet protons at δ 2.64 (m, H-14) and 0.99 (d, J = 6.9 Hz, Me-17). An analysis of the COSY, HMQC and HMBC spectra led to structure **RH3** for this compound.

The HMBC correlations, of a furan proton at δ 6.18 (H-15) with the carbon at δ 31.4 (C-14), of methyl protons at δ 0.99 (Me-17) with the carbons at δ 31.4 (C-14), 35.8 (C-8) and 122.3 (C-13) and of methylene protons at δ 2.32 and 2.60 (2H-11) with carbons at δ 35.8 (C-8), 122.3 (C-13) and 149.1 (C-12) suggested that the Me-17 should be attached to C-14. In the NOESY spectrum, the methine proton at δ 1.62 (H-9) displayed a cross-peak with the methyl protons at δ 0.99 (Me-17), indicating that this methyl group was α-oriented. Thus, the stereostructure of compound **RH3** was concluded to be taepeenin H, a new compound (Cheenpracha et al., 2005).

Table 34 ^{1}H, ^{13}C NMR, DEPT and HMBC spectral data of compound **RH3**

Position	δ_H (mult, J, Hz)	δ_C	DEPT	HMBC
1	1.79 (m)	38.2	CH_2	2, 5, 9
	1.14 (m)			
2	1.62 (m)	18.1	CH_2	4, 10
3	2.38 (m)	29.6	CH_2	1, 4, 5, 18, 19
	1.51 (m)			
4		60.7	C	
5	2.05 (dd, J = 12.9, 2.1)	51.1	CH	4, 7, 9, 10, 18, 19, 20
6	1.99 (m)	23.8	CH_2	7, 10
	1.67 (m)			
7	1.80 (m)	31.3	CH_2	5, 9, 14
	1.51 (m)			
8	1.85 (m)	35.8	CH	6
9	1.62 (m)	44.4	CH	1, 5, 11, 14, 20
10		37.0	C	
11	2.60 (dd, J = 16.8, 6.6)	22.4	CH_2	8, 12, 13
	2.32 (dd, J = 16.8, 10.2)			
12		149.1	C	
13		122.3	C	

Table 34 (Continued)

Position	δ_H (mult, *J*, Hz)	δ_C	DEPT	HMBC
14	2.64 (m)	31.4	CH	9, 12, 15
15	6.18 (d, *J* = 1.8)	109.5	CH	12, 13
16	7.21 (d, *J* = 1.8)	140.5	CH	12, 13, 15
17	0.99 (d, *J* = 6.9)	17.5	CH_3	8, 13, 14
18		173.7	C	
19	9.90 (s)	199.9	CH	3, 4, 18
20	0.76 (s)	14.2	CH_3	1, 5, 9, 10
18-O*Me*	3.73 (s)	52.5	CH_3	18

1.3.2.2.4 Compound RH4

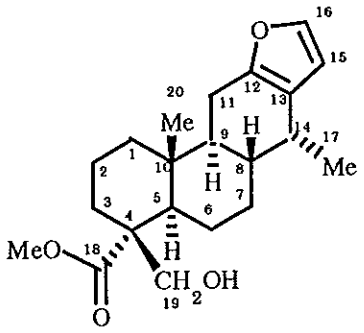

Compound **RH4**, $C_{21}H_{30}O_4$ ([M]$^+$ *m/z* 346.2111 by HREIMS), was found to be a derivative of **RH3**. The ^{1}H NMR spectral data (Tables 35 and 36, Figure 67) of **RH4** was comparable to those of **RH3**, except the aldehydic proton (δ 9.90) in **RH3** was replaced by oxymethylene protons at δ_H 3.84 and 3.96 (each d, *J* = 11.7 Hz), δ_C 61.5. These proton signals showed correlations with carbons at δ 29.9 (C-3), 50.1 (C-5), 53.5 (C-4) and 178.6 (C-18) in the HMBC spectrum, suggesting of their attachment at C-4. Thus the structure of compound **RH4** was concluded to be taepeenin I, a new compound (Cheenpracha et al., 2005).

Table 35 ^{1}H, ^{13}C NMR, DEPT and HMBC spectral data of compound **RH4**

Position	δ_H (mult, *J*, Hz)	δ_C	DEPT	HMBC
1	1.77 (m)	38.6	CH_2	3, 9, 20
	1.25 (m)			
2	1.62 (m)	17.6	CH_2	4, 10
3	2.12 (m)	29.9	CH_2	4, 5, 18
	1.59 (m)			
4		53.5	C	
5	1.79 (m)	50.1	CH	4, 6, 9, 10, 18, 19, 20
6	1.58 (m)	23.9	CH_2	5, 8, 10
	1.28 (m)			
7	1.68 (m)	31.3	CH_2	5, 14
	1.33 (m)			
8	1.73 (m)	35.5	CH	9, 17
9	1.58 (m)	46.0	CH	5, 7, 8, 10, 11, 20
10		36.9	C	
11	2.58 (dd, *J* = 16.8, 6.9)	22.2	CH_2	8, 10, 13
	2.36 (dd, *J* = 16.8, 10.2)			
12		149.2	C	
13		122.4	C	
14	2.60 (m)	31.4	CH	8, 9, 12, 15, 17
15	6.17 (d, *J* = 1.8)	109.5	CH	12, 13, 16
16	7.21 (d, *J* = 1.8)	140.4	CH	12, 13, 15
17	0.96 (d, *J* = 6.9)	17.6	CH_3	8, 13, 14
18		178.6	C	
19	3.96 (d, *J* = 11.7)	61.5	CH_2	3, 4, 5, 18
	3.84 (d, *J* = 11.7)			
20	0.89 (s)	15.1	CH_3	1, 5, 9, 10
18-O*Me*	3.74 (s)	52.1	CH_3	18

Table 36 Comparison of ^{13}C NMR spectral data of compounds **RH1-RH4**

Position	RH1	RH2	RH3	RH4
1	38.6	38.5	38.2	38.6
2	18.9	17.8	18.1	17.6
3	29.4	36.9	29.6	29.9
4	61.1	47.2	60.7	53.5
5	46.8	49.2	51.1	50.1
6	21.8	24.1	23.8	23.9
7	28.4	30.8	31.3	31.3
8	126.9	35.7	35.8	35.5
9	144.7	45.8	44.4	46.0
10	37.9	36.8	37.0	36.9
11	105.0	22.0	22.4	22.2
12	153.5	149.4	149.1	149.2
13	125.8	122.5	122.3	122.4
14	128.5	31.5	31.4	31.4
15	104.9	109.5	109.5	109.5
16	144.5	140.4	140.5	140.4
17	15.9	17.6	17.5	17.6
18	173.5	185.2	173.7	178.6
19	199.8	16.8	199.9	61.5
20	24.5	14.6	14.2	15.1
18-O*Me*	52.6		52.5	52.1

1.3.2.2.5 Compound RH5

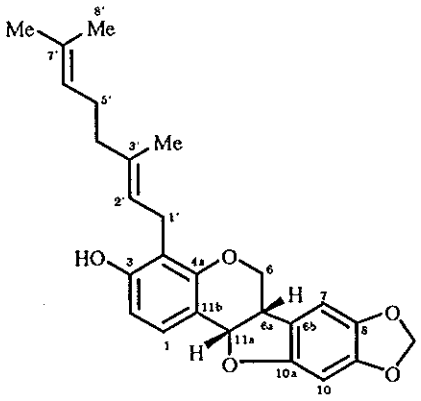

Compound **RH5** was isolated as orange viscous oil, $[\alpha]_D^{27}$ +60.4° (c 0.02, MeOH). The UV spectrum showed absorption band at ν_{max} 206, 234, 283 and 311 nm indicating that structure of **RH5** had a conjugated double bonds. The IR spectrum exhibited absorption band of hydroxyl (3415 cm^{-1}).

The ^{13}C NMR and DEPT spectra (Table 37, Figure 70) displayed 26 signals for 26 carbons including three methyl, five methylene, eight methine and ten quaternary carbons. The ^{1}H NMR spectral data (Table 37, Figure 69) showed the presence of a geranyl unit at δ 5.21 (1H, br t, *J* = 6.9 Hz, H-2′), 5.04 (1H, br s, H-6′), 3.40 (2H, br d, *J* = 6.9 Hz, H-1′), 2.05 (4H, m, H-4′ and H-5′), 1.79 (3H, s, 3′-Me), 1.66 (3H, s, 7′-Me) and 1.58 (3H, s, H-8′). The proton signal at δ 5.90 (2H, d, *J* = 6.9 Hz) was assigned as dioxymethylene ($-OCH_2O-$) which was connected to carbon at δ 101.2 from HMQC experiment. The oxymethylene proton signals at δ 4.25 (1H, dd, *J* = 10.8, 4.8 Hz) and 3.60 (1H, dd, *J* = 11.1, 10.8 Hz), identified as 2H-6, displayed cross-peak with proton at δ 3.46 (1H, dd, *J* = 11.1, 6.9 Hz, H-6a), and proton H-6a with proton at δ 5.48 (1H, d, *J* = 6.9 Hz, H-11a) from COSY spectrum. Two aromatic rings were observed at δ 7.24 and 6.56 (each 1H, d, *J* = 8.4 Hz, H-1 and H-2, respectively) and 6.72 and 6.43 (each 1H, s, H-7 and H-10, respectively) in ^{1}H NMR spectrum. From these data, compound **RH5** was a pterocarpane type. On the basis of HMBC correlation, the geranyl unit was located at C-4 by correlation of H-1′ with carbons at δ 156.0 (C-3), 153.9 (C-4a) and 112.4 (C-4). The dioxymethylene protons at δ 5.90 exhibited correlation with carbons at δ 148.1 (C-8) and 141.6 (C-9), indicating that the dioxymethylene group was attached to the carbons at C-8 and C-9. The ^{1}H and ^{13}C NMR spectrum of compound **RH5** were comparable with nitiducol (Van Heerden et al., 1978), thus compound **RH5** was assigned as nutiducol.

Table 37 ^{1}H, ^{13}C NMR, DEPT and HMBC spectral data of compound **RH5**

Position	δ_H (mult, *J*, Hz)	δ_C	DEPT	HMBC
1	7.24 (d, *J* = 8.4)	129.2	CH	3, 4a, 11a
2	6.56 (d, *J* = 8.4)	110.0	CH	3, 4, 11b
3		156.0	C	
4		112.4	C	
4a		153.9	C	
6	4.25 (dd, *J* = 10.8, 4.8)	66.8	CH_2	4a, 6b, 11a
	3.60 (dd, *J* = 11.1, 10.8)			
6a	3.46 (dd, *J* = 11.1, 6.9)	40.2	CH	7, 10a, 11a, 11b
6b		118.1	C	
7	6.72 (s)	104.7	CH	6a, 6b, 8, 9, 10a
8*		148.1	C	
9*		141.6	C	
10	6.43 (s)	93.8	CH	6b, 8, 9, 10a
10a		154.3	C	
11a	5.48 (d, *J* = 6.9)	79.2	CH	1, 4a, 6, 6a, 6b, 10a, 11b
11b		114.4	C	
1′	3.40 (br d, *J* = 6.9)	22.3	CH_2	3′, 3, 4, 4a
2′	5.21 (br t, *J* = 6.9)	121.5	CH	3′-Me, 3′, 4′, 4
3′		138.5	C	
4′	2.05 (m)	39.7	CH_2	2′, 3′, 4′, 6′
5′	2.05 (m)	26.4	CH_2	2′, 6′, 3′-Me
6′	5.04 (br s)	123.8	CH	4′, 7′, 8′, 7′-Me
7′		131.9	C	
8′	1.58 (s)	17.7	CH_3	6′, 7′, 7′-Me
7′-Me	1.66 (s)	25.7	CH_3	6′, 7′, 8′
OCH_2O	5.90 (d, *J* = 6.9)	101.2	CH_2	8, 9
3′-Me	1.79 (s)	16.2	CH_3	2′, 3′, 4′

* May be interchangeable

1.3.2.2.6 Compound RH6

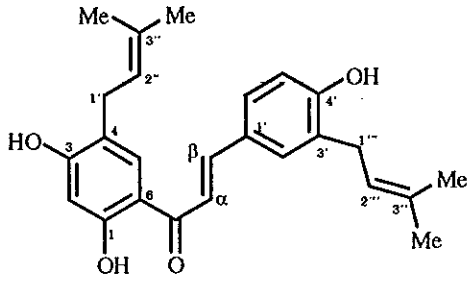

Compound **RH6** was obtained as yellow solid, mp 178-179 °C. The UV (λ_{max} 206, 242, 264 and 377 nm) and IR (3418 and 1635 cm^{-1}) absorption bands showed characteristic of chalcone chromophore.

The ^{13}C NMR and DEPT spectra (Table 38, Figure 72) displayed 25 signals for 25 carbons, including four methyl, two methylene, nine methine and ten quaternary carbons.

The ^{1}H NMR spectral data (Table 38, Figure 71) displayed the presence of a chalcone skeleton as signals at δ 7.85, 7.46 (each 1H, d, *J* = 15.3 Hz, H-β and H-α, respectively), 7.64, 6.42 (each 1H, s, H-5 and H-2, respectively), and ABX system at δ 7.44 (1H, d, *J* = 2.1 Hz, H-2′), 7.40 (1H, dd, *J* = 8.4, 2.1 Hz, H-6′), and 6.86 (1H, d, *J* = 8.4 Hz, H-5′). The proton signal at δ 13.30 showed characteristic of chelated hydroxyl group. In addition, the ^{1}H NMR spectral data exhibited characteristic of two isoprenyl units at δ 5.32 (2H, m, H-2″ and H-2‴), 3.40 (2H, br d, *J* = 7.2 Hz, H-1‴), 3.34 (2H, br d, *J* = 7.2 Hz, H-1″), 1.80 (12H, s, H-4″, 3″-Me, H-4‴ and 3‴-Me).

The locations of two isoprenyl units were deduced from HMBC correlations. The methylene protons at δ 3.34 (2H-1″) showed correlations with carbons at δ 164.9 (C-3), 131.1 (C-5) and 118.7 (C-4), indicating that the first unit of isoprenyl moiety was attached to carbon at C-4. The other unit of proton at δ 3.40 (2H-1‴) showed correlation with carbons at δ 156.9 (C-4′), 135.4 (C-2′) and 128.3 (C-3′), confirming that this unit was connected to the carbon C-3′. Thus compound **RH6** was deduced as stipulin (Ngameni et al., 2004) which was previously isolated from the twigs of *Dorstenia barteri* var. *subtriangularis*.

Table 38 ^{1}H, ^{13}C NMR, DEPT and HMBC spectral data of compound **RH6**

Position	δ_H (mult, *J*, Hz)	δ_C	DEPT	HMBC
α	7.46 (d, *J* = 15.3)	117.8	CH	β, 6, 1′, C=O
β	7.85 (d, *J* = 15.3)	144.5	CH	1′, 2′, 6′, C=O
1	13.30 (s (OH))	161.5	C	
2	6.42 (s)	104.1	CH	1, 3, 4, 6
3		164.9	C	
4		118.7	C	
5	7.64 (s)	131.1	CH	1, 3, 1″, C=O
6		114.4	C	
1′		127.7	C	
2′	7.44 (d, *J* = 2.1)	135.4	CH	β, 3′, 4′, 1‴
3′		128.3	C	
4′		156.9	C	
5′	6.86 (d, *J* = 8.4)	116.4	CH	1′, 3′
6′	7.40 (dd, *J* = 8.4, 2.1)	131.0	CH	β, 1′, 2′, 4′
1″	3.34 (br d, *J* = 7.2)	29.7	CH_2	3, 4, 5, 2″, 3″
2″	5.32 (m)	121.7	CH	4, 1″, 3″, 4″, 3″-Me
3″		135.7	C	
4″	1.80 (s)	18.0	CH_3	3″, 3″-Me, 2″
3″-Me	1.80 (s)	25.8	CH_3	3″, 3″-Me, 2″
1‴	3.40 (br d, *J* = 7.2)	29.2	CH_2	2′, 3′, 4′, 3‴
2‴	5.32 (m)	121.1	CH	3′, 3‴, 4‴, 3‴-Me
3‴		135.7	C	
4‴	1.80 (s)	18.0	CH_3	2‴, 3‴, 3‴-Me
3‴-Me	1.80 (s)	25.8	CH_3	2‴, 3‴, 3‴-Me
C=O		192.0	C	

* May be interchangeable

1.3.2.3 *Determination of isolated pure compounds from the seeds of C. crista*

The seeds collecting from Trang province, Thailand in May 2004, were extracted with acetone at room temperature (5 days) and evaporated under reduced pressure to afford acetone extract. The acetone extract was further chromatographed on silica gel and eluted with hexane-EtOAc mixtures. Purification of fractions obtained from EtOAc-hexane afforded 17-methylvouacapane-8(14),9(11)-diene (**SD1**, 4.8 mg), vouacapane (**SD2**, 11.8 mg), taepeenin J (**SD3**, 17.3 mg), taepeenin K (**SD4**, 7.3 mg), taepeenin L (**SD5**, 12.4 mg) and 6β-hydroxyvouacapane (**SD6**, 6.9 mg). Compound **SD3** possesses a dimeric vouacapane skeleton.

Their structures were elucidated by 1D and 2D NMR spectroscopic data. All carbons were assigned by ^{13}C NMR, DEPT, HMQC and HMBC data.

1.3.2.3.1 Compound SD1

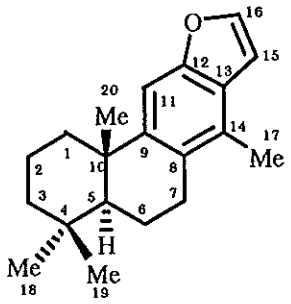

Compound **SD1** was isolated as a yellow solid, mp. 70-71 °C. The UV and IR spectrum were similar to those of compound **SC1**, but the carbonyl functionality was not observed in IR spectrum.

Its ^{1}H and ^{13}C NMR spectral data (Table 39, Figures 73 and 74) were similar to those of **SC1** (Table 20), except that the methoxyl group at δ 3.70 (s, 18-OMe) disappeared and the methyl protons were shown at δ 0.97 (s). For this compound, assignments of carbon and proton signals were confirmed by means of HMQC and HMBC experiments. In the HMBC spectrum, the methyl protons at δ 0.97 (Me-18) showed correlations with carbons at 49.9 (C-5), 41.7 (C-3), 33.5 (C-4) and 21.7 (C-19). Thus compound **SD1** was assigned to be 17-methylvouacapane-8(14),9(11)-diene by comparison of its spectral data with previously reported data (Jadhav et al., 2003).

Table 39 ^{1}H, ^{13}C NMR, DEPT and HMBC spectral data of compound SD1

Position	δ_H (mult, *J*, Hz)	δ_C	DEPT	HMBC
1	2.37 (m)	39.8	CH_2	2, 5, 10, 20
	1.47 (m)			
2	2.00 (m)	19.2	CH_2	10
	1.82 (m)			
3	1.53 (m)	41.7	CH_2	4, 5, 18
	1.25 (m)			
4		33.5	C	
5	1.36 (dd, *J* = 12.6, 2.4)	49.9	CH	4, 7, 9, 10, 18, 19, 20
6	1.67 (m)	19.5	CH_2	4, 5
7	2.92 (dd, *J* = 17.4, 7.2)	28.0	CH_2	5, 6, 8, 9, 14
	2.73 (ddd, J = 17.4, 11.1, 7.2)			
8		128.1	C	
9		146.0	C	
10		38.4	C	
11	7.33 (s)	104.4	CH	8, 10, 12, 13
12		153.0	C	
13		125.5	C	
14		128.1	C	
15	6.71 (dd, *J* = 2.1, 0.9)	104.9	CH	12, 13
16	7.51 (d, *J* = 2.1)	144.1	CH	12, 13, 15
17	2.35 (s)	15.7	CH_3	8, 13, 14
18	0.97 (s)	33.3	CH_3	3, 4, 5, 19
19	0.95 (s)	21.7	CH_3	3, 4, 5, 18
20	1.24 (s)	25.4	CH_3	1, 5, 9, 10

1.3.2.3.2 Compound SD2

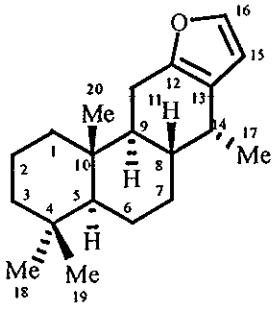

Compound SD2 was isolated as a colorless viscous oil. This compound exhibited UV absorption similar to compound SC8. Comparison of the ^{1}H and ^{13}C NMR spectral data (Tables 40 and 27, Figures 75 and 76) of compound SD2 and SC8 revealed closed structural similarity. The difference was shown in the absence of methoxyl group at δ 3.69 (s, 18-OMe) and the methyl protons were shown at δ 0.89 (s) which was confirmed by HMBC experiment in which the methyl protons at δ 0.89 (Me-18) showed correlation with carbons at δ 55.2 (C-5), 42.0 (C-3), 33.2 (C-4) and 22.2 (C-19). Thus on the basis of its spectroscopic data and comparison with previously reported data of vouacapane (De O. Godoy, et al., 1989), compound SD2 was assigned as vouacapane.

Table 40 ^{1}H, ^{13}C NMR, DEPT and HMBC spectral data of compound SD2

Position	δ_H (mult, *J*, Hz)	δ_C	DEPT	HMBC
1	1.74 (m), 1.12 (m)	39.7	CH_2	5, 9, 10, 20
2	1.59 (m), 1.46 (m)	18.7	CH_2	3
3	1.45 (m), 1.18 (m)	42.0	CH_2	1, 5, 10, 18, 19
4		33.2	C	
5	0.91 (m)	55.2	CH	1, 3, 7, 9, 10, 18, 19, 20
6	1.68 (m), 1.34 (m)	21.5	CH_2	5, 8
7	1.72 (m), 1.43 (m)	31.2	CH_2	5, 9, 14
8	1.79 (m)	35.7	CH	7, 9, 14, 17
9	1.48 (m)	45.6	CH	1, 5, 10,14
10		37.4	C	

Table 40 (Continued)

Position	δ_H (mult, *J*, Hz)	δ_C	DEPT	HMBC
11	2.56 (dd, *J* = 16.5, 6.6)	22.2	CH_2	8, 9, 10, 12, 13
	2.35 (dd, *J* = 16.5, 10.2)			
12		149.9	C	
13		122.5	C	
14	2.61 (m)	31.5	CH	8, 9, 12, 13, 15, 17
15	6.17 (d, *J* = 1.8)	109.5	CH	12, 13, 16
16	7.21 (d, *J* = 1.8)	140.3	CH	12, 13, 15
17	0.94 (d, *J* = 5.7)	17.5	CH_3	8, 13, 14
18	0.89 (s)	33.7	CH_3	3, 4, 5, 19
19	0.86 (s)	22.2	CH_3	3, 4, 5, 18
20	0.89 (s)	14.4	CH_3	1, 5, 9, 10

1.3.2.3.3 Compound SD3

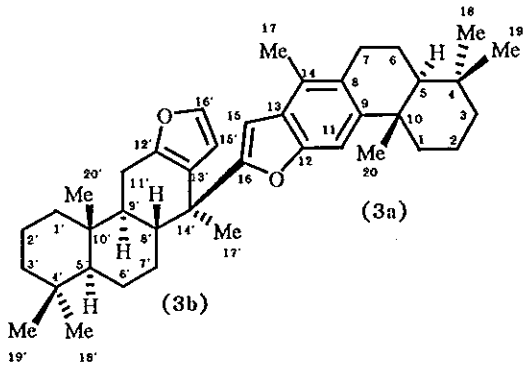

Compound SD3, $[\alpha]_D^{27}$ +36.6° (c 0.27, $CHCl_3$), was obtained as a viscous oil and had a molecular formula $C_{40}H_{54}O_2$ by HREIMS ($[M]^+$ *m/z* 566.4109, calcd 566.4124). The UV spectrum (λ_{max} 217, 255, 283 and 293 nm) suggested a benzofuran chromophore (Lyder et al., 1998). The ^{13}C NMR and DEPT spectral data (Tables 41 and 42, Figure 78) showed 40 carbons; twelve of these were sp^2 carbons: attributable to four methine and eight quaternary carbons.

The ^1H NMR spectral data of SD3 (Tables 41 and 42, Figure 77) displayed two fragments (3a and 3b) of cassane-type diterpenes. The fragment 3a

displayed the presence of three tertiary methyl groups at δ 1.24 (Me-20), 0.95 (Me-18) and 0.94 (Me-19), one aromatic methyl at δ 2.28 (Me-17), a methine proton at δ 1.35 (dd, J = 12.6, 2.1 Hz, H-5), and two aromatic protons at δ 7.26 (s, H-11) and 6.08 (s, H-15). These data indicated that fragment **3a** and **SD1** (Jadhav et al., 2003) were closely related, except for the disappearance of the aromatic proton signal at δ 7.51 (H-16) in fragment 3a.

The ^{1}H NMR spectral data (Table 42) of fragment 3b showed the presence of four tertiary methyl groups at δ 1.64 (s, Me-17′), 0.90 (s, Me-20′), 0.82 (s, Me-19′) and 0.75 (s, Me-18′), and three aliphatic methine proton signals at δ 1.70 (m, H-9′), 1.67 (m, H-8′) and 0.73 (dd, J = 10.8, 2.1 Hz, H-5′). Resonances at δ 7.22 and 6.08 (each d, J = 1.8 Hz) were typical of 1,2-disubstituted furan. Its ^{1}H NMR spectral data was almost identical to those of **SD2** (De O. Godoy, et al., 1989), except for the splitting pattern of methyl protons (Me-17′) in **3b** was shown as a singlet at δ 1.64 but a doublet at δ 0.94 in **SD2** (De O. Godoy, et al., 1989).

The connectivity of both fragments was confirmed by HMBC correlations. The methyl protons at δ 1.64 (Me-17′) showed correlations with the carbons at δ 162.3 (C-16), 121.9 (C-13′), 44.2 (C-8′) and 40.3 (C-14′), a methine proton at δ 1.67 (H-8′) with the carbons at δ 162.3 (C-16) and 40.3 (C-14′), and an aromatic proton at δ 6.08 (H-15) with δ 162.3 (C-16), 153.3 (C-12), 127.3 (C-14), 126.4 (C-13) and 40.3 (C-14′), confirming that fragments **3a** and **3b** were connected at C-16 and C-14′, respectively. The stereochemistry at C-14′ was determined on the basis of NOESY experiments (Fig. 2). A methine proton at δ 0.73 (H-5′) showed cross-peaks with δ 1.70 (H-9′) and 1.64 (Me-17′), suggesting that Me-17′ should be α-axial oriented. From these data, a dimer **SD3** was deduced to be taepeenin J, a new compound.

Table 41 ^{1}H, ^{13}C NMR, DEPT and HMBC spectral data of fragment 3a (SD3)

Position	δ_H (mult, J, Hz)	δ_C	DEPT	HMBC
1	2.33 (m), 1.48 (m)	39.9	CH_2	2, 10, 20
2	2.00 (m), 1.83 (m)	19.2	CH_2	1
3	1.47 (m), 1.39 (m)	41.7	CH_2	1, 5, 18, 19
4		33.5	C	

Table 41 (Continued)

Position	δ_H (mult, *J*, Hz)	δ_C	DEPT	HMBC
5	1.35 (dd, *J* = 12.6, 2.1)	49.9	CH	4, 7, 9, 18, 19, 20
6	1.62 (m), 1.48 (m)	19.5	CH_2	4, 10
7	2.90 (dd, *J* = 17.1, 3.3)	28.0	CH_2	5, 6, 8, 9, 14
	2.70 (m)			
8		127.3	C	
9		146.8	C	
10		38.4	C	
11	7.26 (s)	104.3	CH	8, 10, 12, 13
12		153.3	C	
13		126.4	C	
14		127.3	C	
15	6.08 (s)	102.6	CH	12, 13, 14, 16, 14′
16		162.3	C	
17	2.28 (s)	15.9	CH_3	8, 13, 14
18	0.95 (s)	33.3	CH_3	3, 4, 5, 19
19	0.94 (s)	21.7	CH_3	3, 4, 5, 18
20	1.24 (s)	25.3	CH_3	1, 5, 9, 10

Table 42 ^{1}H, ^{13}C NMR, DEPT and HMBC spectral data of fragment 3b (SD3)

Position	δ_H (mult, *J*, Hz)	δ_C	DEPT	HMBC
1′	1.71 (m), 1.02 (m)	39.4	CH_2	2′, 5′, 9′, 20′
2′	1.65 (m), 1.49 (m)	18.8	CH_2	1′
3′	1.21 (m), 1.15 (m)	41.8	CH_2	2′
4′		33.1	C	
5′	0.73 (dd, *J* = 10.8, 2.1)	54.2	CH	1′, 9′, 18′, 19′, 20′
6′	1.53 (m), 1.21 (m)	21.4	CH_2	7′, 8′
7′	2.11 (m), 2.06 (m)	28.6	CH_2	8′
8′	1.67 (m)	44.2	CH	14′, 16

Table 42 (Continued)

Position	δ_H (mult, *J*, Hz)	δ_C	DEPT	HMBC
9′	1.70 (m)	47.5	CH	1′
10′		37.6	C	
11′	2.76 (dd, *J* = 16.5, 6.0)	22.1	CH_2	8′, 9′, 10′, 12′
	2.45 (dd, *J* = 16.5, 9.6)			
12′		150.6	C	
13′		121.9	C	
14′		40.3	C	
15′	6.08 (d, *J* = 1.8)	108.5	CH	12′, 13′
16′	7.22 (d, *J* = 1.8)	140.6	CH	12′, 13′, 15′
17′	1.64 (s)	24.6	CH_3	8′, 13′, 14′, 16
18′	0.75 (s)	33.4	CH_3	3′, 4′, 5′, 19′
19′	0.82 (s)	22.1	CH_3	3′, 4′, 5′, 18′
20′	0.90 (s)	14.3	CH_3	1′, 5′, 9′, 10′

1.3.2.3.4 Compound SD4

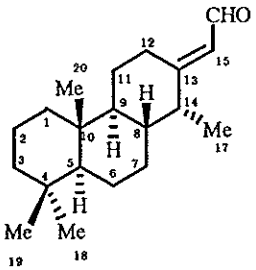

Compound SD4 had the molecular formula $C_{20}H_{32}O$ ($[M]^+$ *m/z* 288.2466) as determined by HREIMS. The IR (1682 cm^{-1}) and UV (λ_{max} 224 nm) absorption bands were characteristics of conjugated carbonyl functionality. The ^{13}C NMR and DEPT spectrum (Table 43, Figure 80) exhibited a total of 20 carbons with one carbonyl carbon at δ 191.0 and two sp^2 carbons at δ 172.0 and 123.9.

The ^1H NMR spectral data (Table 43, Figure 79) showed the presence of an aldehydic proton at δ 10.00 (d, *J* = 8.4 Hz, H-16) which coupled with an olefinic proton at δ 5.83 (dd, *J* = 8.4, 0.9 Hz, H-15). This indicated that conjugated carbonyl

group was an exocyclic double bond. Signals of three tertiary methyl groups at δ 0.87 (Me-18), 0.83 (Me-19) and 0.81 (Me-20), and a doublet methyl group at δ 1.05 (d, J = 7.2 Hz, Me-17) were displayed similarly to those of **SD2** (De O. Godoy, et al., 1989). The observed HMBC correlations between the methyl protons at δ 1.05 (Me-17) with carbons at δ 45.2 (C-14), 40.8 (C-8) and 172.0 (C-13), and of an olefinic proton at δ 5.83 (H-15) with carbons at δ 24.5 (C-12) and 45.2 (C-14), confirmed that the double bond was attached to carbon C-13. The relative stereochemistry of **SD4** was determined on the basis of coupling constants and NOESY experiments. The *E*-double bond was determined by NOESY cross-peak between an olefinic proton at δ 5.83 (H-15) and a methine proton at δ 2.35 (H-14). Thus, compound **SD4** was assigned as taepeenin K, a new compound.

Table 43 ^{1}H, ^{13}C NMR, DEPT and HMBC spectral data of compound **SD4**

Position	δ_H (mult, J, Hz)	δ_C	DEPT	HMBC
1	1.70 (m)	39.6	CH_2	2
	0.98 (m)			
2	1.68 (m)	18.8	CH_2	
	1.48 (m)			
3	1.45 (m)	42.1	CH_2	5
	1.19 (m)			
4		33.2	C	
5	0.86 (m)	55.2	CH	1, 4, 9, 18, 19, 20
6	1.00 (m)	21.6	CH_2	10
7	1.51 (m)	31.3	CH_2	5, 6
	1.35 (m)			
8	1.49 (m)	40.8	CH	13
9	1.18 (m)	48.0	CH	1, 5, 14, 20
10		37.1	C	
11	1.91 (m)	27.0	CH_2	12
	1.23 (m)			
12	3.18 (br dd, J = 13.8, 3.0)	24.5	CH_2	11, 13, 15
	2.17 (m)			
13		172.0	C	

Table 43 (Continued)

Position	δ_H (mult, *J*, Hz)	δ_C	DEPT	HMBC
14	2.35 (m)	45.2	CH	9, 12, 13, 15
15	5.83 (dd, *J* = 8.4, 0.9)	123.9	CH	12, 14
16	10.00 (d, *J* = 8.4)	191.0	CH	13
17	1.05 (d, *J* = 7.2)	14.1	CH_3	8, 13, 14
18	0.87 (s)	33.7	CH_3	3, 5, 19
19	0.83 (s)	22.0	CH_3	3, 5, 18
20	0.81 (s)	14.0	CH_3	1, 5, 9, 10

1.3.2.3.5 Compound SD5

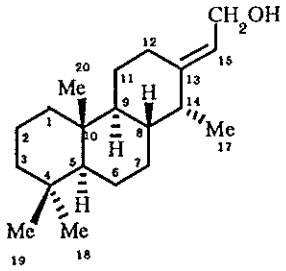

Compound **SD5** showed the molecular ion $[M]^+$ at *m/z* 290.2603 in HREIMS spectrum in agreement with the formula $C_{20}H_{34}O$. The presence of hydroxyl (3409 cm^{-1}) functionality was evident from IR absorption.

The ^1H and ^{13}C NMR spectral data of **SD5** (Table 44, Figures 81 and 82) showed characteristics similar to those of **SD4** except that the oxymethylene protons at δ 4.12 (d, *J* = 7.2 Hz) replaced the aldehydic proton signal at δ 10.00. This finding was supported by HMBC spectrum of **SD5**, in which the oxymethylene protons at δ 4.12 (2H-16) were correlated with the carbons at δ 151.0 (C-13) and 118.7 (C-15). Compound **SD5** displayed the same relative stereochemistry as that of **SD4**. Therefore, compound **SD5** was determined to be taepeenin L, a new compound.

Table 44 ^{1}H, ^{13}C NMR, DEPT and HMBC spectral data of compound **SD5**

Position	δ_H (mult, *J*, Hz)	δ_C	DEPT	HMBC
1	1.70 (m)	39.7	CH_2	2, 5, 10, 20
	0.97 (m)			
2	1.52 (m)	18.9	CH_2	1, 3
	1.39 (m)			
3	1.43 (m)	42.2	CH_2	5, 18, 19
	1.18 (m)			
4		33.2	C	
5	0.83 (m)	55.8	CH	1, 7, 9, 18, 19, 20
6	1.64 (m)	21.7	CH_2	10
	1.30 (m)			
7	1.50 (m)	31.7	CH_2	5
8	1.53 (m)	40.7	CH	7
9	1.13 (m)	48.4	CH	1, 5, 7
10		37.0	C	
11	1.78 (m)	26.6	CH_2	8, 9, 12, 13
	0.96 (m)			
12	2.43 (m)	23.7	CH_2	9, 11, 13, 14, 15
	1.90 (m)			
13		151.0	C	
14	2.20 (m)	44.3	CH	9, 13, 15, 17
15	5.37 (td, J = 7.2, 1.5)	118.7	CH	12, 14, 16
16	4.12 (d, J = 7.2)	58.7	CH_2	13, 15
17	0.95 (d, J = 7.2)	14.4	CH_3	8, 13, 14
18	0.86 (s)	33.7	CH_3	3, 4, 5, 19
19	0.82 (s)	22.1	CH_3	3, 4, 5, 18
20	0.79 (s)	14.2	CH_3	1, 5, 9, 10

1.3.2.3.6 Compound SD6

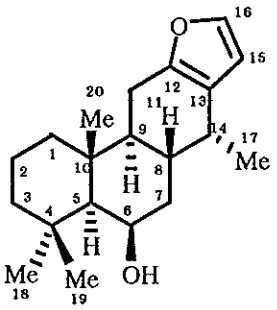

Compound SD6 was obtained as colorless viscous oil. The UV spectrum exhibited absorption bands similar to those of SD2. The IR spectrum showed absorption band of hydroxyl group at 3484 cm^{-1}. The ^{1}H and ^{13}C NMR spectral data (Table 45, Figures 83 and 84) were closely related to those of SD2, except for the oxymethine proton signal at δ 4.47 (dd, J = 4.8, 3.0 Hz) assignable to H-6. On the basis of HMBC experiment, this proton was correlated with carbons at δ 56.4 (C-5), 37.7 (C-10), 34.1 (C-4) and 30.5 (C-8), indicating that the hydroxyl group was located at C-6. Judging from the small J values (J = 4.8, 3.0 Hz) of oxymethine proton H-6, the hydroxyl group should have an axial orientation. Thus compound SD6 was assigned as 6β-hydroxyvouacapane (Mendes et al., 1994).

Table 45 ^{1}H, ^{13}C NMR, DEPT and HMBC spectral data of compound SD6

Position	δ_H (mult, J, Hz)	δ_C	DEPT	HMBC
1	1.70 (m), 1.07 (m)	42.5	CH_2	5, 9, 20
2	1.67 (m), 1.47 (m)	18.9	CH_2	1, 10
3	1.44 (m), 1.21 (m)	43.8	CH_2	1, 18, 19
4		34.1	C	
5	0.97 (m)	56.4	CH	3, 6, 7, 10, 18, 19, 20
6	4.47 (dd, J = 4.8, 3.0)	67.5	CH	4, 5, 8, 10
7	1.78 (m), 1.60 (m)	40.3	CH_2	5, 6 , 9, 14
8	2.15 (tt, J = 12.3, 4.5)	30.5	CH	6, 7, 9, 11, 14, 17
9	1.52 (m)	46.0	CH	1, 5, 7, 10, 14, 20
10		37.7	C	

Table 45 (Continued)

Position	δ_H (mult, *J*, Hz)	δ_C	DEPT	HMBC
11	2.60 (dd, *J* = 17.1, 6.9)	21.8	CH_2	8, 9, 10, 13, 15
	2.45 (dd, *J* = 17.1, 10.2)			
12		149.7	C	
13		122.2	C	
14	2.63 (qd, *J* = 7.2, 4.5)	31.2	CH	8, 9, 13, 15
15	6.18 (d, *J* = 1.8)	109.5	CH	12, 13
16	7.22 (d, *J* = 1.8)	144.2	CH	12, 13, 15
17	0.97 (d, *J* = 7.2)	17.7	CH_3	8, 13, 14
18	1.01 (s)	33.9	CH_3	3, 4, 5, 19
19	1.26 (s)	24.3	CH_3	3, 4, 5, 18
20	1.23 (s)	17.7	CH_3	1, 5, 9, 10

Table 46 Comparison of ^{13}C NMR spectral data of compounds SD1-SD6

Position	SD1	SD2	SD3		SD4	SD5	SD6
			3a	3b*			
1	39.8	39.7	39.9	39.4	39.6	39.7	42.5
2	19.2	18.7	19.2	18.8	18.8	18.9	18.9
3	41.7	42.0	41.7	41.8	42.1	42.2	43.8
4	33.5	33.2	33.5	33.1	33.2	33.2	34.1
5	49.9	55.2	49.9	54.2	55.2	55.8	56.4
6	19.5	21.5	19.5	21.4	21.6	21.7	67.5
7	28.0	31.2	28.0	28.6	31.3	31.7	40.3
8	128.1	35.7	127.3	44.2	40.8	40.7	30.5
9	146.0	45.6	146.8	47.5	48.0	48.4	46.0
10	38.4	37.4	38.4	37.6	37.1	37.0	37.7
11	104.4	22.2	104.3	22.1	27.0	26.6	21.8
12	153.0	149.9	153.3	150.6	24.5	23.7	149.7
13	125.5	122.5	126.4	121.9	172.0	151.0	122.2
14	128.1	31.5	127.3	40.3	45.2	44.3	31.2

Table 46 (Continued)

Position	SD1	SD2	SD3		SD4	SD5	SD6
			3a	3b*			
15	104.9	109.5	102.6	108.5	123.9	118.7	109.5
16	144.1	140.3	162.3	140.6	191.0	58.7	144.2
17	15.7	17.5	15.9	24.6	14.1	14.4	17.7
18	33.3	33.7	33.3	33.4	33.7	33.7	33.9
19	21.7	22.2	21.7	22.1	22.0	22.1	24.3
20	25.4	14.4	25.3	14.3	14.0	14.2	17.7

*The position was 1′, 2′, 3′,...

1.3.3 Structural elucidation of compounds from the bark of *S. multiflora*

Two new *ent*-kaurene type diterpenes, named as *ent*-16-kaurene-3β,15β,18-triol (BMC1) and *ent*-16-kaurene-3-oxo-15β,18-diol (BMC2), were isolated from a dichloromethane extract from the bark of *Suregada multiflora* along with five known diterpenes: *ent*-kaur-16-ene-3β,15β-diol (BMC3), abbeokutone (BMC4), helioscopinolide A (BMC5), helioscopinolide C (BMC6) and helioscopinolide I (BMC7). Their structures were elucidated on the basis of spectroscopic analysis.

1.3.3.1 Compound BMC1

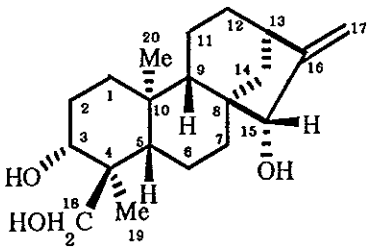

Compound BMC1 was isolated as a white solid. It showed the $[M]^+$ at *m/z* 320.2351 ($C_{20}H_{32}O_3$) in the HREIMS spectrum. The presence of hydroxyl (3337 cm^{-1}) functionality was evident from IR absorption.

The ^{13}C NMR and DEPT spectral data (Table 47, Figure 86) exhibited 20 carbons, attributable to two methyl, nine methylene, five methine and four quaternary carbons indicating a diterpenoid. Two low-field signals at δ 108.3 and 159.1 represented two carbons of an exocyclic double bond and the signals at δ 82.6, 74.9 and 69.5 indicating the presence of three oxygenated carbons in the molecule.

The ^{1}H NMR spectral data (Table 47, Figure 85) displayed the presence of two singlet signals at δ 1.02 (3H, s, Me-20) and 0.80 (3H, s, Me-19), a set of methylene protons at δ 5.19, 5.09 (each 1H, br s, 2H-17), two oxymethine protons at δ 3.59 (1H, dd, J = 10.8, 6.0 Hz, H-3) and 3.78 (1H, s, H-15), and a methine proton at δ 2.73 (1H, br s, H-13). These data indicated that compound **BMC1** and **BMC3** (Das et al., 1994) were closely related, except for the replacement of the methyl proton signal at δ 1.00 with oxymethylene proton signals at δ 3.58 and 3.33 (each 1H, d, J = 10.8 Hz, 2H-18). The location of oxymethylene protons was established as follows. An oxymethine proton at δ 3.59 (H-3) showed HMBC correlations with the carbons at δ 69.5 (C-18), 48.7 (C-5), 26.1 (C-2) and 11.5 (C-19), a methine proton at δ 0.90 (H-5) with the carbons at δ 69.5 (C-18), 54.2 (C-9), 41.7 (C-4), 38.9 (C-10), 17.9 (C-20) and 11.5 (C-19), and the methyl protons at δ 0.80 (Me-19) with the carbons at δ 74.9 (C-3), 69.5 (C-18), 48.7 (C-5) and 41.7 (C-4), confirming that oxymethylene protons were attached to carbon C-18.

The relative stereochemistry at the important chiral centers was determined on the basis of coupling constants and NOESY experiments. The large J value of proton H-3 (J = 10.8 Hz) indicated an axial orientation (β-phase). On biogenetic grounds, the methyl Me-20 was deduced to be α-oriented (Dewick P.M., 2001), and this methyl group displayed NOESY cross-peaks with Me-19 and H-14α. Hence Me-19 should also be α-oriented. On the other hand, the cross-peaks between H-3/H-5, H-5/H-9 and H-9/H-15 suggested the β-orientation of H-3, H-5, H-9 and H-15. The appearance of an oxymethine proton H-15 as a singlet also supported its β-orientation (Jia et al., 1994). The structure of compound **BMC1** was elucidated as *ent*-16-kaurene-3β,15β,18-triol, a new compound.

Table 47 ^{1}H, ^{13}C NMR, DEPT and HMBC spectral data of compound **BMC1**

Position	δ_H (mult, *J*, Hz)	δ_C	DEPT	HMBC
1	1.85 (m)	38.4	CH_2	2, 5, 9, 10, 20
2	1.60 (m)	26.1	CH_2	10
3	3.59 (dd, *J* = 10.8, 6.0)	74.9	CH	2, 5, 18, 19
4		41.7	C	
5	0.90 (m)	48.7	CH	4, 9, 10, 18, 19, 20
6	1.54 (m)	18.0	CH_2	10
7	1.63 (m)	34.7	CH_2	9
	1.39 (m)			
8		47.3	C	
9	1.00 (m)	54.2	CH	1, 8, 10, 15, 20
10		38.9	C	
11	1.63 (m)	19.0	CH_2	8, 9, 10
	1.42 (m)			
12	1.48 (m)	32.6	CH_2	9, 14
13	2.73 (br s)	42.2	CH	11, 12
14	1.85 (m)	36.1	CH_2	7, 9, 15, 16
	1.35 (m)			
15	3.78 (s)	82.6	CH	9, 13, 14, 16, 17
16		159.1	C	
17	5.19 (br s)	108.3	CH_2	13, 15, 16
	5.09 (br s)			
18	3.58 (d, *J* = 10.8)	69.5	CH_2	3, 4, 5, 19
	3.33 (d, *J* = 10.8)			
19	0.80 (s)	11.5	CH_3	3, 4, 5, 18
20	1.02 (s)	17.9	CH_3	1, 5, 9, 10

1.3.3.2 Compound BMC2

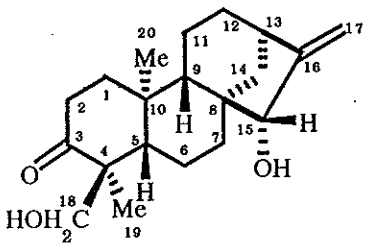

Compound **BMC2**, $C_{20}H_{30}O_3$ ($[M]^+$ *m/z* 318.2195), was obtained as colorless viscous oil. The IR (3407 and 1694 cm^{-1}) absorption bands were characteristic of hydroxyl and carbonyl groups, respectively. The ^{13}C NMR spectral data (Table 48) showed a total of 20 carbons with one carbonyl carbon at δ 219.0. The ^{1}H and ^{13}C NMR spectra of **BMC2** (Table 48, Figures 87 and 88) resembled those of **BMC1** except that the hydroxyl at C-3 in **BMC1** was replaced by a keto group in **BMC2** which was displayed as the disappearance of an oxymethine proton signal (H-3) of **BMC1** at δ 3.59. This finding was supported by HMBC spectrum of **BMC2**, in which the methyl protons at δ 1.03 (Me-19) were correlated with the carbons at δ 219.0 (C-3), 67.3 (C-18), 52.2 (C-4) and 48.6 (C-5) and oxymethylene protons at δ 3.64 and 3.43 (2H-18) with the carbons at δ 219.0 (C-3), 48.6 (C-5) and 16.8 (C-19). Thus, compound **BMC2** was determined as *ent*-16-kaurene-3-oxo-15β,18-diol.

Table 48 ^{1}H, ^{13}C NMR, DEPT and HMBC spectral data of compound BMC2

Position	δ_H (mult, *J*, Hz)	δ_C	DEPT	HMBC
1	2.12 (dd, *J* = 13.2, 2.7)	38.6	CH_2	2
	2.09 (dd, *J* = 13.2, 2.7)			
2	2.61 (ddd, *J* = 16.8, 12.3, 7.2)	35.4	CH_2	3, 10
	2.35 (ddd, *J* = 16.8, 6.6, 2.7)			
3		219.0	C	
4		52.2	C	
5	1.74 (m)	48.6	CH	6, 10
6	1.67 (m), 1.59 (m)	18.5	CH_2	7

Table 48 (Continued)

Position	δ_H (mult, *J*, Hz)	δ_C	DEPT	HMBC
7	1.78 (br dd, *J* = 9.6, 3.3)	34.2	CH_2	
	1.56 (m)			
8		52.7	C	
9	1.16 (br d, *J* = 6.6)	54.2	CH	5, 8
10		38.5	C	
11	1.51 (m), 1.48 (m)	20.2	CH_2	12
12	1.74 (m)	32.5	CH_2	
13	2.79 (br s)	42.1	CH	
14	1.92 (br d, *J* = 12.0)	36.2	CH_2	7, 15, 16
	1.46 (m)			
15	3.84 (s)	82.6	CH	
16		159.8	C	
17	5.24 (br s)	108.7	CH_2	13, 15, 16
	5.11 (br s)			
18	3.64 (d, *J* = 11.1)	67.3	CH_2	3, 5, 19
	3.43 (d, *J* = 11.1)			
19	1.03 (s)	16.8	CH_3	3, 4, 5, 18
20	1.20 (s)	17.5	CH_3	1, 5, 9, 10

1.3.3.3 Compound BMC3

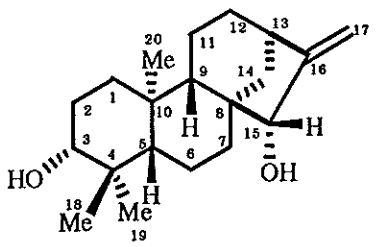

Compound BMC3 was obtained as a colorless viscous oil. The IR spectrum displayed the hydroxyl functionality at 3358 cm^{-1}. By comparison of ^1H and ^{13}C NMR spectral data (Table 49, Figures 89 and 90) and BMC1 (Table 47), the signals of the two oxymethylene protons at δ 3.58 and 3.33 (each d, *J* = 10.8 Hz) were not observed in

BMC3 and three methyl singlets were displayed at δ 1.03, 1.00 and 0.79. This data suggested that oxymethylene protons in **BMC1** were replaced with methyl protons in **BMC3** which was located at C-18 based on HMBC experiment in which H-3 (δ 3.21) showed long-range correlation with carbons at δ 38.8 (C-4), 28.4 (C-18) and 15.5 (C-19). On the basis of its spectroscopic data and comparison with those reported in the literature (Das et al., 1994), compound **BMC3** was assigned to be *ent*-kaurene-3β,15β-diol.

Table 49 ^{1}H, ^{13}C NMR, DEPT and HMBC spectral data of compound **BMC3**

Position	δ_H (mult, *J*, Hz)	δ_C	DEPT	HMBC
1	1.87 (m), 0.91 (m)	38.7	CH_2	2, 5, 10, 20
2	1.69 (m), 1.63 (m)	27.1	CH_2	1, 10
3	3.21 (dd, *J* = 10.8, 5.4)	79.0	CH	4, 18, 19
4		38.8	C	
5	0.76 (dd, *J* = 8.1, 2.7)	55.0	CH	4, 6, 7, 18, 19, 20
6	1.72 (m), 1.63 (m)	19.2	CH_2	5, 8
7	1.75 (m), 1.47 (m)	35.2	CH_2	5, 9
8		47.5	C	
9	1.01 (m)	54.1	CH	5, 8, 14, 15, 20
10		39.2	C	
11	1.43 (m), 1.29 (m)	18.1	CH_2	8, 12
12	1.67 (m), 1.54 (m)	32.7	CH_2	14
13	2.75 (br s)	42.3	CH	8
14	1.90 (m)	36.2	CH_2	8, 12, 15, 16
15	3.80 (s)	82.9	CH	9, 13, 14
16		160.3	C	
17	5.21 (br s)	108.3	CH_2	13
	5.08 (br t, *J* = 0.6)			
18	1.00 (s)	28.4	CH_3	3, 4, 5, 19
19	0.79 (s)	15.5	CH_3	3, 4, 5, 18
20	1.03 (s)	17.6	CH_3	1, 5, 9, 10

1.3.3.4 Compound BMC4

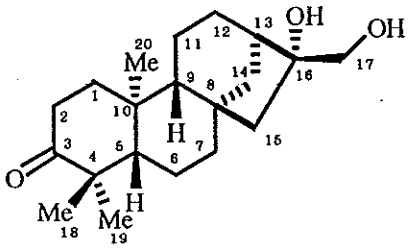

Compound **BMC4** was isolated as colorless viscous oil. The IR spectrum exhibited absorption bands of hydroxyl (3407 cm^{-1}) and carbonyl (1698 cm^{-1}) groups. The ^{1}H and ^{13}C NMR spectral data (Table 50, Figures 91 and 92) were comparable to those of **BMC2**. The differences were shown in the absence of olefinic protons at δ 5.24 and 5.11 (each br s, 2H-17) and an oxymethine proton at δ 3.84 (s, H-15). A closer analysis of the ^{13}C NMR data and DEPT experiments allowed the identification of three oxygenated carbons including an oxymethylene, an oxyquarternary and a carbonyl carbons. In ^{1}H NMR spectral data, the presence of the oxymethylene protons at δ 3.74 and 3.62 (each d, J = 10.8 Hz) was observed which showed correlations with carbons at δ 81.7 (C-16), 52.8 (C-15) and 45.3 (C-13) by HMBC experiments indicating that hydroxyl groups were attached to C-16 and C-17. The correlation of methyl protons at δ 0.98 (Me-19) with carbons at δ 216.0 (C-3), 54.3 (C-5), 47.2 (C-4) and 27.2 (Me-18) confirmed the location of carbonyl carbon at C-3. The relative stereochemistry of **BMC4** showed similarity with **BMC2**.

A survey of the literature for 16, 17-dihydroxy-*ent*-kauranoids revealed that the chemical shifts for tertiary hydroxyl group at C-16 and C-17 positions are sensitive towards the relative orientations of these substituents at C-16. In general, C-16 and C-17 of *ent*-kauranoids showed resonances between δ 79.7-79.8 (C-16β) and 69.5-70.4 (CH_2-17α) and between δ 81.6-81.8 (C-16α) and 66.2-66.5 (CH_2-17β). This characteristic of ^{13}C NMR shielding behaviour led to assignment of the stereochemistry (Agrawal et al., 1995). The C-16 and C-17 signals for this compound were found to appear at δ 81.7 and 66.3, thus reflecting the α-orientation of the tertiary hydroxyl group at C-16. This meant that **BMC4** was identified to be abbeokutone which was previously isolated from *Euphorbia sieboldiana* (Agrawal et al., 1995).

Table 50 ^{1}H, ^{13}C NMR, DEPT and HMBC spectral data of compound BMC4

Position	δ_H (mult, *J*, Hz)	δ_C	DEPT	HMBC
1	1.94 (dd, *J* = 13.2, 6.3)	39.2	CH_2	2, 3, 5, 10, 20
	1.33 (m)			
2	2.42 (dd, *J* = 8.7, 6.3)	34.0	CH_2	1, 3, 4, 10
3		216.0	C	
4		47.2	C	
5	1.37 (m)	54.3	CH	3, 18, 19, 20
6	1.47 (m), 1.39 (m)	21.6	CH_2	5, 7
7	1.63 (m), 1.45 (m)	40.9	CH_2	5, 8, 14
8		44.4	C	
9	1.04 (m)	55.3	CH	1, 5, 7, 10, 12, 15
10		38.5	C	
11	1.52 (m)	18.8	CH_2	8, 10, 13
12	1.54 (m)	26.0	CH_2	14
13	2.02 (br d, *J* = 3.6)	45.3	CH	
14	1.86 (m), 1.56 (m)	39.9	CH_2	15
15	1.52 (m), 1.44 (m)	52.8	CH	16
16		81.7	C	
17	3.74 (d, *J* = 10.8)	66.3	CH_2	13, 15, 16
	3.62 (d, *J* = 10.8)			
18	1.03 (s)	27.2	CH_2	3, 4, 5, 19
19	0.98 (s)	20.9	CH_3	3, 4, 5, 18
20	1.03 (s)	17.8	CH_3	1, 5, 9, 10

1.3.3.5 Compound BMC5

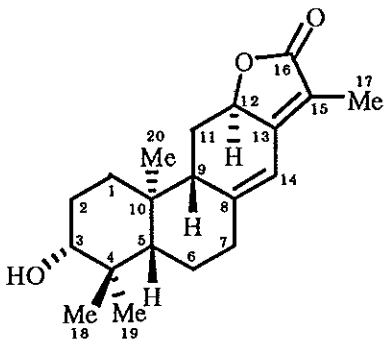

Compound BMC5 was isolated as a white solid, mp 175-176 °C. The IR spectrum suggested hydroxyl (3463 cm^{-1}), conjugated ester (1739 cm^{-1}) and double bond (1663 cm^{-1}) functionalities. The UV absorption maxima at 205 and 275 nm again suggested the presence of conjugation in the molecule.

Its ^{13}C NMR spectral data (Table 51, Figure 94) showed 20 signals for 20 carbons suggesting that compound BMC5 was a diterpenoid. The ^{1}H NMR spectral data (Table 51, Figure 93) displayed typical signals of abiatene-type diterpene as three singlet methyl signals at δ 1.04 (Me-19), 0.94 (Me-20) and 0.83 (Me-18), one vinylic methyl signal at δ 1.83 (d, J = 1.5 Hz, Me-17), one olefinic proton signal at δ 6.29 (s, H-14), and one oxymethine proton signal at δ 4.87 (ddd, J = 13.5, 6.6, 1.5 Hz, H-12). The oxymethine proton signals at δ 3.29 (dd, J = 11.4, 4.2 Hz), two AB systems of methylene proton signals at δ 2.55 (dd, J = 13.5, 6.6 Hz), 1.77 (dd, J = 13.5, 4.2 Hz) and 2.53 (ddd, J = 13.5, 4.2, 2.4 Hz), 2.22 (br dd, J = 13.5, 5.1 Hz), and two methine proton signals at δ 2.16 (br d, J = 8.7 Hz) and 1.16 (dd, J = 12.3, 2.4 Hz) were assigned as H-3, 2H-11, 2H-7, H-9 and H-5, respectively. On the basis of HMBC experiment, the correlations of a methine proton at δ 3.29 (H-3) with carbons at δ 39.1 (C-4), of methine proton at δ 1.16 (H-5) with carbons at δ 78.5 (C-3), 39.1 (C-4), 51.6 (C-9), 41.2 (C-10), 28.7 (Me-19), 16.7 (C-20) and 15.6 (Me-18), and of olefinic proton at δ 6.29 (H-14) with carbons at δ 156.3 (C-13), 116.4 (C-15), 76.1 (C-12), 51.6 (C-9) and 36.9 (C-7) confirmed the structure of BMC5.

The relative stereochemistry at the important chiral centers was determined on the basis of coupling constants and NOESY experiments. The large J value of proton H-3 (J = 11.4 Hz) indicated an axial orientation (β-phase). On biogenetic grounds, the

methyl Me-20 was deduced to be α-oriented (Dewick P.M., 2001), and this methyl group displayed NOESY cross-peak with Me-19. Hence Me-19 should also be α-oriented. Thus, compound **BMC5** was identified as helioscopinolide A (Borghi et al., 1991).

Table 51 ^{1}H, ^{13}C NMR, DEPT and HMBC spectral data of compound **BMC5**

Position	δ_H (mult, *J*, Hz)	δ_C	DEPT	HMBC
1	1.97 (dt, *J* = 12.9, 3.6)	37.4	CH_2	2, 9, 10, 20
	1.25 (m)			
2	1.60 (m)	27.4	CH_2	3
	1.50 (m)			
3	3.29 (dd, *J* = 11.4, 4.2)	78.5	CH	4, 18, 19
4		39.1	C	
5	1.16 (dd, *J* = 12.3, 2.4)	54.4	CH	3, 4, 9, 10, 18, 19, 20
6	1.87 (m)	23.4	CH_2	5
	1.45 (m)			
7	2.53 (ddd, *J* = 13.5, 4.2, 2.4)	36.9	CH_2	8, 13
	2.22 (br dd, *J* = 13.5, 5.1)			
8		151.7	C	
9	2.16 (br d, *J* = 8.7)	51.6	CH	8, 10, 11, 12, 14, 20
10		41.2	C	
11	2.55 (dd, *J* = 13.5, 6.6)	27.5	CH_2	8, 9, 10, 12, 13
	1.77 (dd, *J* = 13.5, 4.2)			
12	4.87 (ddd, *J* = 13.5, 6.6, 1.5)	76.1	CH	11, 13
13		156.3	C	
14	6.29 (s)	114.2	CH	7, 9, 12, 13, 15
15		116.4	C	
16		174.0	C	
17	1.83 (d, *J* = 1.5)	8.2	CH_3	13, 15, 16
18	0.83 (s)	15.6	CH_3	3, 4, 5, 19
19	1.04 (s)	28.7	CH_3	3, 4, 5, 18
20	0.94 (s)	16.7	CH_3	1, 5, 9, 10

1.3.3.6 Compound BMC6

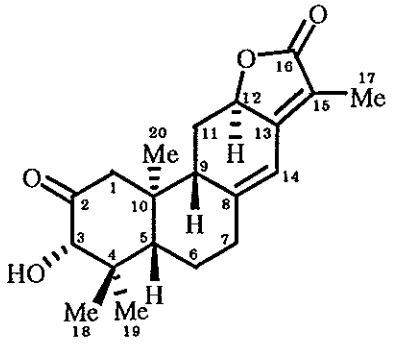

Compound **BMC6** was isolated as a white solid, mp 197-198 °C. Its IR and UV spectrum showed absorption bands similar to compound **BMC5**. The ^{13}C and ^{1}H NMR spectral data (Table 52, Figures 95 and 96) of compound **BMC6** revealed close structural similarity to compound **BMC5**, except that compound **BMC6** displayed a signal of carbonyl carbon at δ_C 209.4 and those of methylene protons at δ_H 2.74 and 2.39 (each d, J = 12.3 Hz, H-1) in **BMC6** were more downfield than methylene protons in **BMC5** because of deshielding zone of the carbonyl group. On the basis of HMBC correlations, an oxymethine proton at δ 3.97 (H-3) showed correlations with carbons at δ 209.4 (C-2), 45.1 (C-4), 29.6 (C-19) and 16.5 (C-18) confirming the attachment of a carbonyl group at C-2. Thus compound **BMC6** was assigned as helioscopinolide C (Crespi-Perellino et al., 1996).

Table 52 ^{1}H, ^{13}C NMR, DEPT and HMBC spectral data of compound **BMC6**

Position	δ_H (mult, J, Hz)	δ_C	DEPT	HMBC
1	2.74 (d, J = 12.3)	51.3	CH_2	2, 3, 5, 10, 20
	2.39 (d, J = 12.3)			
2		209.4	C	
3	3.97 (d, J = 1.2)	82.5	CH	2, 4, 18, 19
4		45.1	C	
5	1.83 (dd, J = 13.8, 2.4)	53.5	CH	1, 4, 6, 7, 9, 10, 18, 19, 20
6	1.99 (m)	23.1	CH_2	4, 5, 7, 8, 10
	1.54 (td, J = 12.9, 4.2)			

Table 52 (Continued)

Position	δ_H (mult, *J*, Hz)	δ_C	DEPT	HMBC
7	2.61 (m)	36.4	CH_2	8, 9
	2.28 (m)			
8		149.2	C	
9	2.50 (br d, *J* = 8.7)	51.4	CH	1, 8, 10, 11, 14, 20
10		46.9	C	
11	2.41 (m)	27.8	CH_2	8, 9, 10, 12, 13
	1.63 (m)			
12	4.85 (dd, *J* = 13.8, 5.1)	75.3	CH	13
13		155.0	C	
14	6.36 (s)	115.5	CH	7, 9, 12, 13, 15
15		117.6	C	
16		174.9	C	
17	1.85 (d, *J* = 1.2)	8.4	CH_3	13, 15, 16
18	0.71 (s)	16.5	CH_3	4, 5, 19
19	1.23 (s)	29.6	CH_3	4, 5, 18
20	0.92 (s)	17.4	CH_3	1, 5, 9, 10

1.3.3.7 Compound BMC7

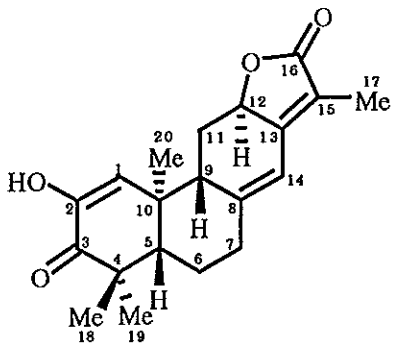

Compound BMC7 was obtained as a white solid, mp 211-212.5 °C. The UV and IR spectrum showed absorption bands similar to those of BMC6. The ^1H and ^{13}C NMR spectral data (Table 53, Figures 97 and 98) were closely related to those of BMC6,

except for the appearance of the olefinic proton signal at δ 6.42 (s) and hydroxyl signal at δ 6.10 (s) assignable, respectively to H-1 and OH at C-2 on the A ring of diterpene. On the basis of HMBC experiment, the double bond was located at C-1 and C-2 by correlation of methyl protons at δ 1.16 (Me-20) with carbons at δ 123.4 (C-1), 52.6 (C-5), 48.2 (C-9) and 41.7 (C-10). Thus compound **BMC7** was identified to be helioscopinolide I (Crespi-Perellino et al., 1996).

Table 53 ^{1}H, ^{13}C NMR, DEPT and HMBC spectral data of compound **BMC7**

Position	δ_H (mult, *J*, Hz)	δ_C	DEPT	HMBC
1	6.42 (s)	123.4	CH	2, 3, 5, 9, 20
2		145.1	C	
3		200.1	C	
4		44.0	C	
5	2.00 (dd, *J* = 12.6, 2.4)	52.6	CH	4, 18, 19, 20
6	1.86 (m), 1.63 (m)	23.0	CH_2	5, 8, 10
7	2.63 (ddd, *J* = 13.5, 3.0, 2.7)	36.7	CH_2	5, 6
	2.30 (m)			
8		148.9	C	
9	2.49 (br d, *J* = 8.7)	48.2	CH	8, 10, 11, 12, 14, 20
10		41.7	C	
11	2.70 (dd, *J* = 6.3, 3.8)	27.6	CH_2	8, 9, 10, 12, 13
	1.70 (dd, *J* = 13.8, 8.7)			
12	4.88 (dd, *J* = 13.2, 4.8)	75.4	CH	
13		155.0	C	
14	6.39 (br s)	116.0	CH	7, 8, 9, 12, 13
15		117.6	C	
16		174.9	C	
17	1.86 (d, *J* = 1.2)	8.4	CH_3	13, 15, 16
18	1.15 (s)	22.1	CH_3	3, 4, 5, 19
19	1.27 (s)	27.0	CH_3	3, 4, 5, 18
20	1.16 (s)	19.4	CH_3	1, 5, 9, 10
OH	6.10 (s)			1, 2, 3

Table 54 Comparison of ^{13}C NMR spectral data of compounds BMC1-BMC7

Position	BMC1	BMC2	BMC3	BMC4	BMC5	BMC6	BMC7
1	38.4	38.6	38.7	39.2	37.4	51.3	123.4
2	26.1	35.4	27.1	34.0	27.4	209.4	145.1
3	74.9	219.0	79.0	216.0	78.5	82.5	200.1
4	41.7	52.2	38.8	47.2	39.1	45.1	44.0
5	48.7	48.6	55.0	54.3	54.4	53.5	52.6
6	18.0	18.5	19.2	21.6	23.4	23.1	23.0
7	34.7	34.2	35.2	40.9	36.9	36.4	36.7
8	47.3	52.7	47.5	44.4	151.7	149.2	148.9
9	54.2	54.2	54.1	55.3	51.6	51.4	48.2
10	38.9	38.5	39.2	38.5	41.2	46.9	41.7
11	19.0	20.2	18.1	18.8	27.5	27.8	27.6
12	32.6	32.5	32.7	26.0	76.1	75.3	75.4
13	42.2	42.1	42.3	45.3	156.3	155.0	155.0
14	36.1	36.2	36.2	39.9	114.2	115.5	116.0
15	82.6	82.6	82.9	52.8	116.4	117.6	117.6
16	159.1	159.8	160.3	81.7	174.0	174.9	174.9
17	108.3	108.7	108.3	66.3	8.2	8.4	8.4
18	69.5	67.3	28.4	27.2	15.6	16.5	22.1
19	11.5	16.8	15.5	20.9	28.7	29.6	27.0
20	17.9	17.5	17.6	17.8	16.7	17.4	19.4

1.3.4 Bioactivities of isolated compounds from *B. pandurata*, *C. crista* and *S. multiflora*

In this research, we isolated several compounds from *B. pandurata*, *C. crista* and *S. multiflora* including diterpene and chalcone groups. These plants showed different biological activities. However, the bioactive tests were chosen according to literature report such as *B. pandurata* exhibited anti-HIV-1 PR activity, *C. crista*: antimalarial activity and *S. multiflora*: anti-allergic activity.

1.3.4.1 *Activity of isolated compounds from B. pandurata on anti-HIV-1 PR activity*

The human immunodeficiency virus type-1 (HIV-1), a member of retrovirus family, has been a causative organism in an acquired immunodeficiency syndrome (AIDS). One of the important enzymes necessary for the replication of this virus is HIV-1 protease (HIV-1 PR). HIV-1 PR belongs to the aspartyl protease class and functions as a dimer of 99 amino acids each. This enzyme plays a crucial role in the process of viral maturation and infectivity. Thus, searching for HIV-1 PR inhibitors from natural sources has become a promising approach. Herein, I report the activity against HIV-1 PR of chalcone derivatives from this plant. The compounds (**BP1-BP6**) isolated from the rhizomes of *B. pandurata* were investigated for anti-HIV-1 PR activity. Among the isolated compounds tested, **BP3** exhibited the most potent HIV-1 PR inhibitory activity with an IC_{50} value of 5.6 μM, followed by **BP2** (IC_{50} = 18.7 μM), whereas other compounds possessed weak activity (Table 55). Structure-activity relationships of these class of compounds for anti- HIV-1 PR activity are summarized as follows: (1) hydroxyl moiety at position 4 conferred higher activity than the methoxyl group as observed in **BP3** (IC_{50} = 5.6 μM) versus **BP2** (IC_{50} = 18.7 μM); and (2) prenylation of dihydrochalcone (**BP3**, IC_{50} = 5.6 μM) produced higher activity than non-prenylated one (**BP5**, IC_{50} > 100 μM). The potency of **BP3** against HIV-1 PR was also comparable to that of acetyl pepstatin, a positive control (IC_{50} = 3.4 μM).

Table 55 HIV-1 PR inhibitory activity of compounds BP1-BP6 of *B. pandurata*[a], ( ) = %inhibition at 100 μM

Compounds	IC_{50} (μM)
Panduratin C (BP1)	> 100 (43.1%)
Panduratin A (BP2)	18.7 ± 0.8
Hydroxypanduratin A (BP3)	5.6 ± 0.7
Helichrysetin (BP4)	>100 (14.1%)
2′, 4′, 6′-Trihydroxyhydrochalcone (BP5)	>100 (7.5%)
Uvagoletin (BP6)	>100 (2.7%)
Acetyl pepstatin, positive control	3.4 ± 0.2

[a] Each value represents the mean ± SD of the three determinations.

1.3.4.2 *Activity of isolated compounds from C. crista on antimalarial activity*

The effective dose (ED_{50}) of cassane and norcassane type diterpenes, SC1-SC10, RH1-RH4 and SD1-SD6 for antimalaria suggested inactivity (ED_{50} >50 μg/ml), whereas rosane-type diterpene (SC10) exhibited significant antimalaria with ED_{50} values of 4.1 μg/ml.

1.3.4.3 *Activity of isolated compounds from S. multiflora on antiallergic activity*

As shown in Table 56, *ent*-16-kaurene-3β,15β,18-triol (BMC1) exhibited the most potent activity with an IC_{50} value of 22.5 μM, followed by *ent*-16-kaurene-3-oxo-15β,18-diol (BMC2, IC_{50} = 22.9 μM), helioscopinolide A (BMC5, IC_{50} = 26.5 μM), *ent*-kaurene-3β,15β-diol (BMC3, IC_{50} = 28.7 μM), helioscopinolide I (BMC7, IC_{50} = 29.3 μM), helioscopinolide C (BMC6, IC_{50} = 37.0 μM) and abbeokutone (BMC4, IC_{50} = 42.1 μM). All these compounds possessed stronger anti-allergic activity than ketotifen fumarate, a positive control (IC_{50} = 47.5 μM). These compounds were also tested on the enzyme activity of β-hexosaminidase. As a result, they showed weak inhibition against this enzyme activity at 100 μM, whose results indicated

the inhibition of the antigen-induced degranulation but not the activity of β-hexosaminidase.

Table 56 Anti-allergic activity of compounds (BMC1-BMC7) from *S. multiflora*[a]

Compound	IC_{50} (μM)	Enzyme inhibition at 100 μM
ent-16-Kaurene-3β,15β,18-triol (BMC1)	22.5	14.3%
ent-3-Oxo-16-kaurene-15β,18-diol (BMC2)	22.9	17.9%
ent-16-Kaurene-3β,15β-diol (BMC3)	28.7	21.0%
Abbeokutone (BMC4)	42.1	16.1%
Helioscopinolide A (BMC5)	26.5	19.5%
Helioscopinolide C (BMC6)	37.0	18.6%
Helioscopinolide I (BMC7)	29.3	21.7%
Ketotifen fumarate	47.5	15.8%

[a]Each value represents mean ± S.E.M. of four determinations.

CHAPTER 1.4
CONCLUSION

Searching for anti-HIV-1 protease (PR) inhibitors from Thai medicinal plants led to the isolation of a new cyclohexenylchalcone named panduratin C (**BP1**), chalcone derivatives: panduratin A (**BP2**), hydroxypanduratin A (**BP3**), helichrysetin (**BP4**), 2′,4′,6′-trihydroxyhydrochalcone (**BP5**), uvangoletin (**BP6**), two aromatics: dihydro-pinosylvin (**BP7**), methyl *trans*-cinnamate (**BP8**), and three flavanones: pinocembrin (**BP9**), pinostrobin (**BP10**) and alpinetin (**BP11**) from methanol extract of *B. pandurata* rhizomes. The structures of all compounds were elucidated on the basis of chemical and spectroscopic methods. It was found that **BP3** possessed the most potent anti-HIV-1 PR activity with an IC_{50} value of 5.6 μM, followed by **BP2** (IC_{50} = 18.7 μM), whereas other compounds exhibited only mild activity. Structure-activity relationships of these compounds on anti-HIV-1 PR activity are summarized as follows: (1) hydroxyl moiety at position 4 conferred higher activity than methoxyl group; (2) prenylation of dihydrochalcone was essential for activity; and (3) introduction of double bond at C-α and C-β of chalcone gave higher activity. As regards of active constituents contained in *B. pandurata* rhizomes, hydroxypanduratin A (**BP3**) and panduratin A (**BP2**) are active principles against HIV-1 PR.

Eight new cassane-type diterpenes, named taepeenin A-D, F and G (**SC1-SC5, SC9**), and two new norcassane-type diterpenes, named nortaepeenin A and B (**SC6** and **SC7**), were isolated from the stems of *C. crista* along with two known diterpenes: methyl vinhaticoate (**SC8**) and *ent*-11β-hydroxy-rosa-5,15-diene (**SC10**). In addition, the structure of **SC1** was confirmed by X-ray diffraction analysis. Six compounds were isolated from roots of *C. crista* including three new cassane-type diterpenes: taepeenin E (**RH1**), H (**RH3**) and I (**RH4**), and three known compounds: vinhaticoic acid (**RH2**), nutiducol (**RH5**) and stipulin (**RH6**). A new dimer **SD3** and two new cassane-type diterpenes **SC4** and **SC5**, designated taepeenin J-L, together with three known compounds: 17-methylvouacapane-8(14),9(11)-diene (**SD1**), vouacapane (**SD2**) and 6β-hydroxyvouacapane (**SD6**) were isolated from the seeds of this plants. **SD3** possesses a dimeric vouacapane skeleton.

Two *ent*-kaurene diterpenes, *ent*-16-kaurene-3β,15β,18-triol (**BMC1**) and *ent*-3-oxo-16-kaurene-15β,18-diol (**BMC2**), were isolated from a dichloromethane extract of the bark of *Suregada multiflora* along with five known diterpenes: *ent*-16-kaurene-3β,15β-diol (**BMC3**), abbeokutone (**BMC4**), helioscopinolide A (**BMC5**), helioscopinolide C (**BMC6**) and helioscopinolide I (**BMC7**). Compounds **BMC1-BMC7** possessed appreciable anti-allergic activities in RBL-2H3 cells model with IC_{50} values ranging from 22.5 to 42.2 μM.

Part II

Search for Novel Terpenes in *Erythropodium caribaeorum* and Study for Carotenoids from a Coral-Derived *Micrococcus* strain PAH83

CHAPTER 2.1
INTRODUCTION

2.1.1 Search for novel terpenes in *Erythropodium caribaeorum*

2.1.1.1 *Introduction*

Natural products from terrestrial plants have been exploited by humans for a long time for many purposes such as food, medicines, fragrances, pigments, pesticides, herbicides, fungicides and insecticides. However, during the 1960s, the use of scuba diving technology opened up areas of unexplored marine environments that enabled researchers to collect the marine organisms which led to the discovery of a broad spectrum of novel molecular structures. Since investigations of the 1970s, drug discovery from the world's oceans has already become a valuable tool in biomedicine. Even with this success, chemists and pharmacologists are still just beginning to explore the world's ocean because the oceans cover over 70% of the Earth's surface.

The marine environment is a rich source of biologically active natural products, many of which have not been found in terrestrial sources (Carte, 1996). This is due to the physical, chemical and biological differences between marine and terrestrial environments: (i) the high quantity of elemental compounds in the sea such as salt content and halogen elements (Cl^-, 19,000 mg l^{-1}; Br^-, 65 mg l^{-1}; and I^-/IO^{3-}, 5 x 10^{-4} mg l^{-1}) (Proksch, et al. 2002); (ii) the various pressure that increases 1 atm at every ten meters in the depths of the ocean; and (iii) unusually high or low temperatures and reduced light in the seawater. These properties make the food chains in ocean environments exceedingly complex.

Gorgonians, also known as sea whips, sea fans or sea plumes, are prominent members of tropical and subtropic habitats world wide. In the Bahamas and Florida, gorgonians represent an estimated 38% of the known fauna with over 195 species documented from the families Briareidae, Plexauridae and Gorgoniidae (Bayer, 1961). These organisms have proven to be a prolific source of novel bioactive natural products, particularly terpenes which exhibit a range of biomedical activities (Fenical, 1987 and Rodriguez, 1995).

Eleutherobin is a microtubule-stabilizing diterpenoid glycoside originally isolated from the rare Australian octoacoral *Eleutherobia* sp. (Lindel et al., 1997). Although two elegant total syntheses of eleutherobin have been reported (Nicolaou et al., 1998; Chen et al., 1999), the anticancer potential of eleutherobin has never been fully evaluated because total synthesis and the original natural source both failed to provide sufficient material for effective in vivo testing. Recently, it was discovered that *Erythropodium caribaeorum*, a relatively abundant Caribbean gorgonian, is a good source of eleuthesides, and it has provided sufficient eleutherobin for preliminary animal studies (Scafati et al., 2002) and chemical transformations to new analogues.

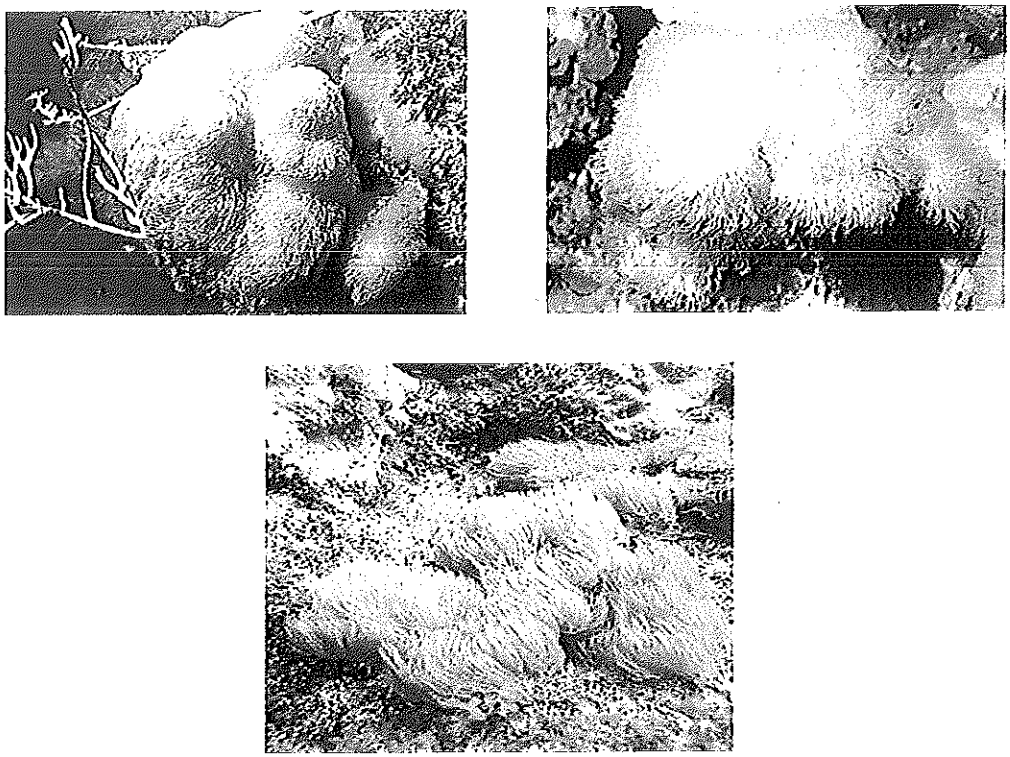

Figure 5 *Erythropodium caribaeorum*

2.1.1.2 Review of literatures

E. caribaeorum is an encrusting gorgonian, and previous chemical investigations of this organism resulted in the isolation of over 10 briarane and eunicellane skeleton, including erythrolides A-Q (Look et al., 1984; Pordesimo et al., 1991; Dookran et al., 1993; Banjoo et al.,2002), acetate analogues of E, F, and H (Maharaj et al., 1999), and eleuthesides (Scafati, 2002).

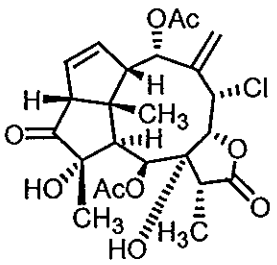

1: Aquariolide A

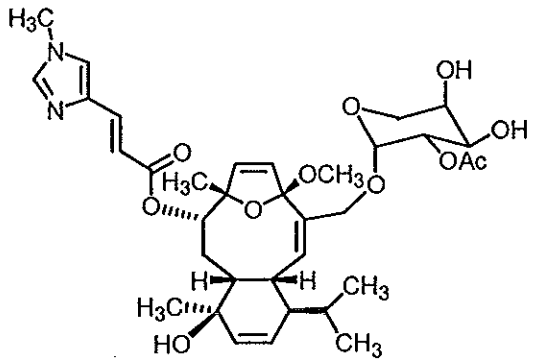

2: Caribaeoside

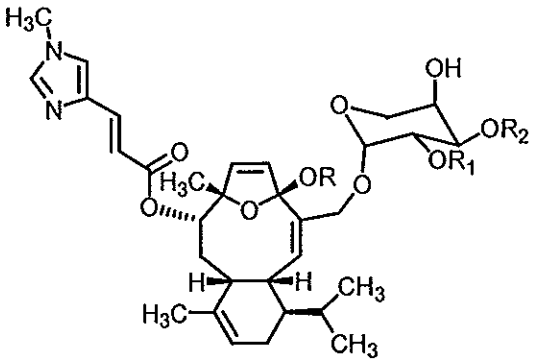

3: R = CH_3, R_1 = Ac, R_2 = H; Eleutherobin

4: R = H, R_1 = Ac, R_2 = H; Desmethyleleutherobin

5: R = CH_3, R_1 = H, R_2 = Ac; Isoeleutherobin

6: R = CH_3, R_1 = R_2 = H; Desacetyleleutherobin

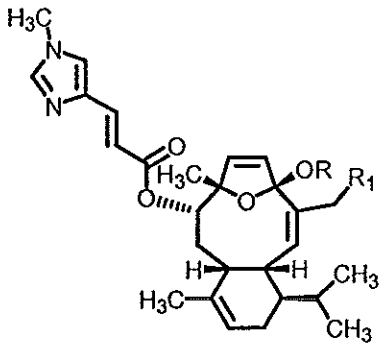

7: R = H, R_1 = CO_2CH_3; Sarcodictyin

8: R = CH_3, R_1 = H; Methylcaribaeorane

9: R = CH_3, R_1 = H; 15-Hydroxycaribae

10: R = R_1 = H; Caribaeorane

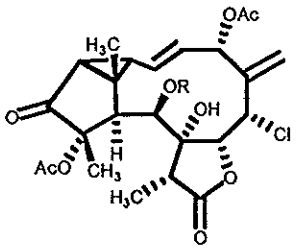

11: R = Ac; Erythrolide A

12: R = $COCH_2OC(O)CH_3$; Erythrolide L

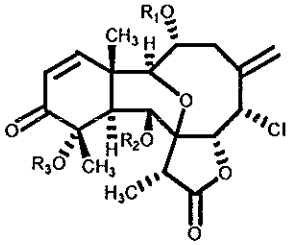

13: R_1 = R_2 = R_3 = Ac; 3-Acetylerythrolide E

14: R_1 = $(CO)CH_2O(CO)CH_3$, R_2 = R_3 = Ac; 3-Acetylerythrolide I

15: R_1 = R_3 = Ac, R_2 = H; Erythrolide E

16: R_1 = $(CO)CH_2O(CO)CH_3$, R_2 = H, R_3 = Ac; Erythrolide I

17: R_1 = H, R_2 = $(CO)CH_2O(CO)CH_3$, R_3 = Ac; Erythrolide F

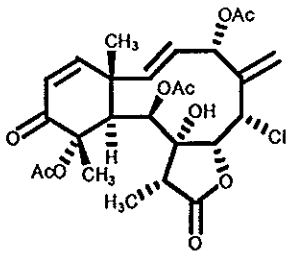

18: Erythrolide B

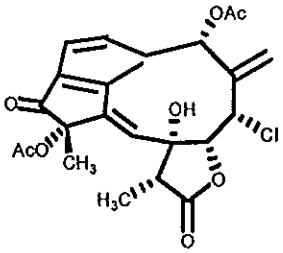

19: Erythrolide K

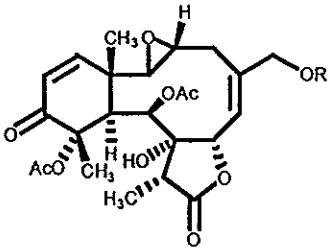

20: R = Ac; 16-Acetylerythrolide H

21: R = H; Erythrolide H

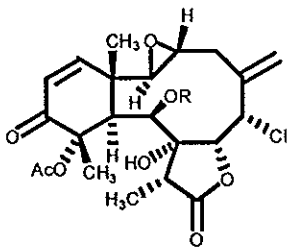

22: R = Ac; Erythrolide C

23: R = $(CO)CH_2O(CO)CH_3$; Erythrolide D

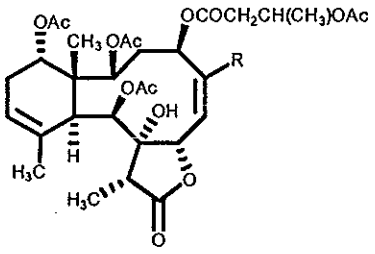

24: R = CH_3; Erythrolide M

25: R = CH_2OH; Erythrolide N

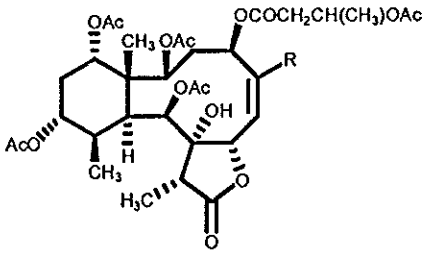

26: Erythrolide J

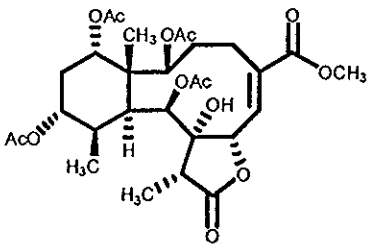

27: Erythrolide O

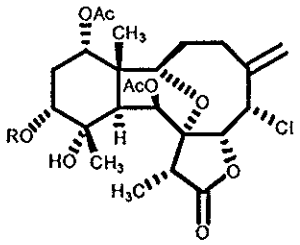

28: R = H; Erythrolide P

29: R = Ac; Erythrolide Q

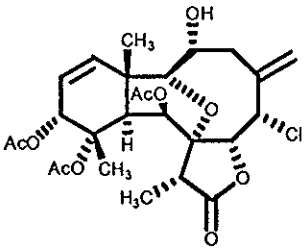

30: Erythrolide G

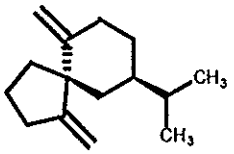

31: Erythrodiene

2.1.2 Production of carotenoids by *Micrococcus* strain PAH83

2.1.2.1 *Introduction*

Carotenoids, found widely in microorganisms and plants, are important natural pigments, displaying yellow, orange, and red colors. Carotenoids are generally C_{40} tetraterpenoids formed from eight C_5 isoprenoid units joined head-to-tail, except at the center where a tail-to-tail linkage reverses the order, resulting in a symmetrical molecule. An important feature is a centrally located, extended conjugated double-bond system, which constitutes the light-absorbing chromophore that gives carotenoids their attractive color and provides the visible absorption spectrum that serves as a basis for their

identification and quantification. The basic skeleton may be modified in many ways, including cyclization, hydrogenation, dehydrogenation, introduction of oxygen functions, rearrangement, chain shortening, or combinations thereof, resulting in a multitude of structures. Hydrocarbon carotenoids (e.g. β-carotene, lycopene) are known as carotenes, and oxygenated derivatives are called xanthophylls. Common oxygen substituents are the hydroxy (as in β-cryptoxanthin), keto (as in canthaxanthin), epoxy (as in violaxanthin), and aldehyde (as in β-citraurin) groups. Carotenoids can be acyclic (e.g. lycopene), monocyclic (e.g. γ-carotene), or bicyclic (e.g. α- and β-carotene). In nature, carotenoids exist primarily in the more stable all-*trans* (or all-*E*) form, but small amounts of *cis* (or *Z*) isomers do occur.

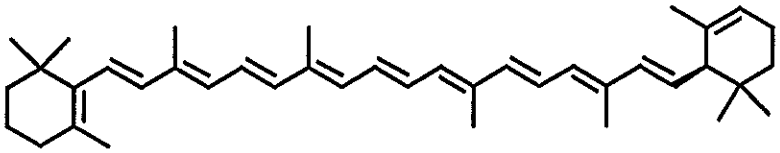

α-Carotene

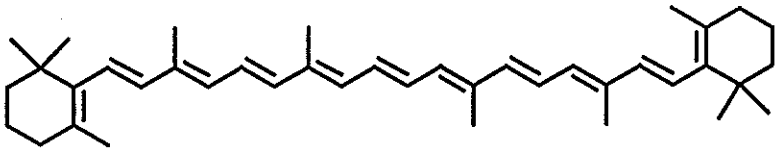

β-Carotene

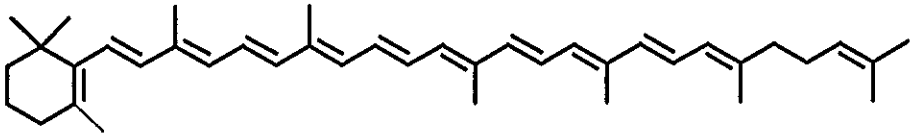

γ-Carotene

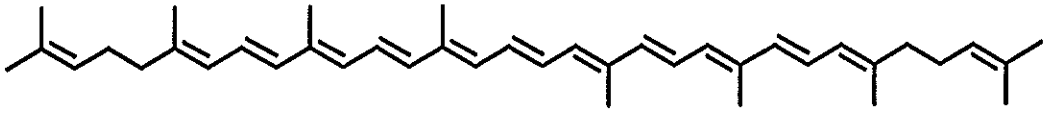

Lycopene

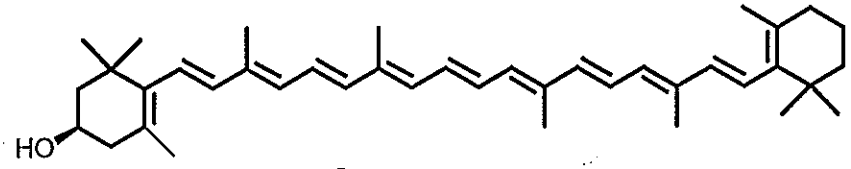

β-Cryptoxanthin

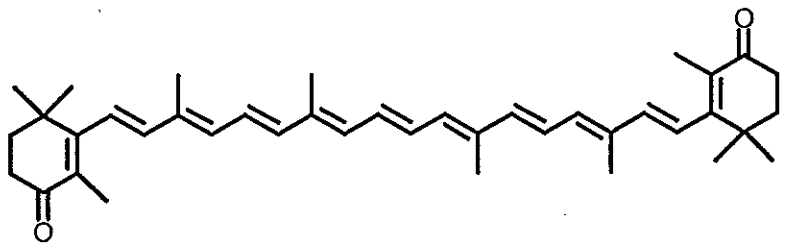

Canthaxanthin

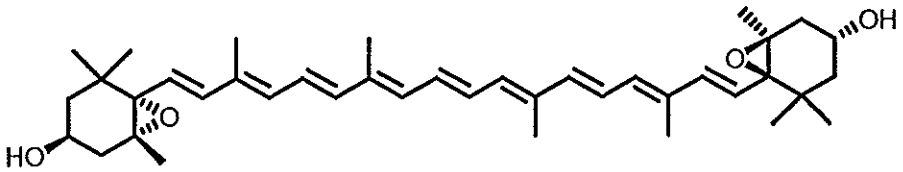

Violaxanthin

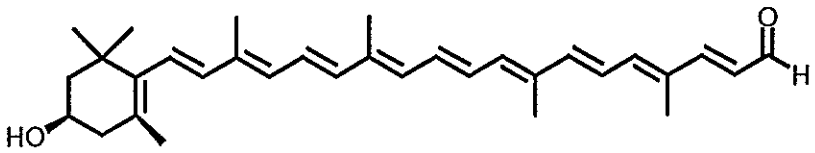

β-Citraurin

Industrially, carotenoid pigments such as β-carotene and astaxanthin, are used as natural food colourants or feed additives in aquaculture. Several studies have shown that carotenoids combat various types of cancer and other diseases because of their antioxidant and/or provitamin A potential.

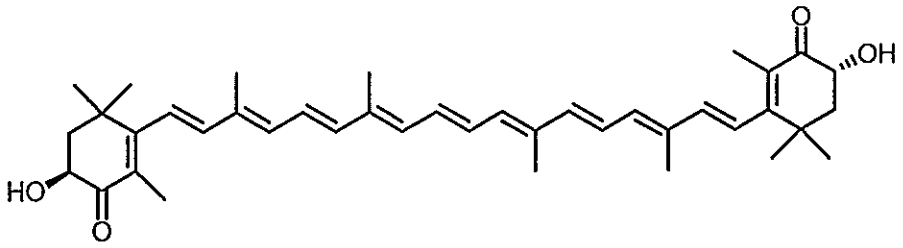

Astaxanthin

Micrococcus is a Gram-positive, aerobic bacterium which is a member of the Micrococcaceae family. *Micrococcus* cells can be observed under the microscope as spherical cells forming pairs or clusters. If cultured in broth or on nutrient agar, the colonies may be red or yellow when observed unstained. Although these bacteria are common human skin contaminant, they are relatively harmless to humans because they maintain a saprophytic lifestyle. They can also be found in freshwater environments or in soil. Three common species of *Micrococcus* are *M. luteus*, *M. roseus*, and *M. varians*

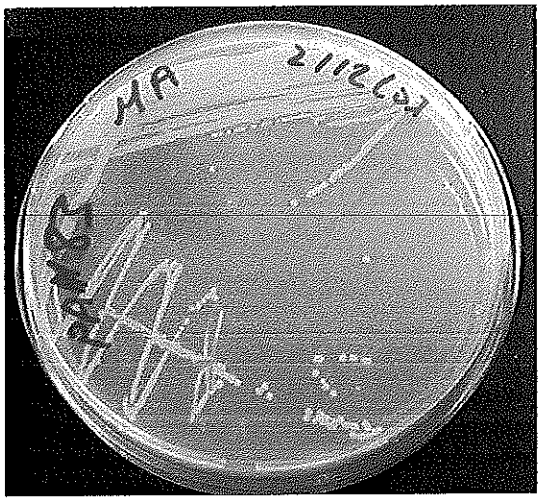

Figure 6 *Micrococcus* strain PAH83

2.1.2.2 Characterization of carotenoids in bacteria

The chemistry of carotenoids in photosynthetic bacteria has been reviewed by Liaasen-Jensen (Liaaen-Jensen, 1978). About 80 different carotenoids are synthesized by photosynthetic bacteria. Their distribution in four major families of photosynthetic bacteria, namely the Rhodospirillaceae, Chromatiaceae, Chlorobiaceae, and Chloroflexaceae, has been reviewed. In general, the characteristics of carotenoids in photosynthetic bacteria are as follows: (1) Most carotenoids are an aliphatic type, except for some aromatic or β end group types in the Chlorobiaceae, and Chloroflexaceae; (2) the cross-conjugated aldehyde and the tertiary methoxy group are confined to the carotenoids of photosynthetic bacteria; (3) several kinds of carotenoids are found in each species; (4) all the carotenoids are bound to light-harvesting or reaction center complexes; and (5) structural elements such as allenic or acetylenic bonds, epoxides or furanoxides, or C_{45} or C_{50} carotenoids are not encountered (Takaichi and Shimada, 1992).

It is well known that the positions on the main λ_{max} are characteristic of the chromophores of the individual carotenoids. λ_{max} is mainly influenced by the number of conjugated C=C double bonds (N) in compounds, and λ_{max} increases as N increases. The main λ_{max} of phytoene (N = 3) in methanol is 285 nm and that spirilloxanthin (N = 13) is 492 nm. The conjugated β ring influences the chromophore. A carotenoid in which the conjugation extends into the β ring has its λ_{max} at shorter wavelengths than a nonconjugated

β ring-type carotenoid with the same *N* value. Thus, in *N* = 11 carotenoids, lycopene (nonconjugated β ring-type) has its main λ_{max} at 468 nm, while rubixanthin (one-conjugated β ring-type) and β-carotene (two-conjugated β ring-type) have their main λ_{max} at 458 and 449 nm, respectively.

2.1.3 Objective

A key finding in any terpene biosynthetic study is identifying the structure of the terpene synthase product. From a recent study using radioactivity-guided isolations coupled with a detailed NMR-guided analysis of the hydrocarbon fraction of *E. caribarorum*, Kerr lab has shown that compound 32 is the cyclase product leading to desmethyleleutherobin (4). As reported by the Andersen group (Cinel et al., 1999), eleutherobin is an artifact and its desmethyl derivative is the true natural product. Thus, this research is now in a position to purify and sequence the terpene synthase responsible for the production of 32 and study for production of carotenoids from *Micrococcus* strain PAH83.

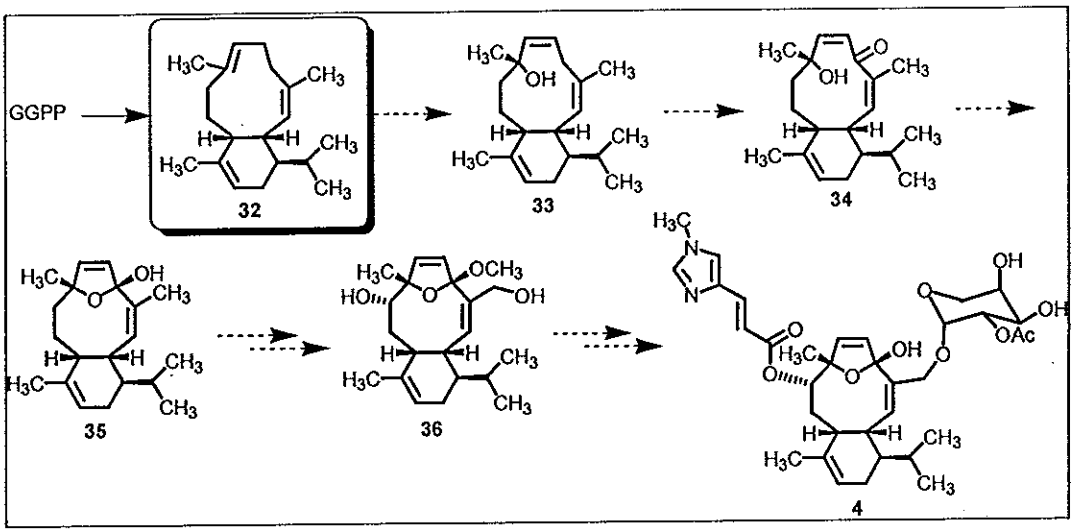

Scheme 8 Proposed biosynthesis of desmethyleleutherobin (4)

CHAPTER 2.2
EXPERIMENTAL

2.2.1 Instruments and Chemicals

Absorbance measurements were carried out by using a Nanodrop ND-1000 spectrophotometer. HPLC apparatus (Series 200 pump, 785A UV/Vis detector; series 250 Binary and Isocratic LC pump, LC 235 diode array and LC 30 RI detector) was from Perkin Elmer. HPLC-APCI-MS from an Accela instrument (Thermo Electron Corporation) equipped with automatic sample injector, photodiode-array detector (PDA) and Finnigan LXQ series APCI mass selectivity detector was used. GC-MS was carried out on Focus GC from Thermo Electron Corporation. Nuclear magnetic resonance spectra were recorded on FTNMR Bruker Ultra Shield™ 300 MHz in chloroform-*d*, benzene-d_6 and methanol-d_4 solutions. Solvents for extraction and chromatography were HPLC and LC grade reagent. Flash column chromatography (FCC) was performed on silica gel 200-425 mesh of Fisher ChemAlert Guide. Precoated plates of silica gel 60 GF_{254} (EMD) was used for analytical purposes.

2.2.2 Material

Samples of *E. caribaeorum* were collected at a depth of 20 ft off Dania Beach, Florida, USA. The *Micrococcus* strain PAH83 was isolated from the octocoral *Pseudopterogorgia acerosa* collected from the Bahamas.

2.2.3 Extractions and Isolations

2.2.3.1 Isolation and Chemical Investigation from E. caribaeorum

Freeze-dried *E. caribaeorum* (383.3 g) was immersed in EtOAc-MeOH (1:1, v/v) (each 3 x 4l, 3 days) at room temperature. The crude extract was filtered and

evaporated under reduced pressure (rotatory evaporator) to afford a dark-brown gum (28.42 g). This crude extract was further subjected to FCC using silica gel 190 g with hexane and increasing polarity with EtOAc and MeOH, respectively (each 4 x 250 ml). On the basis of their TLC characteristic, the collected fractions which contained the same major components were combined; fractions EC1A-EC1Q were obtained (Table 57).

Table 57 Fractions from FCC of crude extract

Fractions	Weight (g)	Solvent systems
EC1A	0.2603	100% hexane
EC1B	0.3593	100% hexane
EC1C	7.0468	90% hexane in EtOAc
EC1D	1.5806	90% hexane in EtOAc
EC1E	1.6302	80% hexane in EtOAc
EC1F	0.0876	80% hexane in EtOAc
EC1G	0.4525	70% hexane in EtOAc
EC1H	0.2386	70% hexane in EtOAc
EC1I	2.7693	50% hexane in EtOAc
EC1J	2.0318	50% hexane in EtOAc
EC1K	0.7927	50% hexane in EtOAc
EC1L	0.1873	25% hexane in EtOAc
EC1M	1.1772	100% EtOAc
EC1N	0.1372	50% EtOAc in MeOH
EC1O	1.2057	50% EtOAc in MeOH
EC1P	0.9988	100% MeOH
EC1Q	1.2263	100% MeOH

Fractions EC1A was analyzed using ^{1}H NMR (300 MHz) and GCMS. From ^{1}H NMR spectrum, the major compound was interested and was further separated by HPLC on 250 x 4.6 mm ZORBAX RX C18, 5 µm column with 100% MeOH at a flow of 1 ml/min. Spectra were recorded on-line from the elution peaks with a RI detector to give fourteen peaks (fourteen subfractions, EC1A1-EC1A14). Subfraction EC1A7 (5.5 mg) afforded a pure sesquiterpene which was assigned as erythrodiene.

Fractions EC1B-EC1D were identified by the same method as fraction EC1A. These fractions showed NMR signals of long chain fatty acid derivatives and were not further investigated.

For fraction EC1E, a pure steroid was crystallized from CH_2Cl_2 which was not further identified.

Fractions EC1F-EC1K were analyzed by LCMS on an Accela instrument (Thermo Electron Corporation) equipped with automatic sample injector, photodiode-array detector (PDA) and LXQ series APCI mass selectivity detector. Separation was performed on 50 mm x 2.1 mm x 1.9 μm Hypersil Gold C18 column using the gradient solvent system as follows: 0 to 1 min, 30% MeOH:H_2O; 1 to 10 min, 100% MeOH; 10 to 15 min, 100% MeOH. The flow rate was set to 0.4 ml/min, and injection volume was 1 μl. Erythrolides A and B were found as major components in fractions EC1K and EC1I, respectively, and erythrolide A was crystallized with MeOH.

Fraction EC1P was separated by HPLC on Phenomenex Gemini C-18, 5μ, 250x10 mm column using the gradient solvent system as follows: 0 to 10 min, 70%MeOH:H_2O; 10 to 30 min, 100% MeOH, and then reequilibration to the starting condition. Absorbance spectra were recorded on-line with LC-235 diode array detector (Perkin Elmer) at 290 nm. The retention time at 22.52 and 26.32 min was suggested to desacetyleleutherobin and eleutherobin which was confirmed by ^1H NMR spectrum. In addition, eleutherobin was compared with authentic sample.

2.2.3.2 Study for Production of Carotenoids from *Micrococcus* strain PAH83

2.2.3.2.1 Growth Conditions

The microorganism was grown in a sterilized marine broth (Difo) medium containing 5.0 g l^{-1} peptone, 1.0 g l^{-1} yeast extract at 30 °C. The initial pH was adjusted to desired value with dilute HCl and NaOH solutions and the medium was heat sterilized.

2.2.3.2.2 Analytical Methods

A 10 ml sample was taken from each flask at definite time intervals. Great care was taken to protect the samples from light. Absorbance measurements were

carried out by using a Nanodrop ND-1000 spectrophotometer. The medium without yeast growth was used as the blank. The total carotenoid content was also determined spectrophotometrically. The procedure used for the extraction of carotenoids was essentially a modification of published methods (Jagannadham et al., 1991). Cells were first centrifuged at 6,500g for 15 min. The supernatant was discarded. The cell pellet was rinsed twice with deionized water, then centrifuged again (6,500g, 15 min) and the supernatant was discarded. Cells were mixed with methanol and blended to prevent clotting. Samples were then wrapped with aluminum foil to protect them from light, and the extraction was vortexed until the methanol layer turned yellow (within 10 min). The methanol extract was purified from cell debris by further centrifugation at 8,000g for 10 min, and its absorbance at 440 nm was measured. β-Carotene (Sigma) was used as the standard.

2.2.3.2.3 HPLC Analysis

Methanol extracts were evaporated to dryness under vacuum at 30 °C in a Buchi rotavapor, within minutes. Purification of carotenoids was carried out without saponification. Dry pigments were dissolved in 1 ml methanol injected (50 µl) onto a µBondapak C18 column (300 x 4.6 mm, 5 µm particle size, RCM type; Water, USA). All other HPLC apparatus (Series 200 pump, 785A UV/Vis detector at 440 nm) was from Perkin Elmer. Separation was achieved using reversed phase HPLC at a flow rate of 1.0 ml min^{-1}. Solvents and conditions for separation were as follows: 0 to 10 min, 90% methanol:H_2O; 10 to 20 min, 90% methanol:H_2O to 100% methanol; 20 to 40 min, 100% methanol.

2.2.3.2.4 LC-MS

For analysis of carotenoids by HPLC-APCI-MS, an Accela instrument (Thermo Electron Corporation) equipped with automatic sample injector, photodiode-array detector (PDA) and LXQ series APCI mass selectivity detector was used. The mass spectra were recorded in the positive ion mode in the mass range from m/z 50 to 1500. The voltage of the corona needle was +3.9 kV, cone voltage of +17 V, probe temperature of 300 °C and source temperature of 200 °C. Separation was performed on 50 mm x 2.1

mm x 1.9 μm Hypersil Gold C18 column using the gradient solvent system as follows: 0 to 1 min, 30% MeOH:H_2O; 1 to 10 min, 100% MeOH; 10 to 15 min, 100% MeOH. The flow rate was set to 0.4 ml min^{-1}, and injection volume was 1 μl. The PDA was operated at 200–800 nm.

CHAPTER 2.3
RESULTS AND DISCUSSION

2.3.1 Search for intermediates involved in eleutherobin biosynthesis

The primary problem in pathway elucidation work is the very low levels of incorporation of labeled metabolites thus "forcing" researchers to use radioisotopes rather than stable isotope methodology. In this part of the work, a search was conducted for potential intermediates by NMR and LC-MS to evaluate extracts for general terpene diversity and GC-MS for examining hydrocarbon fractions for potential terpene cyclase products.

In an effort to identify plausible intermediates involved in desmethyl-eleutherobin biosynthesis, we used coral material from Florida for this search for new presumed intermediates.

The dried sample of *E. caribaeorum* was extracted with EtOAc-MeOH (1:1, v/v) and the organic solvents were removed by rotary evaporation. The crude extract was subjected to silica column chromatography and eluted with 100% hexane and increasing polarity with EtOAc and MeOH to afford 17 fractions (EC1A-EC1Q, Table 57). From the ^{1}H NMR spectrum, fraction EC1A (Figure 114) showed characteristics of a terpene cyclase product at δ 1.0-1.5 and 5.0-5.5 ppm. The GC-MS spectrum (Figures 99 and 100) displayed the peak at retention time 9.20 min which showed the molecular weight at *m/z* 204 corresponding to $C_{15}H_{24}$. This fraction was injected on reversed-phase C-18 HPLC with 100% MeOH using RI detector. The subfraction **EC1A7** at retention time 9.20 min was collected and further identified by NMR techniques. The ^{13}C NMR spectrum exhibited 15 carbons with four olefinic carbons. From above data, this compound was suggested to be a sesquiterpene with two carbocyclic rings. The observed double bonds were assigned as terminal exocyclic olefinics on the basis of their ^{1}H and ^{13}C NMR characteristics. Thus, compound **EC1A7** was identified as the previously reported erythrodiene (Pathirana and Fenical, 1993).

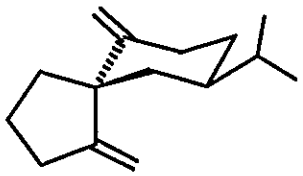

Erythrodiene

Table 58 ^{13}C NMR spectra (75 MHz, C_6D_6) of compound EC1A7 and erythrodiene

Compound EC1A7	Erythrodiene (50 MHz, $CDCl_3$)
158.0	158.0
152.9	152.8
107.5	109.9
106.8	106.7
51.9	51.3
41.6	41.1
40.3	39.7
40.1	39.6
34.3	33.8
33.5	33.0
33.0	32.5
31.6	31.1
21.2	20.8
20.2	20.1
20.1	19.7

The ^1H NMR and GC-MS of fractions EC1B-EC1D (Figures 101-103, 116-118) showed characteristics of long chain fatty acids which were not further investigated.

Investigation of fraction EC1E indicated the presence of a steroid as a major compound in this fraction. The ^1H NMR spectrum was clear which was not further identified.

Purification of fraction EC1K by recrystallization with MeOH afforded a pure compound which was identified as erythrolide A (Dookran et al., 1999). The LC-MS

spectrum (Figure 109) confirmed the peak at 3.67 min (*m/z* 538.6). All compounds were not isolated except for erythrolide A because the required molecular peak was not found in the spectrum. The same methods for analysis in other fractions were used. Interestingly, the fraction EC1H (Figure 7) with the molecular ion at *m/z* 303 on APCI source showed the same molecular ion with the intermediate in Scheme 8. In addition, this peaks displayed the absorbance at 236 nm on PDA. Thus, this fraction was further isolated by HPLC with 70% MeOH:H_2O, 0 to 10 min; 100% MeOH, 10-30 min. The peak at retention time 24.72 min was collected (Figure 7) but the sample was not enough for further NMR investigation.

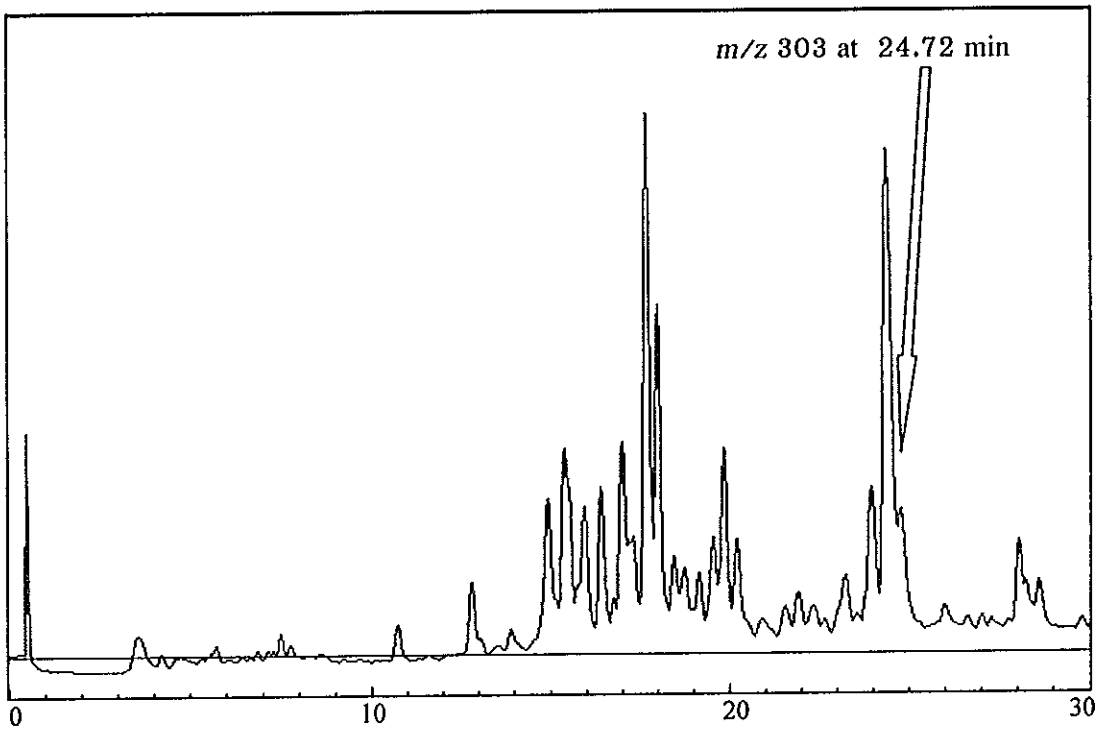

Figure 7 Elution profiles of fraction **EC1H** reversed-phase HPLC eluted with MeOH:H_2O (7:3, v/v) and increasing polarity with MeOH at 235 nm

For fraction EC1I, the ^1H NMR spectrum showed characteristics of erythrolide B, which was found to be the major compound in *E. caribaeorum*. Erythrolide A appears to be produced in nature from erythrolide B by a di-π-methane rearrangement. From the LCMS spectrum, fractions EC1P-EC1Q (Figures 112 and 113) were found to be the peaks of eleutherobin analogs. The HPLC chromatogram of fraction EC1P was compared with authentic sample and the retention time at 26.30 and 22.50 min was

assigned as eleutherobin and desacetyleleutherobin, respectively. These compounds were confirmed by ^{1}H NMR spectrum.

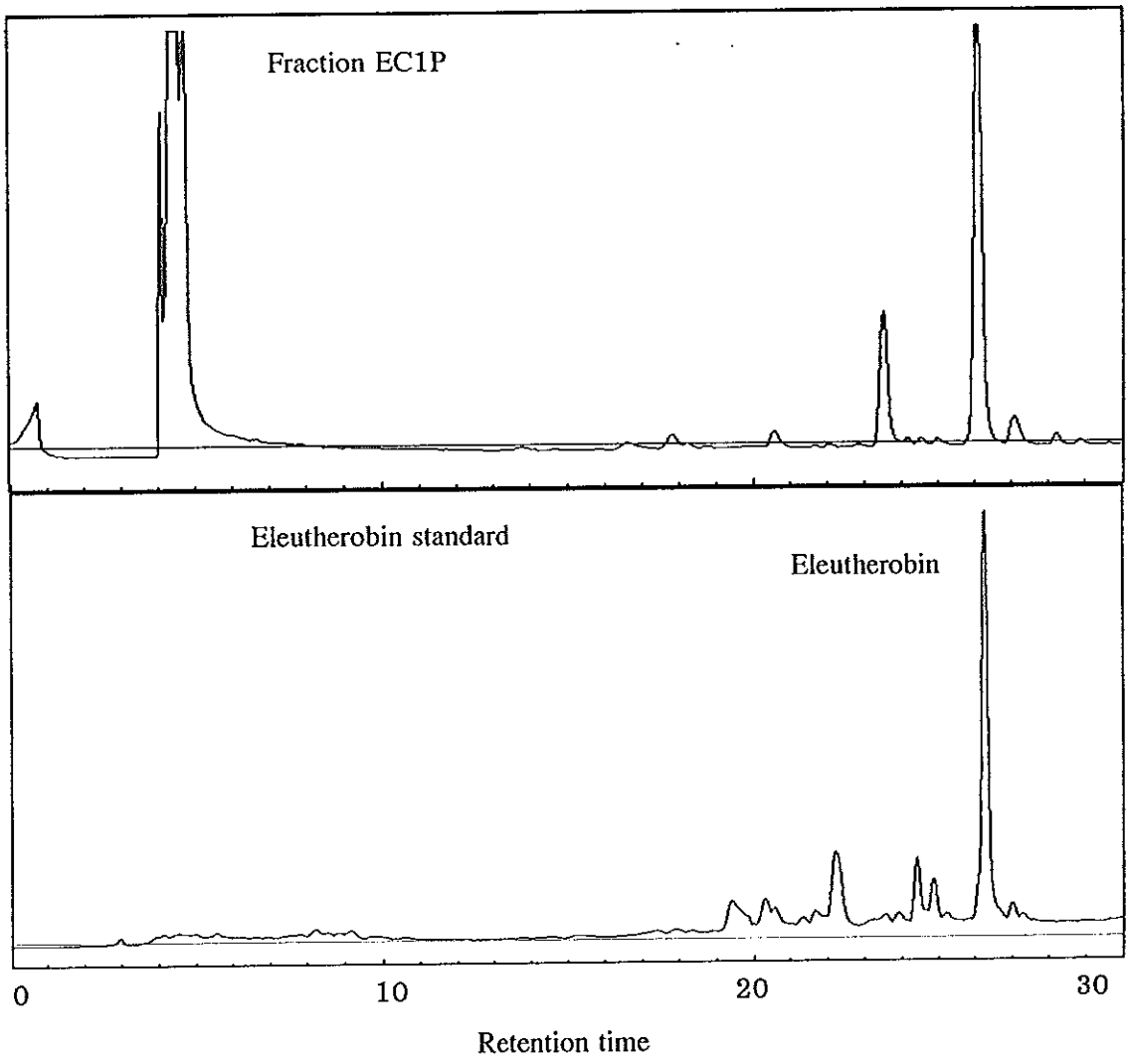

Figure 8 Comparison of HPLC chromatogram of fraction **EC1P** and eleutherobin at 290 nm

The ^{1}H NMR spectrum of eleutherobin displayed the signals at δ 7.72 (s, H-7′), 7.59 (d, J = 15.6 Hz, H-3′), 7.48 (s, H-5′), 6.48 (d, J = 15.6 Hz, H-2′), 3.76 (s, 6′-NMe), 6.26 (d, J = 5.6, H-6), 6.19 (d, J = 5.6 Hz, H-5), 5.61 (d, J = 9.0 Hz, H-2), 5.31 (m, H-12), 5.00 (dd, J = 9.4, 3.0 Hz, H-2″), 4.92 (d, J = 3.0 Hz, H-1″), 3.24 (s, 4-OMe), 2.11 (s, 2″-OAc), 1.02 (d, J = 6.6 Hz, H-19), and 0.99 (d, J = 6.6 Hz, H-20) which were characteristics of this compound and comparable

with the literature report. For desacetyleleutherobin, the ^{1}H NMR spectrum showed similarities with eleutherobin, except for the absence of acetyl group at δ 2.11. In addition, comparison of ^{1}H NMR spectral data between this compound and literature revealed the same data.

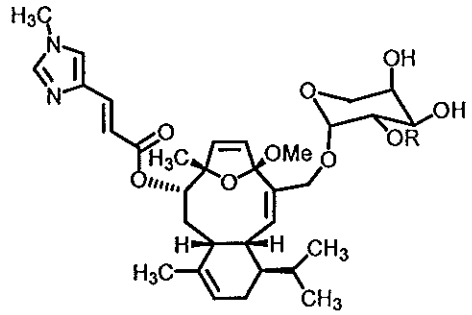

R = Ac; Eleutherobin

R = H; Desacetyleleutherobin

2.3.2 Investigation for Production of Carotenoids in *Micrococcus* strain PAH83

The effects of pH, temperature, aeration, different incubation periods, inoculation, media and sugar on the growth and carotenoids biosynthesis of *Micrococcus* strain PAH83 were investigated. The results are presented as the units of total carotenoids concentration at any time and at the end of growth (P, P_m; mg l^{-1}), crude extract concentration at any time and at the end of growth (X, X_m, g l^{-1}) and product yields determined as the amount of carotenoids produced per unit of dry weight of crude extract ($Y_{P/X}$), respectively. Three replicates were performed for pH, temperature, aeration, incubation, inoculation, media and sugar.

2.3.2.1 *Calibration curve of β-carotene*

The known concentration of β-carotene was used as the standard for calculating the concentration of carotenoids. Figure 9 shows the calibration curve of β-carotene and linear equation.

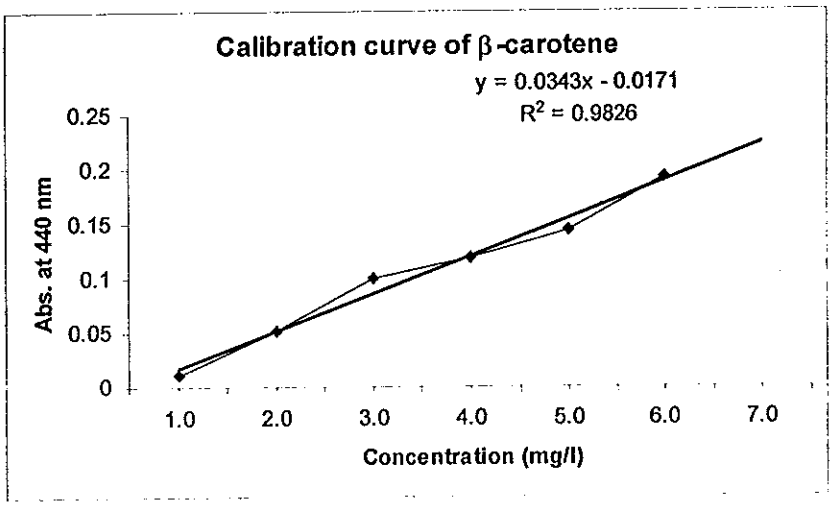

Figure 9 Calibration curve of β-carotene

2.3.2.2 *Effect of initial pH*

Table 59 Effect of initial pH on the maximum crude extract and carotenoids concentrations (X_m, P_m) and product yield ($Y_{P/X}$)

pH	X_m (g l^{-1})	P_m (mg l^{-1})	$Y_{P/X}$ (mg g^{-1})
4	0.4	0.0	0.00
5	6.2	4.2	0.67
6	6.8	4.7	0.69
7	15.8	5.3	0.34
8	14.4	5.3	0.37

The pH value of the growth medium affects not only biosynthetic activity of culture, but also culture growth rate. Figure 10 shows the total carotenoids production concentration in batch fermentation with marine broth media at various initial pH values ranging from 4 to 8. As seen from Figure 10, with raising the pH, carotenoids production concentration increased to a maximum level at pH 6. On the other hand, a further increase of the pH over 6 resulted in a reduction of carotenoids production concentration.

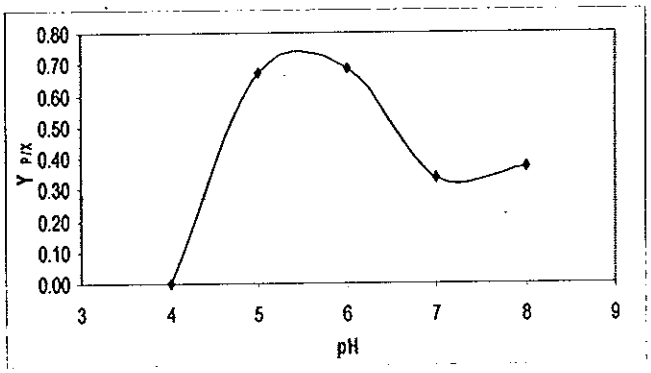

Figure 10 Effect of initial pH on the product yield (2% inoculation, 30 °C, 150 rpm, 24 h)

2.3.2.3 *Effect of temperature*

Table 60 Effect of temperature on the maximum crude extract and carotenoids concentrations (X_m, P_m) and product yield ($Y_{P/X}$)

T (°C)	X_m (g l^{-1})	P_m (mg l^{-1})	$Y_{P/X}$ (mg g^{-1})
30	4.8	4.6	0.96
37	6.4	5.2	0.81
45	1.2	1.0	0.83

Temperature is another important parameter affecting the performance of cells and product formation. The temperature of the growth medium had also a considerable effect on both the growth and carotenoids production of *Micrococcus* strain PAH83. The total carotenoids production decreased sharply above 30 °C likely due to the denaturation of enzyme system of microorganism at higher temperatures and/or poor bacterial growth. Maximum production were determined as 5.2 mg l^{-1} at 37 °C. Results in Table 60 also indicate that carotenoids yield based on maximum crude extract was highest at 30 °C due to low crude extract concentration and relatively high product concentration obtained at this temperature.

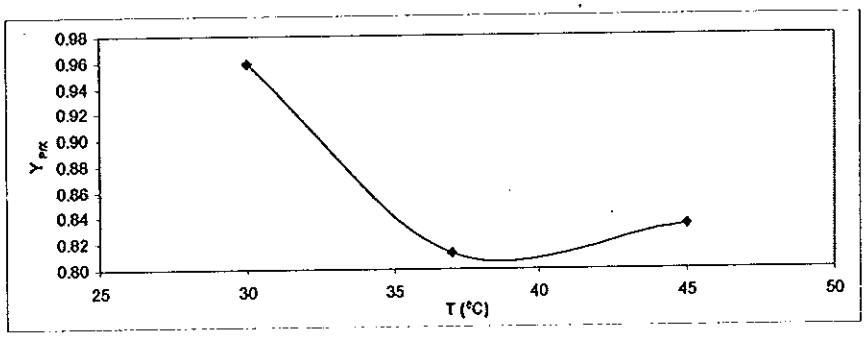

Figure 11 Effect of temperature on the product yield (2% inoculation, pH 6, 150 rpm, 24 h)

2.3.2.4 *Effect of aeration*

Table 61 Effect of aeration on the maximum crude extract and carotenoids concentrations (X_m, P_m) and product yield ($Y_{P/X}$)

Aeration (rpm)	X_m (g l^{-1})	P_m (mg l^{-1})	$Y_{P/X}$ (mg g^{-1})
0	2.0	0.9	0.43
100	6.8	4.7	0.69
150	7.8	5.2	0.67
250	8.4	5.5	0.65

If the microorganism requires oxygen, aerating the growth medium is very important for the successful progress of the fermentation. As *Micrococcus* spp. are known to be aerobic microorganisms, the effect of the aeration rate on the growth and total carotenoids production was examined and results obtained are shown in Figure 12 and Table 61. Both the growth and total carotenoids production changed significantly with varying the shaking from 0 to 250 rpm. In the growth medium shake at 250 rpm, the crude extract and total carotenoids production concentration were 8.4 g l^{-1} and 5.5 mg l^{-1}, respectively which were much higher than the values of 2.0 g l^{-1} and 0.9 mg l^{-1} crude extract and total carotenoids production concentration at 0 rpm, respectively but the carotenoids production yield was the highest at 100 rpm (0.69 mg g^{-1}). At this point, increasing of aeration up to 100 rpm increased product yield but the aeration higher than

100 rpm resulted in constant product yield (0.67 and 0.65 mg g^{-1}). Aeration could be beneficial to the growth and performance of microbial cells by improving the mass transfer characteristics with respect to substrate, product and oxygen.

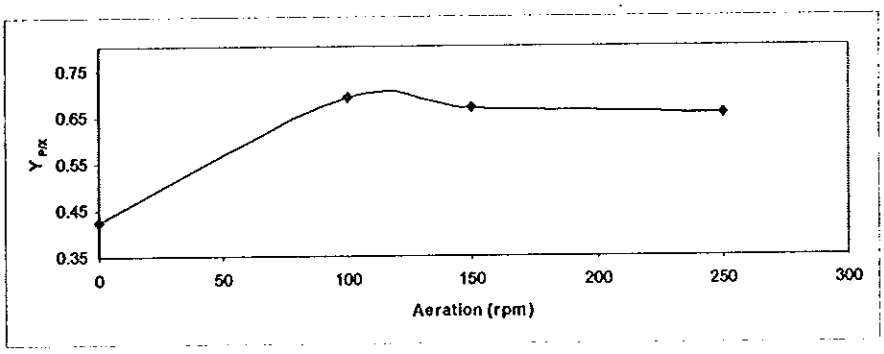

Figure 12 Effect of aeration on the product yield (2% inoculation, pH 6, 30 °C, 24 h)

2.3.2.5 *Effect of inoculation*

Table 62 Effect of inoculation on the maximum crude extract and carotenoids concentrations (X_m, P_m) and product yield ($Y_{P/X}$)

Inoculation (%)	X_m (g l^{-1})	P_m (mg l^{-1})	$Y_{P/X}$ (mg g^{-1})
1	8.8	4.3	0.49
2	9.4	4.3	0.46
3	9.0	4.4	0.49
7.5	8.0	4.4	0.55
10	9.2	4.3	0.47

The growth and carotenoid production properties of *Micrococcus* strain PAH83 were also studied as a function of inoculation. Table 62 showed that total carotenoid production was the highest at 0.55 mg g^{-1} and at 7.5% inoculation. At this %inoculation, the maximum carotenoids production was the highest and the crude extract concentration was the lowest. In the 1% inoculation, the maximum crude extract was 8.8 g l^{-1} and 0.49 mg g^{-1} for product yield. Increasing inoculation up to 10% did not enhance

the product yield; 9.2 g l^{-1} carotenoid concentration and 0.47 mg g^{-1} product yield. Thus, this effect had little influence for *Micrococcus* strain PAH83.

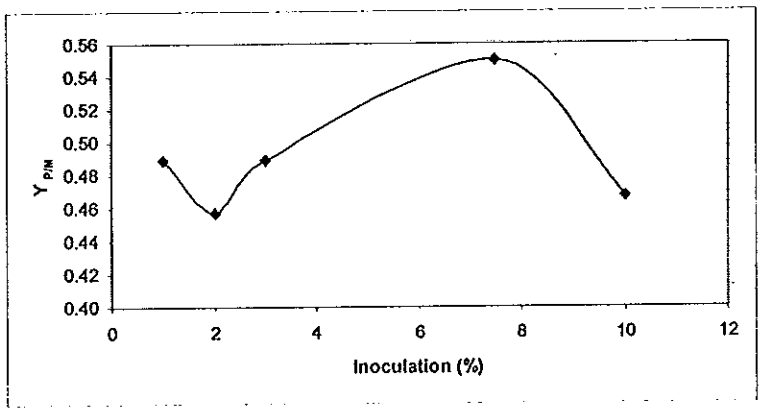

Figure 13 Effect of inoculation on the product yield (100 rpm, pH 6, 30 °C, 24 h)

2.3.2.6 *Effect of media*

Table 63 Effect of media on the maximum crude extract and carotenoids concentrations (X_m, P_m) and product yield ($Y_{P/X}$)

Media	X_m (g l^{-1})	P_m (mg l^{-1})	$Y_{P/X}$ (mg g^{-1})
MB	7.2	3.0	0.42
MB 1/2	3.0	2.4	0.80
MB 1/10	1.0	1.3	1.30

Figure 14 shows the growth and carotenoid production behaviours of *Micrococcus* strain PAH83 in media containing different carbon, nitrogen, phosphorus, and sulfur sources. The experiments were performed in MB (marine broth) and diluted MB (MB 1/2 and MB 1/10). In MB, the growth of microorganism was very fast within 24 h, and microorganism concentration decreased in diluted MB. The maximum of crude extract concentration was found as 7.2 g l^{-1} in MB.

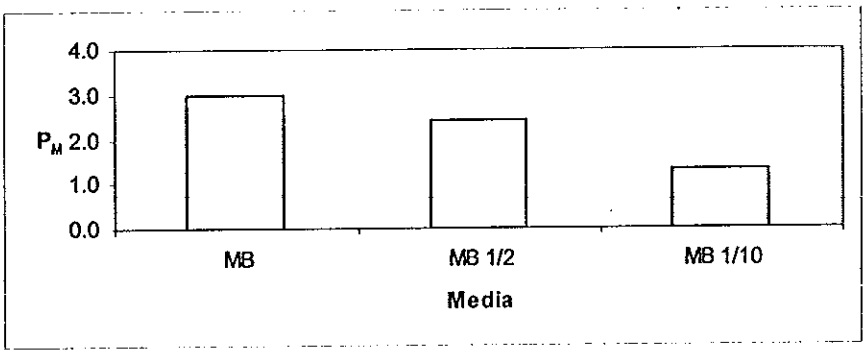

Figure 14 Effect of media on the product yield (7.5% inoculation, 100 rpm, pH 6, 30 °C, 24 h)

2.3.2.7 *Effect of different incubation periods*

Table 64 Effect of different incubation periods on the maximum crude extract and carotenoids concentration (X_m, P_m) and product yield ($Y_{P/X}$)

Time (days)	X_m (g l^{-1})	P_m (mg l^{-1})	$Y_{P/X}$ (mg g^{-1})
1	5.2	4.2	0.81
2	8.0	4.3	0.54
3	7.6	2.6	0.34

Production of carotenoids was also examined at different times (1-3 days). From Figure 15, the product yield of carotenoids was found as 0.81 mg g^{-1} at 24 h. The microorganism grew most quickly within 24 h whereas the product yield lessened above 24 h.

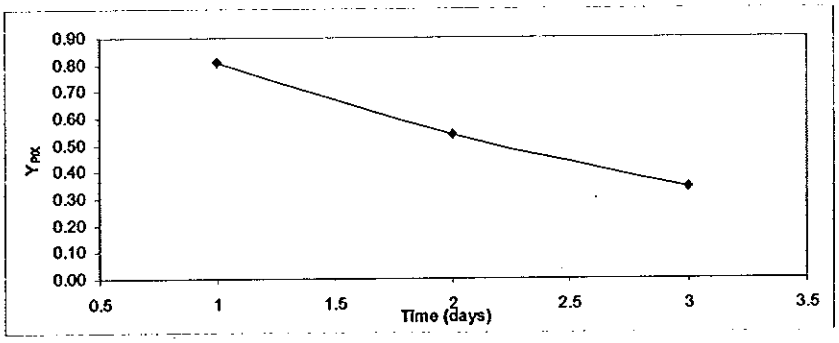

Figure 15 Effect of different incubation periods on the product yield (7.5% inoculation, 100 rpm, pH 6, 30 °C)

2.3.2.8 *Effect of sugar*

Table 65 Effect of sugars on the maximum crude extract and carotenoids concentrations (X_m, P_m) and product yield ($Y_{P/X}$)

Sugars	X_M (g l^{-1})	P_M (mg l^{-1})	$Y_{P/X}$ (mg g^{-1})
0.5% Glucose	9.5	8.5	0.89
1% Glucose	9.8	8.8	0.90
3% Glucose	10.5	6.4	0.61
Arabinose	3.8	4.3	1.13
Glycerol	7.4	2.8	0.38
Xylose	5.0	2.8	0.56
MB 1/10	2.9	2.4	0.83
MB	21.8	9.9	0.45

The effects of different carbon sources: glucose, arabinose, glycerol and xylose on the growth and carotenoids production properties of *Micrococcus* were also examined. The carotenoid concentration was the highest in glucose medium and reached a maximum level (8.8 mg l^{-1}) at 1% glucose concentration. It is well known that glucose is a readily metabolizable carbon source by many organisms so glucose is the substrate which *Micrococcus* strain PAH83 prefers for maximum carotenoids which is obtained in the medium containing this sugar. The microorganism reached the maximal dry crude extract at 3% glucose whereas the growth of microorganism decreased in arabinose source but it was still higher than the control source (MB 1/10).

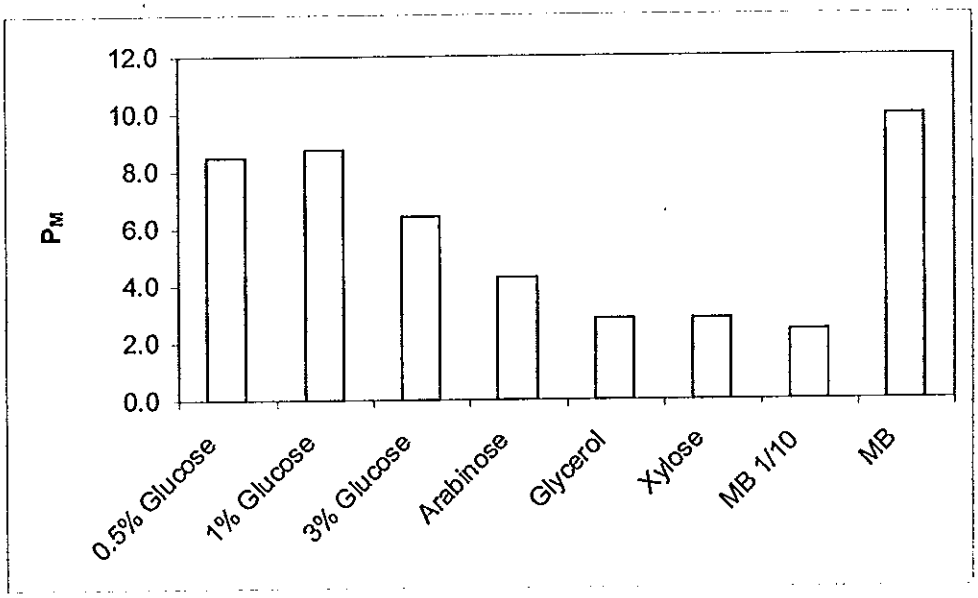

Figure 16 Effect of sugars on the product yield (7.5% inoculation, 100 rpm, pH 6, 30 °C, 24 h)

2.3.3 The Major Carotenoid Pigments of *Micrococcus* strain PAH83

In the genus *Micrococcus*, the chemical nature of pigments has been determined so far only for two mesophilic species. For *M. luteus*, it was found to be a dihydroxy C_{50} carotenoid (Thirkell and Hunter, 1969a and 1969b; Thirkell and Strang, 1967), and for *M. roseus* the pigments were found to be mainly α- or β-carotene derivatives, with canthaxanthin as the main pigment (Schwartzel and Cooney, 1974). Studies have indicated that carotenoids in *M. roseus* do not protect the bacterium against photodynamic killing.

The procedure of extraction and purification of the pigment used (Jensen, 1971) in the present investigation was highly efficient and effective by totally extracting the pigment from pellet of *Micrococcus* strain PAH83 into methanol. The cell pellet and the methanol extract after the first cycle of extraction were pale pink and yellow, respectively. Subsequent extraction with methanol rendered the cell pellet white, but a little pigment could be detected spectrophotometrically in the methanol layer. The procedure was carried out at room temperature, and all the glassware was covered with aluminum foil to protect the pigment from light. Reversed-phase HPLC of the crude pigment in methanol yielded three pigments, **P-1** to **P-3** (Figure 17). UV-visible absorption spectra of carotenoid pigments are of immense importance, since they aid a great deal in determining

the structure of carotenoids (Goodwin, 1976). Table 66 gives the absorption maxima of the three isolated pigments, the predicted number of double bonds in each of the pigments, and the percentage of total pigment of each pigment.

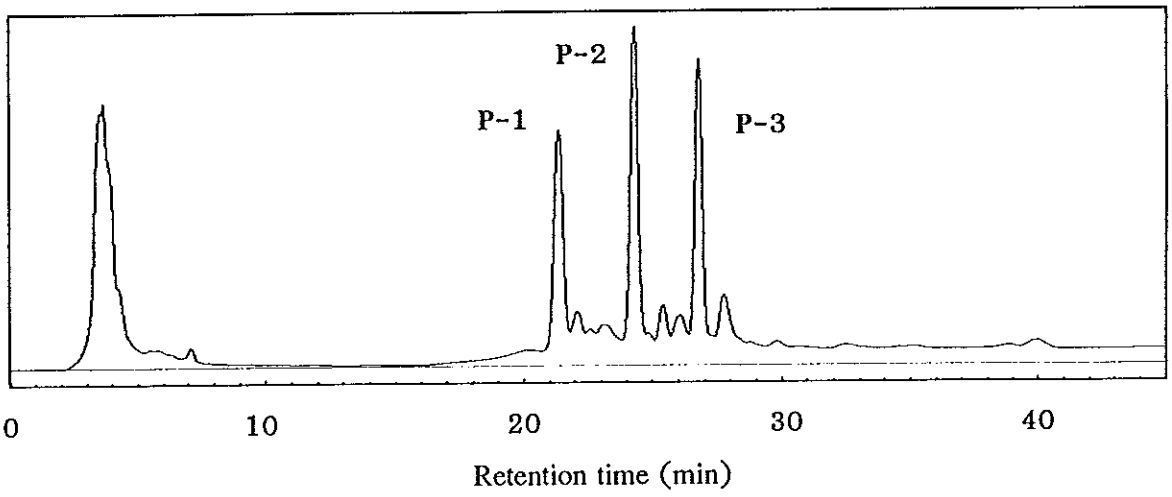

Figure 17 Elution profiles of carotenoids from *Micrococcus* strain PAH83 by reverse-phase HPLC eluted with MeOH:H_2O (9:1, v/v) and increasing polarity with MeOH.

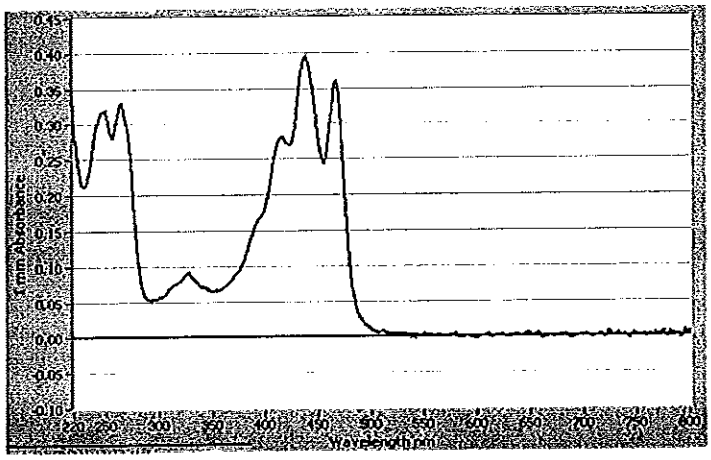

Figure 18 UV-Vis Spectrum of MeOH extract of *Micrococcus* strain PAH83

Table 66 Characteristics of pigments **P-1** to **P-3** from *Micrococcus* strain PAH83

Pigments	t_R (min)	Absorption maxima[a] (λ_{max})	Mol wt	No. of double bonds	% of total pigment[b]
P-1	10.35	415, 439, 467	1029	9	30.0
P-2	10.72	416, 438, 467	867	9	38.1
P-3	11.13	415, 438, 467	705	9	31.9

[a]Absorption spectra were recorded by using an on-line PDA of HPLC-MS.

[b]The percentage of the total pigment represented by each pigment was determined by HPLC profiles by expressing the area of each pigment peak as a percentage of the total area of the three pigment peaks.

The UV visible absorption spectra of all the pigments (**P-1** to **P-3**) appeared to be identical and exhibited a fine structure, with three absorption maxima at 415, 438, and 467 nm. The clear three-band shape of the absorption spectrum is characteristic of carotenoids and further reflects its purity. Comparison of the absorption maxima with the absorption data available for various other carotenoids suggested the presence of 9 conjugated double bonds in all pigments; further comparison also suggested the presence of β-cyclic end groups.

The mass spectrum of **P-3** is shown in Figure 127. The molecular ion is at *m/z* 705 $[M+H]^+$ corresponding to $C_{50}H_{72}O_2$. The main features of the spectrum, including the molecular ion value, correspond to those of decaprenoxanthin except for the absence of signals at m/z 562 and 564 in the spectrum of **P-3**. Structural features accounting for the mass spectral signals of decaprenoxanthin have been assigned previously (Liaaen-Jensen, 1968). The signals at m/z 562 $[M-2-140]^+$ and 564 $[M-140]^+$ are diagnostic for decaprenoxanthin and are due to a retro-Diels-Alder rearrangement of the substituted ∈-ring. The mass spectral data indicated that **P-3** is an isomer of decaprenoxanthin and differs in the features of the terminal rings. A probable structure would be that of sarcinaxanthin (Hertzberg and Liaaen-Jensen, 1977).

In the present study, **P-1** and **P-2** were the most polar pigments, and had absorption spectra similar to sarcinaxanthin **P-3** (Table 66). Peak **P-2** showed three major mass signals $[M+H]^+$ at *m/z* 849.3, 687.9 and 669.6 (Figure 128), which were larger than the molecular weight of most of the C_{40} carotenoides. They matched the fragmentation mass of C_{50} carotenoid monoglucoside ($[M+H]^+$: 867) that lost one water molecule (M-18) and/or one glucoside molecule (M-180), respectively. The fragment at *m/z* 1011.5

$[M-18]^+$, 849.2 $[M-180]^+$ and 669.6 $[M-180-180]^+$ of carotenoid **P-1** (Figure 129), corresponding to losses of molecules of water and glucosides, respectively. The features of the mass spectrum detailed above were in agreement with the reported data of sarcinaxanthin monoglucoside and sarcinaxanthin diglucoside for peaks **P-2** and **P-1**, respectively.

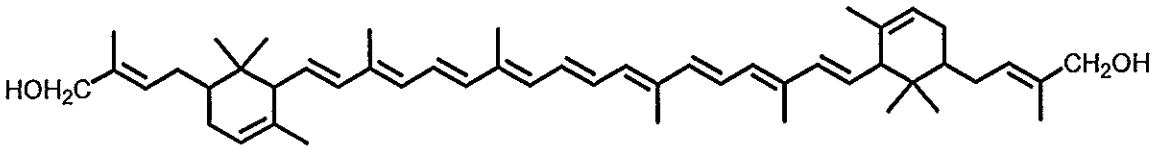

Decaprenoxanthin (*m/z* 704)

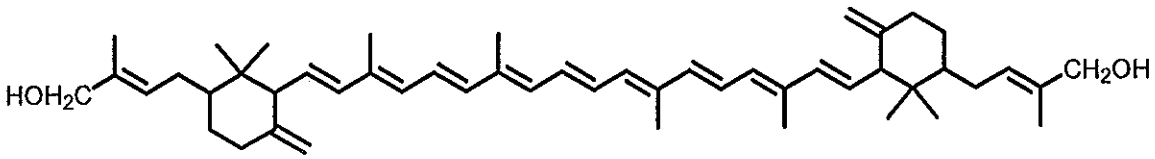

Sarcinaxanthin (**P-3**, *m/z* 704)

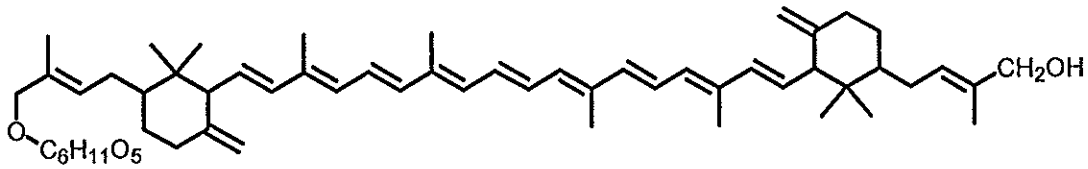

Sarcinaxanthin monoglucoside (**P-2**, *m/z* 866)

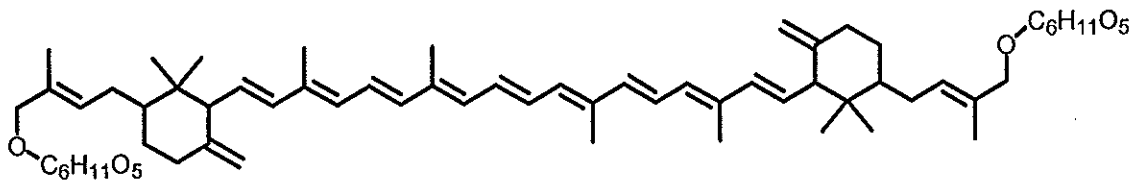

Sarcinaxanthin diglucoside (**P-1**, *m/z* 1028)

CHAPTER 2.4

CONCLUSION

Five known compounds, named erythrolide A and B, eleutherobin, desacetyleleutherobin and erythrodiene were purified from *E. caribaeorum*. Their structures were assigned by NMR, HPLC-MS spectrum and comparison with authentic samples. Interestingly, the fraction EC1H with the molecular ion at *m/z* 303 on APCI source at retention time 24.72 min showed the same molecular ion with the intermediate.

Carotenoids production by Micrococcus strain PAH83 was investigated by using different pH, temperature, aeration, different incubation periods, inoculation, media and sugar. The optimal growth conditions were found at a pH of 6.0, a temperature of 30 $^{\circ}$C, an aeration of 100 rpm, and a 7.5% inoculation, and at 24 hrs. In general, increasing sugar concentration in the growth medium increased the growth of bacterium and carotenoids production. Three carotenoids pigments: sarcinaxanthin, sarcinaxanthin monoglucoside and sarcinaxanthin diglucoside were analyzed and the structures were elucidated by HPLC-MS and UV spectrum. This is the first report of a carotenoid from a bacterium isolated from a coral, which suggests that bacteria from marine invertebrates such as corals may be a useful source of bioactive natural products not previously reported from the invertebrate hosts.

REFERENCES

Ahmad, V. U.; Ali, M. S.; Usmanghani, K. 1997. "Bondenolide, a new diterpenoid from the seeds of *Caesalpinia bonduc*", Z. Naturforsch Ser. B, 52, 410-412.

Ali, E.; Qudrat-I-Khuda, M. 1960. "Bitter constituents from *Caesalpinia bonducella*", Chem. Ind., 463.

Asif Saeed, M.; Sabir, A. W. 2003. "Irritant potential of some constituents from the seeds of *Caesalpinia bonducella* (L.) Fleming", J. Asian Nat. Prod. Res., 5, 35-41.

Awasthi, K. K.; Kumar, A.; Misra, K. 1980. "Two ellagitannins from the stem bark of *Caesalpinia pulcherrima*", Phytochemistry, 19, 1995-1997.

Awasthi, K. K.; Misra, K. 1977. "Chemical constituents of *Caesalpinia pulcherrimas* stem-bark and flowers", J. Indian Chem. Soc., 54, 646.

Awasthi, K. K; Misra, K. 1978. "A novel ellagitannin from *Caesalpinia pulcherrima* bark", Proc. IUPAC 11th International Symp. Chem. Nat. Prod. 1978, 202-205.

Balmain, A.; Bjamer, K.; Connolly, J. D.; Ferguson, G. 1967. "The constitution and stereochemistry of epsilon-caesalpin", Tetrahedron Lett., 5027.

Banskota, A. H.; Attamimi, F.; Usia, T.; Linn, T. Z.; Tezuka, Y.; Kalauni, S. K.; Kakota, S. 2003. "Novel norcassane-type diterpene from the seed kernels of *Caesalpinia crista*", Tetrahedron Lett., 44, 6879-6882.

Canonica, I. L.; Jommi, G.; Manitto, P.; Pagnoni, U. M.; Pelizzoni, F. 1966. "Structure of caesalpines", Gazz. Chim. Ital. 96, 662-686.

Canonica, L.; Jommi, G.; Manitto, P.; Pelizzoni, F. 1963. "Bitter principles of *Caesalpinia bonducella*", Tetrahedron Lett., 2079.

Carte, B. K. 1996. Biomedical potential of marine natural products. Bioscience, 46, 271-286.

Chaudhry, G. R.; Sharma, V. N.; Dhar, M. L. 1954. "Chemical examination of the roots of *Caesalpinia digyna*", J. Sci. Ind. Res., 13, 147.

Chaudhry, S. R. 1957. "Chemical examination of roots of *Caesalpinia digyna*. Identity of vakerin with bergenin", J. Sci. Ind. Res., 16, 511.

Che, C. T.; Mc Pherson, D. D.; Cordell, G. A.; Fong, H. H. A. 1985. "Pulcherralpin, a new diterpene ester from *Caesalpinia pulcherrima* stems", Abstr. Internat Res. Cong. Nat. Prod. Coll. Pharm. Univ. N. Carolina Chapel Hill NC, July 7-12, 176.

Che, C. T.; Mc Pherson, D. D.; Cordell, G. A.; Fong, H. H. S. 1986. "Pulcherralpin, a new diterpene ester from *Caesalpinia pulcherrima*", J. Nat. Prod., 49, 561-569.

Chen, X-T.; Bhattacharya, S. K.; Zhou, B.; Gutteridge, C. E.; Pettus, T. R. R.; Danishefsky, S. J. 1999. The total synthesis of eleutherobin. J. Am. Chem. Soc. 121, 6563-6579.

Choudhary, M. I.; Gondal, H. Y.; Abbaskhan, A.; Jahan, I. A.; Parvez, M.; Nahar, N.; Atta-ur-Rahman 2004. "Revisiting diterpene lactones of *Suregada multiflora*", Tetrahedron, 60, 7933-7941.

Contreras, J. L.; Amor-Prats, D.; Garcia-Argaez, A.; Perez-Amador, M. C.; Bratoeff, E. A.; Labastida, C. 1995. "A chromatographic study of flavonoids and fatty acids of four *Caesalpinia species*", Phyton. (Buenos Aires), 57, 31-35.

Crespi-Perellino, N.; Garofano, L.; Arlandini, E.; Pinciroli, V. 1996. "Idetification of new diterpenoids from Euphorbia calyptrata cell cultures", J. Nat. Prod., 59, 773-776.

Das, B.; Chakravarty, A. K. 1993. "Three flavone glycosides from *Gelonium multiflorum*", Phytochemistry, 33, 493-496.

Das, B.; Chakravarty, A. K.; Masuda, K.; Suzuki, H.; Ageta, H. 1994. "A diterpenoid from roots of *Gelonium multiflorum*", Phytochemistry, 37, 1363-1366.

Delahaye, P.; Verzele, M. 1983. "Analysis of gallic, digallic and trigallic acids in tannic acids by high-performance liquid chromatography", J. Chromatogr., 265, 363-367.

Dookran, R.; Maharaj, D.; Mootoo, B. S.; Ramsewak, R.; McLean, S.; Raynolds, W. F.; Tinto W. F. 1993. Diterpenes from the gorgonian coral *Erythropodium caribaeorum* from the Southern Caribbean. J Nat. Prod., 56, 1051-1056.

Fenical, W. 1987. Marine soft corals of the genus Pseudopterogorgia: a resource for novel anti-inflammatory diterpenoids. J. Nat. Prod. 50, 1001-1008.

Ghatak, N. 1934. "Chemical examination of kernels of the seeds of *Caesalpinia bonducella*", Proc. Acad. Sci. United Provinces Agra Oudh India, 4, 141.

Ghosh, S. 1979. "Chemical investigations on the seeds of *Gelonium muliflorum* A.Juss.", East Pharm., 22, 185-188.

Giral, F.; Aguilar, M. D. 1953. "Vitamin C content of medicinal drugs. II. Barks, roots and rhizomes", Ciencia(Mexico), 12, 283-285.

Goyal, H.; Sukumar, S.; Purushothaman, K. K. 1981. "Anti-malarials from Indian medicinal plants", J. Res. Ayur. Siddha, 2, 286-295.

Goodwin, T. W. 1976. Chemistry and biochemistry of plant pigments, Academic Press, London. vol. 1, p. 225-261.

Griffiths, L. A. 1959. "On the distribution of gentisic acid in green plants", J. Exp Biol., 10, 437.

Hertzberg, S.; Liaaen-Jensen, S. 1977. Bacterial carotenoids. LIII. C_{50} carotenoids. 19. Absolute configuration of sarcinaxanthin and sarcinaxanthin β-D-glucoside. Isolation of sacinaxanthin diglycoside. Acta Chem. Scand. 31, 215-218.

Herunsalee, A.; Pancharoen, O.; Tuntiwachwuttikul, P. 1987. "Further studies of flavonoids of the black rhizomes *Boesenbergia pandurata*", J. Sci. Soc. Thailand, 13, 119-122.

Hosamani, K. M. 1995. "Unique occurrence of novel fatty acids like ricinoleic and cyclopropenoid fatty acids in *Caesalpinia sepiaria* and *Leucaena glauca* seed oils", Indian J. Chem., 34b, 167-168.

Imamura, H.; Umehara, K.; Ohashi, H. 1980. "Constituents of *Caesalpinia japonica* (Leguminosae)", Gifu Daigaku Nogakubu Kenkyu Hokoku, 43, 75-82.

Jadhav, A. N.; Kaur, N.; Bhutani, K. K. 2003. "A new furanoditerpenoid marker for the distinction between the seeds of two species of *Caesalpinia*", Phytochem. Anal., 14, 315-318.

Jagannadham, M. V.; Rao, V. J.; Shivaji, S. 1991. The major carotenoid pigment of a psychrotrophic *Micrococus roseus* strain: purification, structure, and interaction with synthetic membranes. J. Bact. 173, 7911-1917.

Jahan, I. A.; Nahar, N; Mosihuzzaman, M.; Shaheen, F.; Parween, Z.; Atta-ur-Rahman; Choudhary, M. I. 2002. "Novel diterpene lactones from *Suregada multiflora*", J. Nat. Prod., 65, 932-934.

Jaipetch, T.; Kanghae, S.; Pancharoen, O.; Patrick, V. A.; Reutrakul, V.; Tuntiwachwuttikul, P.; White, A. H. 1982. "Constituents of *Boesenbergia pandurata* (syn. *Kaempferia pandurata*): isolation, crystal structure and synthesis of (DL)-boesenbergin A", Aust. J. Chem., 35, 351-361.

Jaipetch, T.; Reutrakul, V.; Tuntiwachwuttikul, P.; Santisuk, T. 1983. "Flavonoids in the black rhizomes of *Boesenbergia pandurata*", Phytochemistry, 22, 625-626.

Jensen, S. L.; Jensen, A. 1971. Quantitative determination of carotenoids in photosynthetic tissues. Methods Enzymol. 23, 586-602.

Jiang, R. W.; But, P. P. H.; Ma, S. C.; Mak, T. C. W. 2001a. "Furanoditerpenoid lactones from the seeds of *Caesalpinia minax* Hance.", Phytochemistry, 57, 517-521.

Jiang, R. W.; But, P. P. H.; Ma, S. C.; Ye, W. C.; Chan, S. P.; Mak, T. C. W. 2002c. "Structure and antiviral properties of macrocaesalmin, a novel cassane furanoditerpenoid lactone from the seeds of *Caesalpinia minax* Hance", Tetrahedron Lett., 43, 2415-2418.

Jiang, R. W.; Ma, S. C.; But, P. P. H.; Mak, T. C. W. 2001b. "Isolation and characterization of spirocaesalmin, a novel rearranged vouacapane diterpenoid from *Caesalpinia minax* Hance.", J. Chem. Soc. Perkin. Trans. I, 22, 2920-2923.

Jiang, R. W.; Ma, S. C.; But, P. P. H.; Mak, R. C. W. 2001c. "New antiviral cassane furanoditerpenes from *Caesalpinia minax*", J. Nat. Prod., 64, 1266-1272.

Jiang, R. W.; Ma, S. C.; He, Z. D.; Huang, X. S.; But, P. P. H.; Wang, H.; Chan, S. P.; Ooi, V. N. C.; Xu, H. X.; Mal, T. C. W. 2002b. "Molecular structures and antiviral activities of naturally occurring and modified cassane furanoditerpenoids and friedelane triterpenoids from *Caesalpinia minax*", Bio. Org. Med. Chem., 10, 2161-2170.

Katti, M. C. T. 1930. "Chemical examination of the seeds of *Caesalpinia bonducella*, Flem. Part I", J. Indian Chem. Soc., 7, 207-220.

Katti, M. C. T.; Puntambekar, S. V. 1930. "Chemical examination of the seeds of *Caesalpinia bonducella* Flem. Part II. Fatty oil", J. Indian Chem. Soc. 7, 221-227.

Khuda, Q. I. M.; Erfan Ali, M.; Ahmed Q. A. 1961. "*Caesalpinia bonducella*. II. Chemical examination of the leaves", Pak. J. Sci. Ind. Res., 4, 104.

Kinoshita, T. 2000. "Chemical studies on the Philippine crude drug calumbibit (seeds of *Caesalpinia bonduc*): the isolation of new cassane diterpenes fused with alpha, beta-butenolide", Chem. Pharm. Bull., 48, 1375-1377.

Kinoshita, T.; Kaneko, M.; Noguchi, H.; Kitagawa, I. 1996. "New cassane diterpenes from *Caesalpinia bonduc* (Fabaceae)", Heterocycles, 43, 409-414.

Kitagawa, I.; Simanjuntak, P.; Mahmud, T.; Kobayashi, M.; Fujii, S.; Uji, T.; Shibuya, H. 1996. "Indonesian medicinal plants. XIII. Chemical structures of caesaldekarins C, D and E, three additional cassane-type furanoditerpenes from the roots of *Caesalpinia major* (Fabaceae)", Chem. Pharm. Bull., 44, 1157-1161.

Kitagawa, I.; Simanjuntak, P.; Watano, T.; Shibuya, H.; Fujii, S.; Yamagata, Y.; Kobayashi, M. 1994. "Indonesian medicinal plants. XI. Chemical structures of caesaldekarins A and B, two new cassane-type furanoditerpenes from the roots of *Caesalpinia major* (Fabaceae)", Chem. Pharm. Bull., 42, 1798-1802.

Lai, M. S.; Shameel, S.; Ahmad, V. U.; Usmanghani, K. 1997. "Chemical constituents of *Caesalpinia bonduc*", Pak. J. Sci. Ind. Res., 40, 20-22.

Liaaen-Jensen, S. "The photosynthetic bacteria" Plenum, New York, 1978, p. 233.

Liaaen-Jensen, S.; Hertzberg, S.; Weeks, O. B.; Schwieter, U. 1968. Bacterial carotenoids. XXVII. C_{50} carotenoids. 3. Structure determination of dehydrogenans-P439. Acta Chem. Scand. 22, 1171-1186.

Lindel, T.; Jensen, P. R.; Fenical, W.; Long, B. H.; Casazza, A. M.; Carboni, J.; Fairchild, C. R. 1997. Eleutherobin, a new cytotoxin that mimics paclitaxel (Taxol) by stabilizing microtubules. J. Am. Chem. Soc. 119, 8744-8745.

Look, S. A.; Fenical, W.; van Engen, D.; Clardy, J. 1984. Erythrolides: Unique marine diterpenoids interrelated by a naturally occurring di-π-methane Rearrangement J. Am. Chem. Soc.,106, 5026.

Lyder, D. L.; Peter, S. R.; Tinto, W. F.; Bissada, S. M.; Mc Lean, S.; Reynolds, W. F. 1998a. "Minor cassane diterpenoids of *Caesalpinia bonduc*", J. Nat. Prod. 61, 1462-1465.

Lyder, D. L.; Tinto, W.; Bissada, S. M.; Mc Lean, S.; Reynolds, W. F. 1998b. "Caesalpinin B, a rearranged cassane furanoditerpene of *Caesalpinia bonduc*", Heterocycles, 48, 1465-1469.

Mahato, S. B.; Sahu, N. P.; Luger, P. 1983. "Structure of caesalpinine A: a novel spermidine alkaloid from *Caesalpinia digyna*", J. Ame. Chem. Soc., 105, 4441-4445.

Mahato, S. B.; Sahu, N. P.; Muller, E.; Luger, P. 1985. "Stereochemistry of a macrocyclic spermidine alkaloid from *Caesalpinia digyna* Rottl. X-ray determination of the structure of caesalpinine C (celallocinnine)", J. Chem. Soc. Perkin Trans. II, 2, 193-196.

Mahidol, C. 1985. "Part I: constituents of *Boesenbergia pandurata* (yellow rhizome) (Zingiberaceae). Part II. Additions of lithio chloromethyl phenylsulfoxide to aldimines and alpha, beta-unsaturated compounds", Dissertation-Ph.D.-Mahidol Univ. 291.

Mahidol, C.; Tuntiwachwuttikul, P.; Reutrakul, V. 1982. "Chemical investigation of Zingiberaceous plants", Nrct-Jsps Rattanakosin Bicentennial Joint Seminar on Chemistry of Natural Products, 2-6 August, Bangkok, Thailand. p 15.

Mahidol, C.; Tuntiwachwuttikul, P.; Reutrakul, V.; Taylor, W. C. 1984. "Constituents of *Boesenbergia pandurata* (syn. *Kaempferia pandurata*). III. Isolation and synthesis of (+)-boesenbergin B", Aust. J. Chem., 37, 1739-1745.

McPherson, D. D.; Che, C. T.; Cordell, G. A.; Soejarto, D. D.; Pezzuto, J. M.; Fong, H. H. S. 1985. "New caesalpin diterpenes from *Caesalpinia pulcherrima* roots", Abstr. Internat. Res. Cong. Nat. Prod. Coll. Pharm. Univ. N. Carolina Chapel Hill NC, July 7-12, 1985. 207.

McPherson, D. D.; Che, C. T.; Cordell, G. A.; Soejarto, D. D.; Pezzuto, J. M.; Fong, H. H. S. 1986. "Diterpenoids from *Caesalpinia pulcherrima*", Phytochemistry, 25, 167-170.

McPherson, D. D.; Cordell, G. A.; Soejarto, D. D.; Pezzuto, J. M.; Fong, H. H. S. 1982. "Constituents of *Caesalpinia pulcherrima*. Novel peltogynoids and homoisoflavanoids", Abstr. 23rd Annual Meeting American Society of Pharmacognosy, August 1-5, 23, 71.

McPherson, D. D.; Cordell, G. A.; Soejarto, D. D.; Pezzuto, J. M.; Fong, H. H. S. 1983. "Peltogynoids and homisoflavonoids from *Caesalpinia pulcherrima*", Phytochemistry, 22, 2835-2838.

Mendes, C. C.; Bahia, M. V.; David, J. M.; David, J. P. 2000. "Constituents of *Caesalpinia pyramidalis*", Fitoterapia, 71, 205-207.

Mondai, D. N.; Barik, B. R.; Dey, A. K.; Kundu, A. B.; Banerji, A.; Maiti, S. 1993. "The structure and stereochemistry of (+)-D-pinitol: application of 2D NMR spectroscopy", J. Indian Chem. Soc., 70, 651-652.

Morota, T.; Nishimura, M.; Sasaki, H.; Sato, S. 1990. "Blood platelet aggregation inhibitors containing caesalpin P, sappanchalcone, 3-deoxysappanone or protosappanin A", Patent-Japan Kokai Tokkyo Koho-02, 264,717.

Murakami, A.; Kondo, A.; Nakamura, Y.; Ohigashi, H.; Koshimizu, K. 1993. "Possible anti-tumor promoting properties of edible plants from Thailand, and identification of an active constituent, cardamonin, of *Boesenbergia pandurata*", Biosci. Biotech. Biochem., 57, 1971-1973.

Nagai, M: Nagumo, S.; Eguchi, I.; Lee, S. M.; Suzuki, T. 1984. "Sappanchalcone from *Caesalpinia sappan* L., the proposed biosynthetic precursor of brazilian", Yakugaku Zasshi, 104, 935-938.

Nageshwar, G.; Radhakrishnaiah, M.; Narayana, L. L. 1984. "Chemotaxonomy of *Caesalpinia*", Curr. Sci., 53, 813-814.

Nakahara, K. 2001. "Physiologically active flavonoids from *Boesenbergia pandurata* grown in Thailand", Nogyo Oyobi Engei, 76, 761-768.

Nakamura, E. S.; Kurosaki, F.; Arisawa, M.; Mukainaka, T.; Okuda, M.; Tokuda, H.; Nishino, H.; Pastore Jr, F. 2002. "Cancer chemopreventive effects of constituents of *Caesalpinia ferrea* and related compounds", Cancer Lett., 177, 119-124.

Namikoshi, M.; Nakata, H.; Nuno, M.; Ozawa, T.; Saitoh, T. 1987. "Homoisoflavonoids and related compounds. III. Phenolic constituents of *Caesalpinia japonica* Sieb. ET Zucc.", Chem. Pharm. Bull., 35, 3568-3575.

Namikoshi, M.; Nakata, H.; Saitoh, T. 1987a. "Homoisoflavonoids from *Caesalpinia sappan*", Phytochemistry, 26, 1831-1833.

Namikoshi, M.; Nakata, H.; Yamada, H.; Nagai, M.; Saitoh, T. 1987b. "Homoisoflavonoids and related compounds. II. Isolation and absolute configurations of 3,4-dihydroxylated homoisoflavans and brazilins from *Caesalpinia sappan* L.", Chem. Pharm. Bull., 35, 2761-2773.

Nicolaou, K. C.; Ohshima, T.; Hosokawa, S.; van Delft, F. L.; Vourloumis, D.; Xu, J. Y.; Pfefferkorn, J.; Kim, S. 1998. Total synthesis of eleutherobin and eleuthosides A and B. J. Am. Chem. Soc. 120, 8674-8680.

Nigam, S. S.; Saxena, V. K.; Yadava, R. N. 1977. "Chemical examination of the heart wood of *Caesalpinia sappan*", Indian J. Pharmacy. 39, 85.

Nigam, S. S.; Saxena, V. K.; Yadava, R. N. 1978. "Analysis of fixed oil from heart wood of *Caesalpinia sappan*", J. Inst. Chem.(Calcutta), 50, 65-66.

Ogawa, K.; Aoki, I.; Sashida, Y. 1992. "Caesaljapin, a cassane diterpenoid from *Caesalpinia decapetala* var.*japonica*", Phytochemistry, 31, 2897-2898.

Oswal, V. B.; Garg, S. C. 1984. "Chemical examination of the seeds of *Caesalpinia sappan* Linn.", Seifen Oele Fette Wachse, 110, 577.

Oswal, V. B.; Garg, S. C. 1993. "Unsaponifiable matter of the fixed oil from the seeds of *Caesalpinia sappan* Linn.", Asian J. Chem., 5, 676-678.

Pandji, C.; Grimm, C.; Wray, V.; Witte, L.; Proksch, P. 1993. "Insecticidal constituents from four species of the Zingiberaceae", Phytochemistry, 34, 415-419.

Parmar, V. S.; Singh, S.; Jacobsen, J. P.; Boll, P. M. 1987. "Structure of a new homoisoflavanone from *Caesalpinia pulcherrima*", Acta Chem. Scand. Ser. B, 41, 267-270.

Paris, R. R.; Delaveau, P. 1965. "The flavonoids of *Caesalpinia pulcherrima* isolation of a flavonoid glycoside identified as myricitrin", C. R. Acad. Sci., 260, 271.

Paris, R. R.; Delaveau, P. 1967. "*Caesalpiniae pulcherrimae* folia", Q. J. Crude Drug Res., 7, 964.

Pathirana, C.; Fenical, W. 1993. Erythrodiene: A new spirobicyclic sesquiterpene of a rare skeletal class from the Caribbean gorgonian coral *Erythropodium caribaeorum*. Tetrahedron Lett., 34, 3371-3372.

Parveen, N.; Khan, N. U. 1987. "Luteolin-7,4'-dimethyl ether 3'-glucoside from *Gelonium multiflorum*", Phytochemistry, 26, 2130-2131.

Pascoe, K. O.; Burke, B. A.; Chan, W. R. 1986. "Caesalpin F: a new furanoditerpene from *Caesalpinia bonducella*", J. Nat. Prod., 49, 913-915.

Pathong, A.; Tassaneeyakul, W.; Kanjanapothi, D.; Tantiwachwuttikul, P.; Reutrakul, V. 1989. "Anti-inflammatory activity of 5,7-dimethoxyflavone", Planta Med., 55, 133-136.

Patil, A. D.; Freyer, A. J.; Webb, R. L.; Zuber, G.; Reichwein, R.; Bean, M. F.; Faucette, L.; Johnson, R. K. 1997. "Pulcherrimins A - D, novel diterpene dibenzoates from *Caesalpinia pulcherrima* with selective activity against DNA repair-deficient yeast mutants", Tetrahedron, 53, 1583-1592.

Pelizzoni, F. 1968. "Diterpenoids from *Caesalpinia bonducella* and *Psiadia altissima*", Corsi. Semin. Chim., 11, 53.

Peter, S. R.; Tinto, W. F.; McLean, S.; Reynolds, W. F.; Tay, L. L. 1997b. "Caesalpinin, a rearranged cassane furanoditerpene of *Caesalpinia bonducella*", Tetrahedron Lett., 38, 5767-5770.

Peter, S. R.; Tinto, W. F.; McLean, S.; Reynolds, W. F.; Tay, L. L.; Yu, M.; Chan, W. R. 1998. "Complete ^{1}H and ^{13}C NMR assignments of four caesalpin furanoditerpenes of *Caesalpinia bonducella*", Magn. Reson. Chem., 36, 124-127.

Peter, S. R.; Tinto, W. F.; McLean, S.; Reynolds, W. F.; Yu, M. 1997a. "Bonducellpins A-D, new cassane furanoditerpenes of *Caesalpinia bonduc*", J. Nat. Prod., 60, 1219-1221.

Peter, S.; Tinto, W. F.; McLean, S.; Reynolds, W. F.; Yu, M. 1998. "Cassane diterpenes from *Caesalpinia bonducella*", Phytochemistry, 47, 1153-1155.

Pordesimo, E. O.; Schmitz, F. J.; Ciereszko, L. S.; Hossain, M. B.; van der Helm, D. 1991. New Briarein Diterpenes from the Caribbean Gorgonians *Erythropodium caribaeorum* and *Briareum* sp. J. Org. Chem., 56, 2344-2357.

Proksch, P.; Edrada, R. A.; Ebel, R. 2002. Drugs from the seas current status and microbiological implications. Appl. Microbiol. Biotechnol. 59, 125-134.

Purushothaman, K. K.; Kalyani, K.; Subramaniam, K.; Shanmughanathan, S. P. 1982. "Structure of bonducellin-a new homoisoflavone from *Caesalpinia bonducella*", Indian J. Chem., 21b, 383.

Qudrat-I-Khuda, M.; Erfan Ali, M. 1963. "*Caesalpinia bonducella*. III. Isolation of alpha, beta, and gamma-caesalpin and determination of their functional groups", Pak. J. Sci. Ind. Res., 6, 65.

Ragasa, C. Y.; Ganzon, J.; Hofilena, J.; Tamboong, B.; Rideout, J. A. 2003. "A new furanoid diterpene from *Caesalpinia pulcherrima*", Chem. Pharm. Bull., 51, 1208-1210.

Ragasa, C. Y.; Hofilena, J. G.; Rideout, J. A. 2002a. "New furanoid diterpenes from *Caesalpinia pulcherrima*", J. Nat. Prod., 65, 1107-1110.

Rao, R. V. K.; Prasad, G. R. 1978. "Chemical examination of the flowers of *Caesalpinia pulcherrima*", Indian J. Pharm. Sci., 40, 103-104.

Rastogi, S.; Shaw, A. K.; Dulshreshtha, D. K. 1996. "Characterisation of fatty acids of antifilarial triglyceride fraction from *Caesalpinia bonduc*", Fitoterapia, 67, 63-64.

Reddy, N. L. N.; Ravikanth, V.; Lakshmi, V. V. N. S. J.; Murty, U. S.; Venkateswarlu, Y. 2003. "Inhibitory activity of homoisoflavonoids from *Caesalpinia sappan* against *Beauveria bassiana*", Fitoterapia, 74, 600-602.

Roach, J. S.; Mc Lean, S.; Reynolds, W. F.; Tinto, W. F. 2003. "Cassane diterpenoids of *Caesalpinia pulcherrima*", J. Nat. Prod., 66, 1378-1381.

Roengsumran, S.; Limsuwankesorn, S.; Ngamrojnavanich, N.; Petsom, A.; Chaichantipyuth, C.; Ishikawa, T. 2000. "Cassane diterpenoid from *Caesalpinia major*", Phytochemistry, 53, 841-844.

Rodriguez, A. D. 1995. The natural products chemistry of West Indian gorgonian octocoral. Tetrahedron, 51, 4571-4618.

Saeed, M. A.; Sabir, A. W. 2001. "Antibacterial activity of *Caesalpinia bonducella* seeds", Fitoterapia, 72, 807-809.

Scafati, O. T.; Jangra, U. D.; Campbell, M.; Roberge, M.; Andersen, R. J. 2002. Diterpenoids from cultured *Erythropodium caribaeorum*. Org. Lett. 4, 4085-4088.

Schmidt, O. T.; Eckert, R.; Gunther, E.; Fiesser, H. 1967c. "Natural tannins. XL. Revifolincarboxylic acid, its optically active forms and its binding to D-glucose to form algarobin, a new crystalline compound from algarobilla (*Caesalpinia brevifolia*)", Justus Liebigs Ann. Chem., 204.

Schmidt, O. T., Schanz, R.; Eckert, R.; Wurmb, R. 1967a. "On natural tanning agents. XXXIV. Brevilagin 1 (isolated from *Caesalpinia brevifolia*)". Justus Liebigs Ann. Chem., 706, 131.

Schmidt, O. T.; Schanz, R.; Wurmb, R.; Groebke, W. 1967b. "On natural tanning agents. XXXV. Brevilagin 2 (isolated from *Caesalpinia brevifolia*)", Justus Liebigs Ann. Chem., 706, 154.

Schwartzel, E. H.; Cooney, J. J. 1974. Isolation and characterization of pigmentation mutants of *Micrococcus roseus*. Can. J. Microbiol. 20:1015-1021.

Sengupta, P.; Roy, S.; Das, K. G. 1970. X-caesalpin: a new diterpene from *Caesalpinia pulcherrima* Swartz", Chem. Ind. (London), 534.

Shameel, S.; Usmanghani, S.; Ali, M. S.; Ahmad, V. U. 1997. "*Caesalpinia bonduc* (L.) Rosb. seed oil: lipid composition assessment", Pak. J. Pharm. Sci., 10, 29-38.

Shi, K. L.; Li, R. S.; Zhou, K. H.; Huang, Y. Q.; Hu, S. Z. 1988. "Isolation and X-ray structure characterization of (+)-ononitol from chinense *Caesalpinia crista*. Jiegou Huaxue, 7, 103-106.

Shibuya, H. T.; Kitagawa, I. 1996. "Chemical study of Indonesian medicinal plants", Yakugaku Zasshi, 116, 911-927.

Simin, K.; Khaliq uz Zaman, S. M.; Ahmad, V. U. 2001. "Antimicrobial activity of seed extracts and bondenolide from *Caesalpinia bonduc* (L.) Roxb.", Phytother Res. 15, 437-440.

Srinivas, K. V. N. S.; Rao, Y. K.; Mahender, I.; Das, B.; Krishna, K. V. S. R.; Kishore, K. H.; Murty, U. S. N. 2003. "Flavanoids from *Caesalpinia pulcherrima*", Phytochemistry, 63, 789-793.

Sohns, J.; Kwon, Y. S.; Kim, C. M. 2000. Chemical constituents from the stem of *Caesalpinia japonica*", Korean J. Pharmacog., 31, 430-433.

Steinmetz, E. F. 1960. "*Caesalpinia sappan*", Acta Phytother., 7, 115.

Suarez, S. S.; Cabrera, J. L.; Juliani, H. R. 1984. "Flavonoids, amino acids and carbohydrates of *Caesalpinia gilliesii* (Hook) Benth. (Leguminosae)", An Asoc. Quim. Argent., 72, 261-263.

Supat, P. 1961. "Active principles in *Boesenbergia pandurata*", Thesis-Master, 29.

Suphat, P. 1964. "Active principles in *Boesenbergia pandurata*", Thesis-MS-Chulalongkorn Univ. 31.

Takaichi, S.; Shimada, K. 1992. Characterization of carotenoids in photosynthetic bacteria. Methods in Enzymology, vol. 213, 374-385.

Talapatra, S. K.; Das, G.; Talapatra, B. 1989. "Stereostructures and molecular conformations of six diterpene lactones from *Gelonium multiflorum*", Phytochemistry, 28, 1181-1185.

Thirkell, D.; Hunter, M. I. S. 1969a. Carotenoid-glycoprotein of *Sarcina flava* membrane. J. Gen. Microbiol. 58:289-292.

Thirkell, D.; Hunter, M. I. S. 1969b. The polar carotenoid fraction from *Sarcina flava*. J. Gen. Microbiol. 58:293-299.

Thirkell, D.; Strang, R. H. C. 1967. Analysis and comparison of the carotenoids of *Sarcina flava* and *Sarcina lutea*. J. Gen. Microbiol. 49:53-57.

Trakoontiyakorn, G.; Nakahara, K.; Shinmoto, H.; Takenaka, M.; Onishi Kameyama, M.; Ono, H.; Yoshida, M.; Nagata, T.; Tsushida, T. 2001. "Structural analysis of a novel antimutagenic compound, 4-hydroxypanduratin A, and the antimutagenic activity of flavonoids in a Thai spice, fingerroot (*Boesenbergia pandurata* Schult.) against mutagenic heterocyclic amines", J. Agr. Food Chem., 49, 3046-3050.

Tuchinda, P.; Reutrakul, V.; Claeson, P.; Pongprayoon, U.; Sematong, T.; Santisuk, T.; Taylor, W. C. 2002. "Anti-inflammatory cyclohexenyl chalcone derivatives in *Boesenbergia pandurata*", Phytochemistry, 59, 169-173.

Tuntiwachwuttikul, P.; Kanghae, S.; Jaipetch, T.; Reutrakul, V. 1980. "Chemical constituents of *Boesenbergia pandurata* Schl.(Abstract)", Abstr. 4th Asian Symp. Med. Plants Spices Bangkok, Thailand, September 15-19, 77.

Tuntiwachwuttikul, P.; Pancharoen, O.; Bubb, W. A.; Hambley, T. W.; Taylor, W. C.; Reutrakul, V. 1987. "Constituents of the Zingiberaceae. XI. Structures of (+)-(1R,2S,3R,4S)-2-benzoyloxymethylcyclohex-5-ene-1,2,3,4-tetrol-4-benzoate [(+)-zeylenol] and (+)-(1R,2R,4R,5S,6R,7R)-4-benzoyloxymethyl-3,8-dioxatricyclo-[5.1.0.0.2,4] octane-5,6-diol5-acetate", Aust. J. Chem., 40, 2049-2061.

Tuntiwachwuttikul, P.; Pancharoen, O.; Reutrakul, V.; Byrne, L. T. 1984. "(1'RS,2'SR,6'RS)-(2,6-dihydroxy-4-methoxyphenyl)-[3'-methyl-2'-(3"-methylbut-2"-enyl)-6'-phenylcyclohex-3'-enyl]methanone (panduratin A)-a constituent of the red rhizomes of a variety of *Boesenbergia pandurata*", Aust. J. Chem., 37, 449-453.

Ueda, H.; Tachibana, Y.; Moriyasu, M.; Kawanishi, K.; Alves, S. M. 2001. "Aldose reductase inhibitors from the fruits of *Caesalpinia ferrea* Mart.", Phytomedicine, 8, 377-381.

Varshney, I. P.; Pal, R. 1978. "Chemical studies of the flowers of *Cassia siamea*, *Peltophorum ferrugineum* and *Caesalpinia pulcherrima*", Indian J. pharmacy., 40, 15-16.

Yadava, R. N.; Nigam, S. S. 1987. "Constituents on the heartwood of *Caesalpinia sappan* Linn.", Acta Cienc. Indica Chem., 13, 87-88.

Yadava, R. N.; Saxena, V. K.; Nigam, S. S. 1978. "Analysis of the fixed oil from the heart wood of *Caesalpinia sappan*", Acta Cienc. Indica, 4, 120-121.

APPENDIX

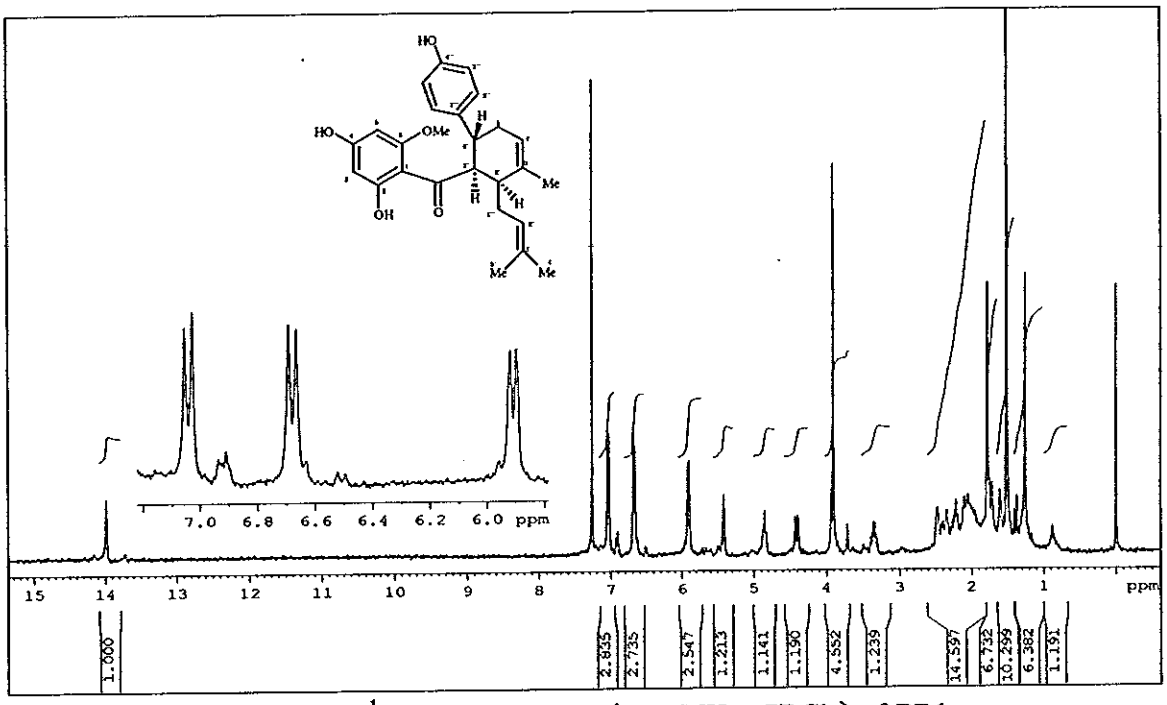

Figure 19 ^{1}H NMR Spectrum (300 MHz, $CDCl_3$) of BP1

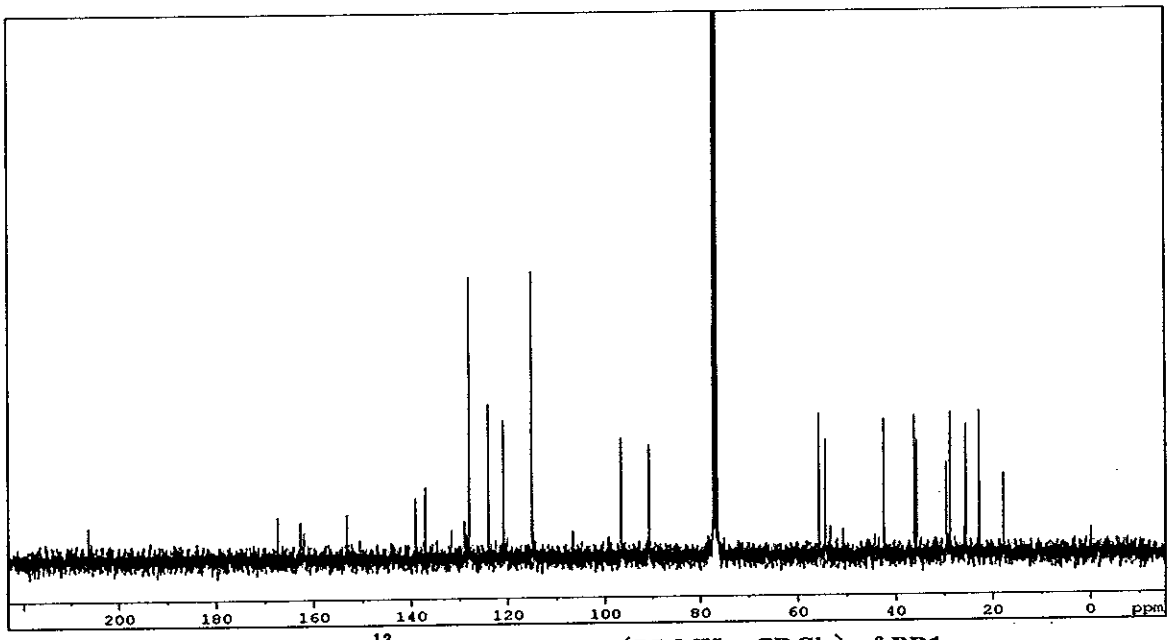

Figure 20 ^{13}C NMR Spectrum (75 MHz, $CDCl_3$) of BP1

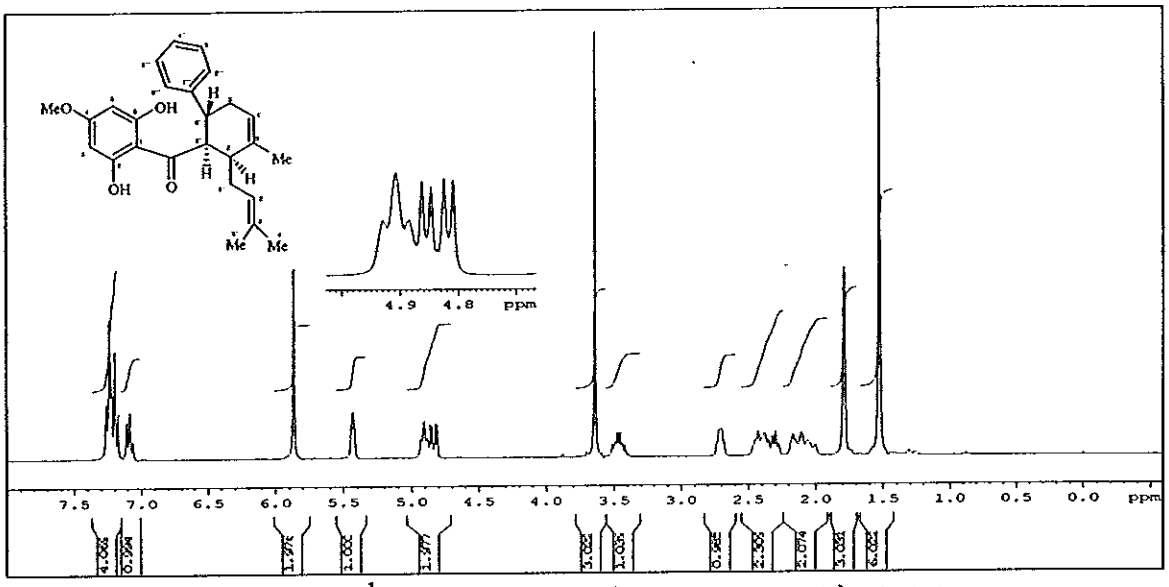

Figure 21 ^{1}H NMR Spectrum (300 MHz, $CDCl_3$) of BP2

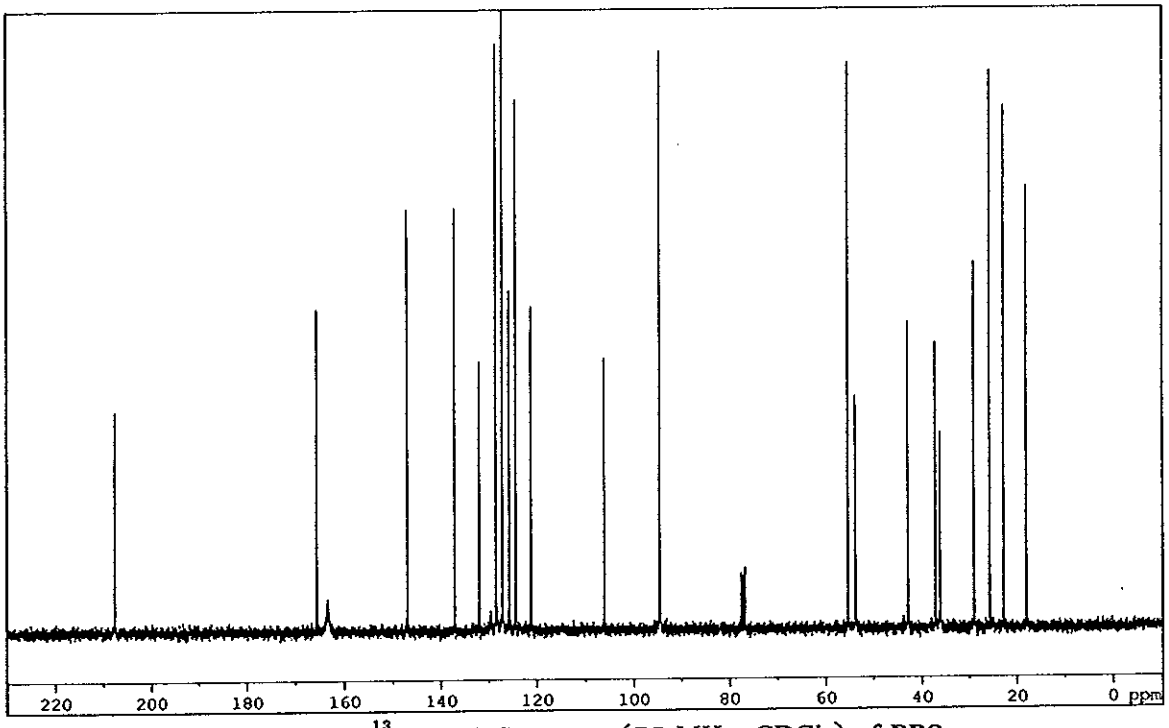

Figure 22 ^{13}C NMR Spectrum (75 MHz, $CDCl_3$) of BP2

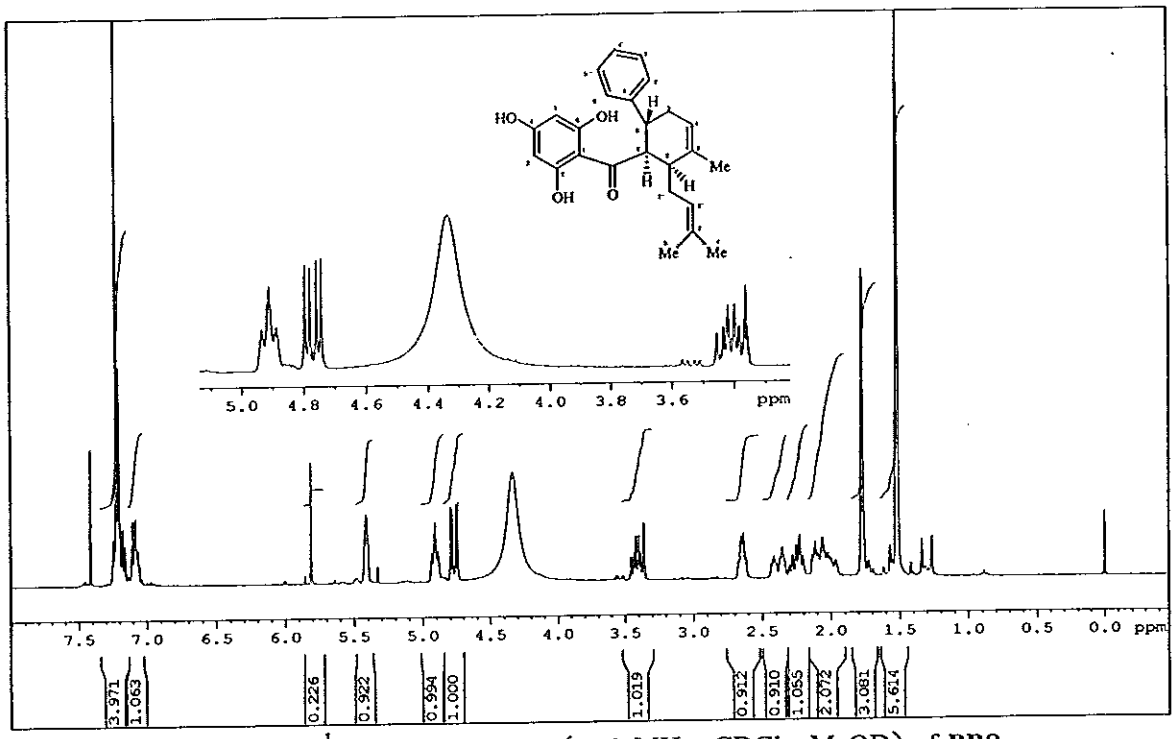

Figure 23 ^{1}H NMR Spectrum (300 MHz, $CDCl_3$+MeOD) of BP3

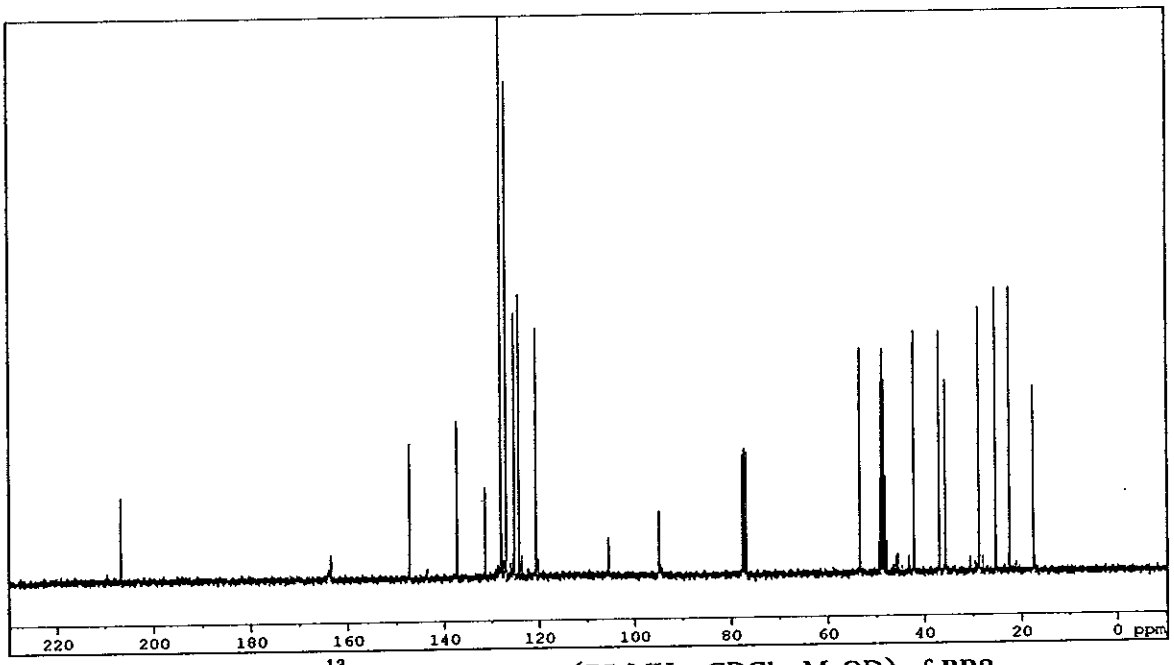

Figure 24 ^{13}C NMR Spectrum (75 MHz, $CDCl_3$+MeOD) of BP3

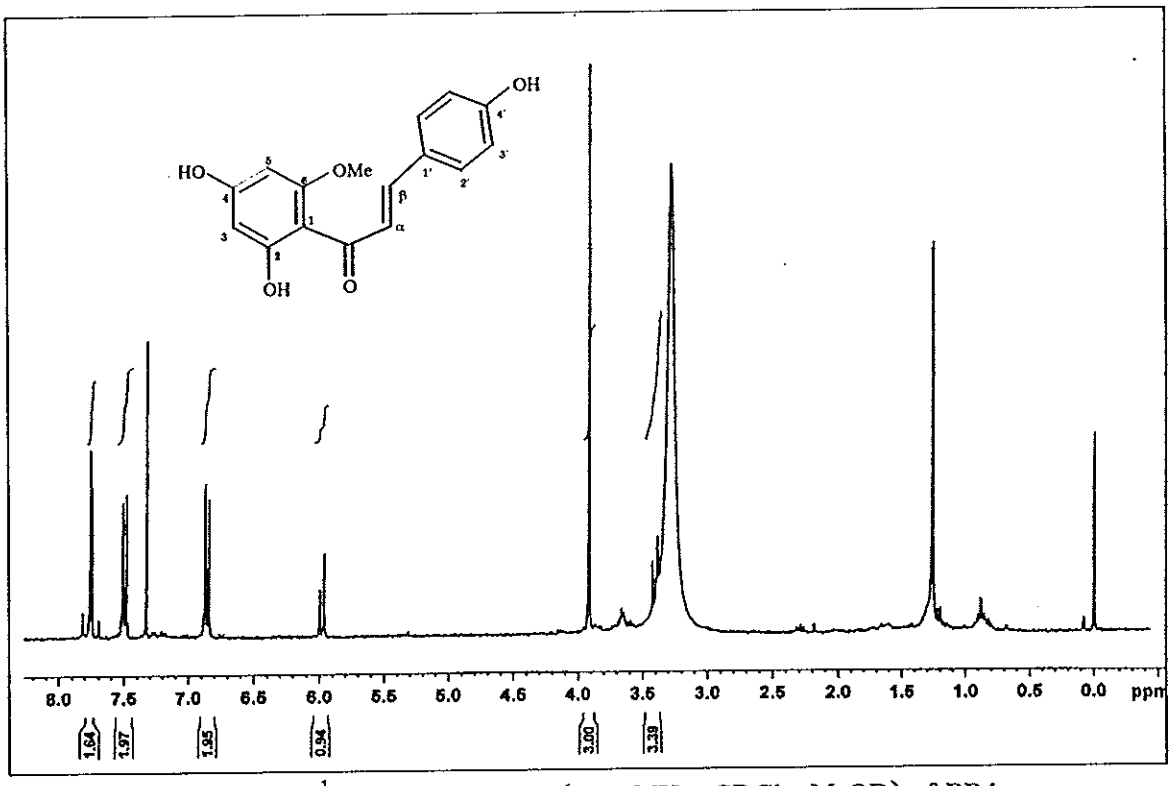

Figure 25 ^{1}H NMR Spectrum (300 MHz, $CDCl_3$+MeOD) of BP4

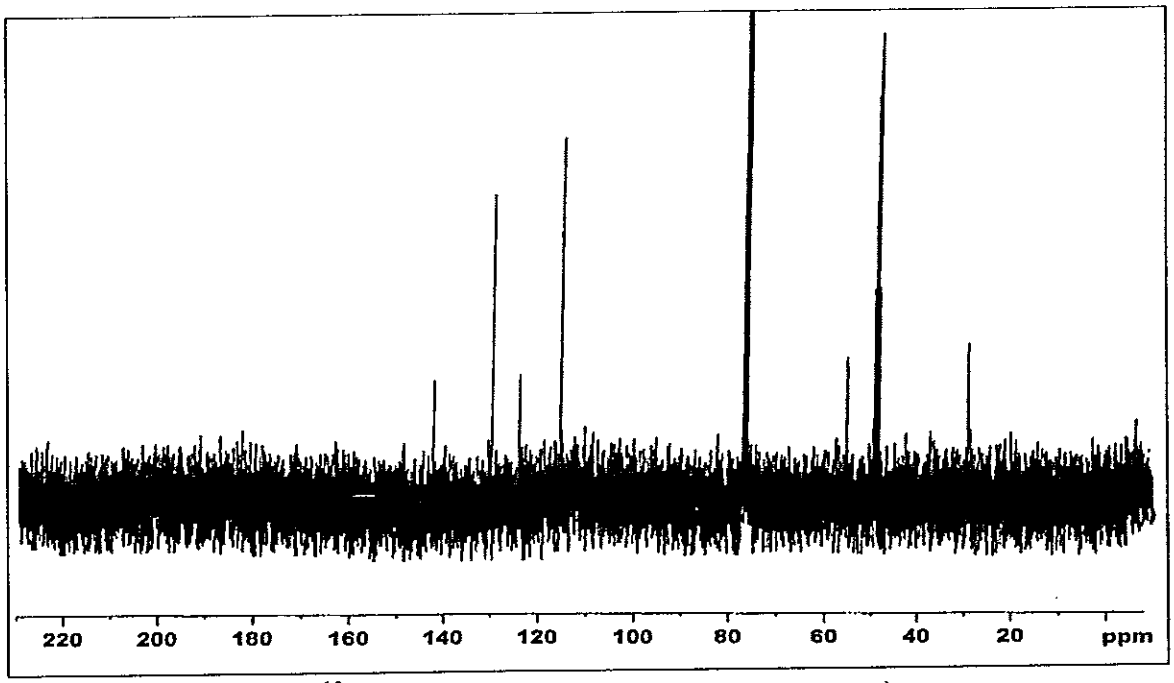

Figure 26 ^{13}C NMR Spectrum (75 MHz, $CDCl_3$+MeOD) of BP4

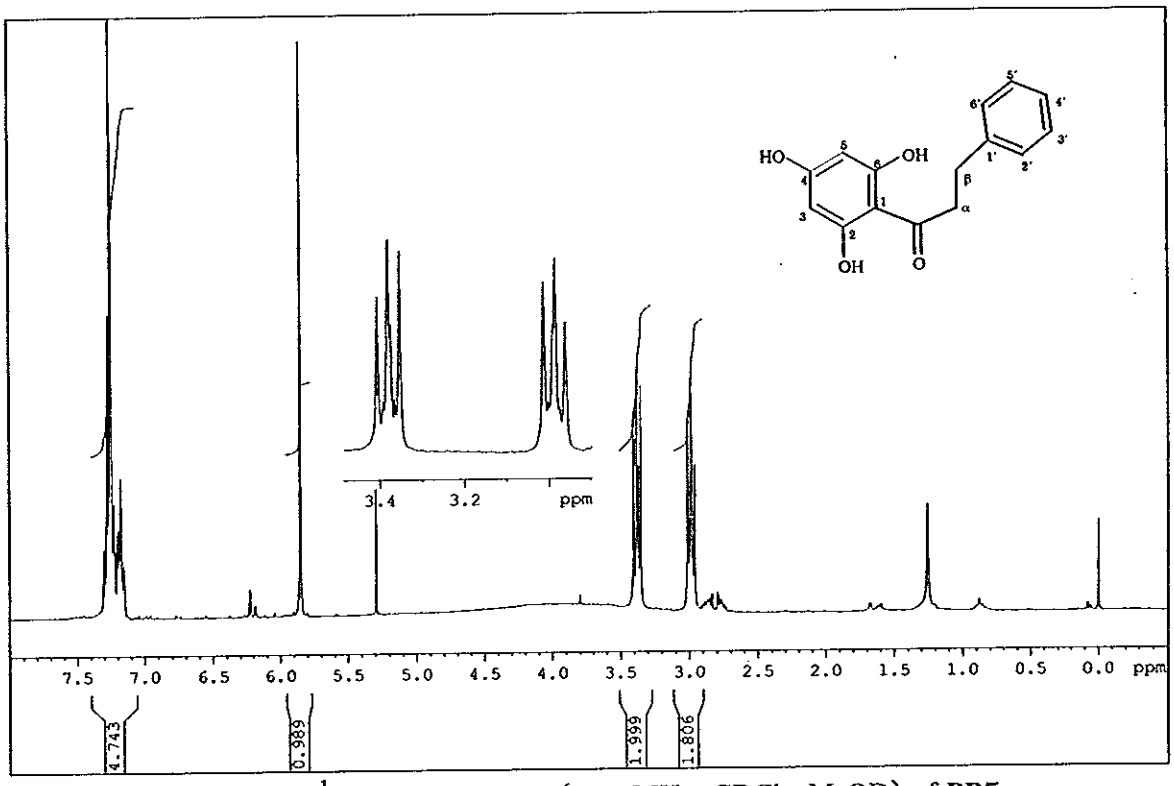

Figure 27 ^{1}H NMR Spectrum (300 MHz, $CDCl_3$+MeOD) of BP5

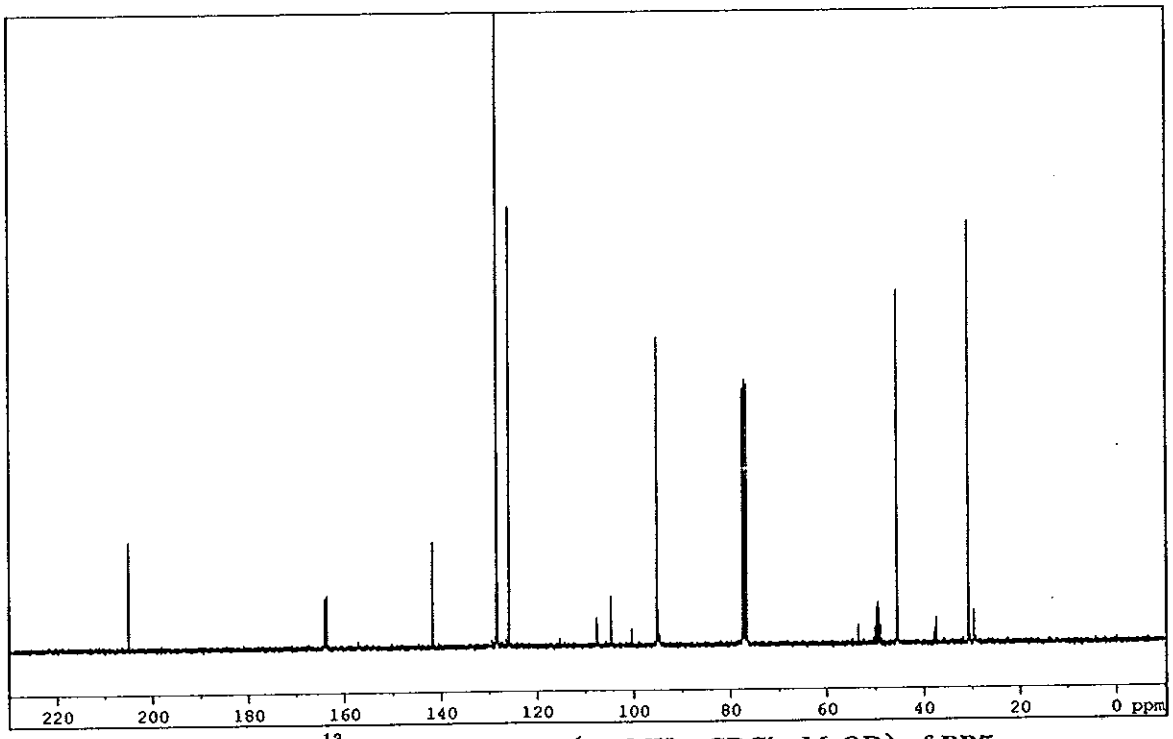

Figure 28 ^{13}C NMR Spectrum (75 MHz, $CDCl_3$+MeOD) of BP5

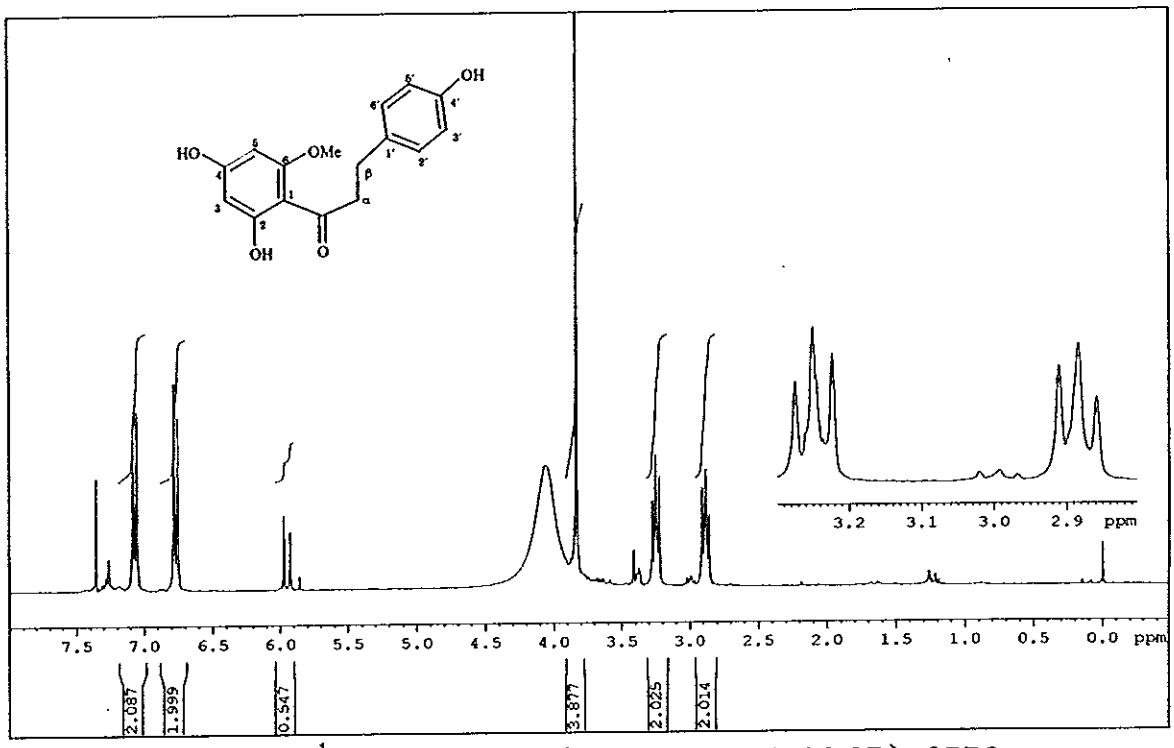

Figure 29 ^{1}H NMR Spectrum (300 MHz, $CDCl_3$+MeOD) of BP6

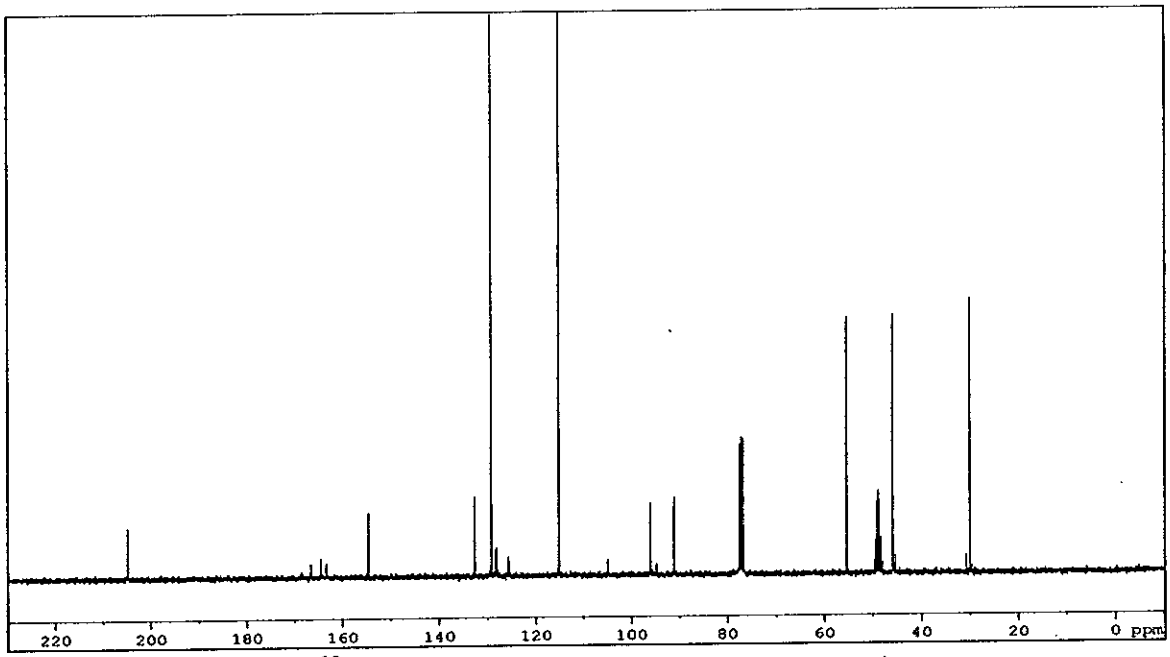

Figure 30 ^{13}C NMR Spectrum (75 MHz, $CDCl_3$+MeOD) of BP6

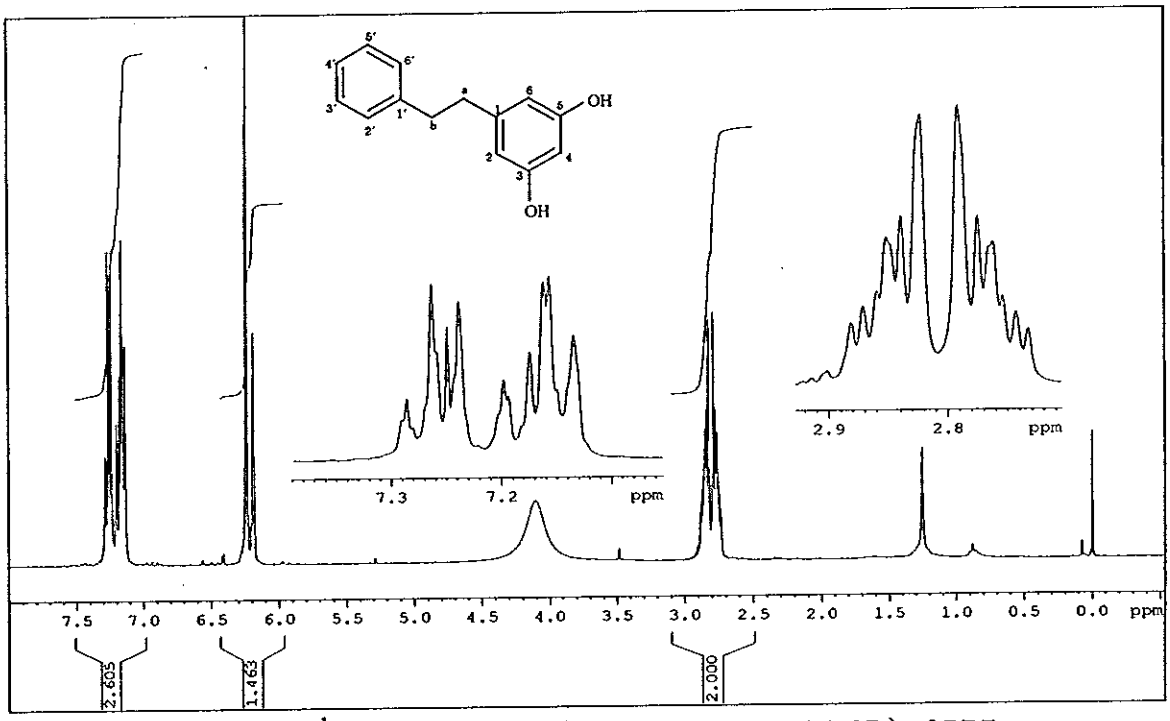

Figure 31 ^{1}H NMR Spectrum (300 MHz, $CDCl_3$+MeOD) of BP7

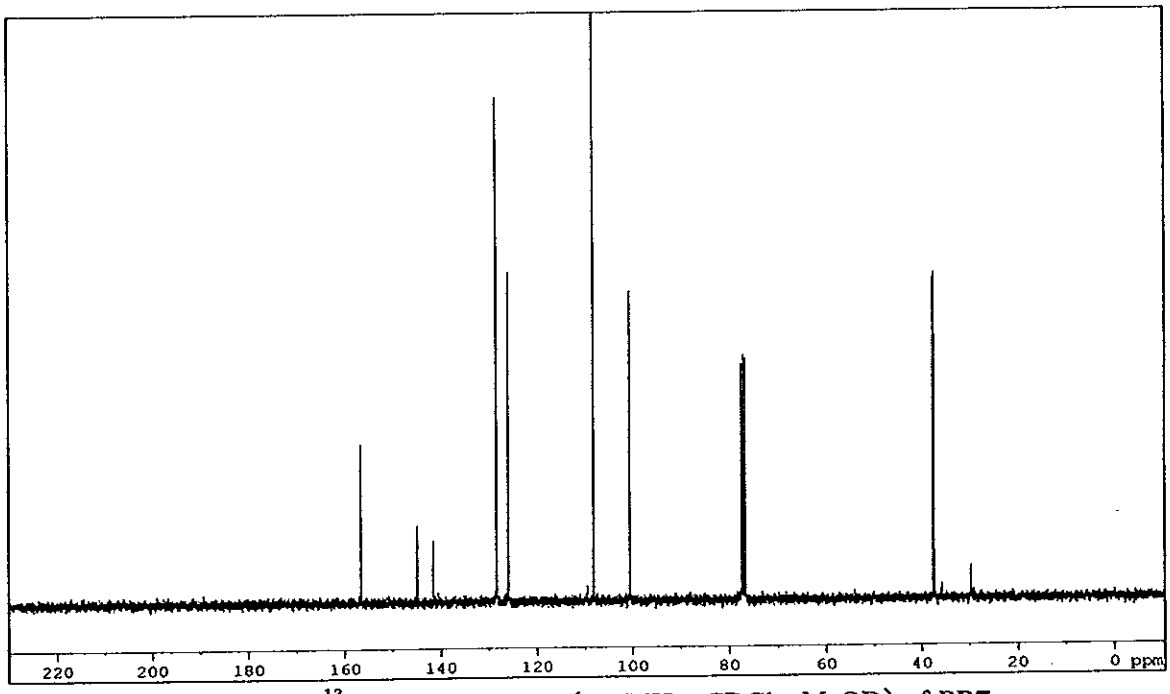

Figure 32 ^{13}C NMR Spectrum (75 MHz, $CDCl_3$+MeOD) of BP7

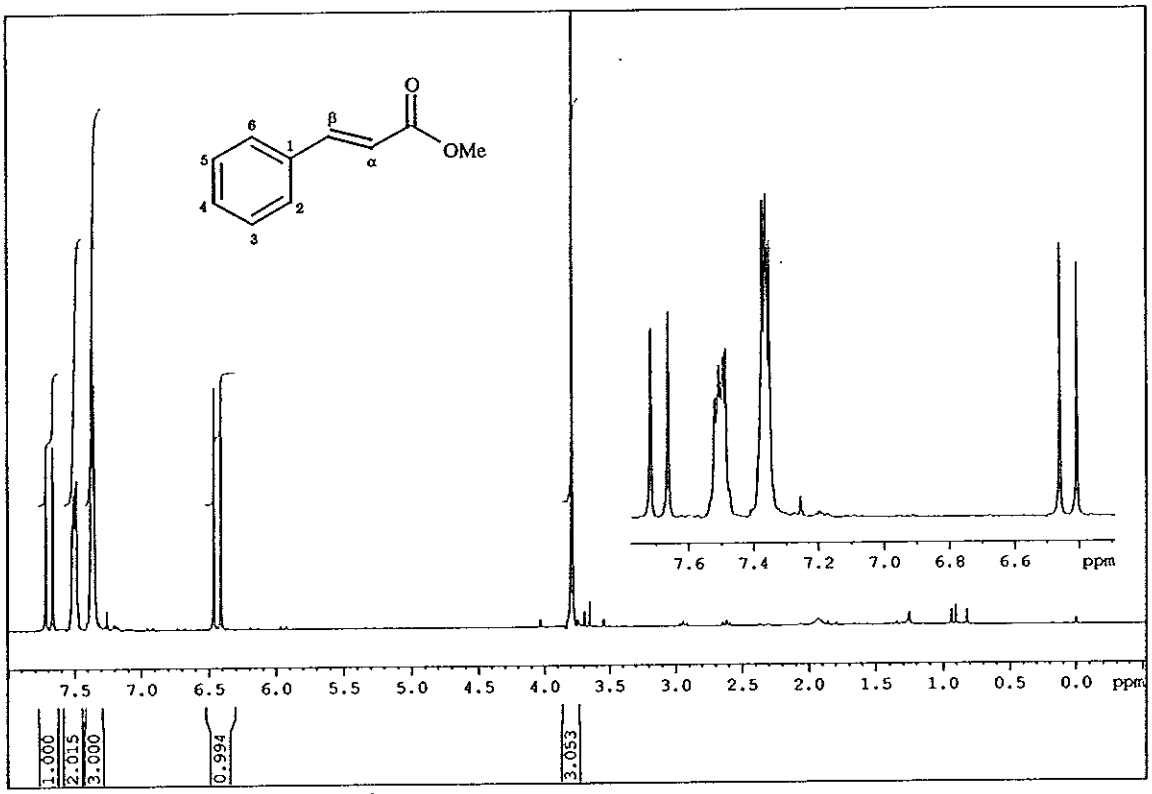

Figure 33 ^{1}H NMR Spectrum (300 MHz, $CDCl_3$) of BP8

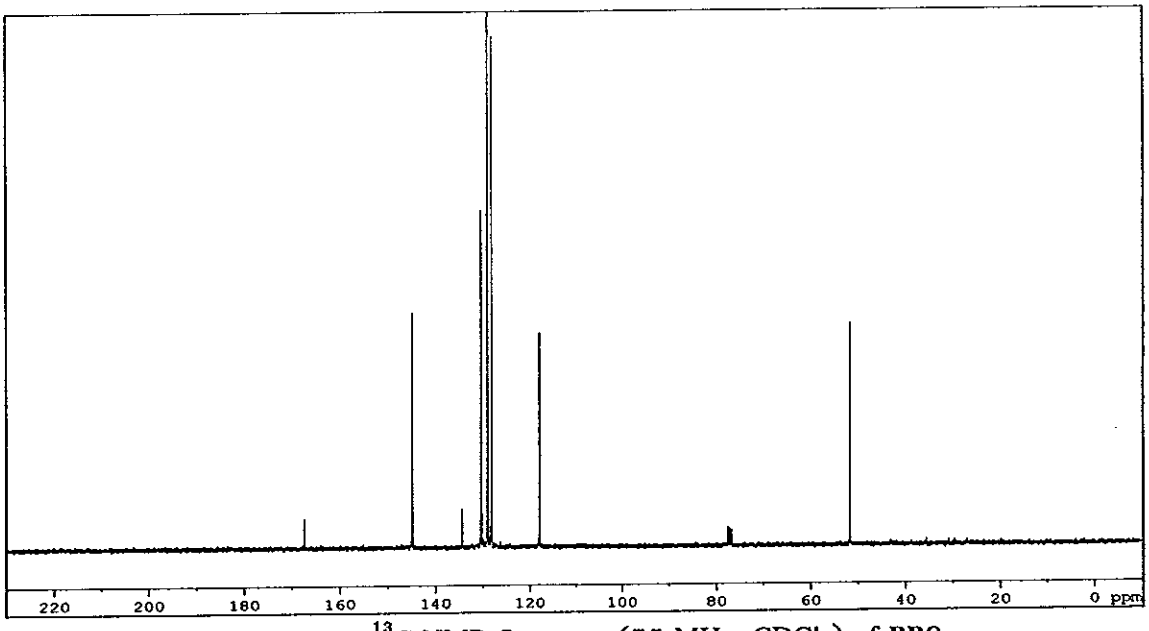

Figure 34 ^{13}C NMR Spectrum (75 MHz, $CDCl_3$) of BP8

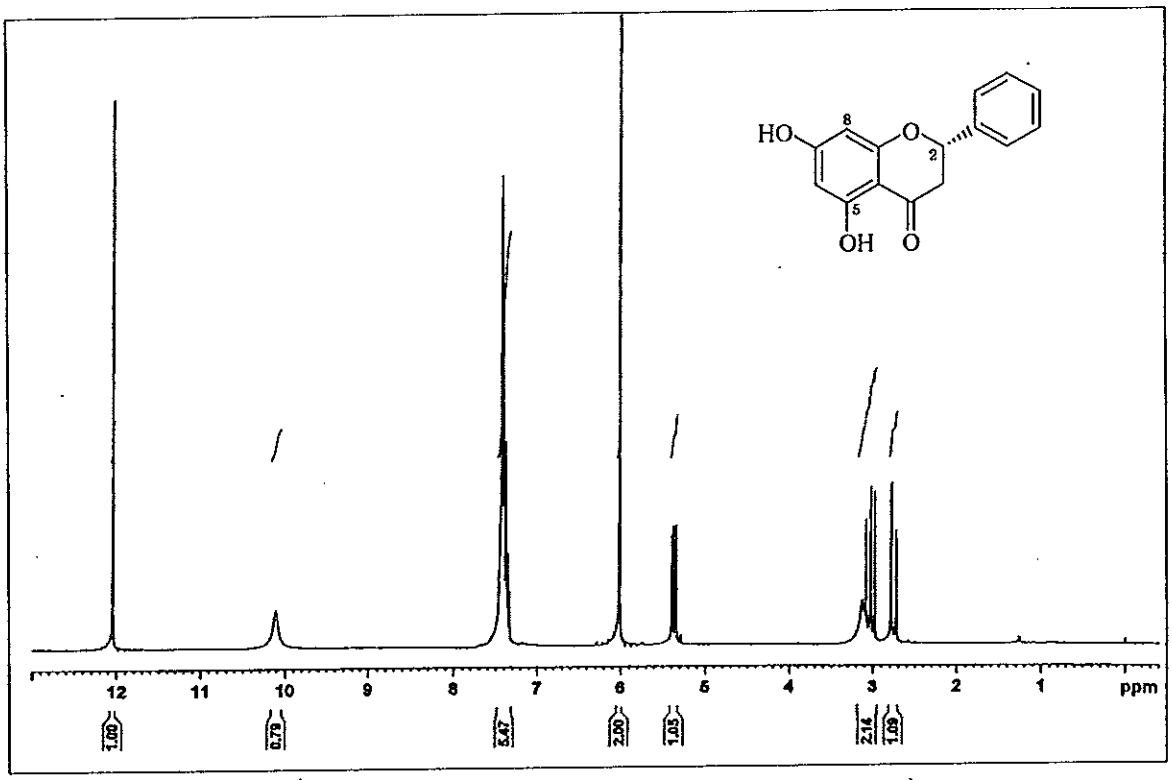

Figure 35 ^{1}H NMR Spectrum (300 MHz, $CDCl_3$+DMSO-d_6) of BP9

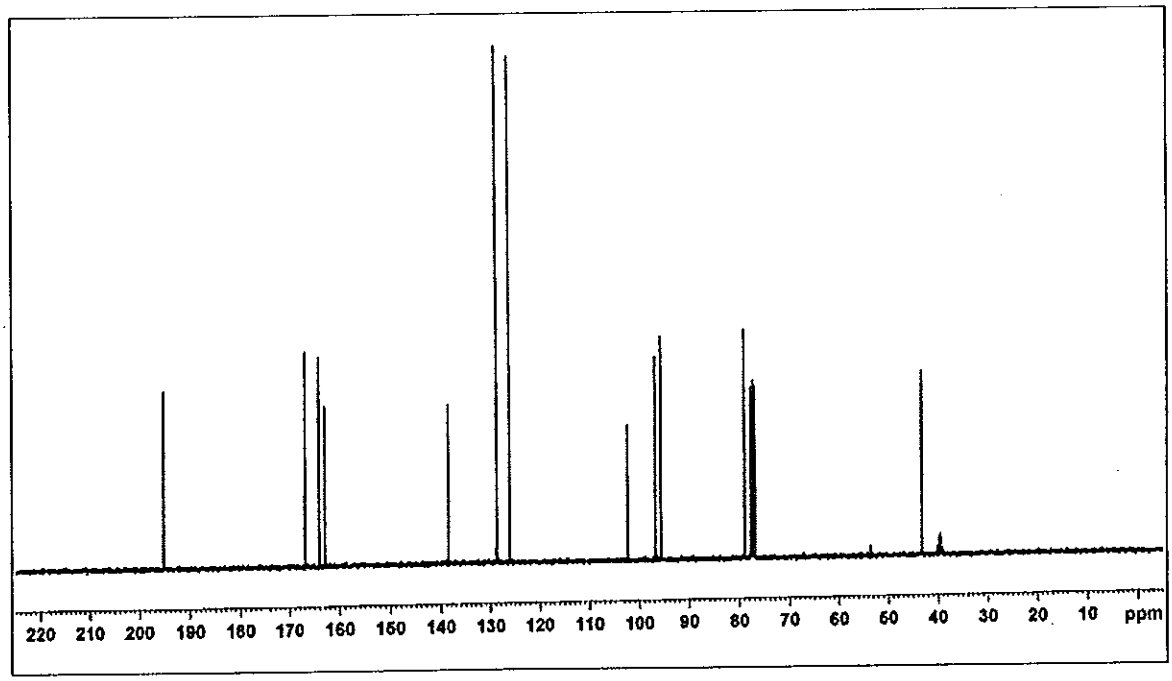

Figure 36 ^{13}C NMR Spectrum (75 MHz, $CDCl_3$+DMSO-d_6) of BP9

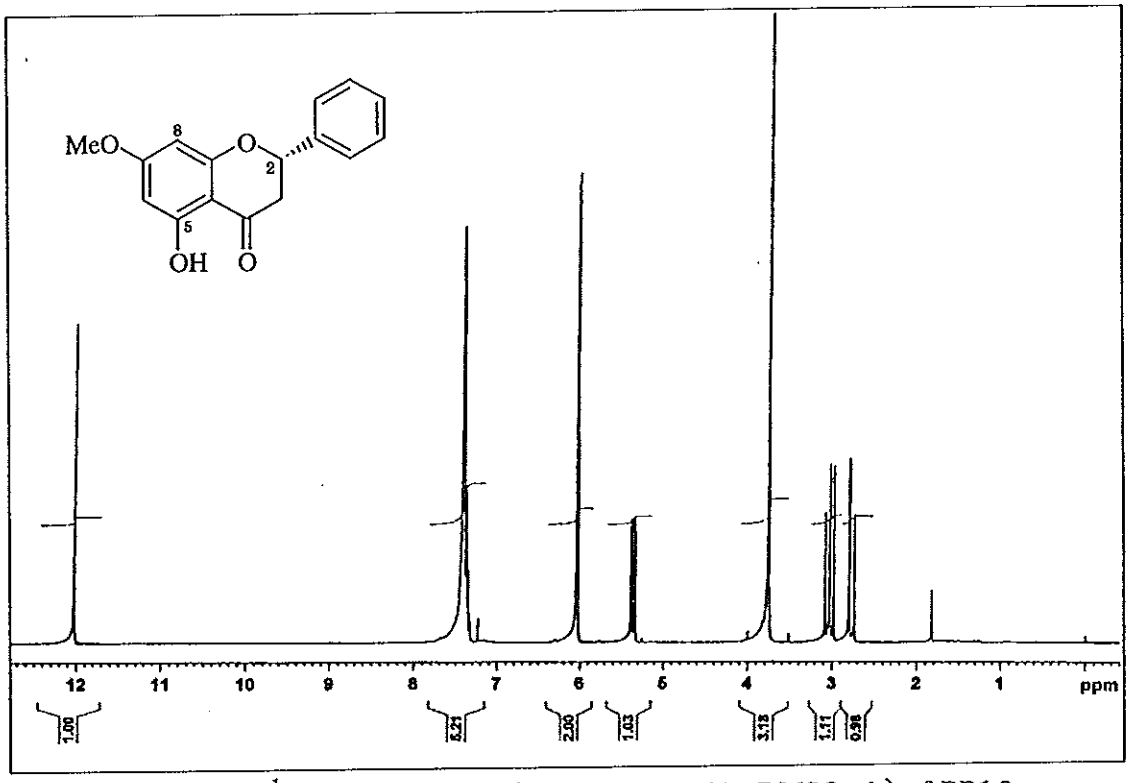

Figure 37 ^{1}H NMR Spectrum (300 MHz, $CDCl_3$+DMSO-d_6) of **BP10**

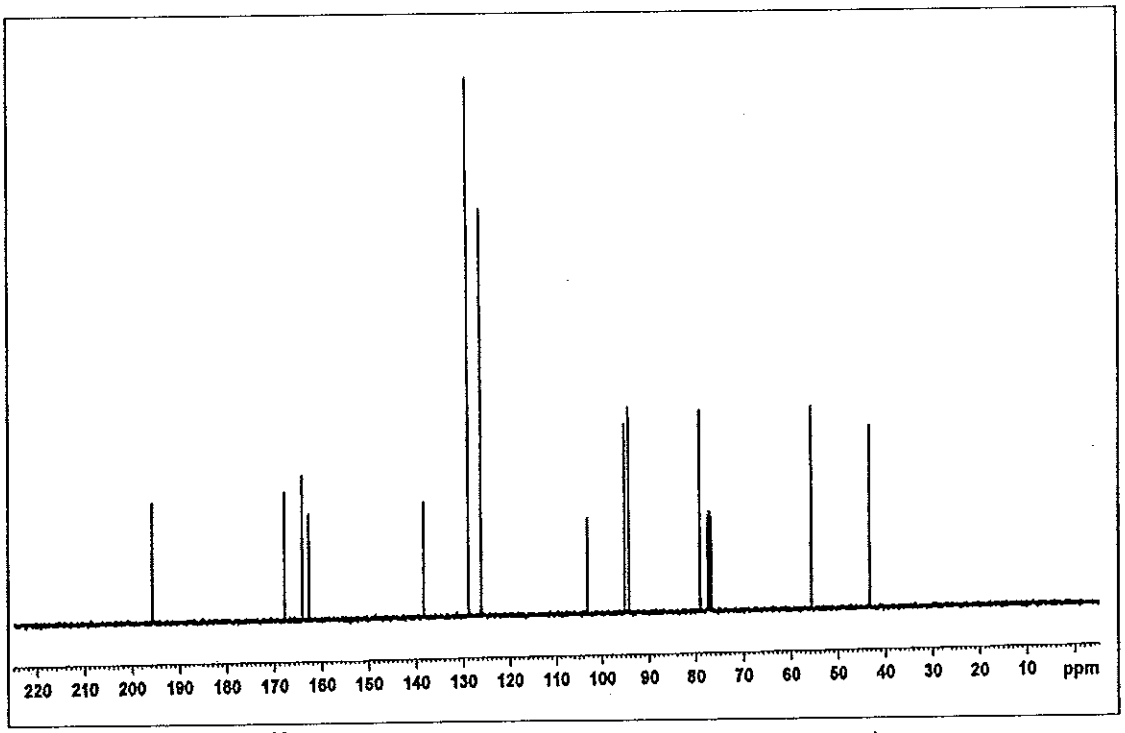

Figure 38 ^{13}C NMR Spectrum (75 MHz, $CDCl_3$+DMSO-d_6) of **BP10**

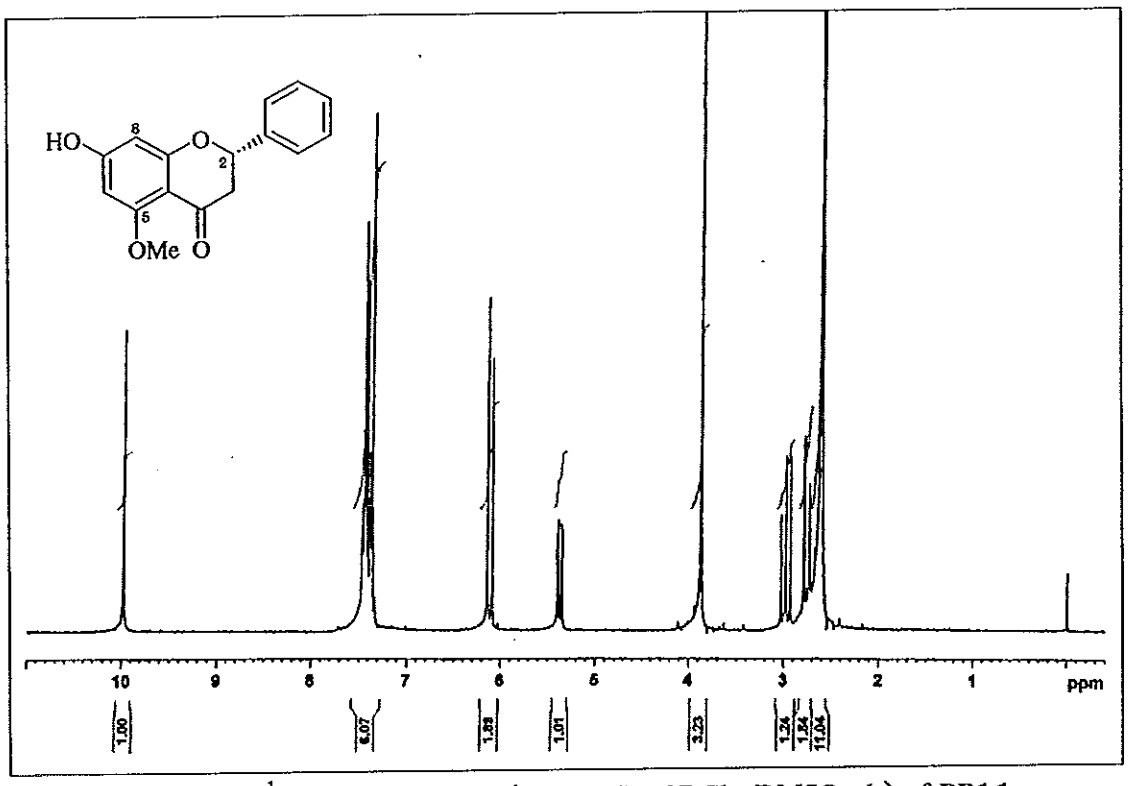

Figure 39 ^{1}H NMR Spectrum (300 MHz, $CDCl_3$+DMSO-d_6) of BP11

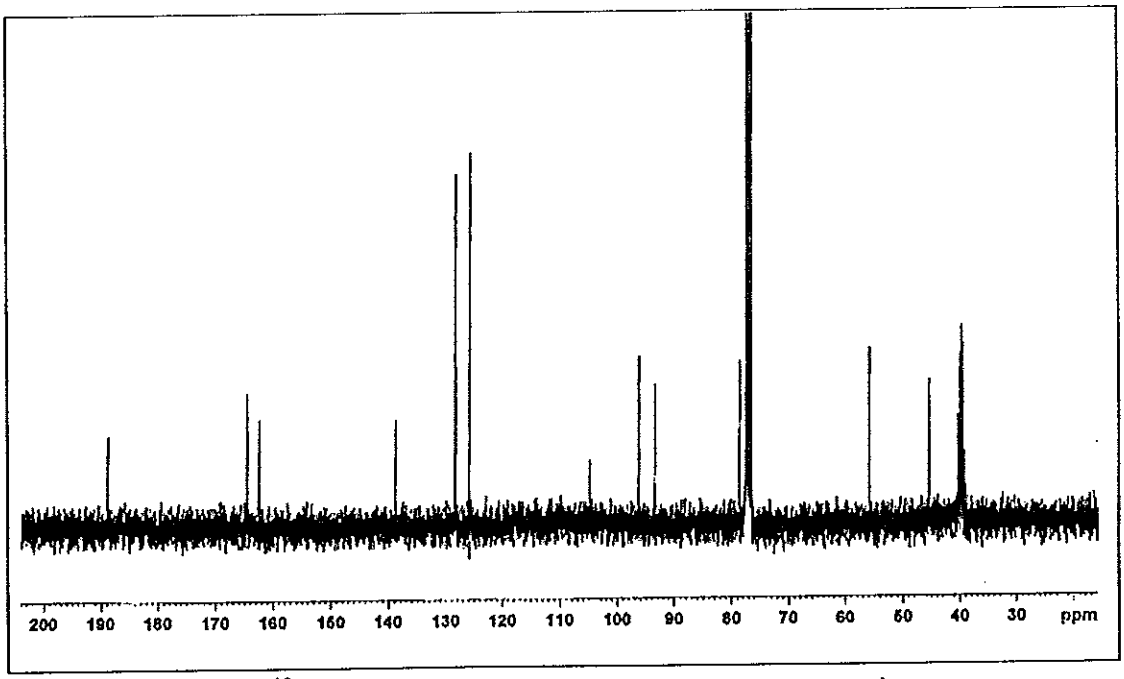

Figure 40 ^{13}C NMR Spectrum (75 MHz, $CDCl_3$+DMSO-d_6) of BP11

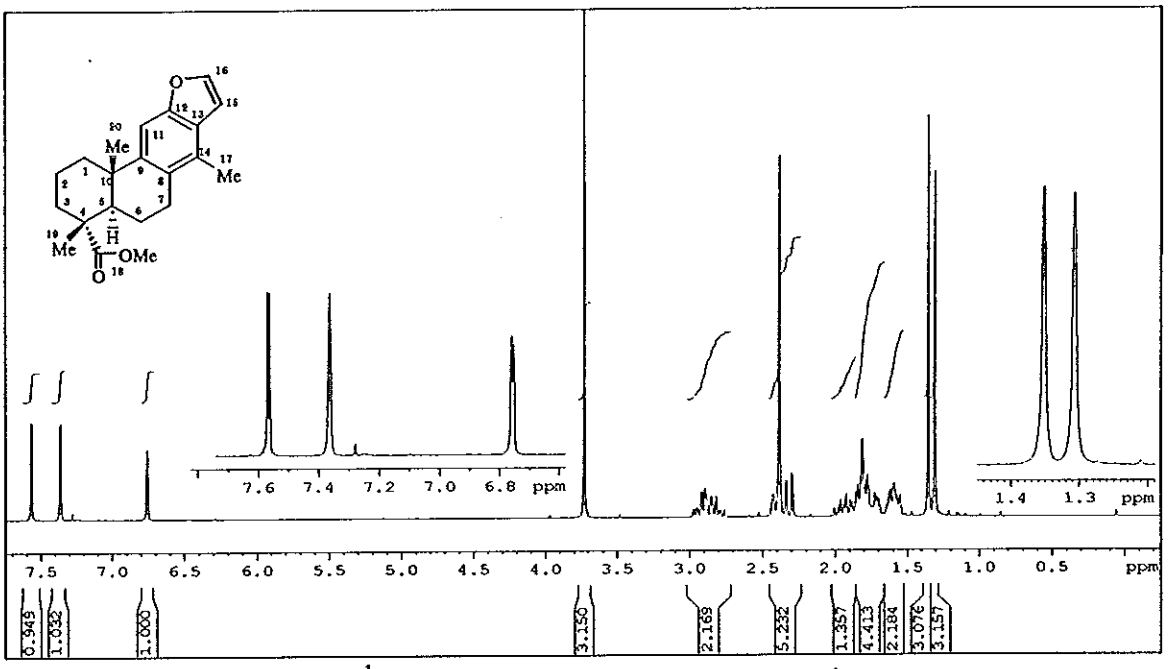

Figure 41 ^{1}H NMR Spectrum (300 MHz, $CDCl_3$) of SC1

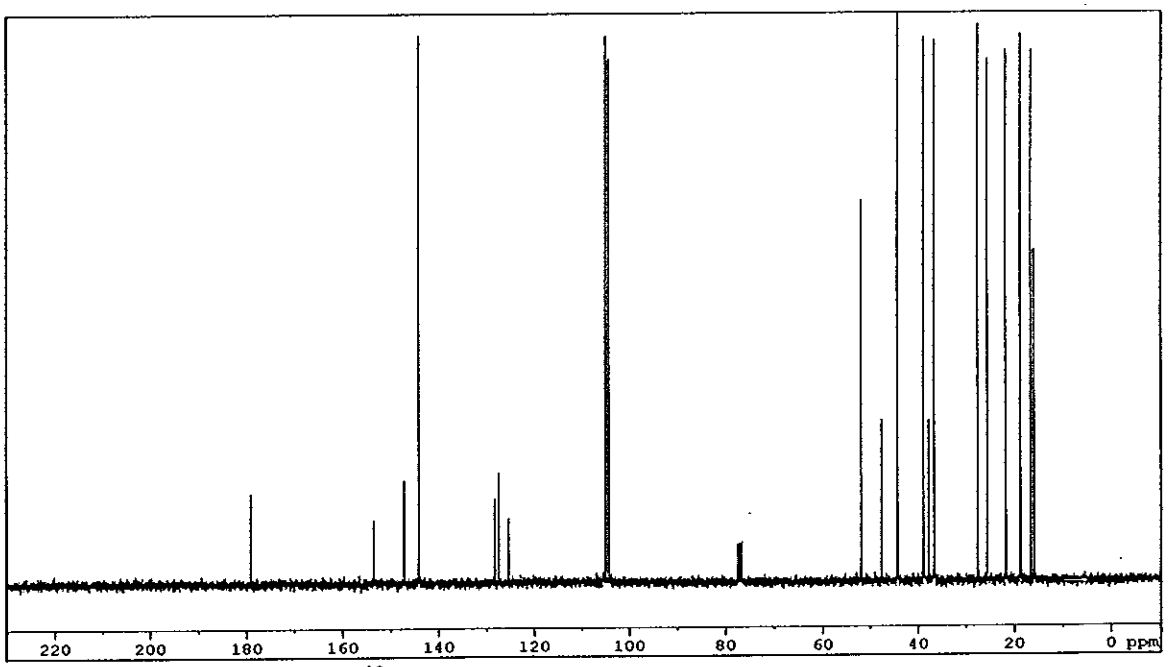

Figure 42 ^{13}C NMR Spectrum (75 MHz, $CDCl_3$) of SC1

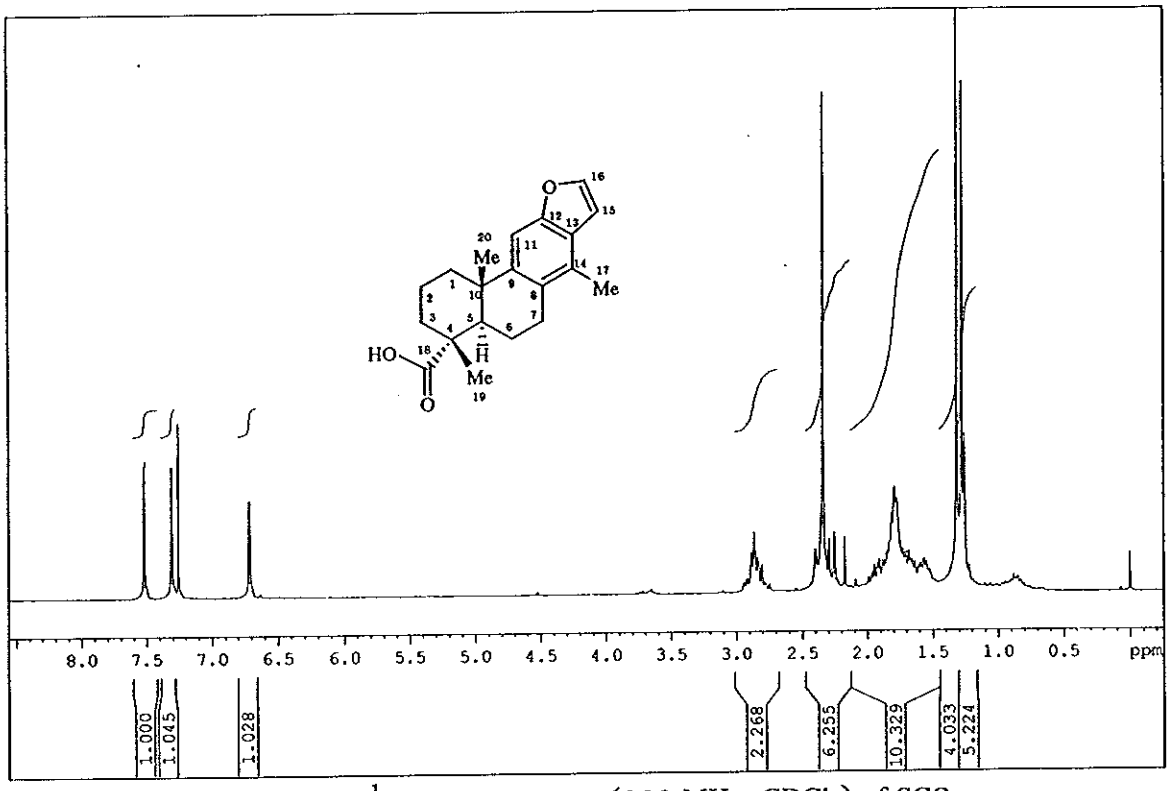

Figure 43 ^{1}H NMR Spectrum (300 MHz, $CDCl_3$) of SC2

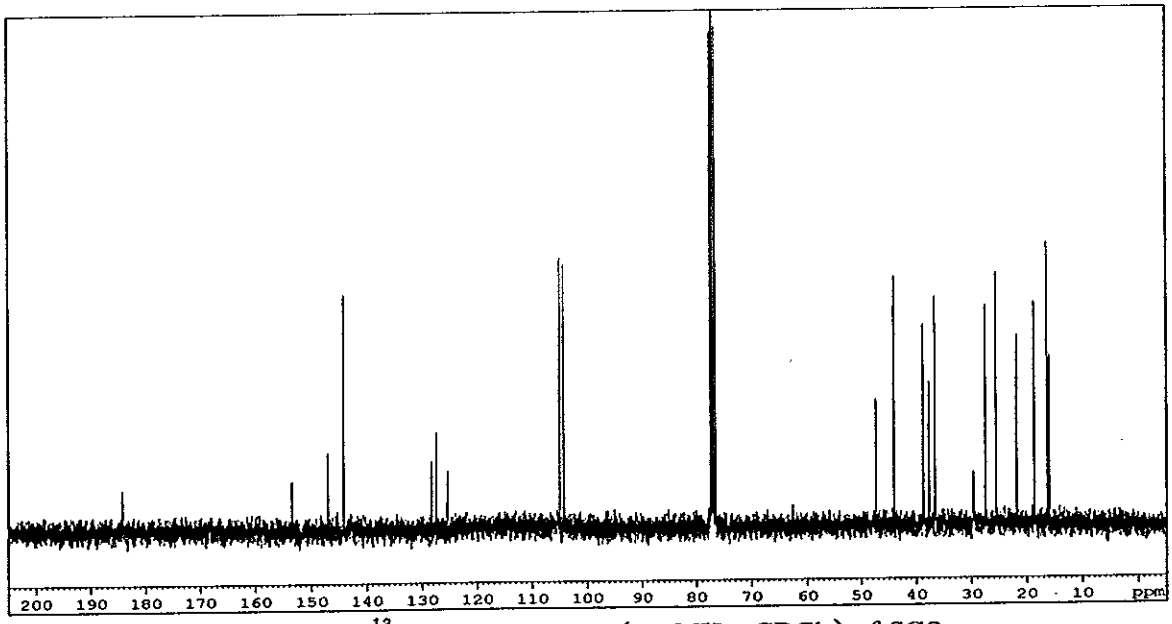

Figure 44 ^{13}C NMR Spectrum (75 MHz, $CDCl_3$) of SC2

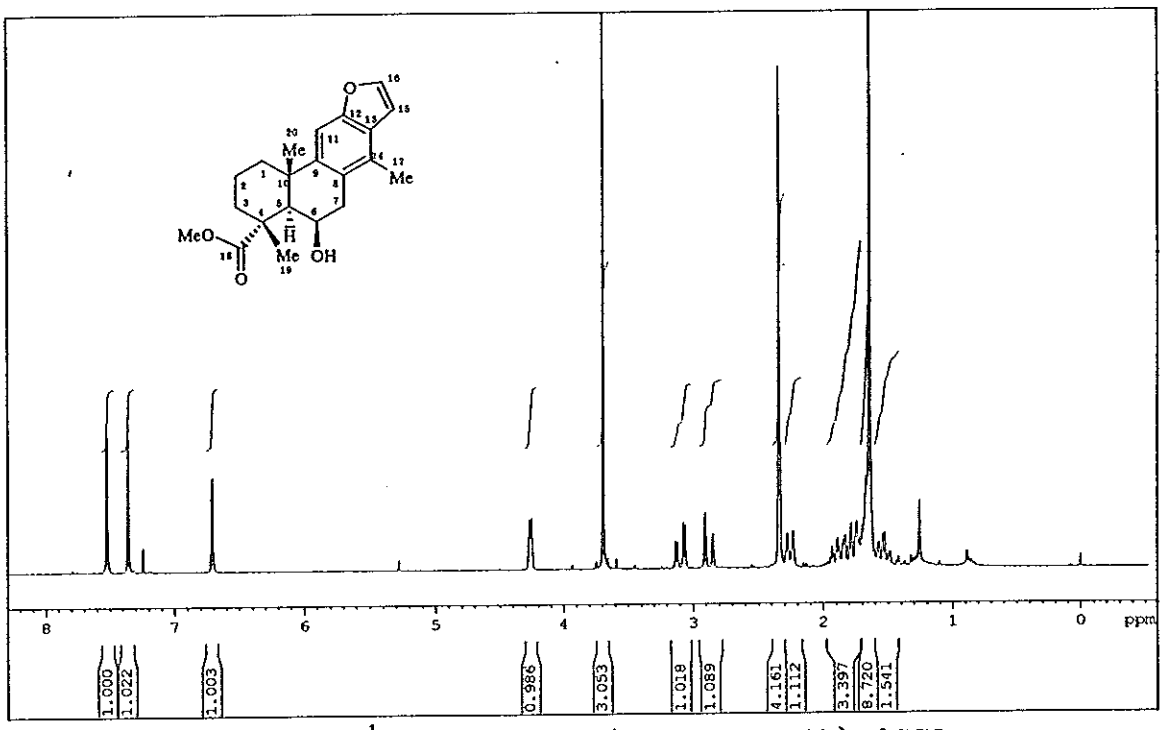

Figure 45 ^{1}H NMR Spectrum (300 MHz, $CDCl_3$) of SC3

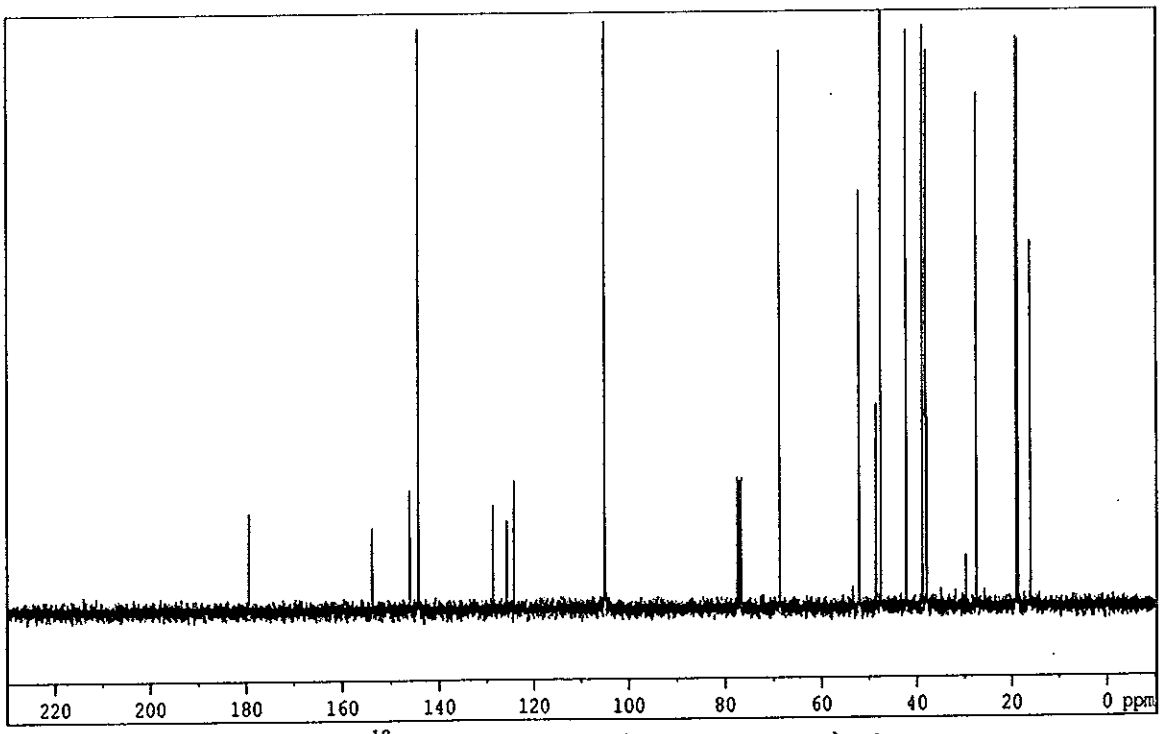

Figure 46 ^{13}C NMR Spectrum (75 MHz, $CDCl_3$) of SC3

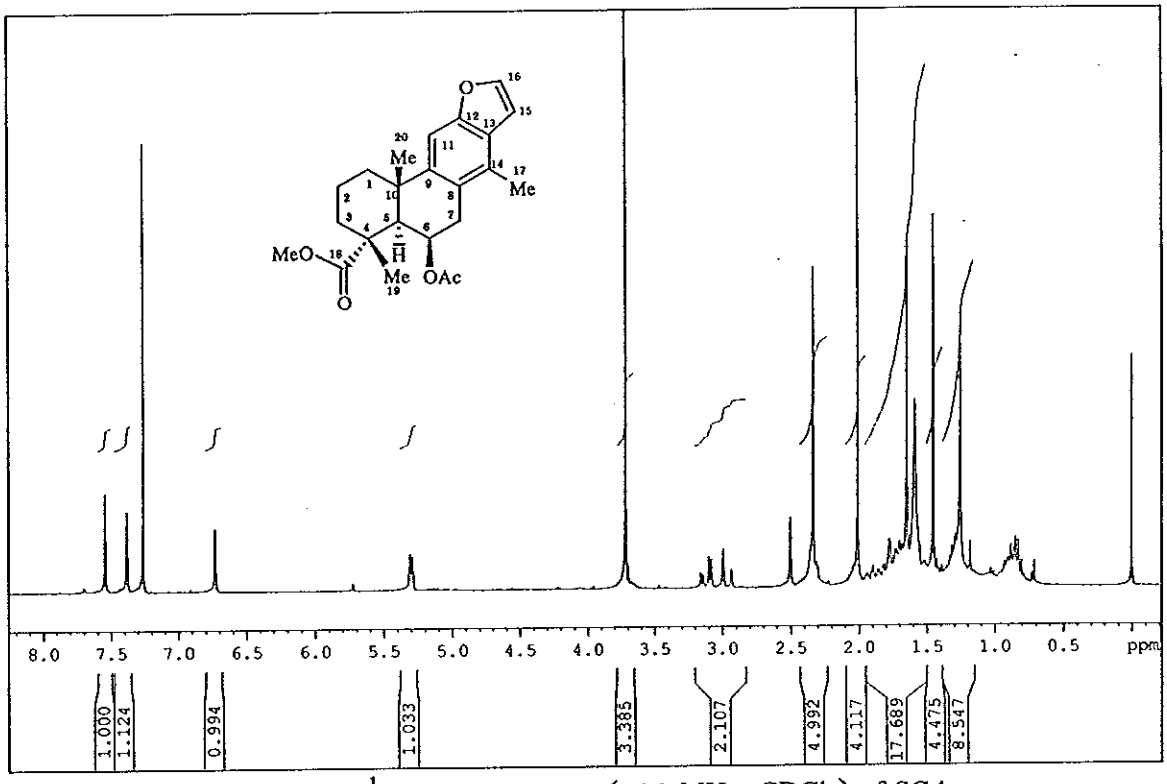

Figure 47 ^{1}H NMR Spectrum (300 MHz, $CDCl_3$) of SC4

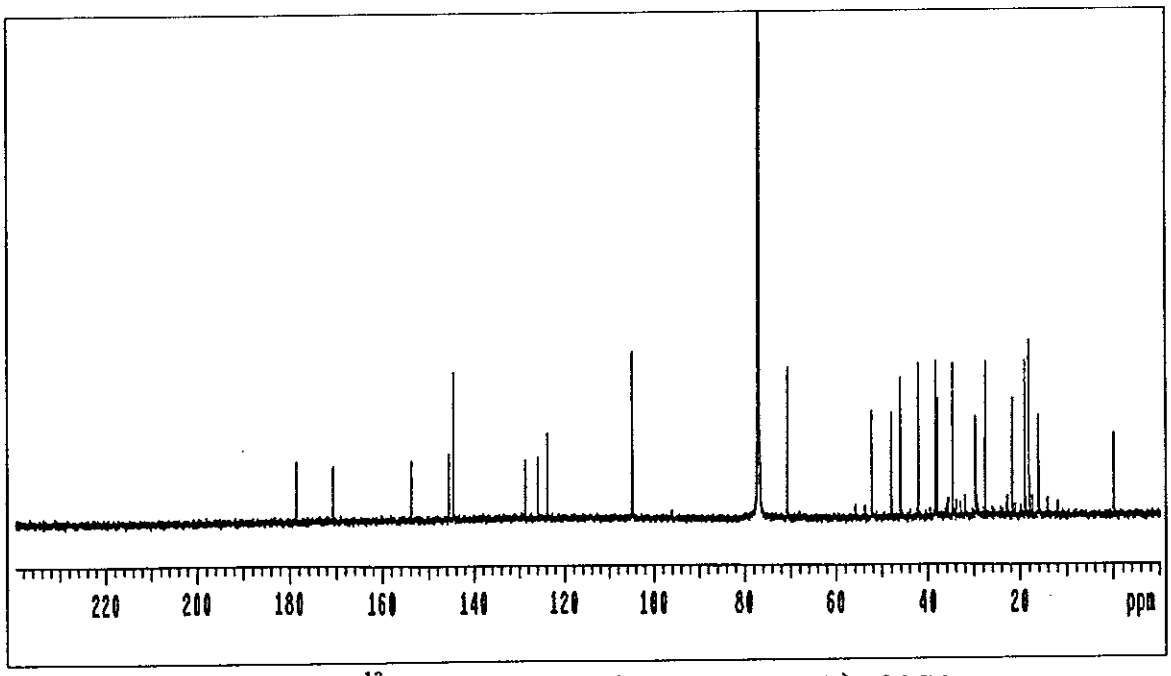

Figure 48 ^{13}C NMR Spectrum (125 MHz, $CDCl_3$) of SC4

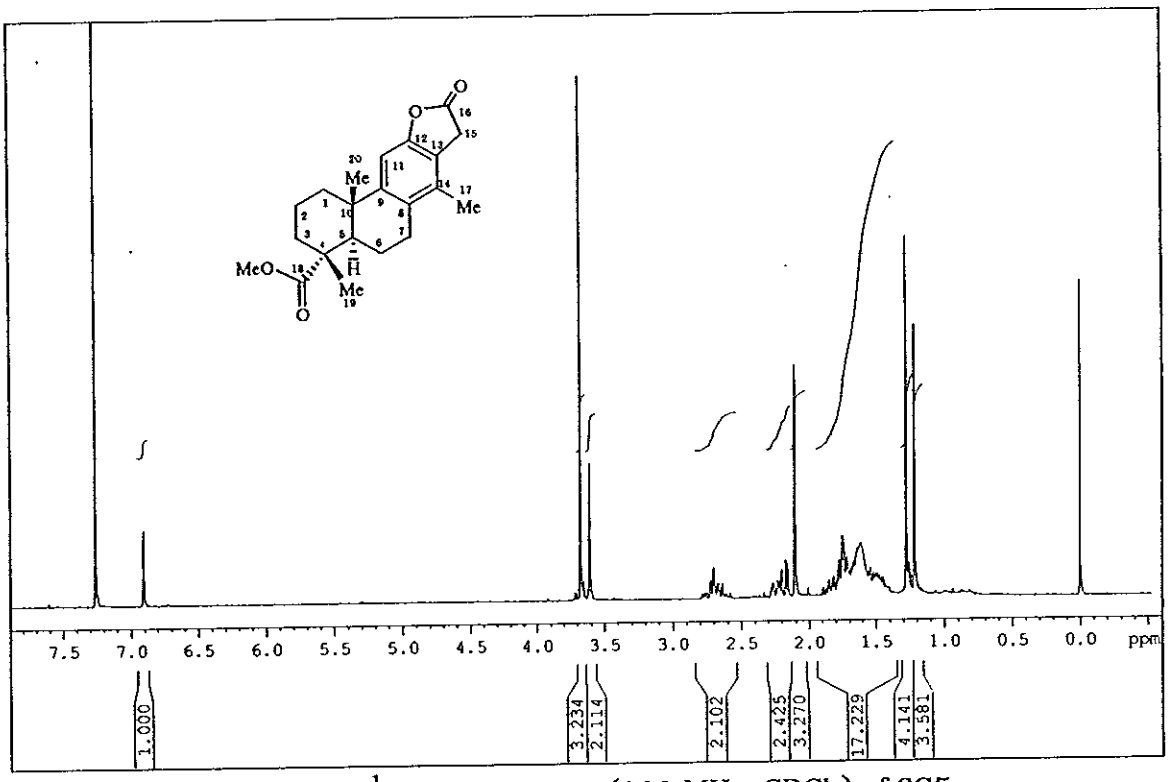

Figure 49 ^{1}H NMR Spectrum (300 MHz, $CDCl_3$) of SC5

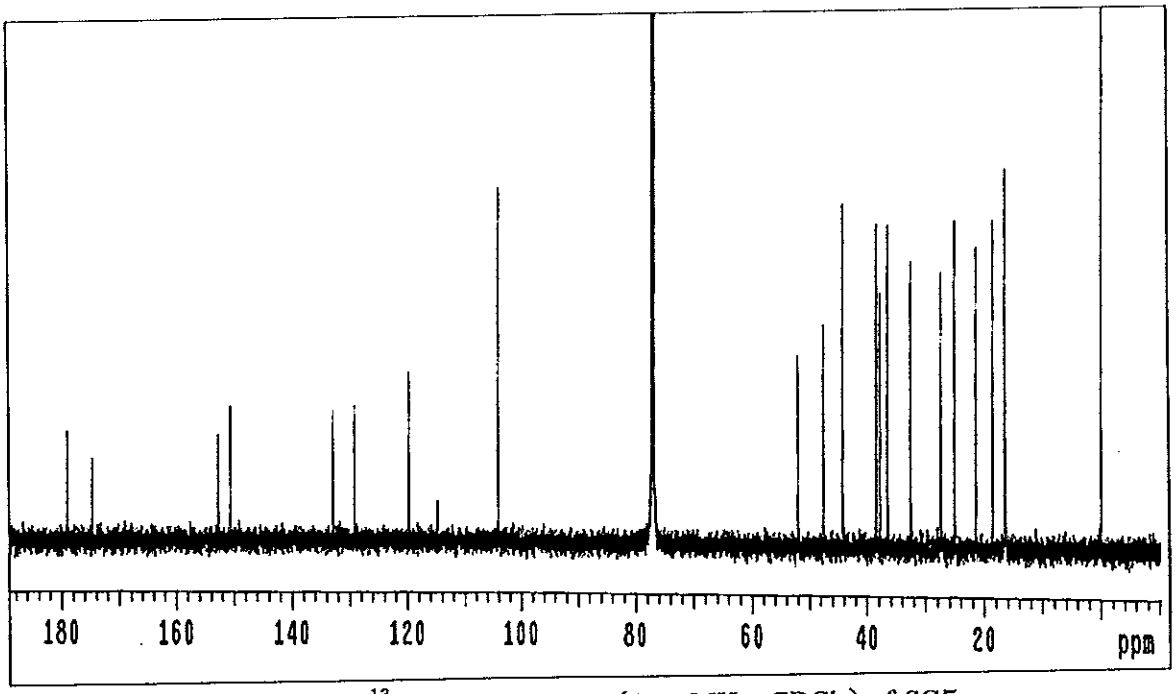

Figure 50 ^{13}C NMR Spectrum (125 MHz, $CDCl_3$) of SC5

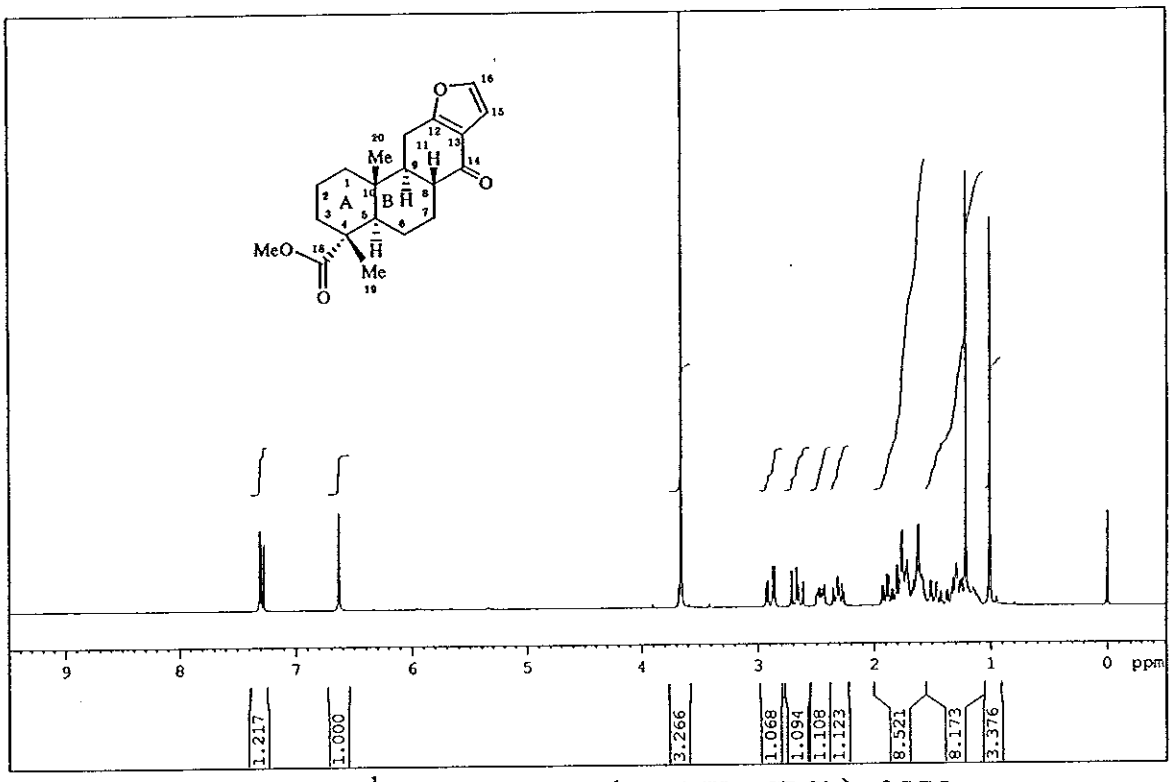

Figure 51 ^{1}H NMR Spectrum (300 MHz, $CDCl_3$) of SC6

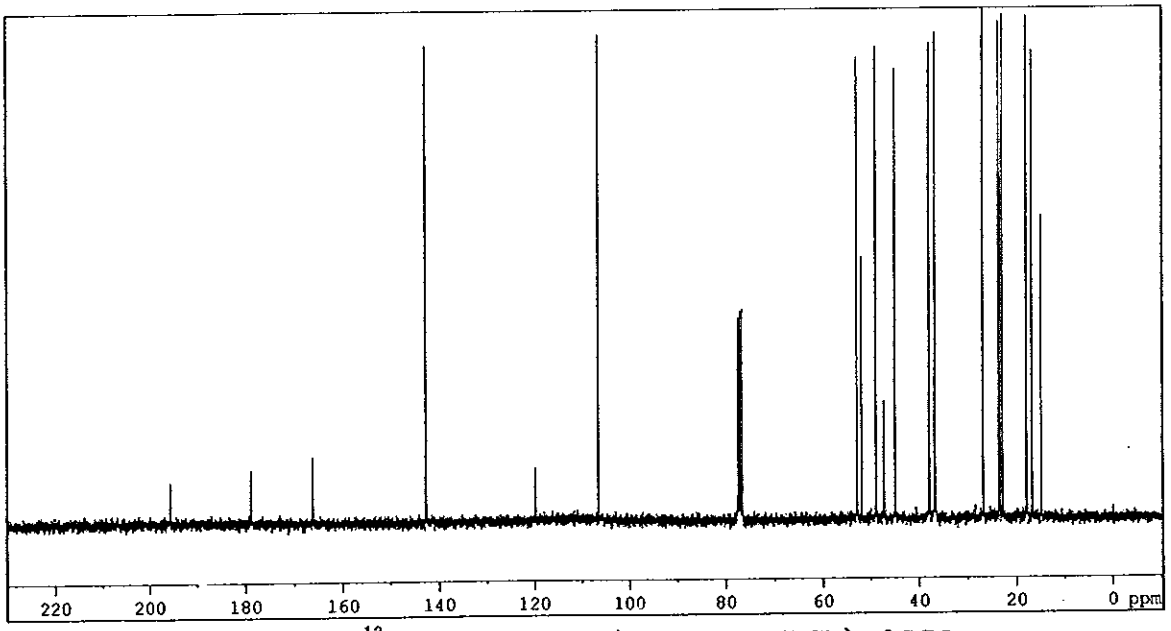

Figure 52 ^{13}C NMR Spectrum (125 MHz, $CDCl_3$) of SC6

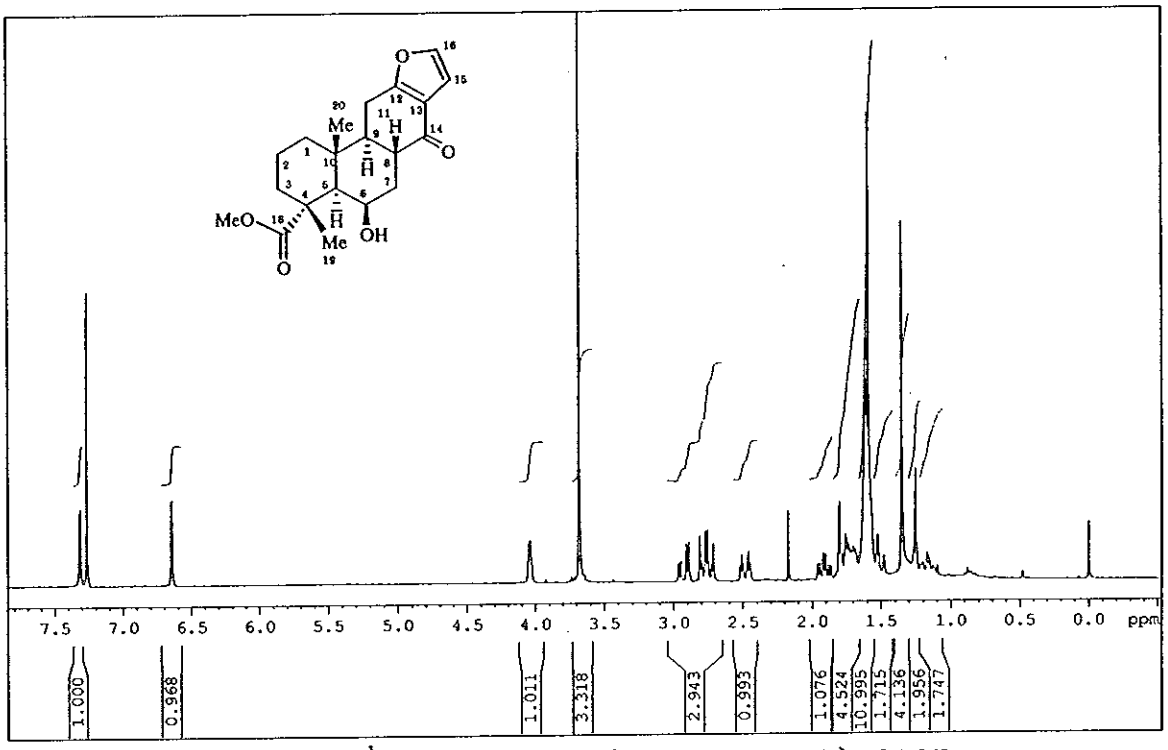

Figure 53 ^{1}H NMR Spectrum (300 MHz, $CDCl_3$) of SC7

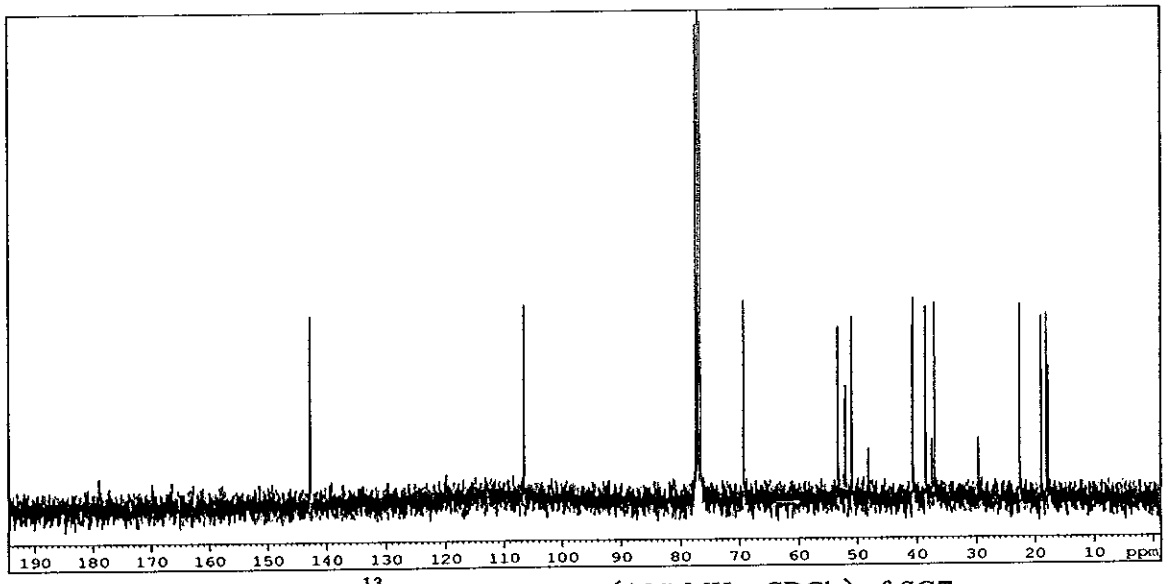

Figure 54 ^{13}C NMR Spectrum (125 MHz, $CDCl_3$) of SC7

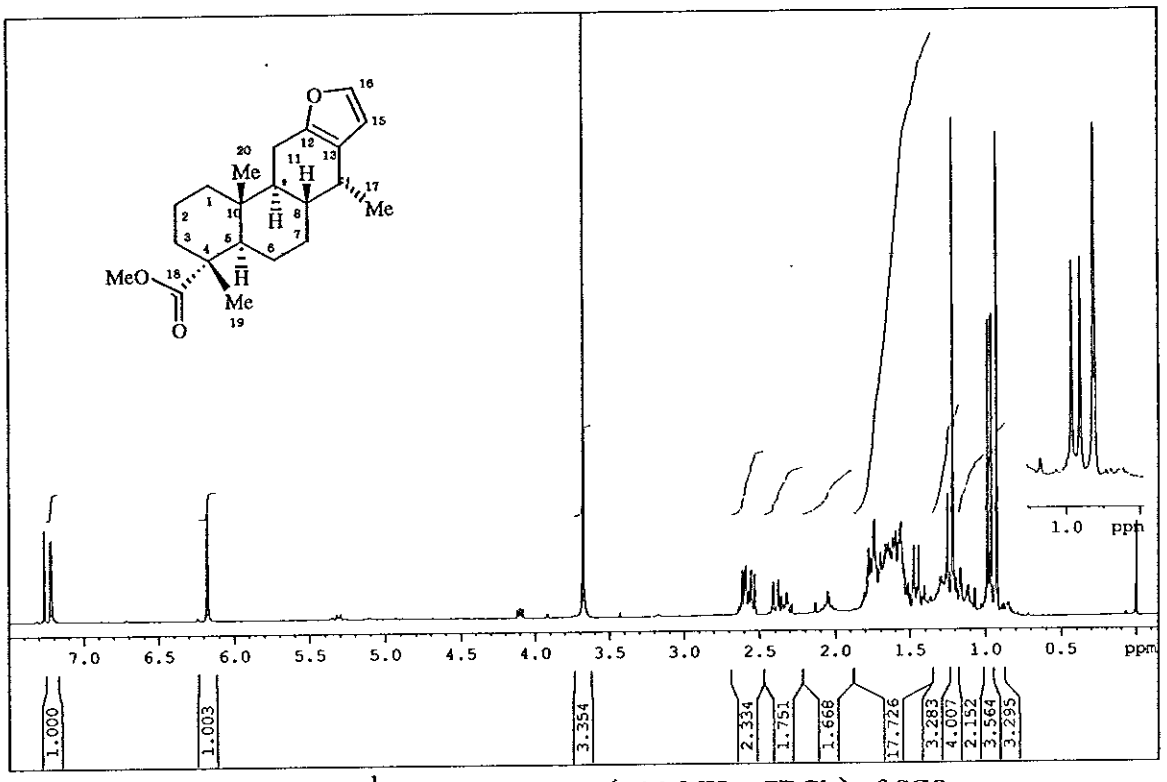

Figure 55 ^{1}H NMR Spectrum (300 MHz, $CDCl_3$) of SC8

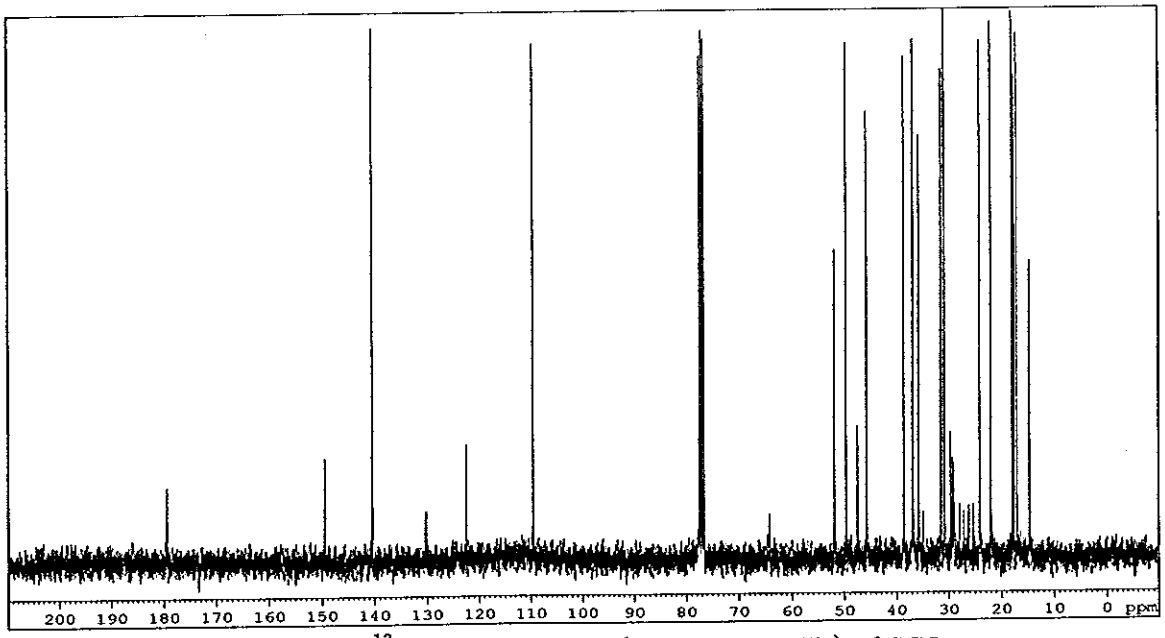

Figure 56 ^{13}C NMR Spectrum (75 MHz, $CDCl_3$) of SC8

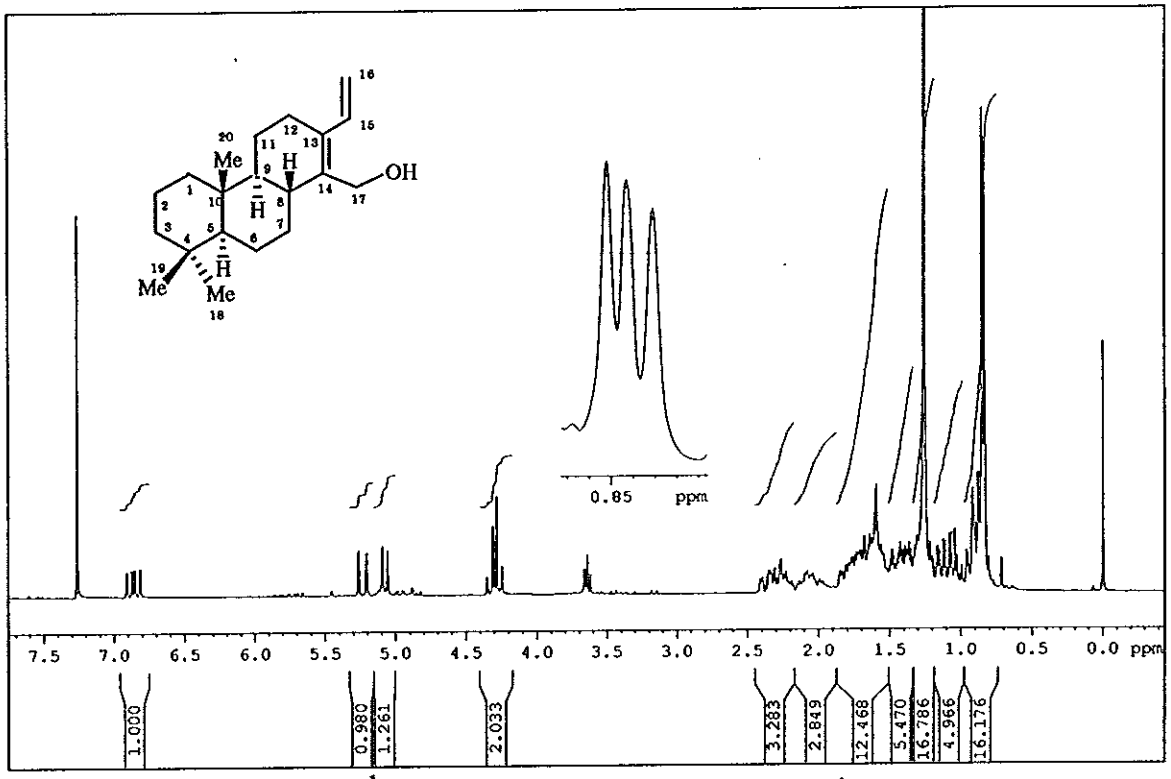

Figure 57 ^{1}H NMR Spectrum (300 MHz, $CDCl_3$) of SC9

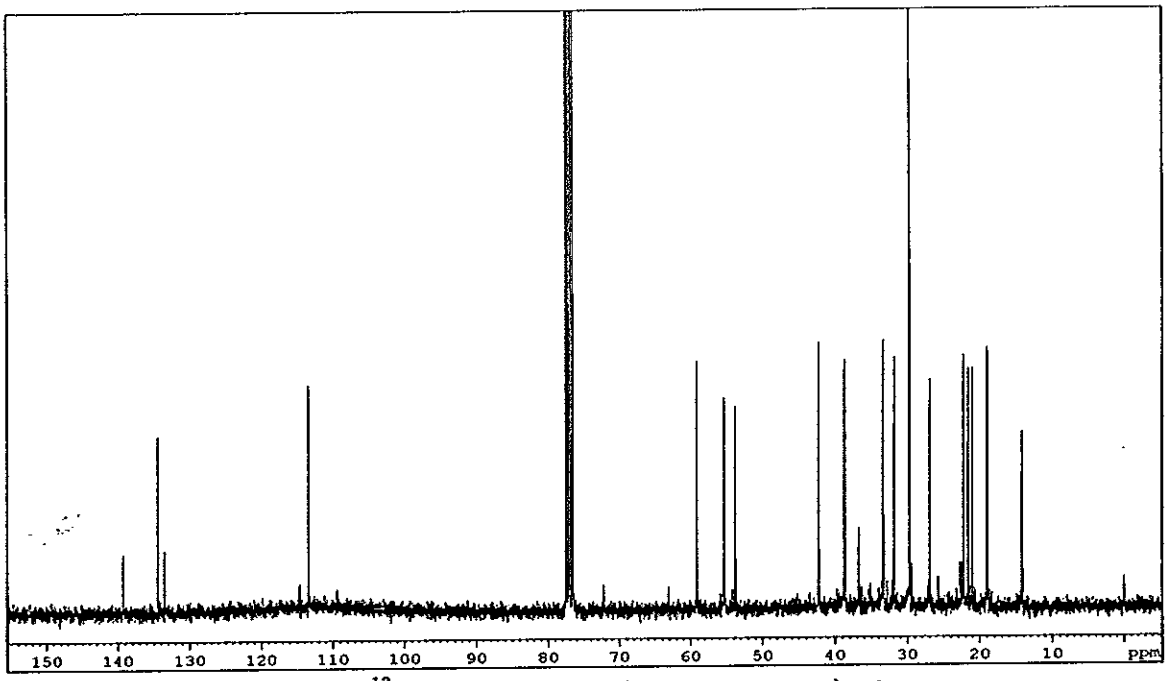

Figure 58 ^{13}C NMR Spectrum (75 MHz, $CDCl_3$) of SC9

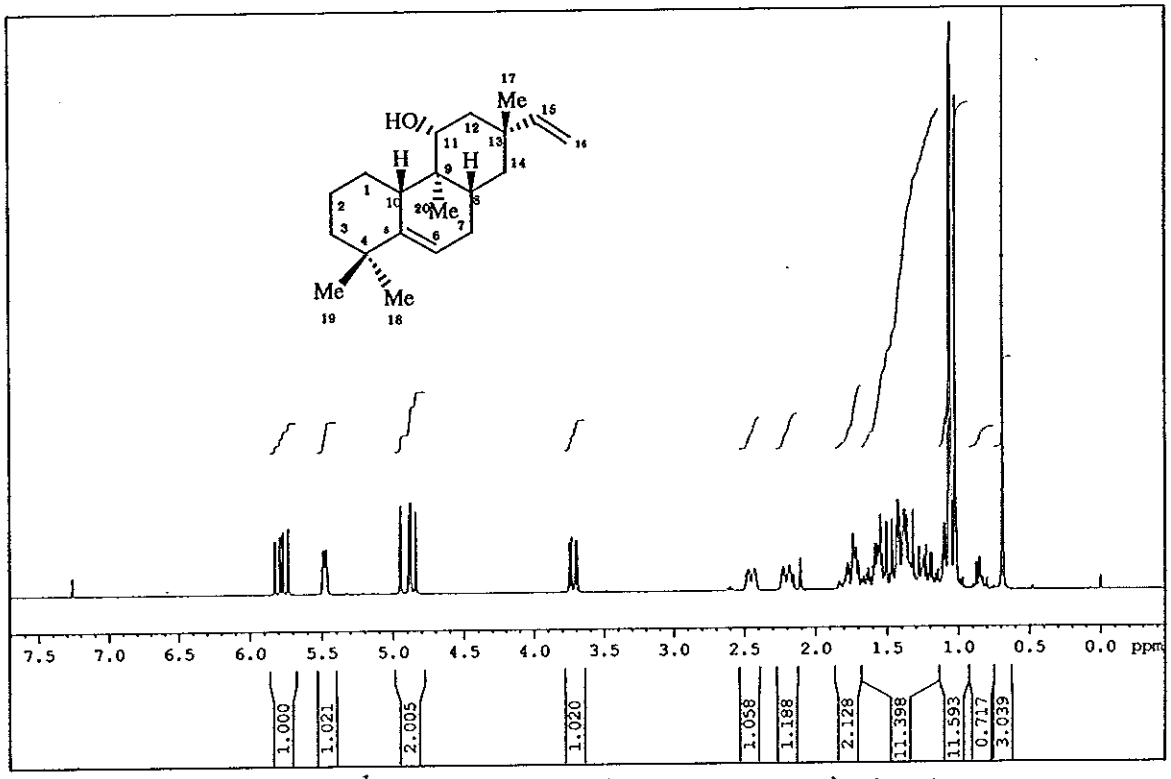

Figure 59 ^{1}H NMR Spectrum (300 MHz, $CDCl_3$) of SC10

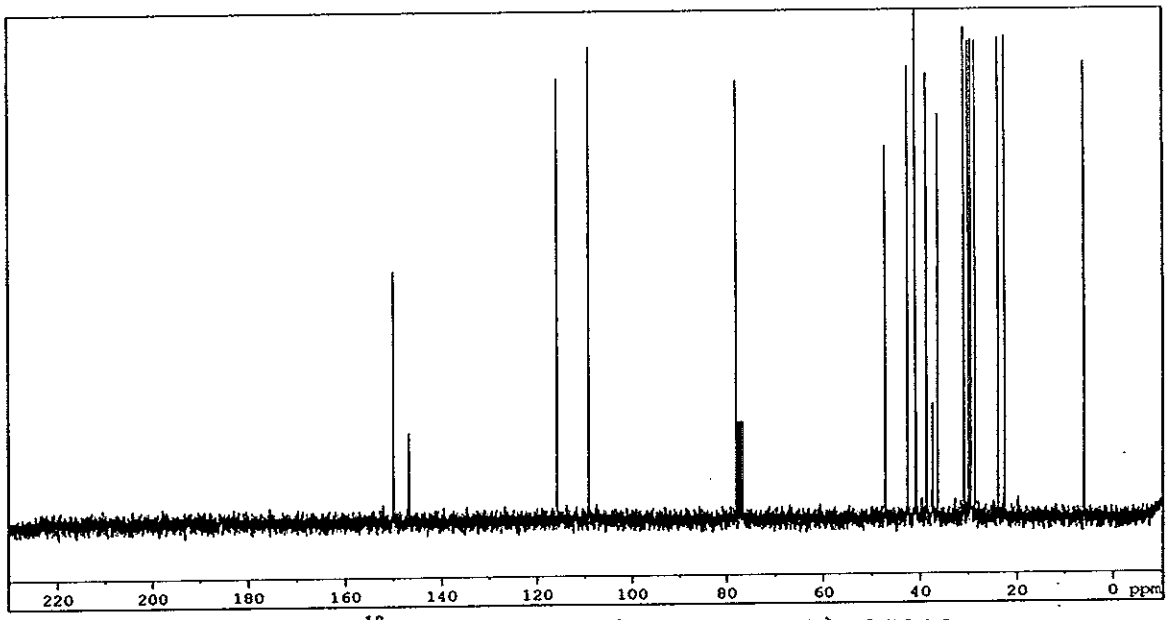

Figure 60 ^{13}C NMR Spectrum (75 MHz, $CDCl_3$) of SC10

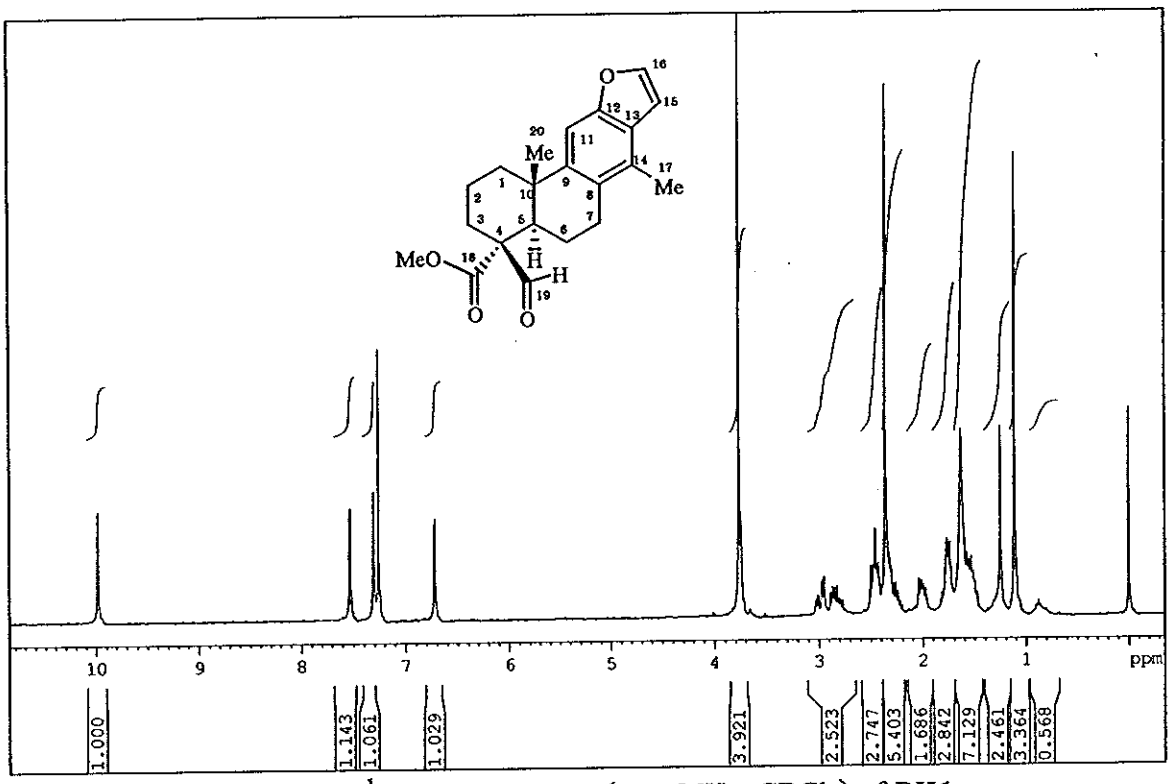

Figure 61 ^{1}H NMR Spectrum (300 MHz, $CDCl_3$) of **RH1**

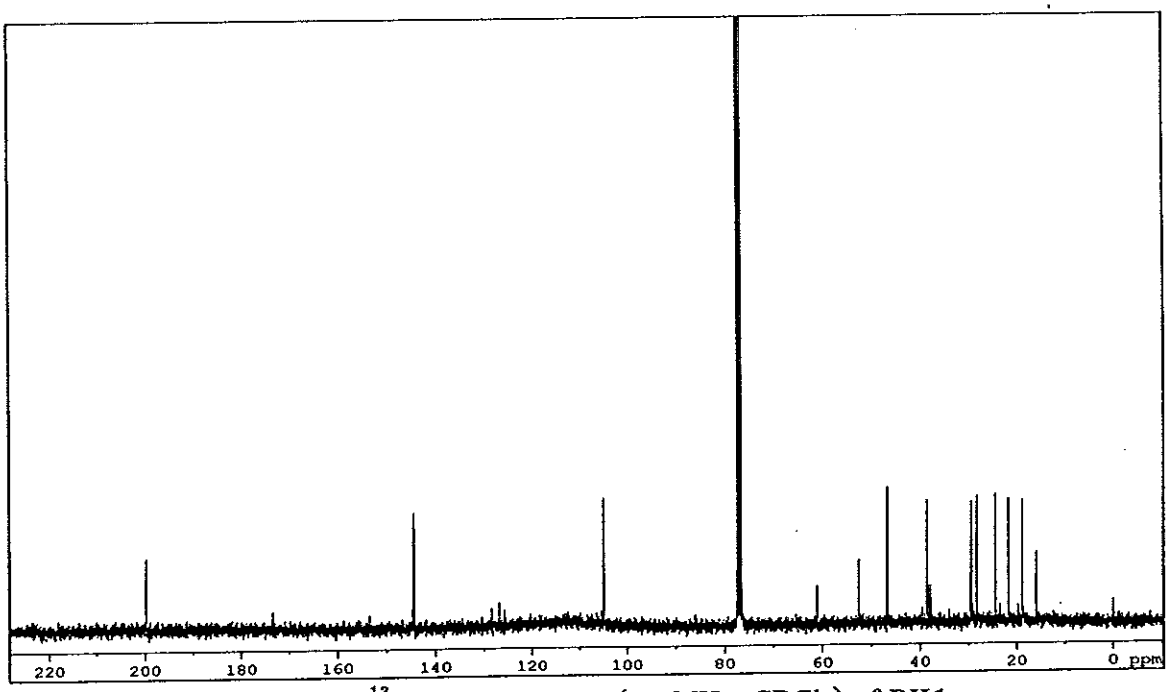

Figure 62 ^{13}C NMR Spectrum (75 MHz, $CDCl_3$) of **RH1**

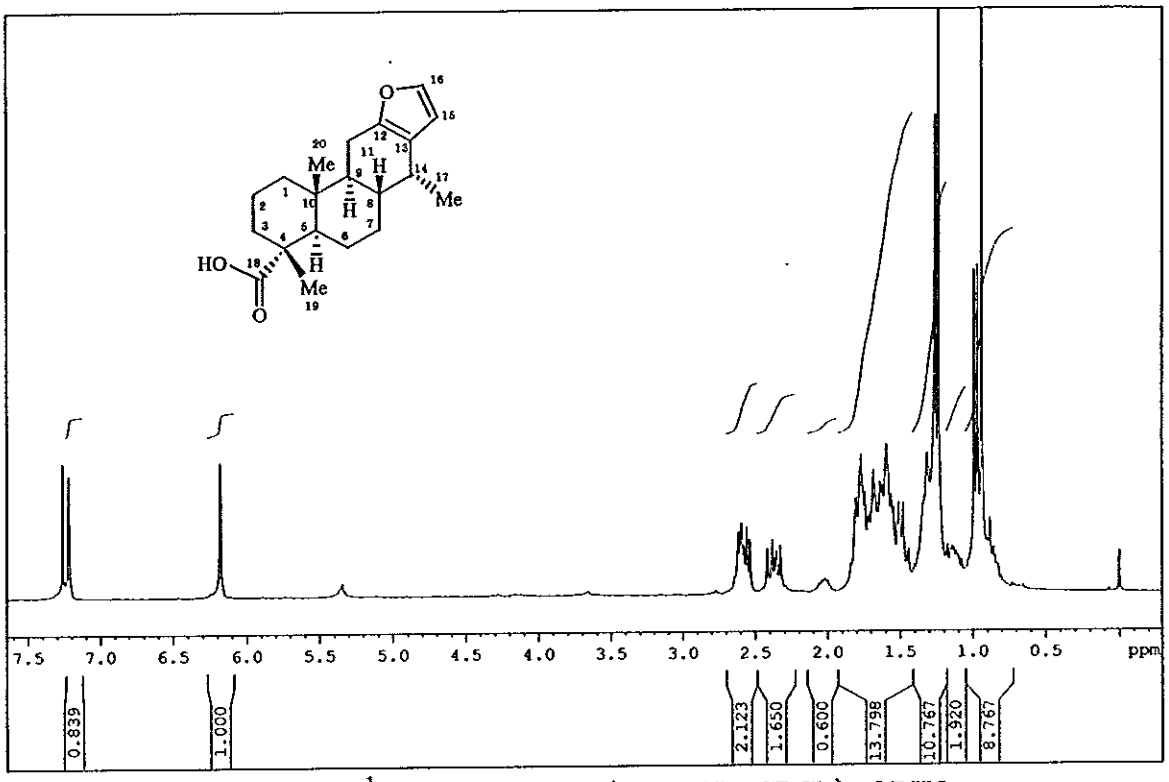

Figure 63 ^{1}H NMR Spectrum (300 MHz, $CDCl_3$) of **RH2**

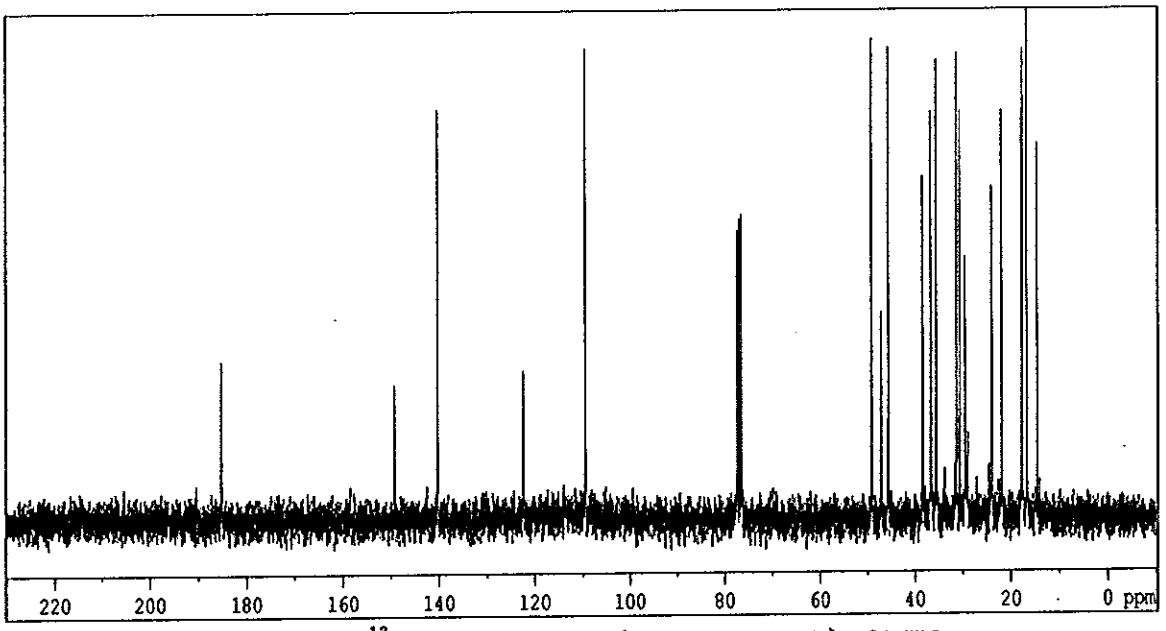

Figure 64 ^{13}C NMR Spectrum (75 MHz, $CDCl_3$) of **RH2**

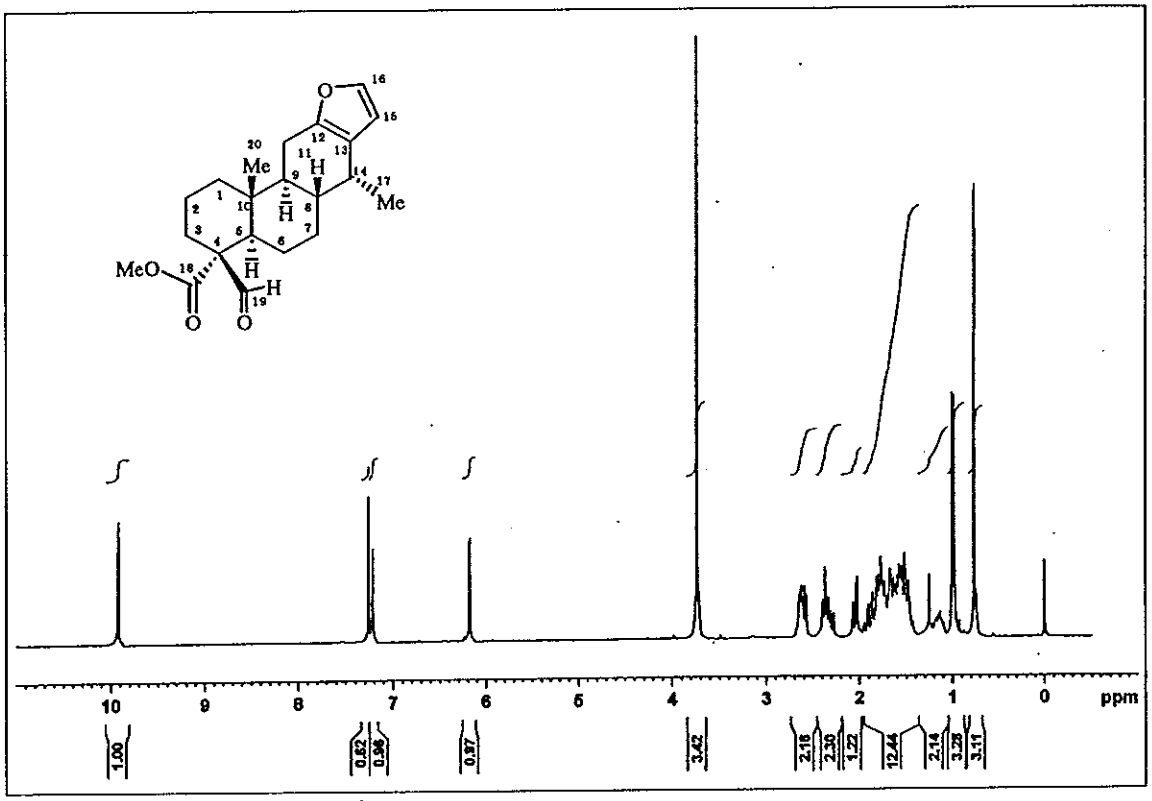

Figure 65 ^{1}H NMR Spectrum (300 MHz, $CDCl_3$) of RH3

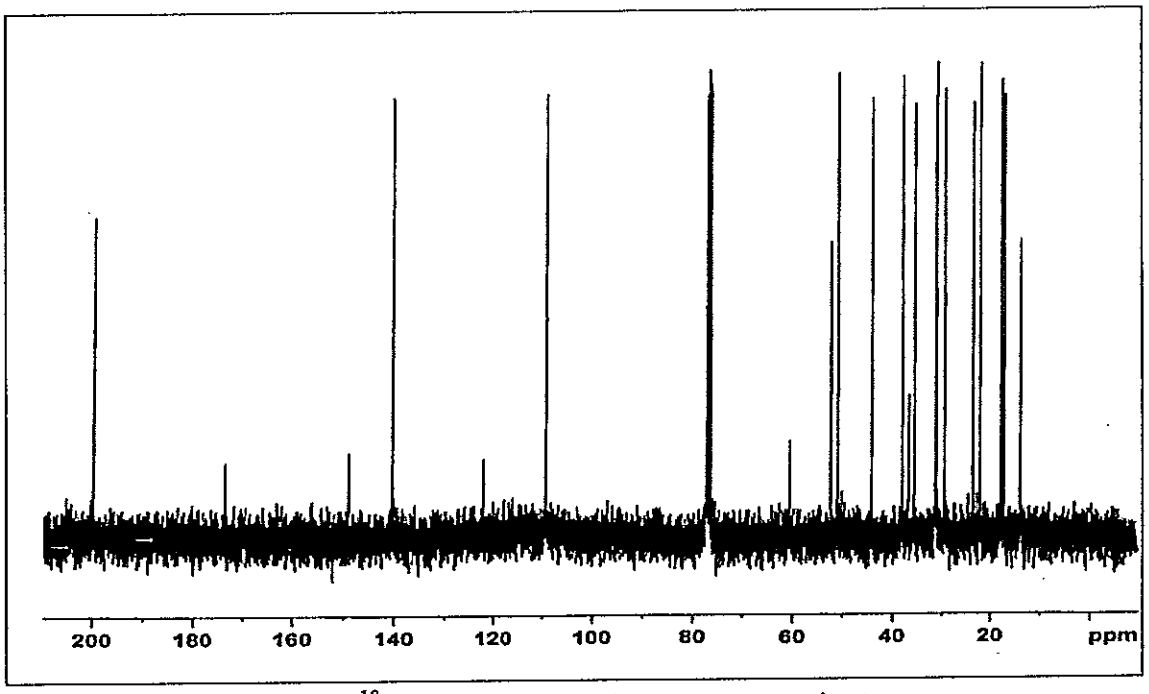

Figure 66 ^{13}C NMR Spectrum (75 MHz, $CDCl_3$) of RH3

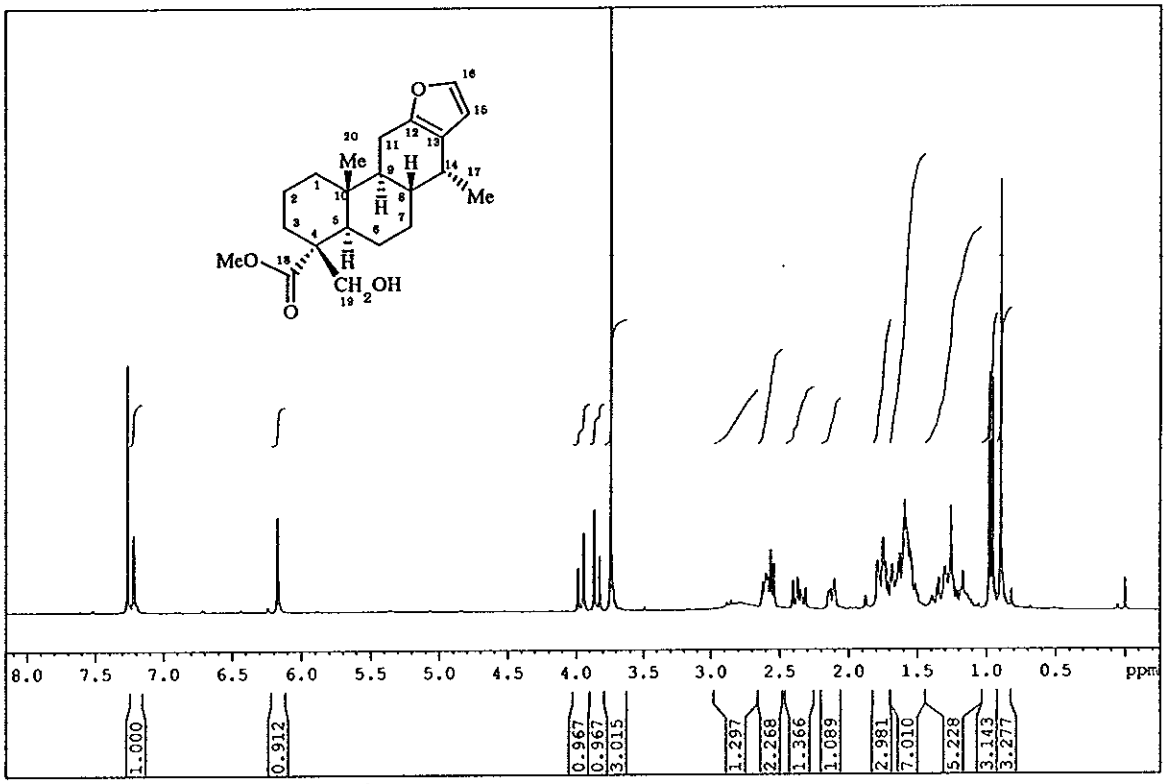

Figure 67 ^{1}H NMR Spectrum (300 MHz, $CDCl_3$) of RH4

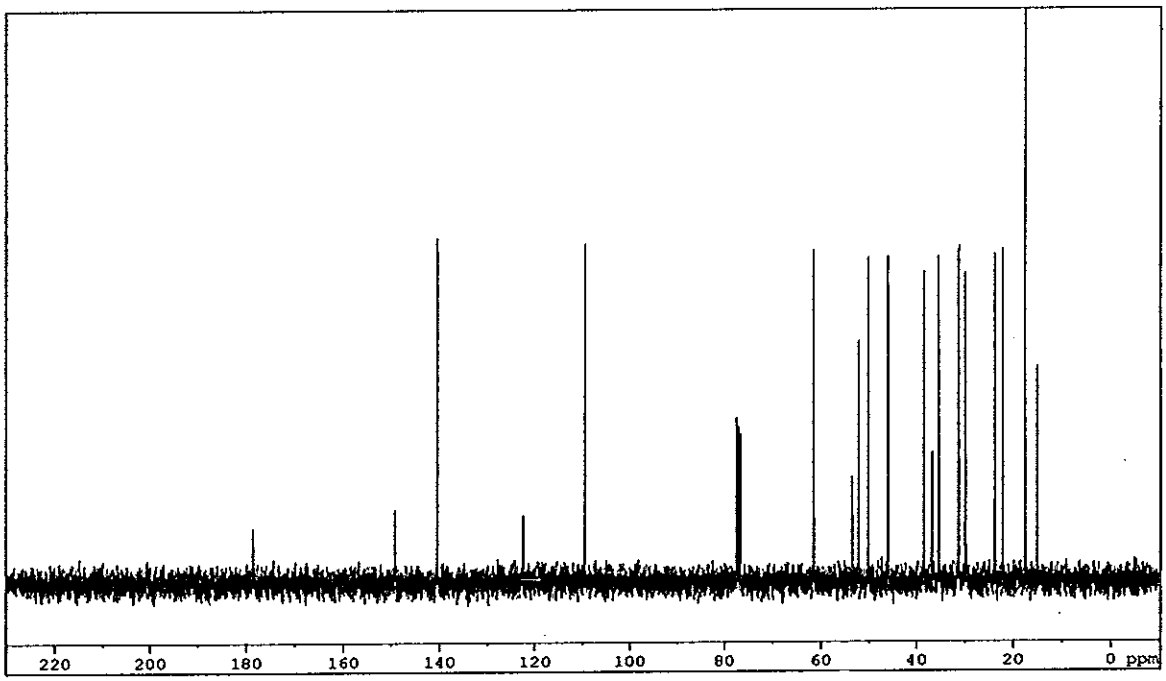

Figure 68 ^{13}C NMR Spectrum (75 MHz, $CDCl_3$) of RH4

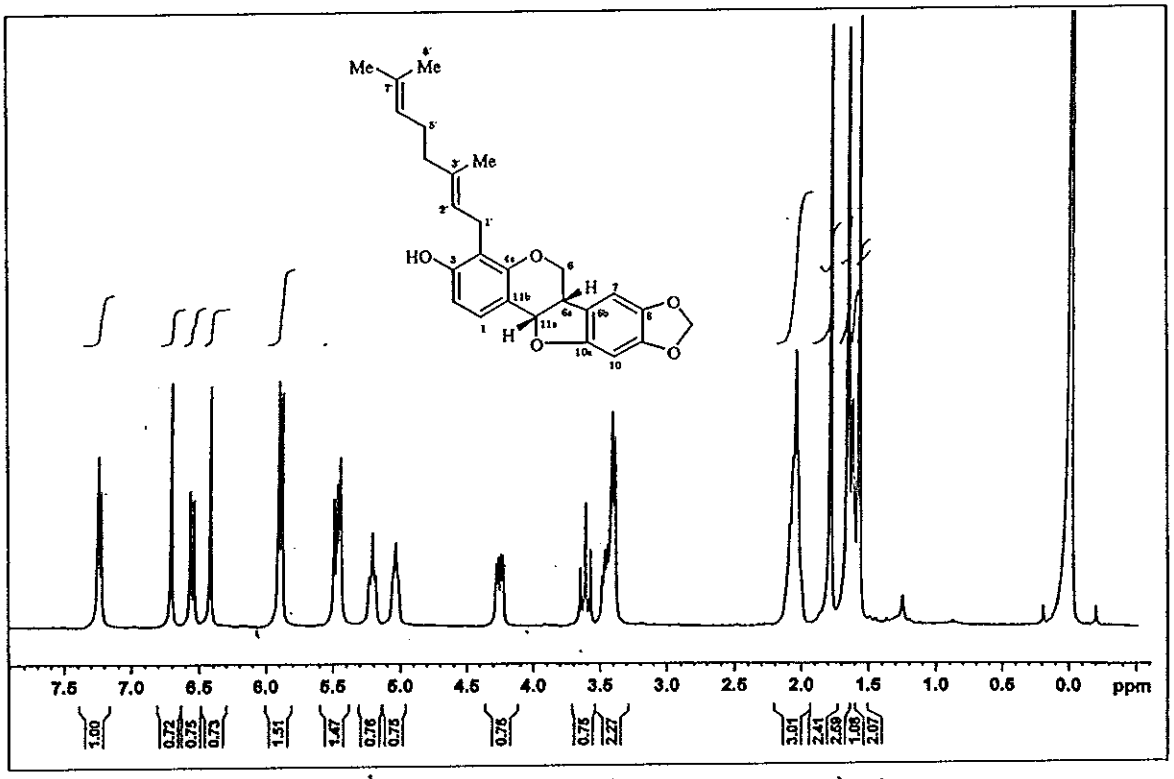

Figure 69 ^{1}H NMR Spectrum (300 MHz, $CDCl_3$) of **RH5**

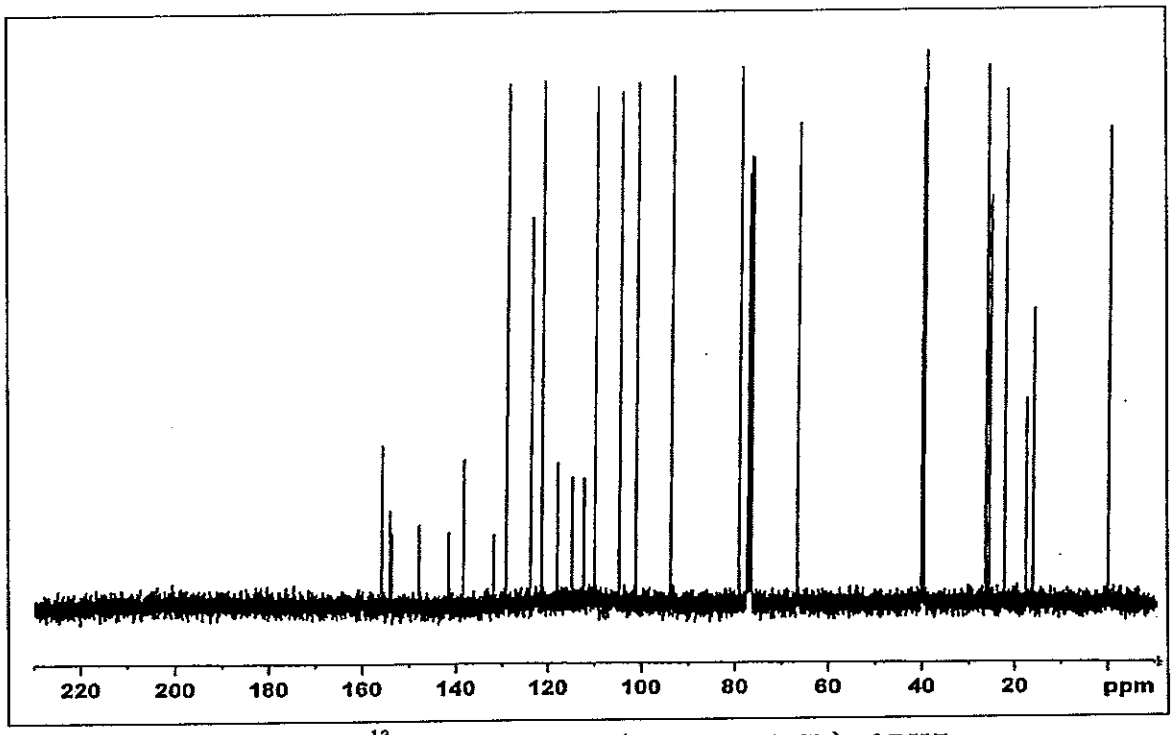

Figure 70 ^{13}C NMR Spectrum (75 MHz, $CDCl_3$) of **RH5**

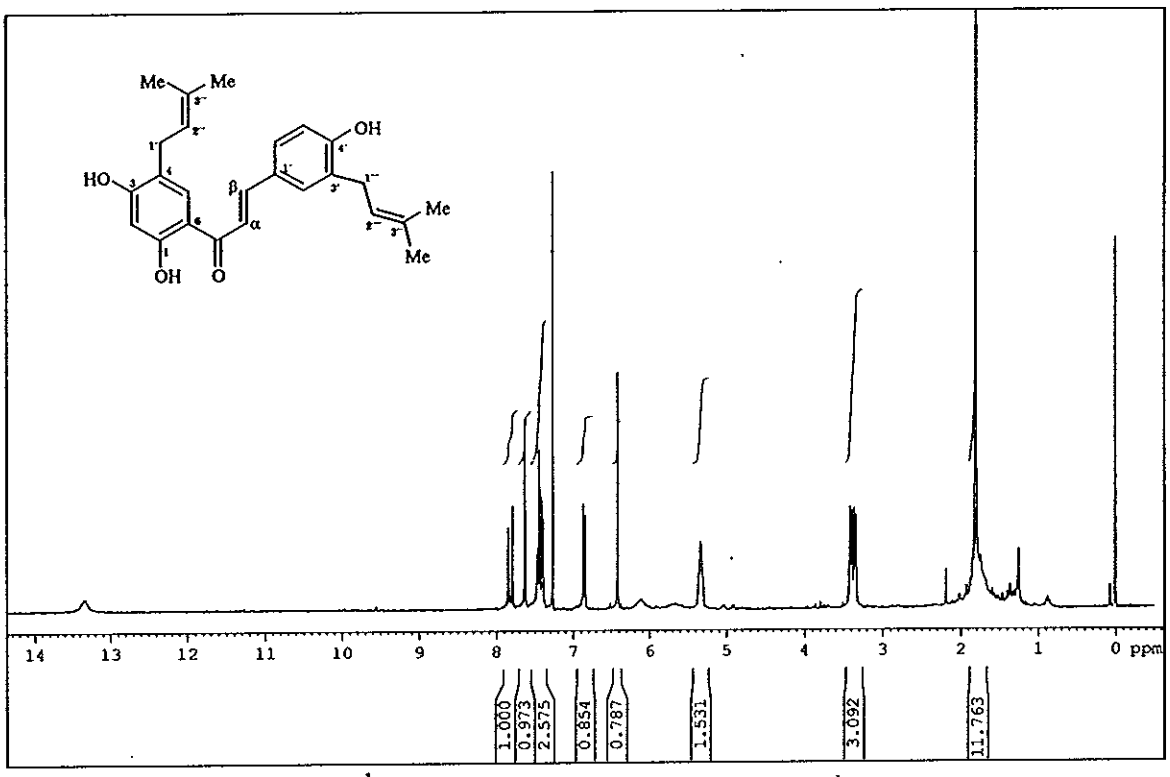

Figure 71 ^{1}H NMR Spectrum (300 MHz, $CDCl_3$) of **RH6**

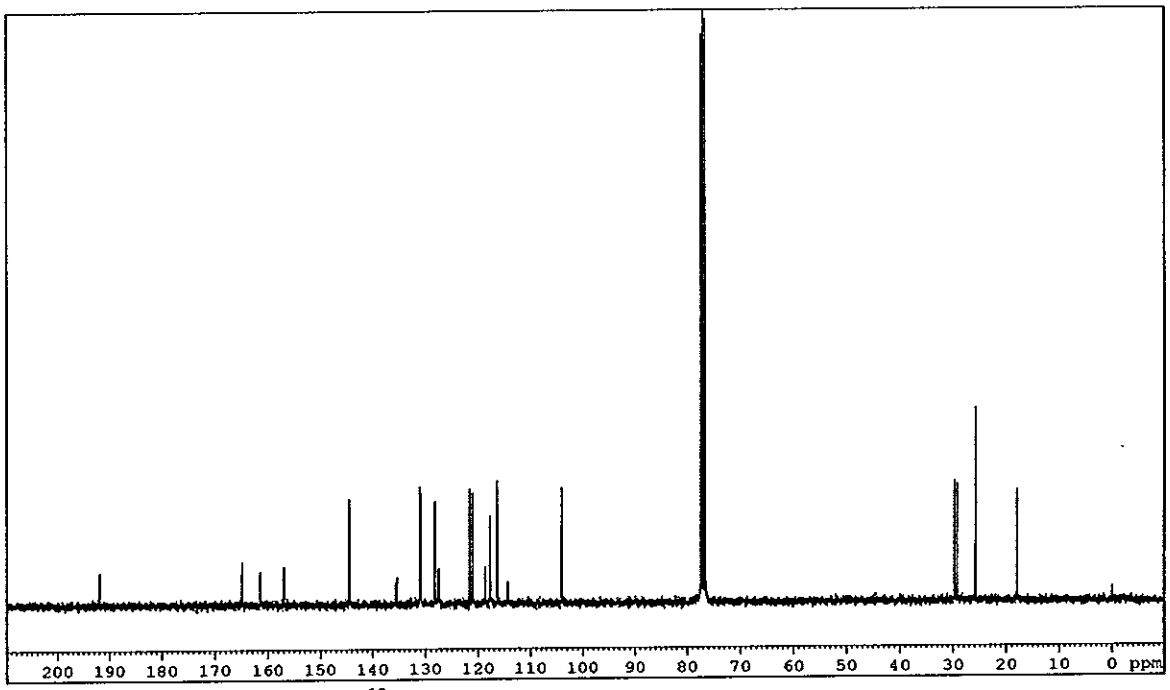

Figure 72 ^{13}C NMR Spectrum (75 MHz, $CDCl_3$) of **RH6**

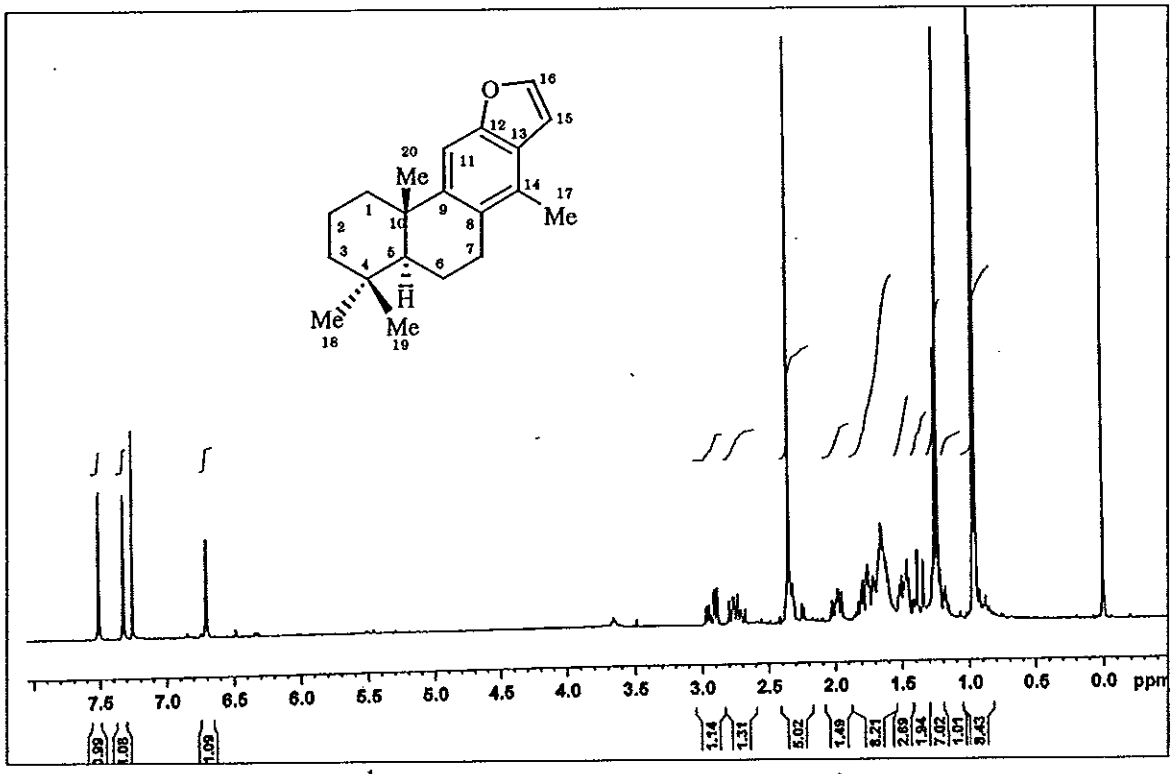

Figure 73 ^{1}H NMR Spectrum (300 MHz, $CDCl_3$) of SD1

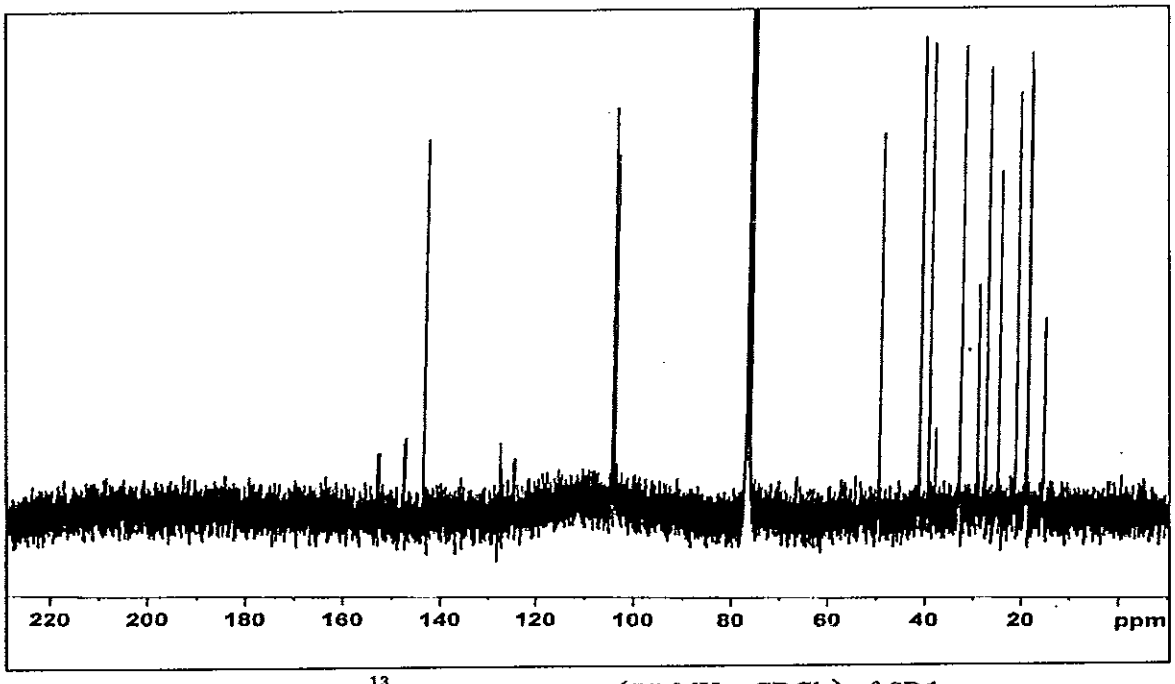

Figure 74 ^{13}C NMR Spectrum (75 MHz, $CDCl_3$) of SD1

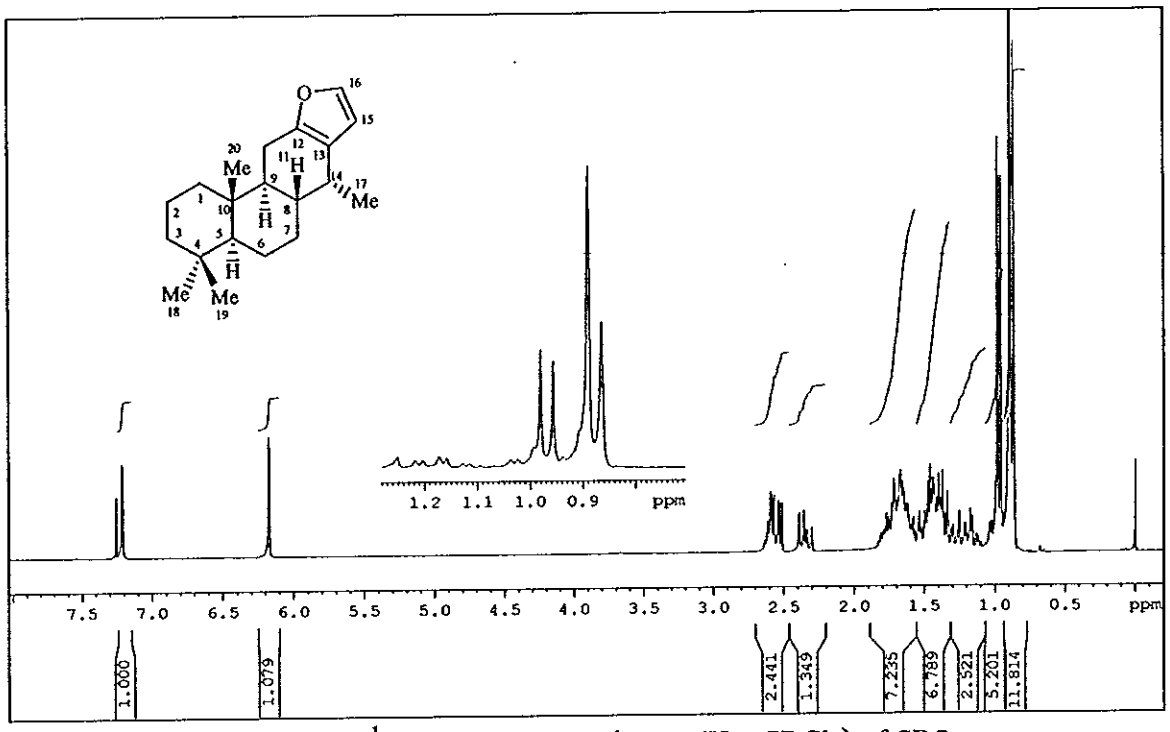

Figure 75 ^{1}H NMR Spectrum (300 MHz, $CDCl_3$) of SD2

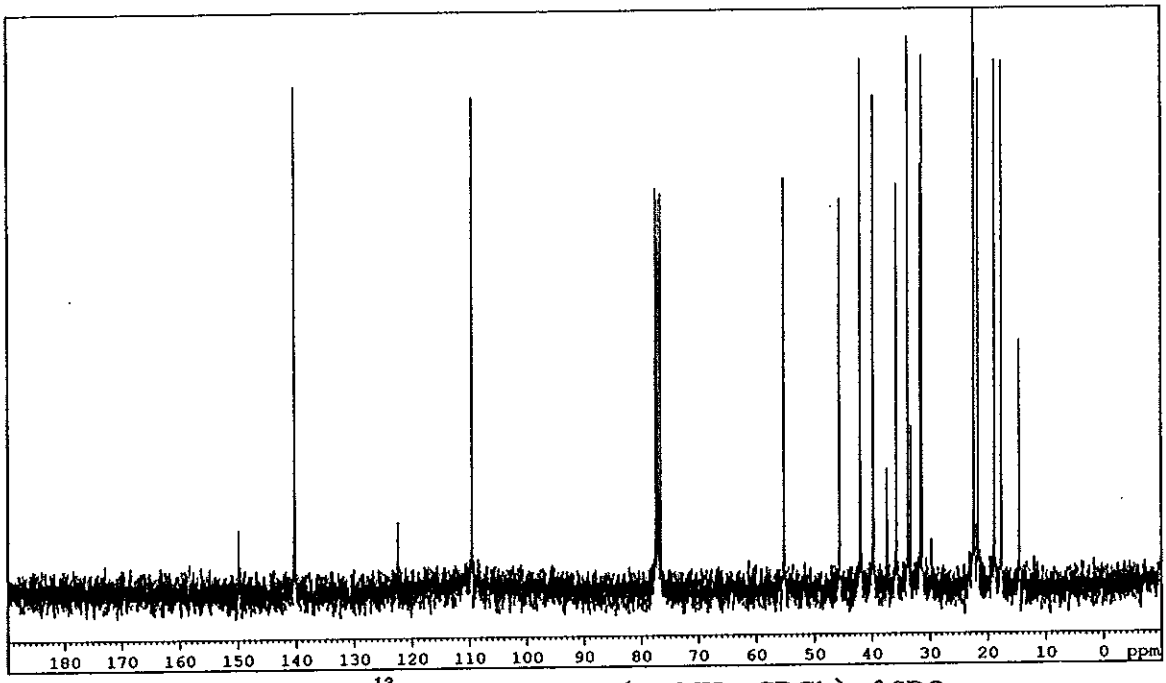

Figure 76 ^{13}C NMR Spectrum (75 MHz, $CDCl_3$) of SD2

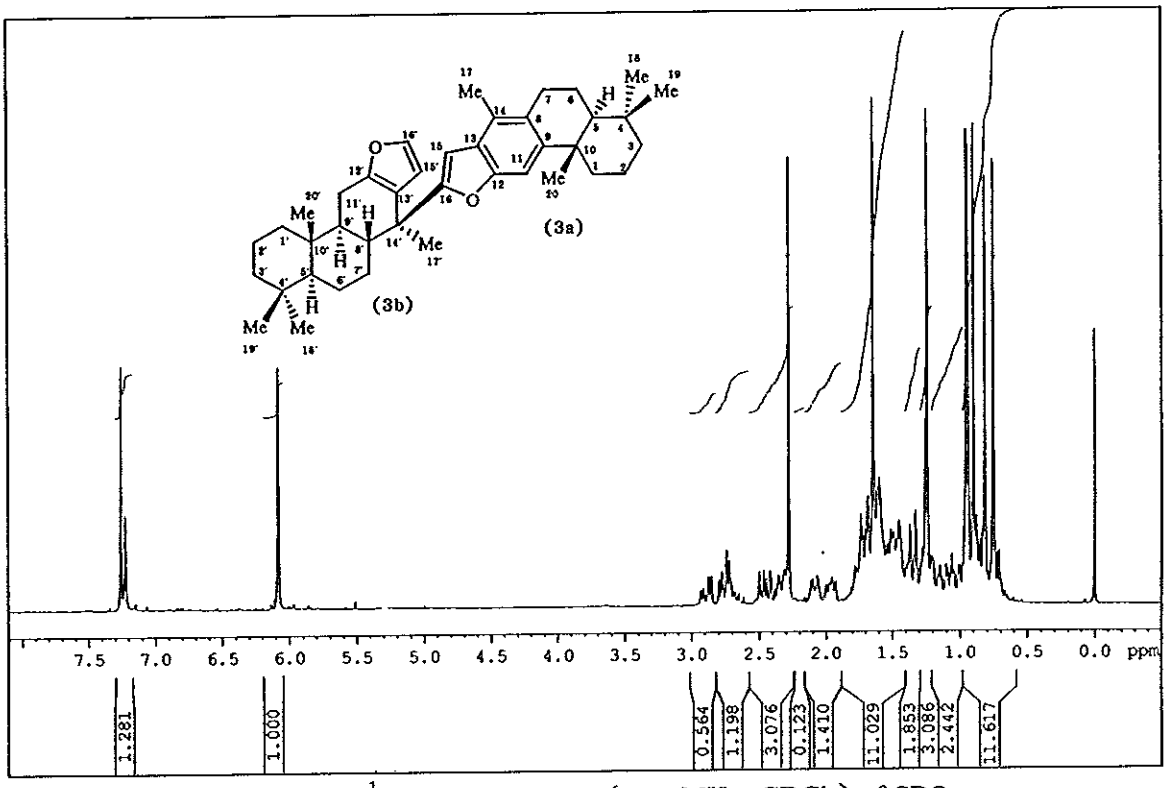

Figure 77 ^{1}H NMR Spectrum (300 MHz, $CDCl_3$) of SD3

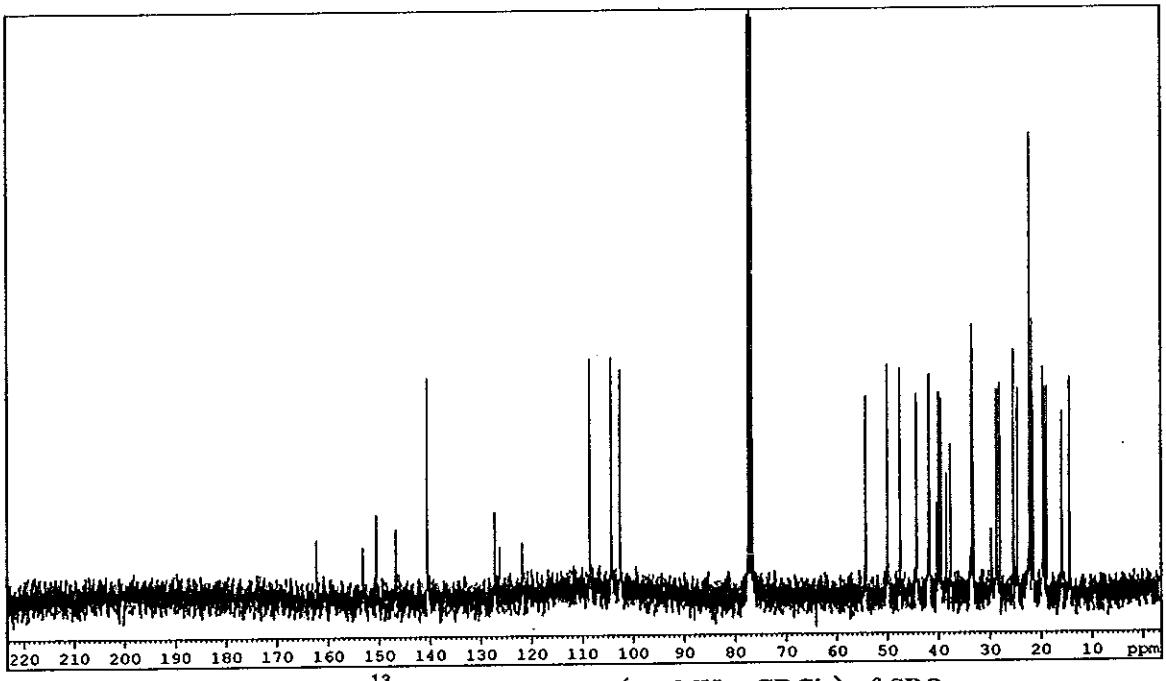

Figure 78 ^{13}C NMR Spectrum (75 MHz, $CDCl_3$) of SD3

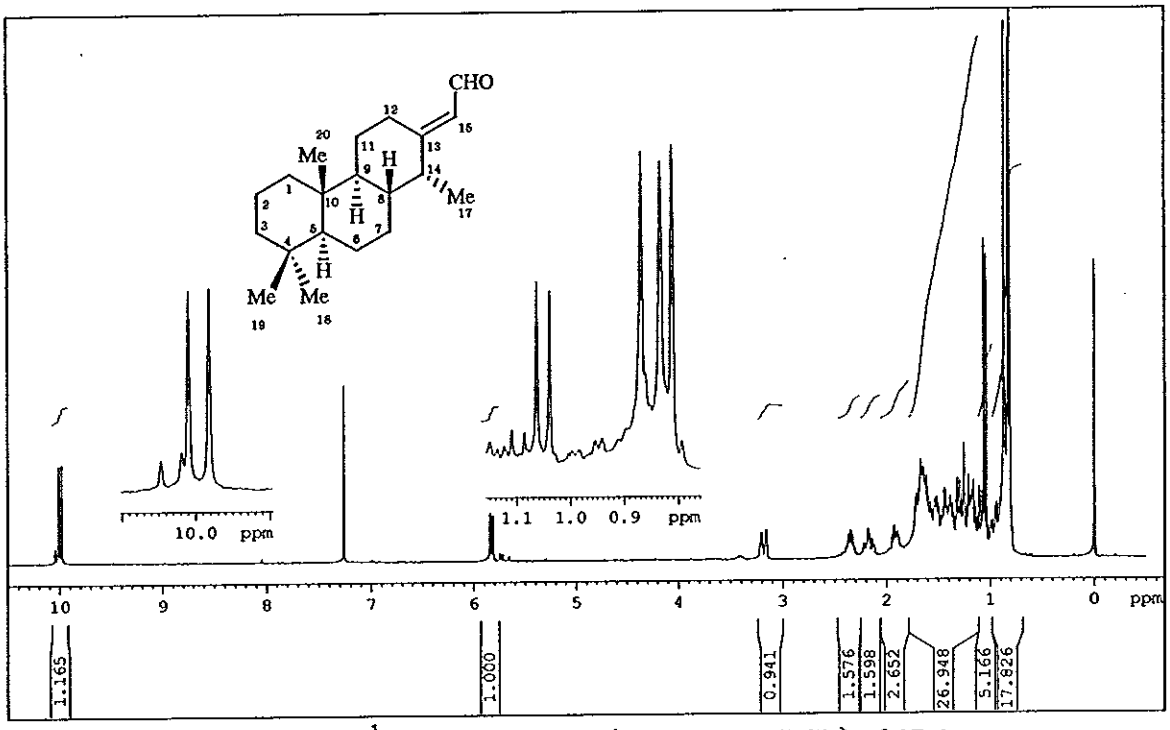

Figure 79 ^{1}H NMR Spectrum (300 MHz, $CDCl_3$) of SD4

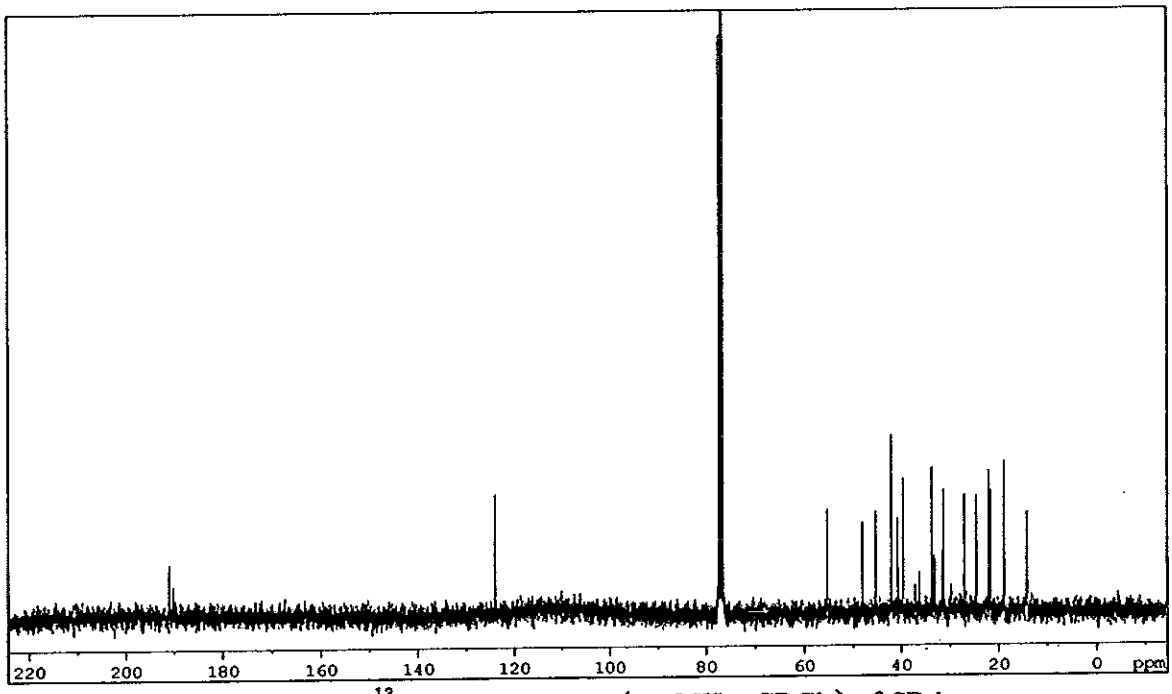

Figure 80 ^{13}C NMR Spectrum (75 MHz, $CDCl_3$) of SD4

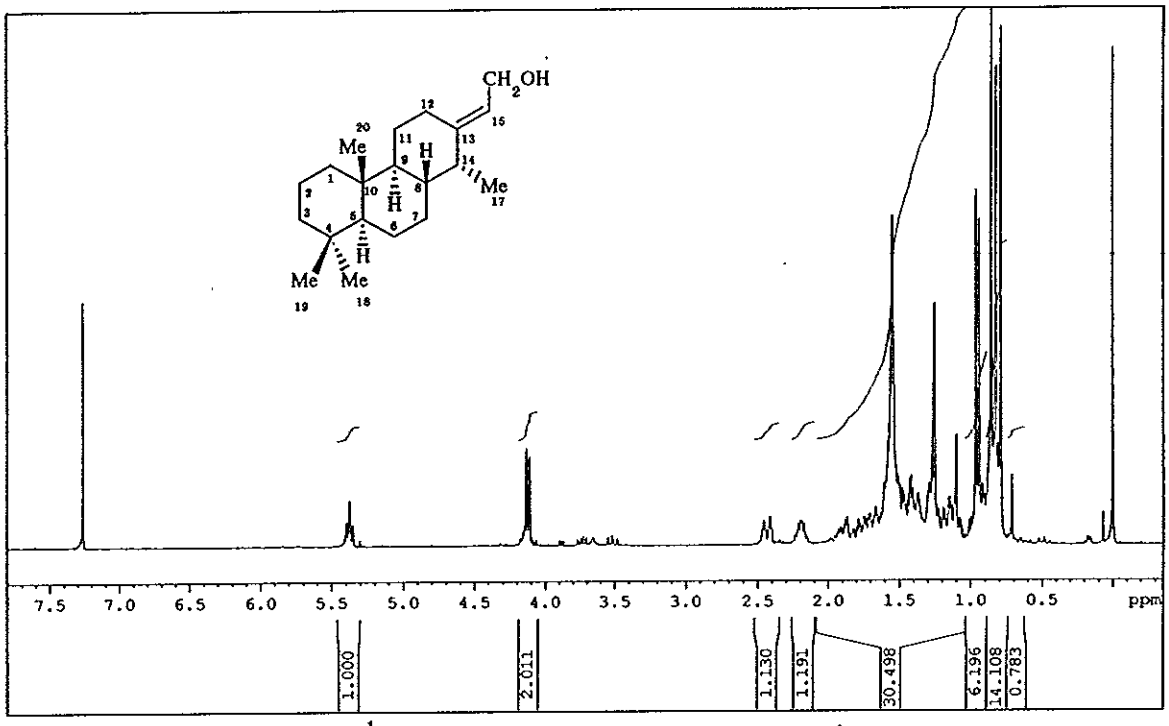

Figure 81 ^{1}H NMR Spectrum (300 MHz, $CDCl_3$) of SD5

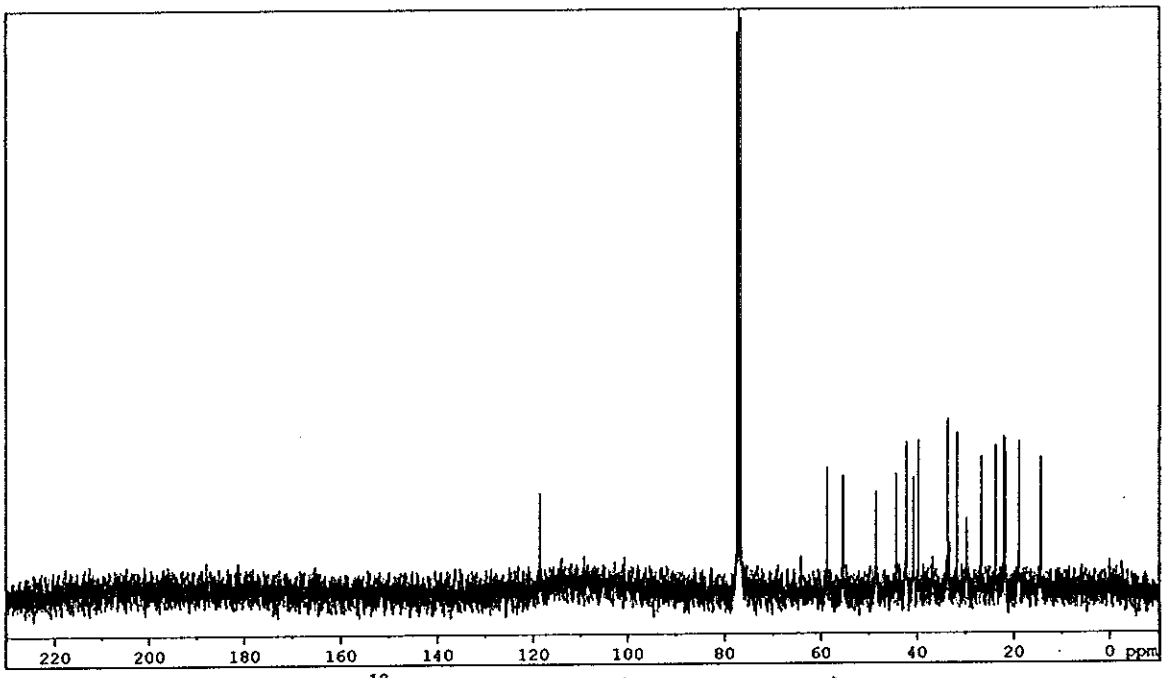

Figure 82 ^{13}C NMR Spectrum (75 MHz, $CDCl_3$) of SD5

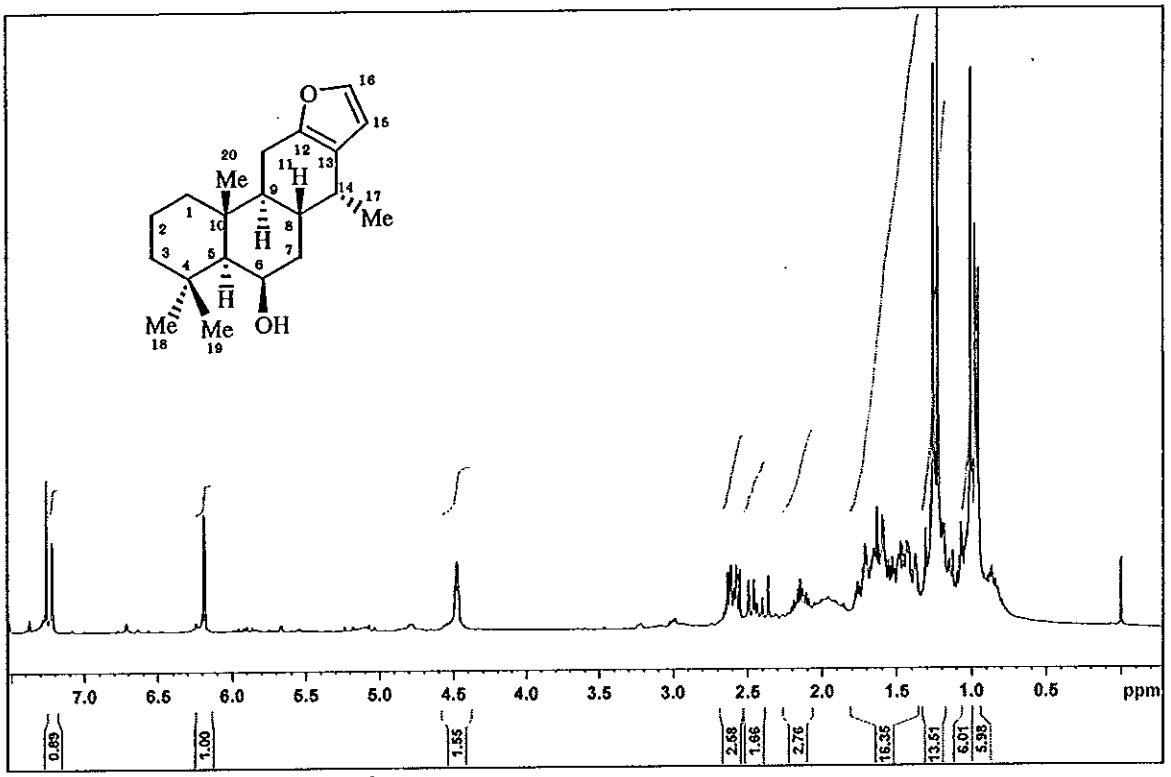

Figure 83 ^{1}H NMR Spectrum (300 MHz, $CDCl_3$) of SD6

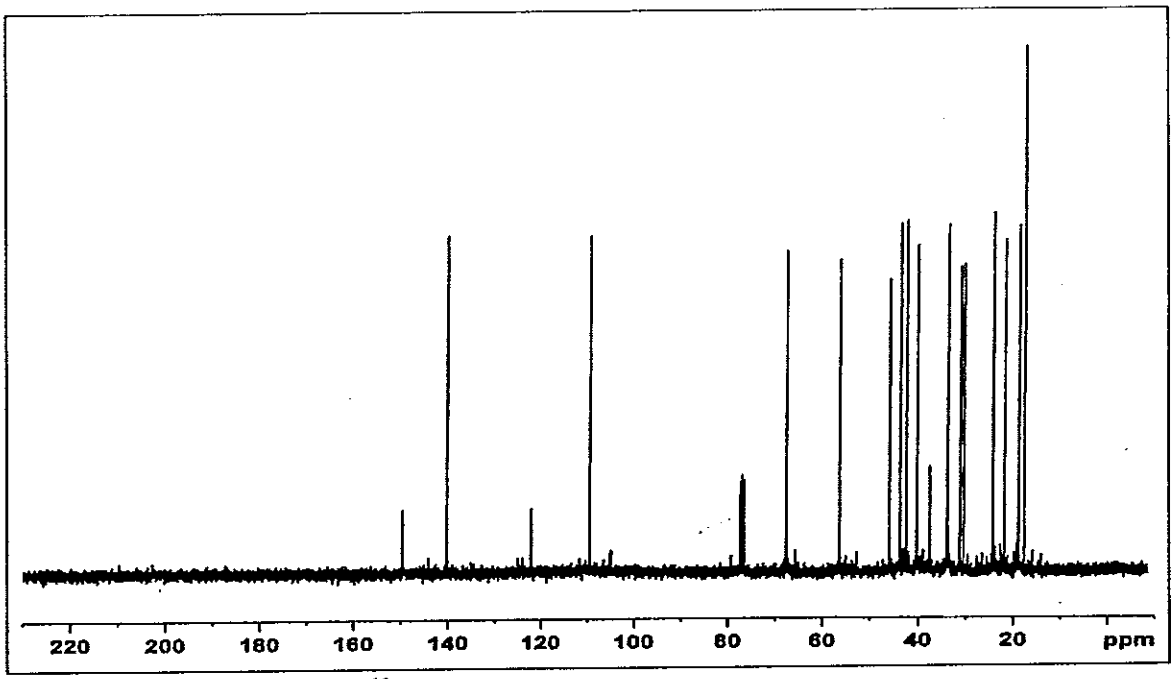

Figure 84 ^{13}C NMR Spectrum (75 MHz, $CDCl_3$) of SD6

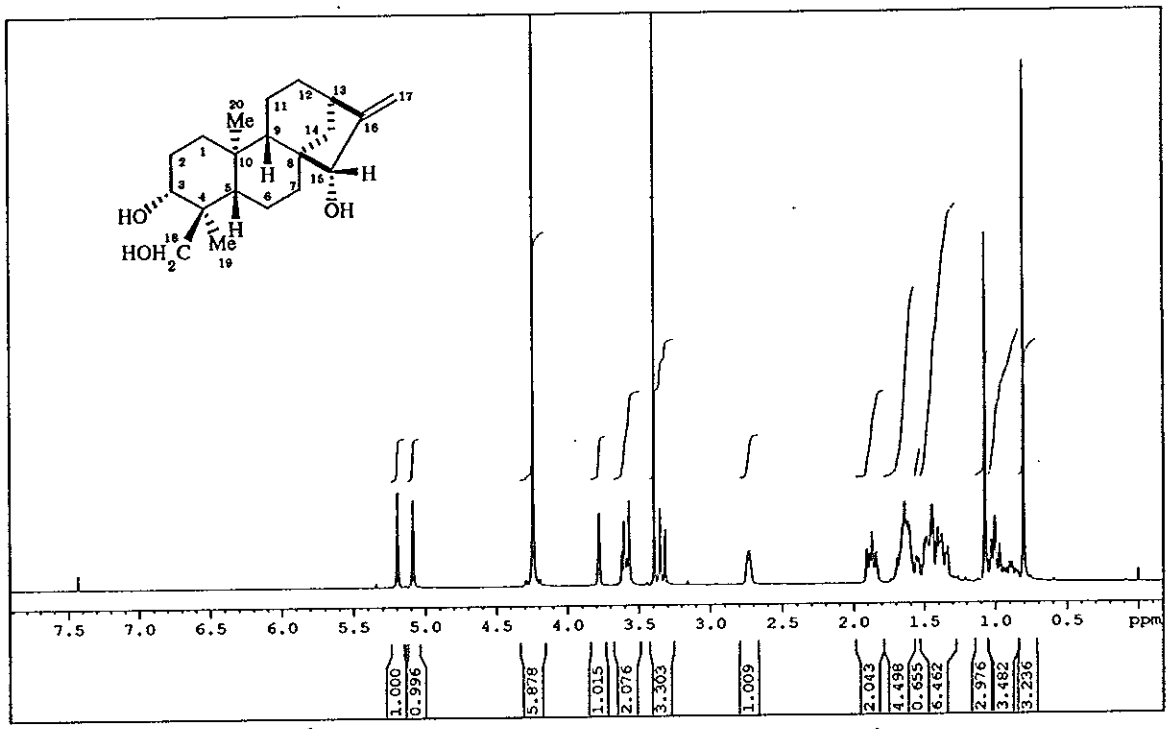

Figure 85 ^{1}H NMR Spectrum (300 MHz, $CDCl_3$+MeOD) of BMC1

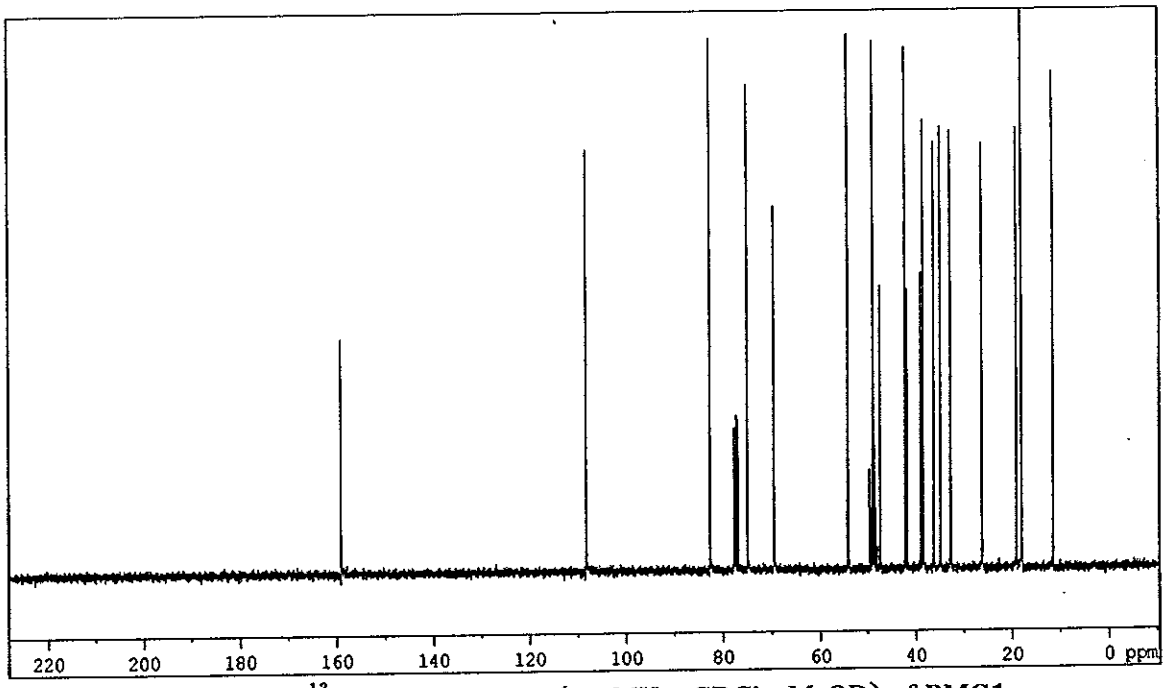

Figure 86 ^{13}C NMR Spectrum (75 MHz, $CDCl_3$+MeOD) of BMC1

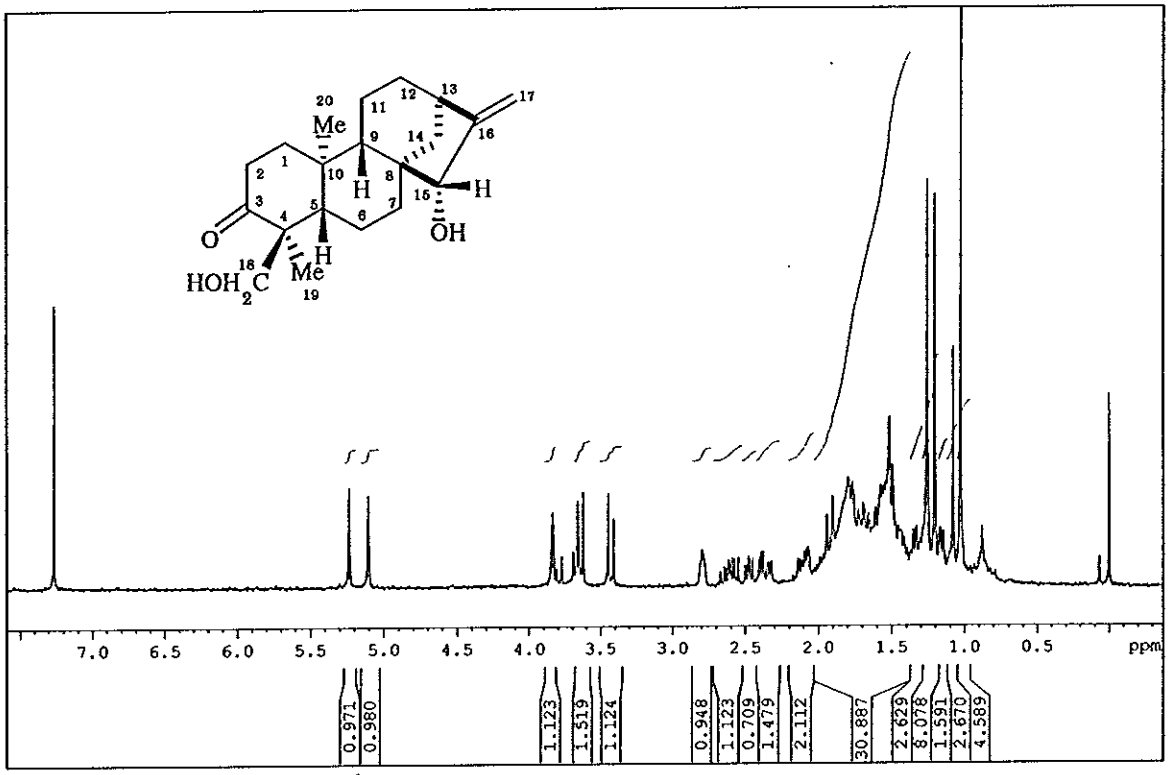

Figure 87 ^{1}H NMR Spectrum (300 MHz, $CDCl_3$) of BMC2

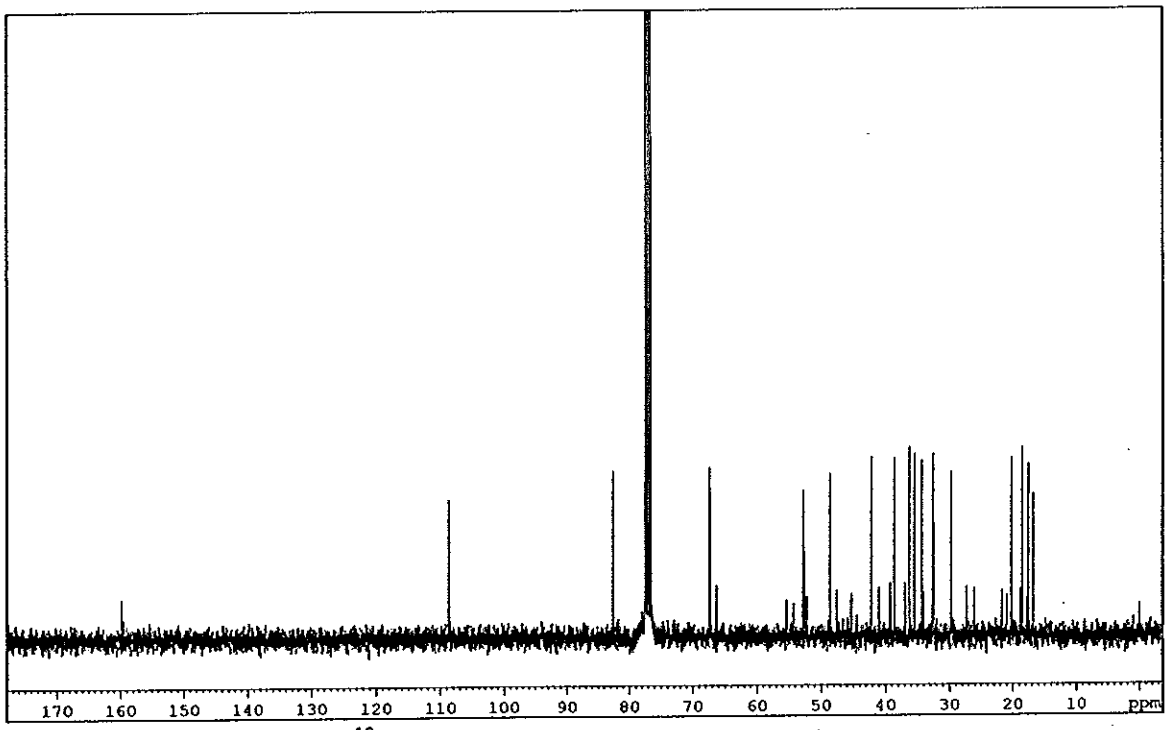

Figure 88 ^{13}C NMR Spectrum (75 MHz, $CDCl_3$) of BMC2

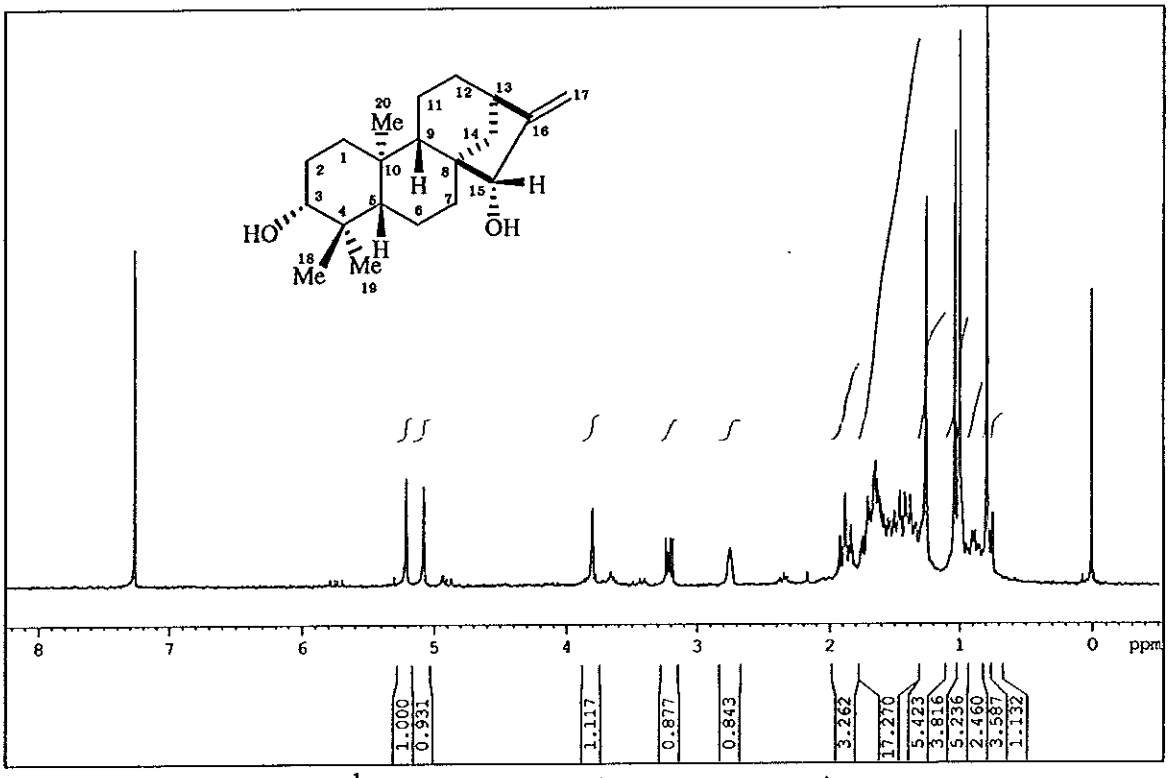

Figure 89 ^{1}H NMR Spectrum (300 MHz, $CDCl_3$) of BMC3

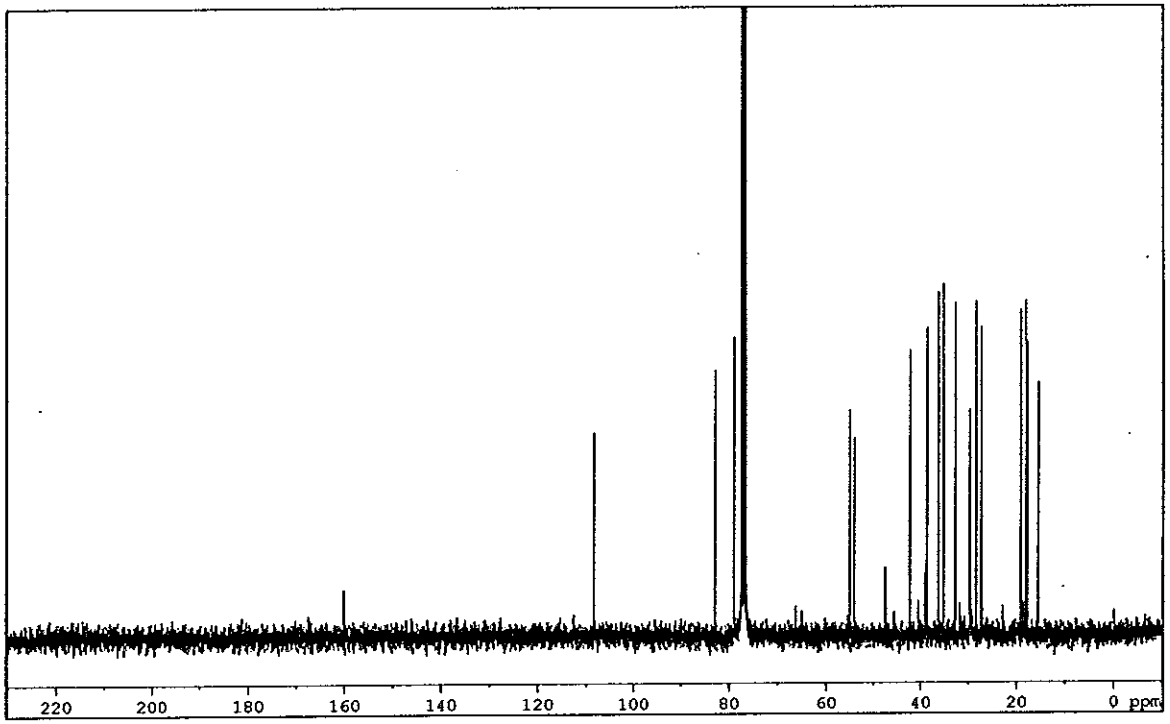

Figure 90 ^{13}C NMR Spectrum (75 MHz, $CDCl_3$) of BMC3

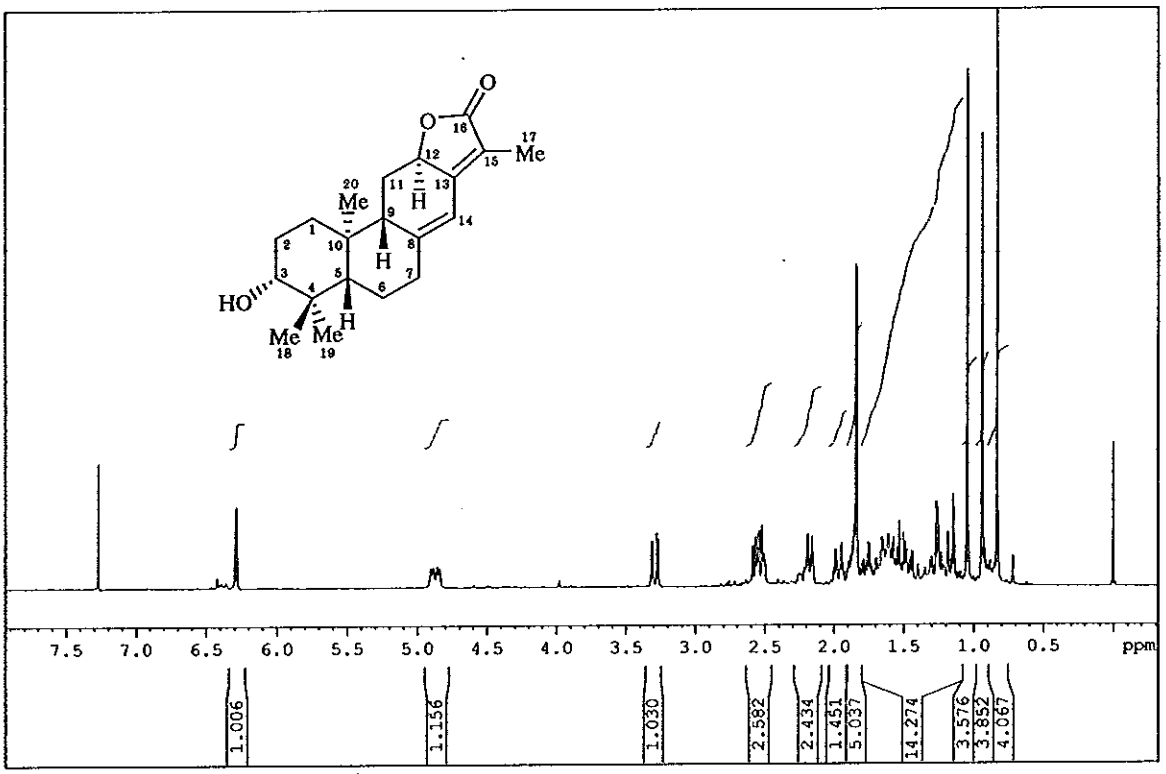

Figure 93 ^{1}H NMR Spectrum (300 MHz, $CDCl_3$) of BMC5

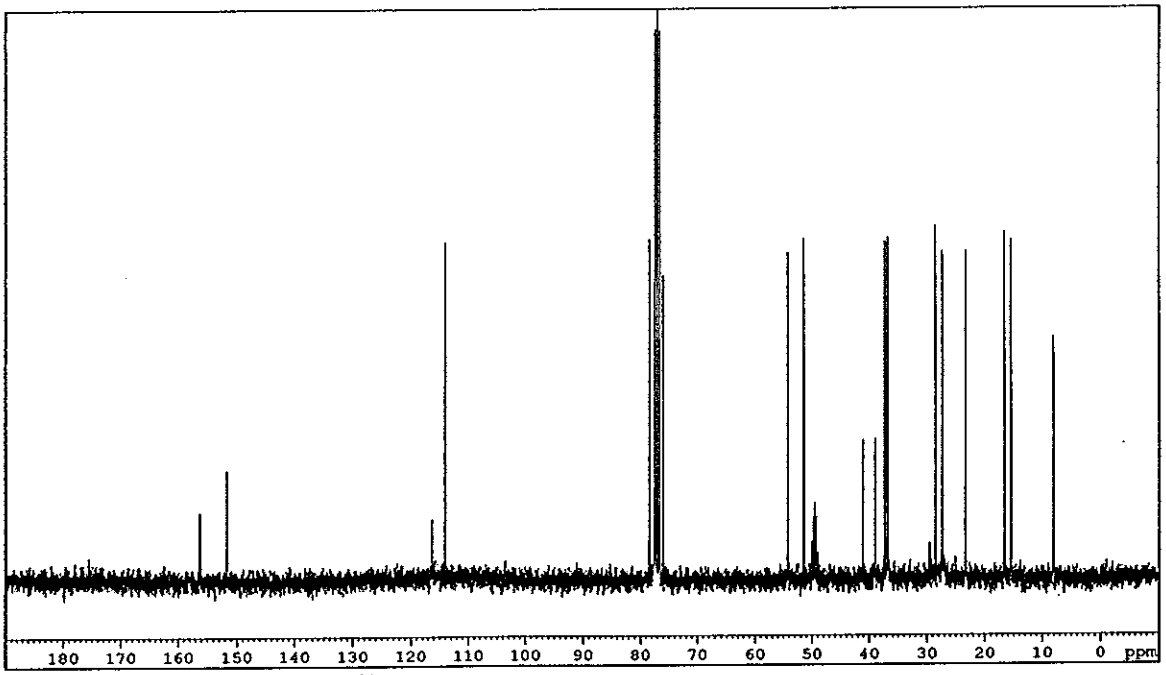

Figure 94 ^{13}C NMR Spectrum (75 MHz, $CDCl_3$) of BMC5

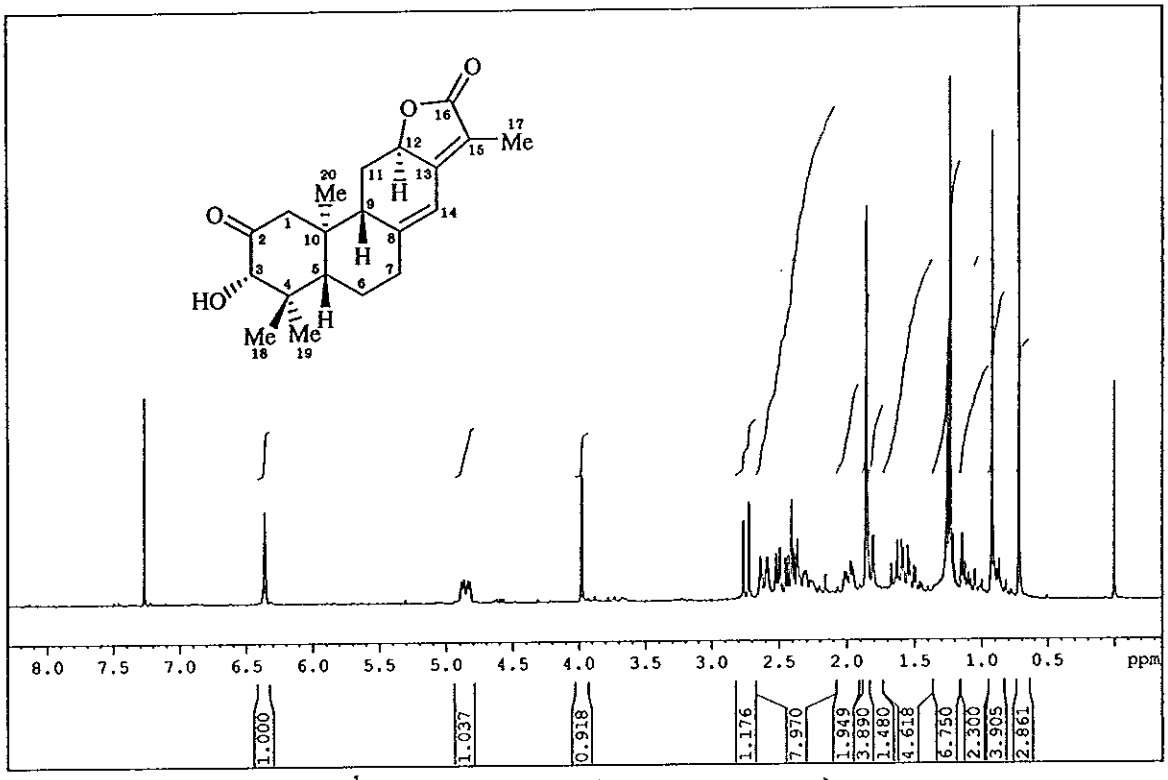

Figure 95 ^{1}H NMR Spectrum (300 MHz, $CDCl_3$) of BMC6

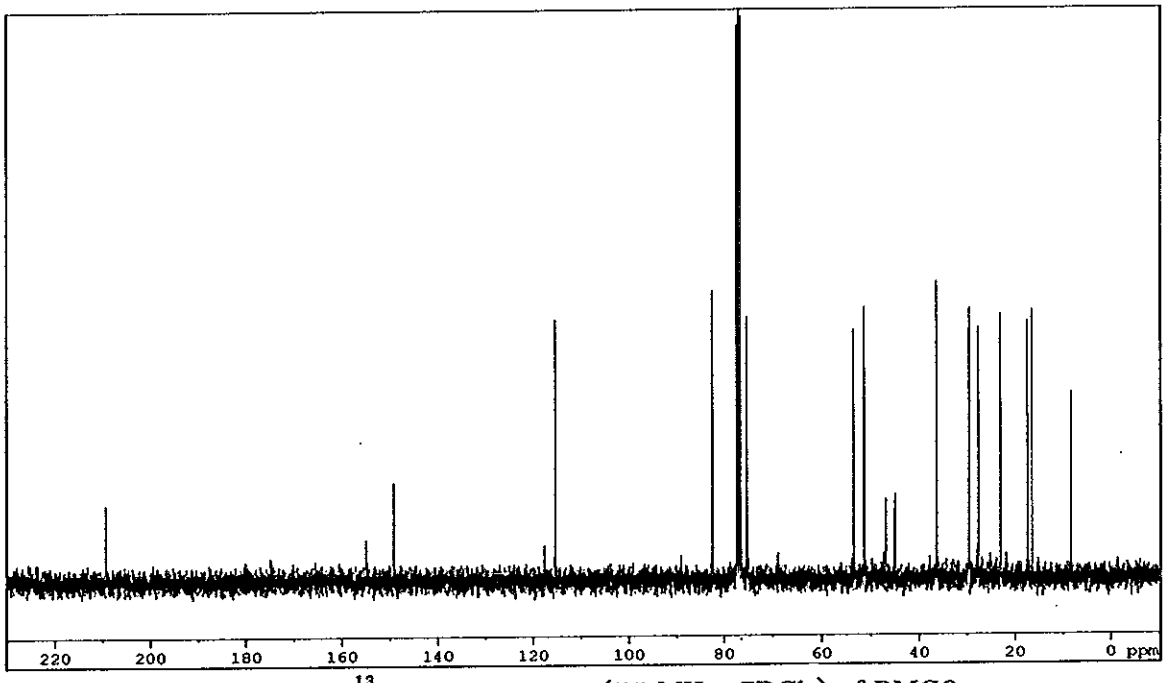

Figure 96 ^{13}C NMR Spectrum (75 MHz, $CDCl_3$) of BMC6

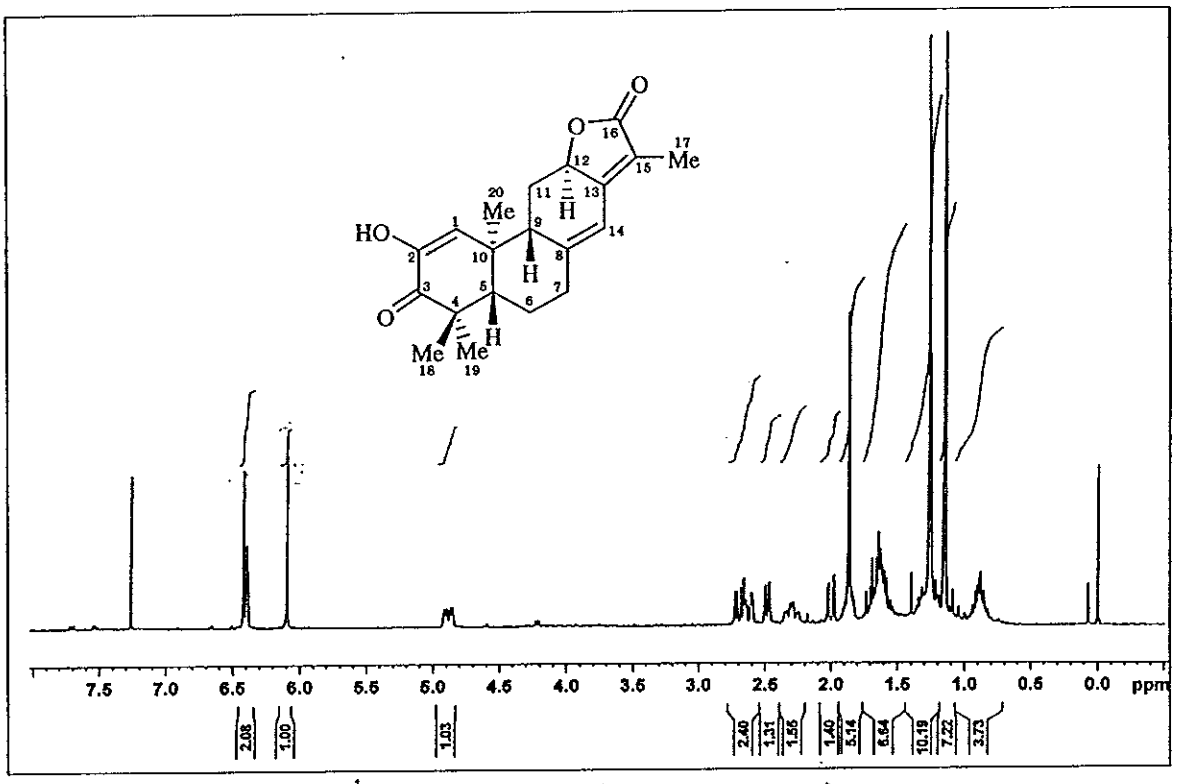

Figure 97 ^{1}H NMR Spectrum (300 MHz, $CDCl_3$) of BMC7

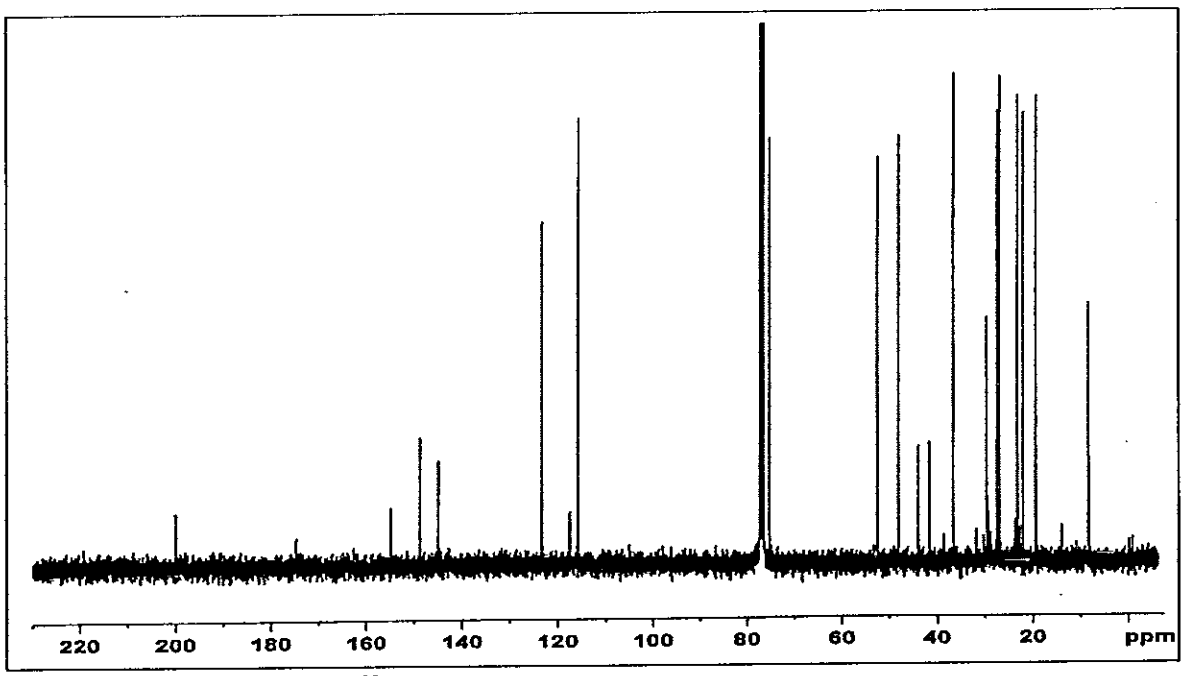

Figure 98 ^{13}C NMR Spectrum (75 MHz, $CDCl_3$) of BMC7

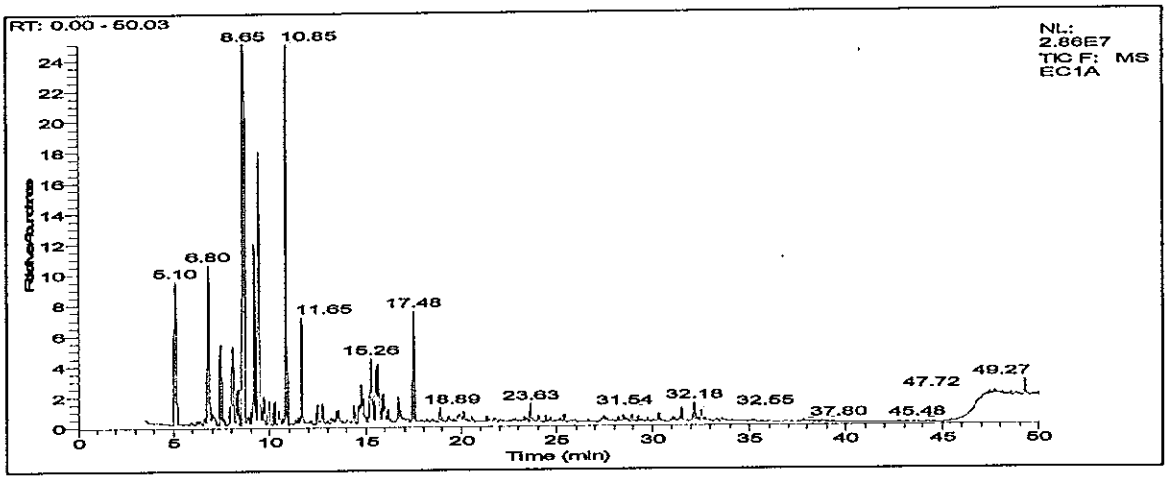

Figure 99 GC Chromatogram of fraction EC1A

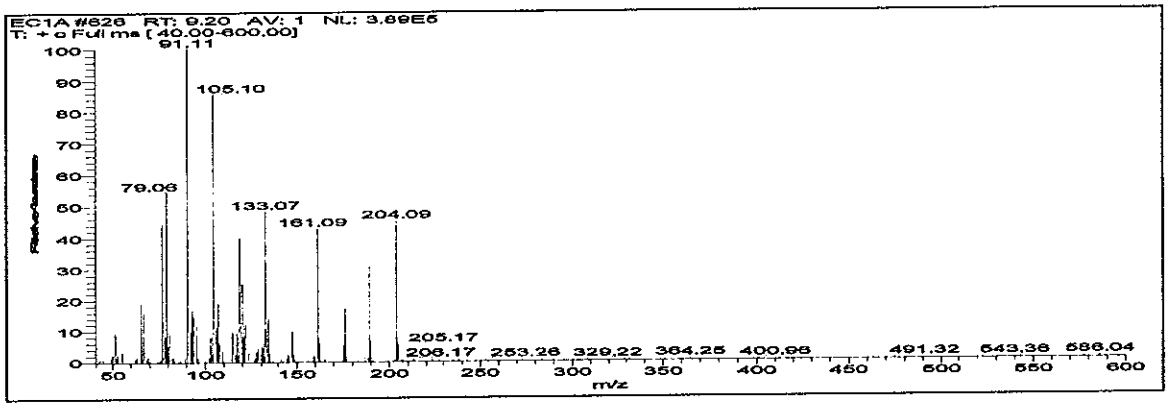

Figure 100 MS Spectrum of fraction EC1A at retention time 9.20 min

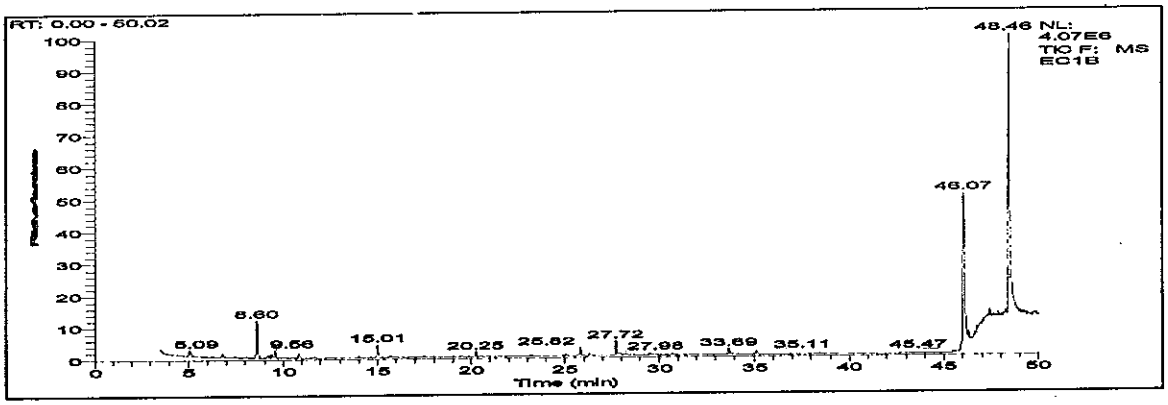

Figure 101 GC Chromatogram of fraction EC1B

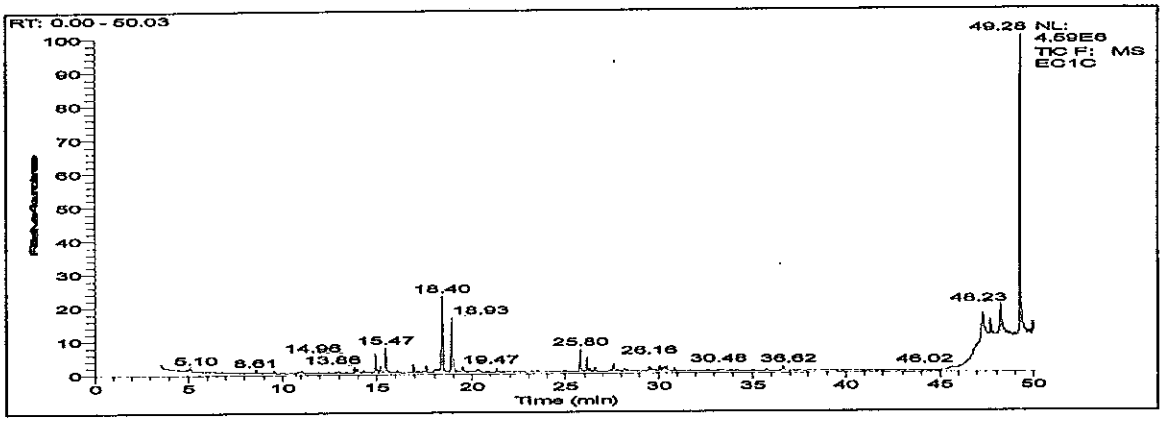

Figure 102 GC Chromatogram of fraction EC1C

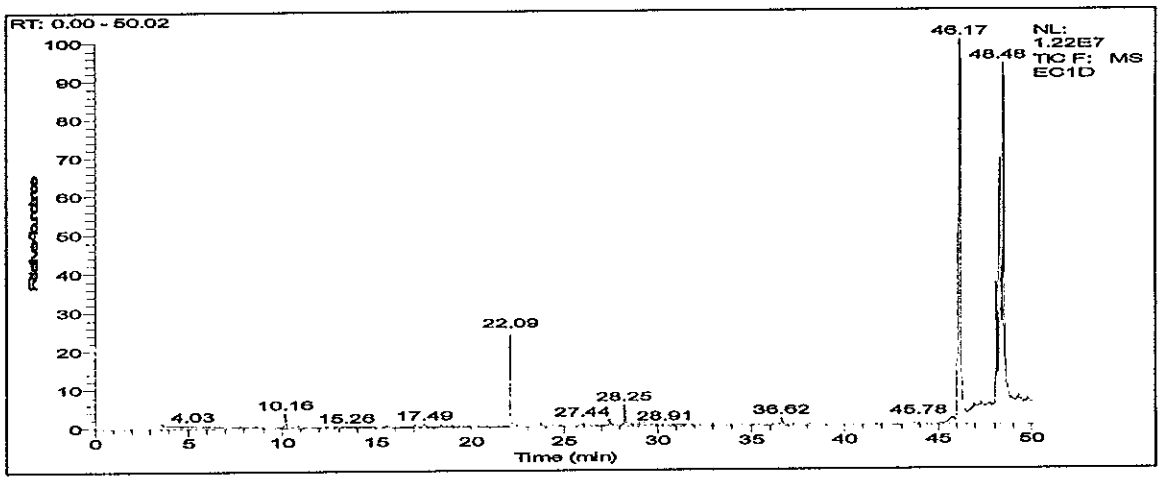

Figure 103 GC Chromatogram of fraction EC1D

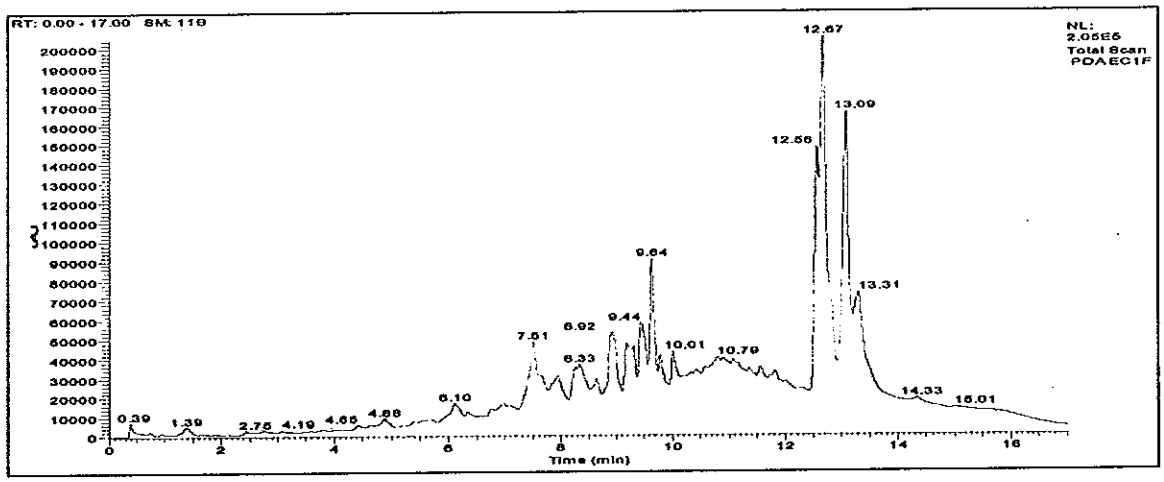

Figure 104 LC Chromatogram (TIC) of fraction EC1F

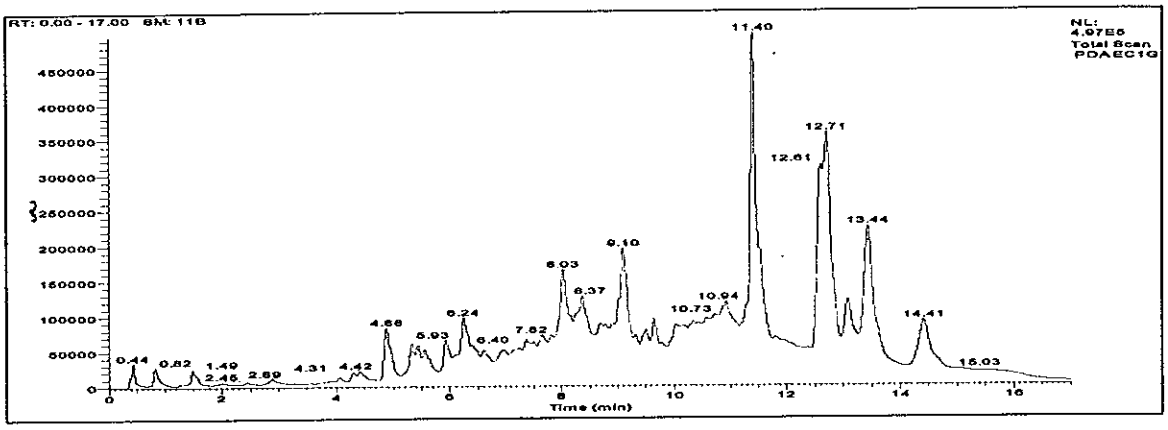

Figure 105 LC Chromatogram (TIC) of fraction EC1G

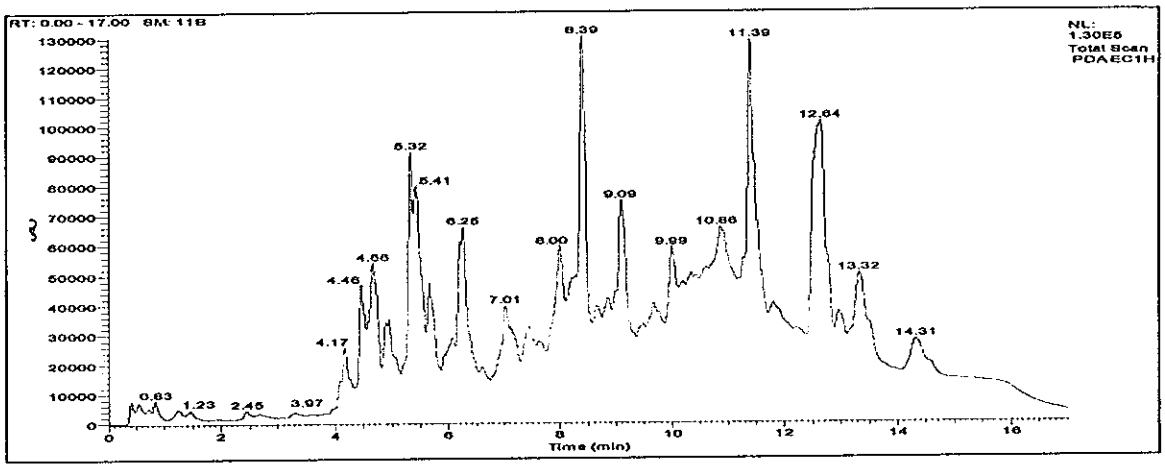

Figure 106 LC Chromatogram (TIC) of fraction EC1H

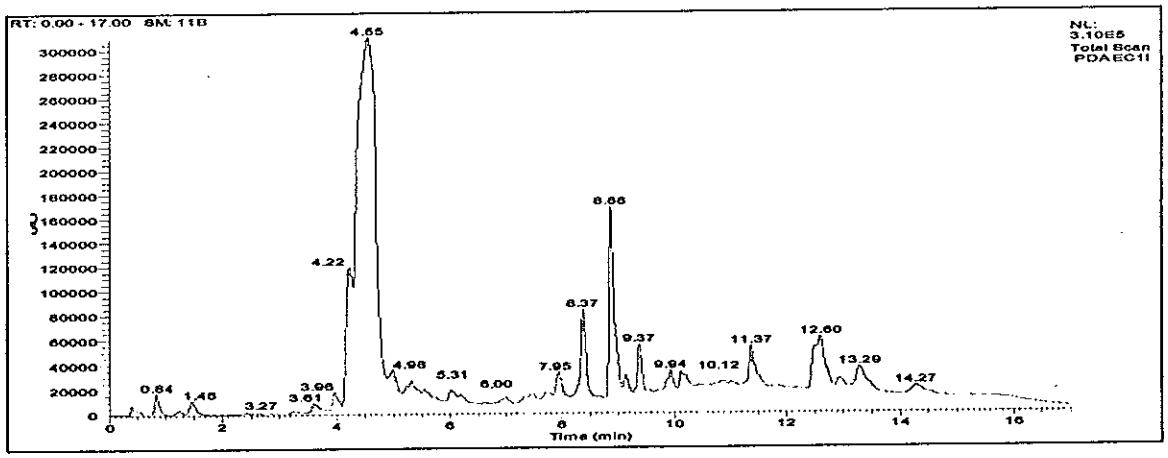

Figure 107 LC Chromatogram (TIC) of fraction EC1I

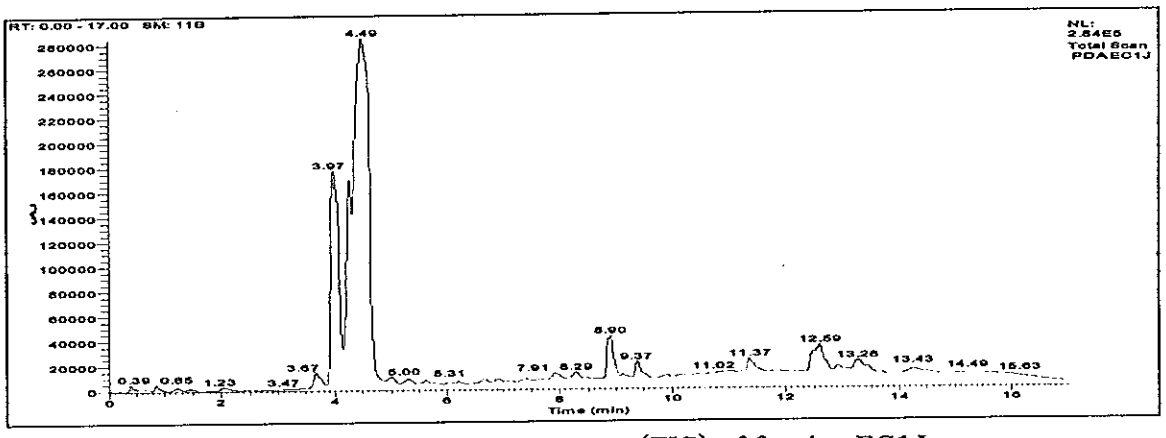

Figure 108 LC Chromatogram (TIC) of fraction EC1J

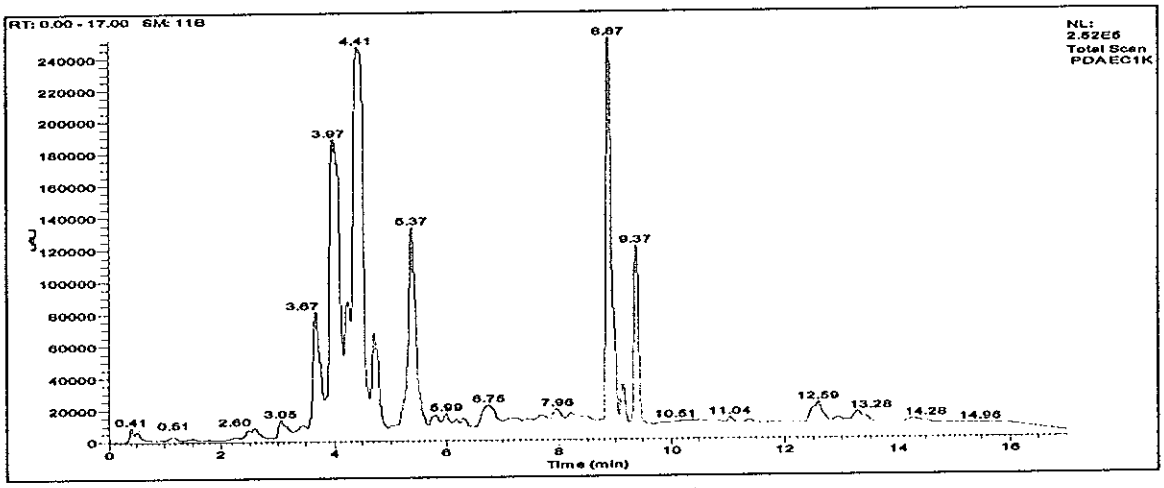

Figure 109 LC Chromatogram (TIC) of fraction EC1K

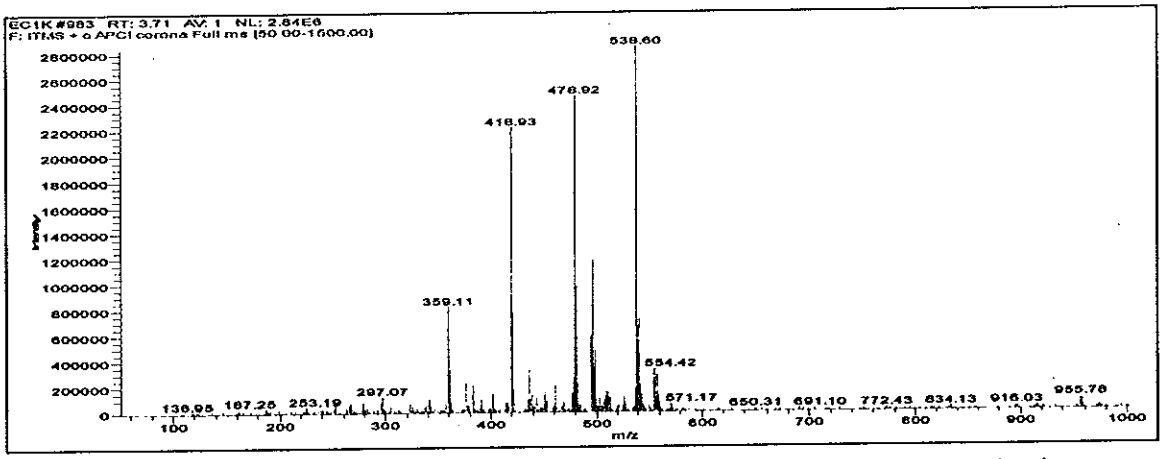

Figure 110 MS-APCI Spectrum of fraction EC1K at retention time 3.71 min

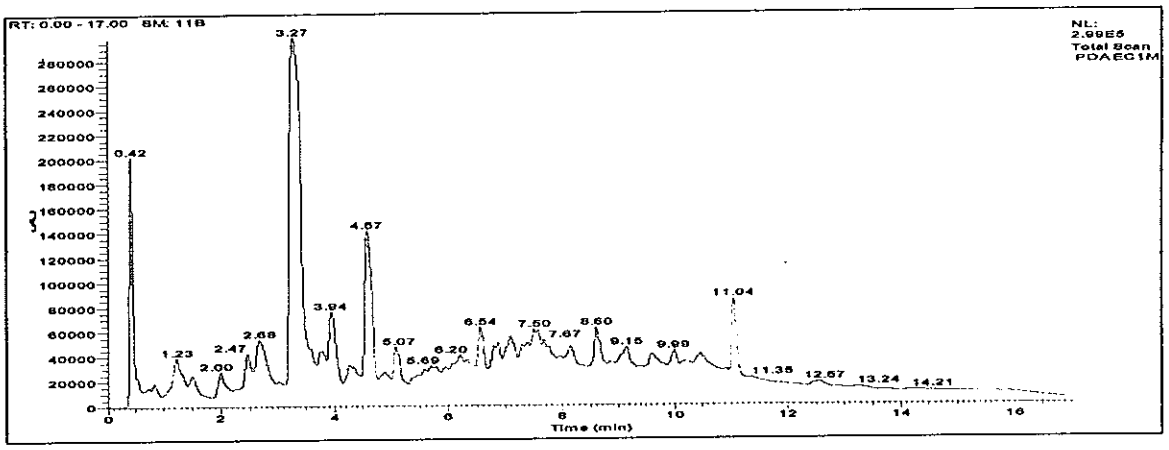

Figure 111 LC Chromatogram (TIC) of fraction EC1M

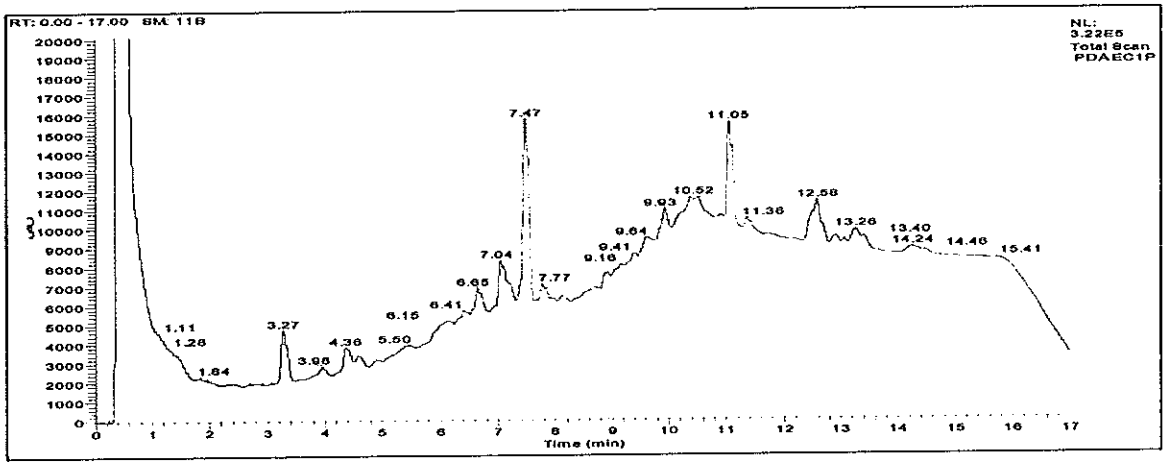

Figure 112 LC Chromatogram (TIC) of fraction EC1P

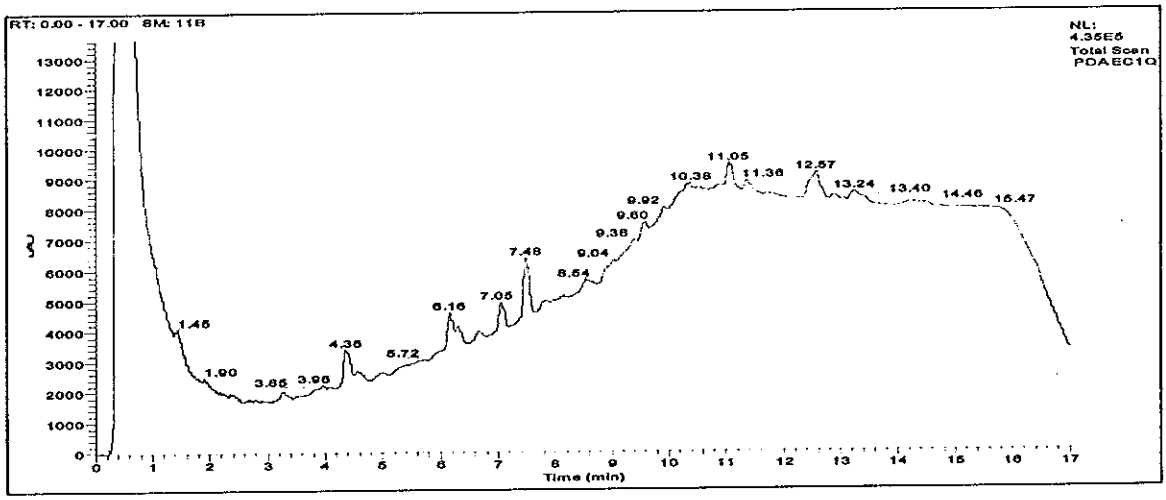

Figure 113 LC Chromatogram (TIC) of fraction EC1Q

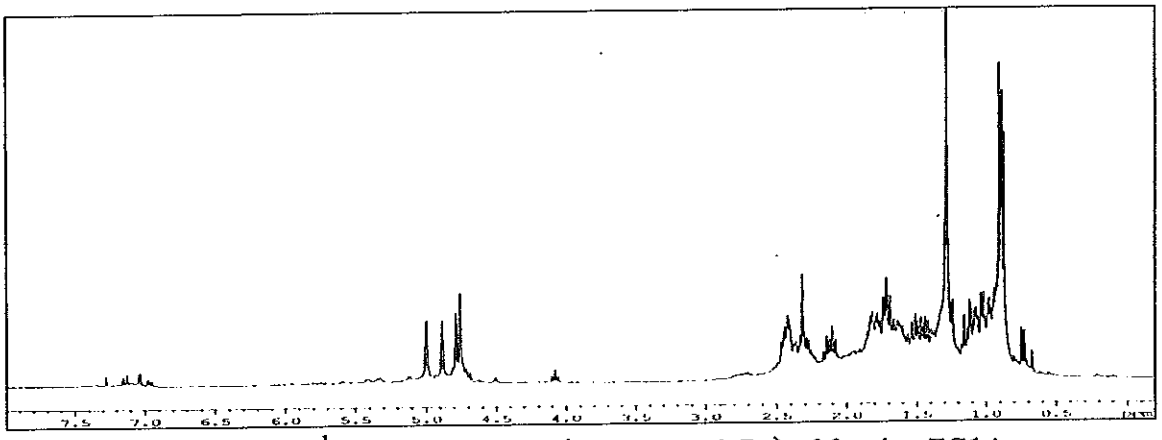

Figure 114 ^{1}H NMR Spectrum (300 MHz, C_6D_6) of fraction EC1A

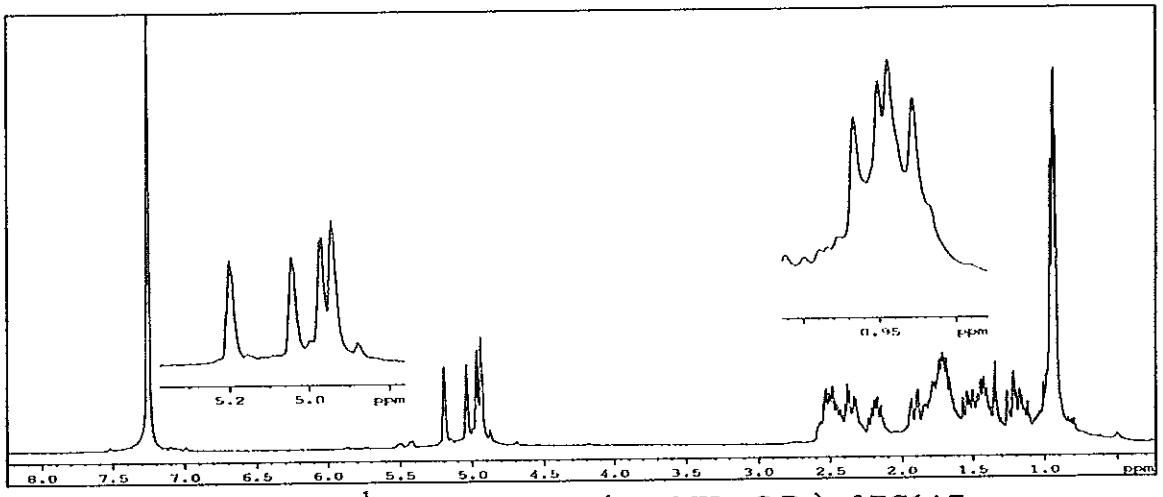

Figure 115 ^{1}H NMR Spectrum (300 MHz, C_6D_6) of EC1A7

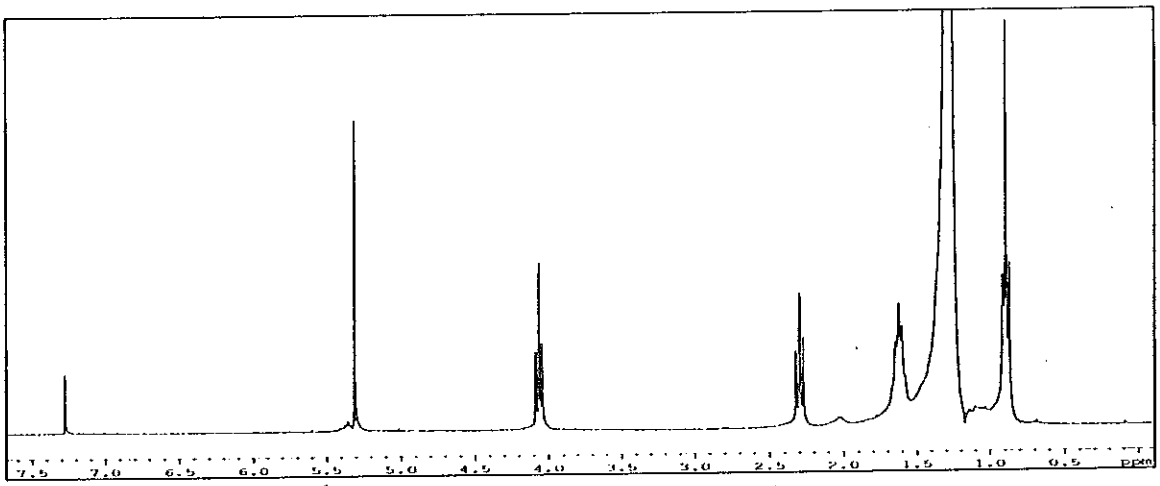

Figure 116 ^{1}H NMR Spectrum (300 MHz, C_6D_6) of fraction EC1B

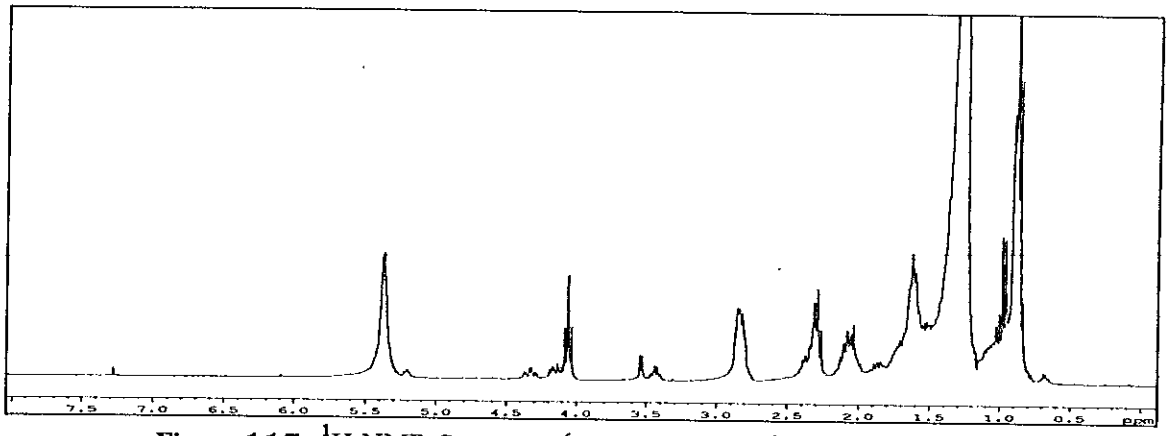

Figure 117 ^{1}H NMR Spectrum (300 MHz, C_6D_6) of fraction EC1C

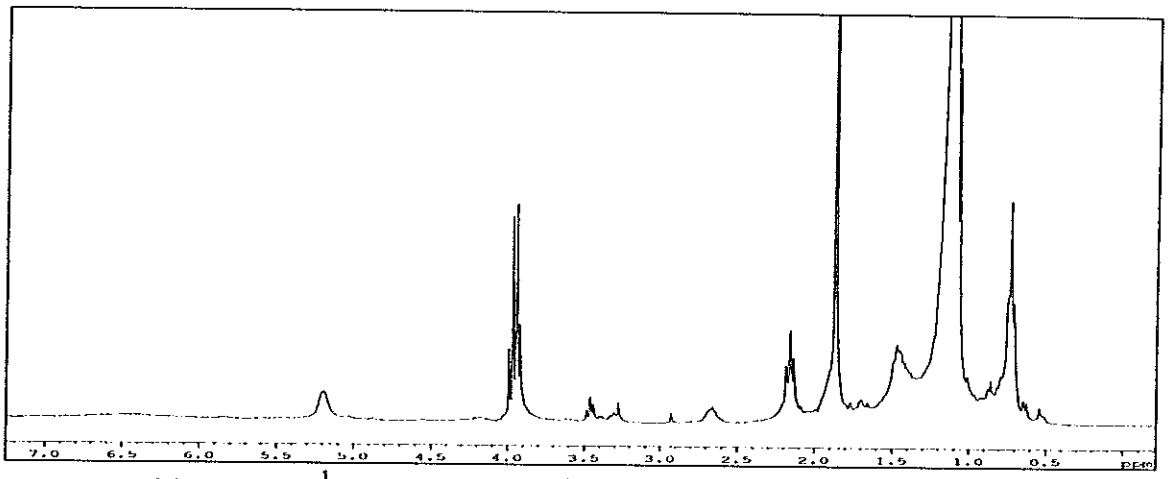

Figure 118 ^{1}H NMR Spectrum (300 MHz, C_6D_6) of fraction EC1D

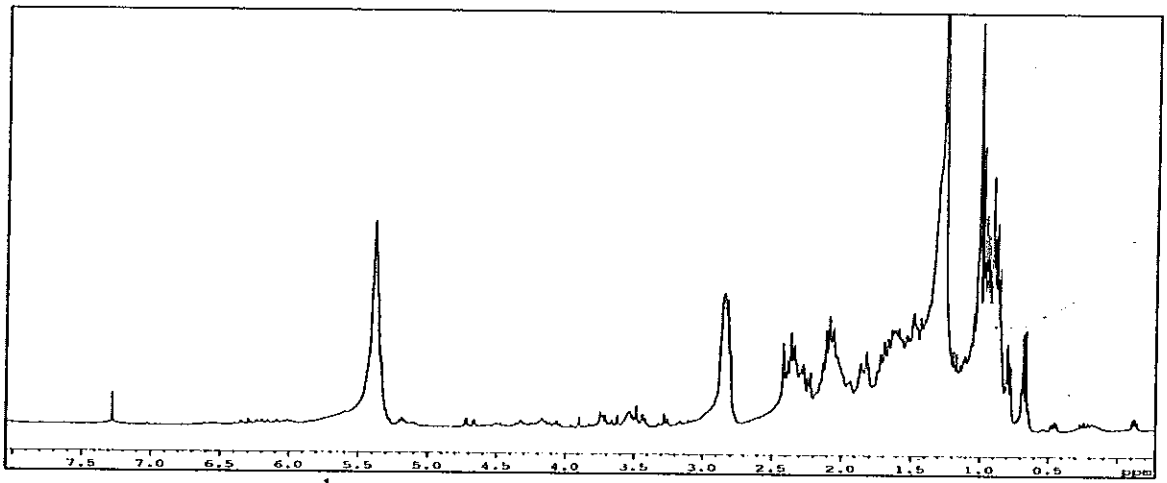

Figure 119 ^{1}H NMR Spectrum (300 MHz, C_6D_6) of fraction EC1F

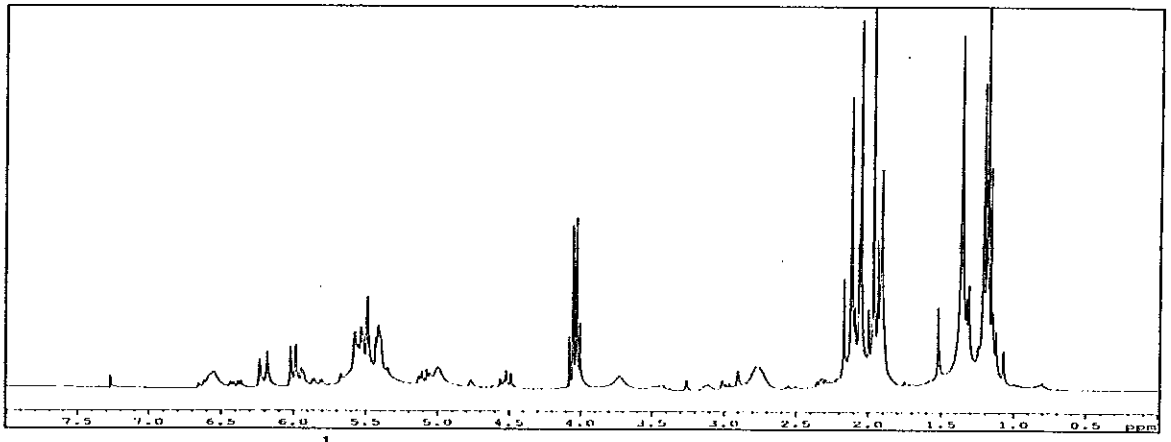

Figure 120 ^{1}H NMR Spectrum (300 MHz, C_6D_6) of fraction **EC1L**

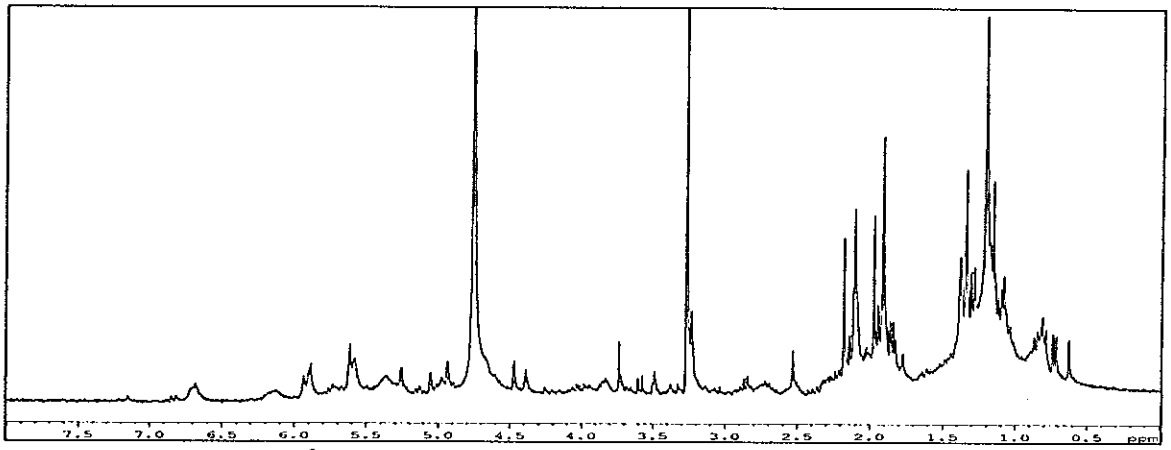

Figure 121 ^{1}H NMR Spectrum (300 MHz, MeOD) of fraction **EC1M**

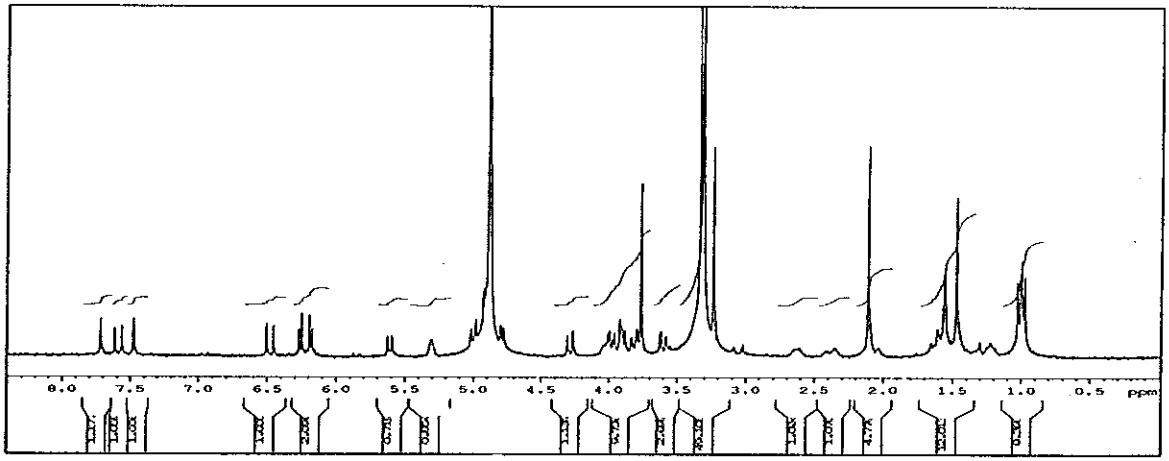

Figure 122 ^{1}H NMR Spectrum (300 MHz, MeOD) of eleutherobin

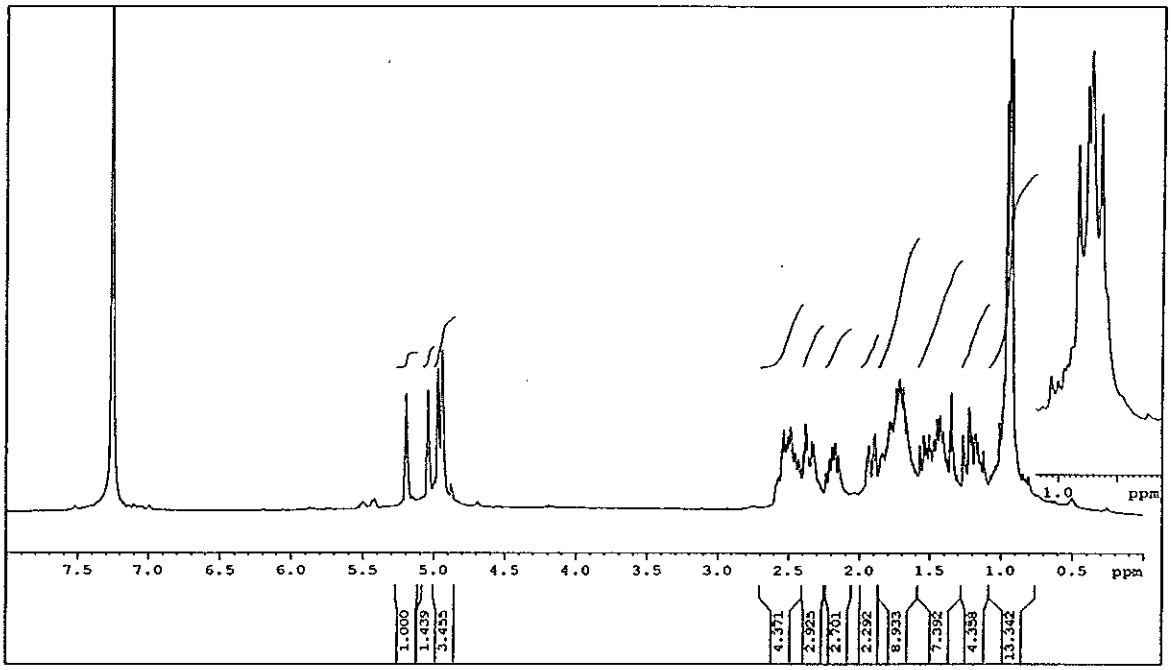

Figure 123 ^{1}H NMR Spectrum (300 MHz, C_6D_6) of erythrodiene

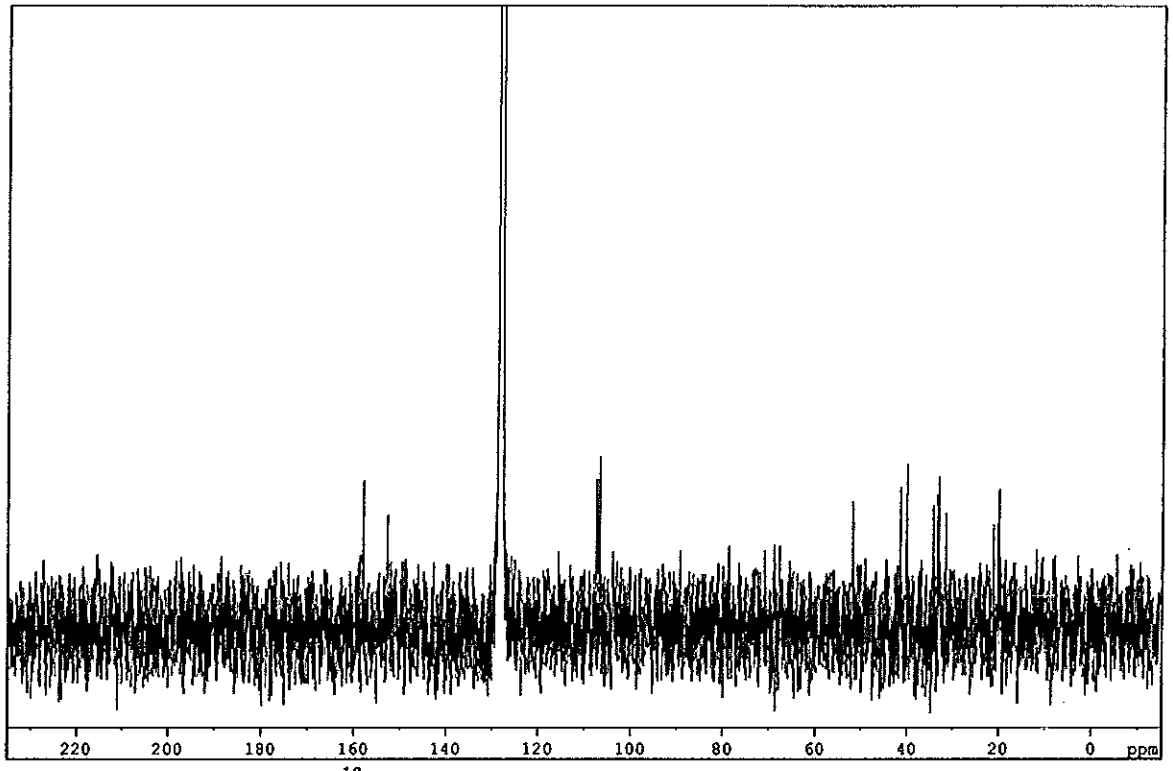

Figure 124 ^{13}C NMR Spectrum (75 MHz, C_6D_6) of erythrodiene

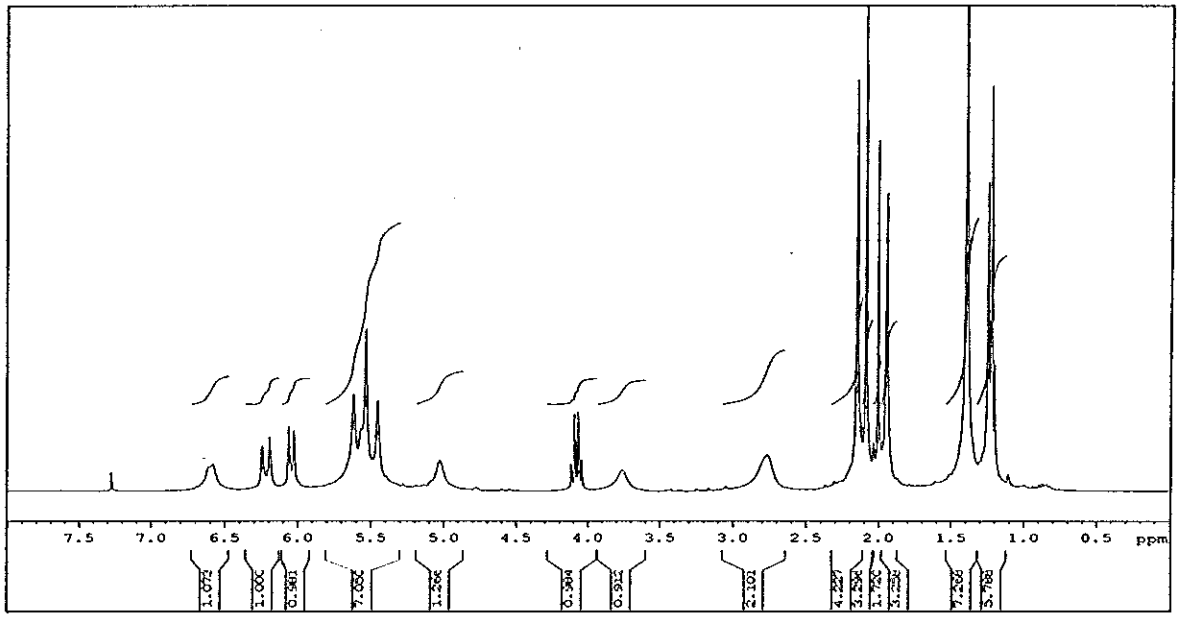

Figure 125 ^{1}H NMR Spectrum (300 MHz, C_6D_6) of erythrolide B

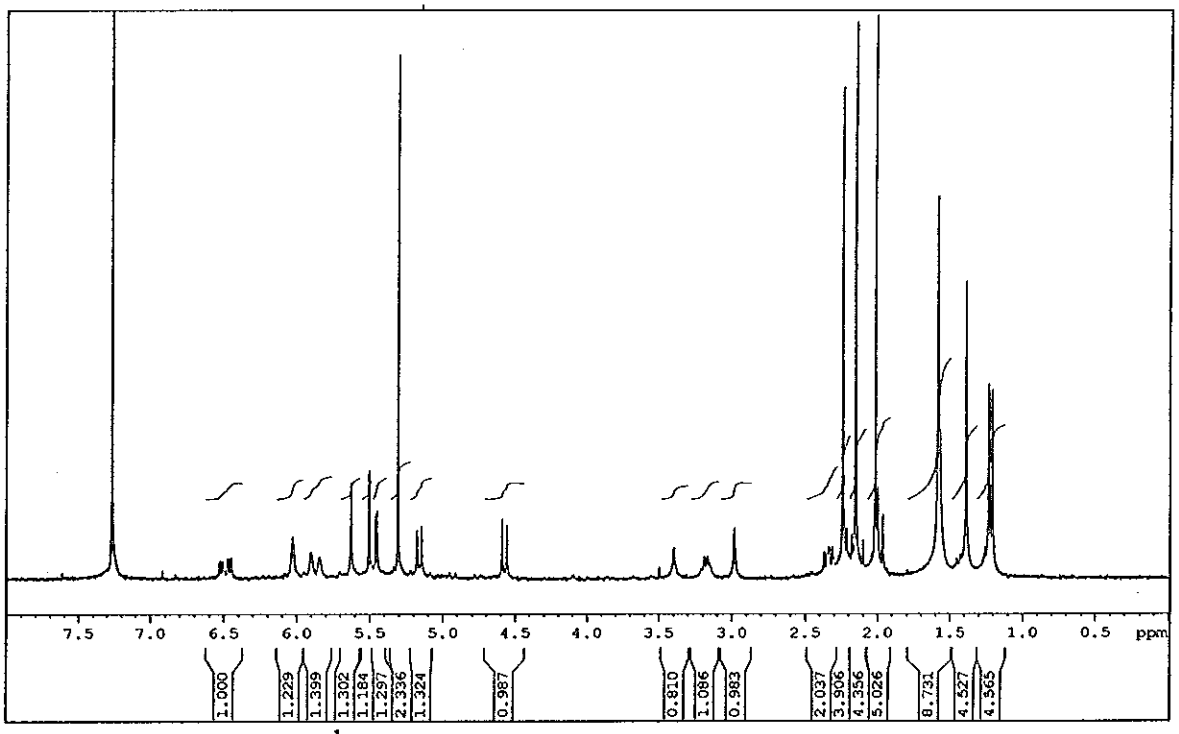

Figure 126 ^{1}H NMR Spectrum (300 MHz, C_6D_6) of erythrolide A

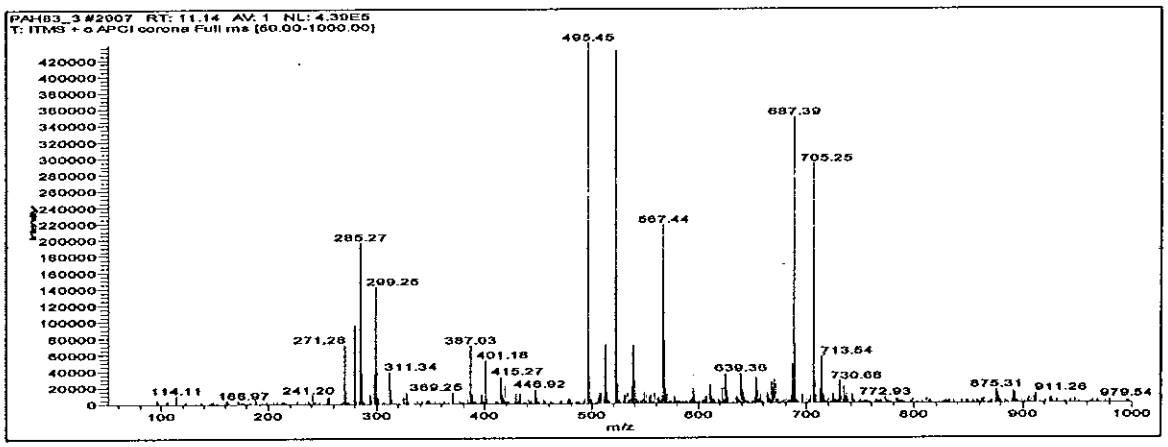

Figure 127 Mass spectrum (MS-APCI) of P-3

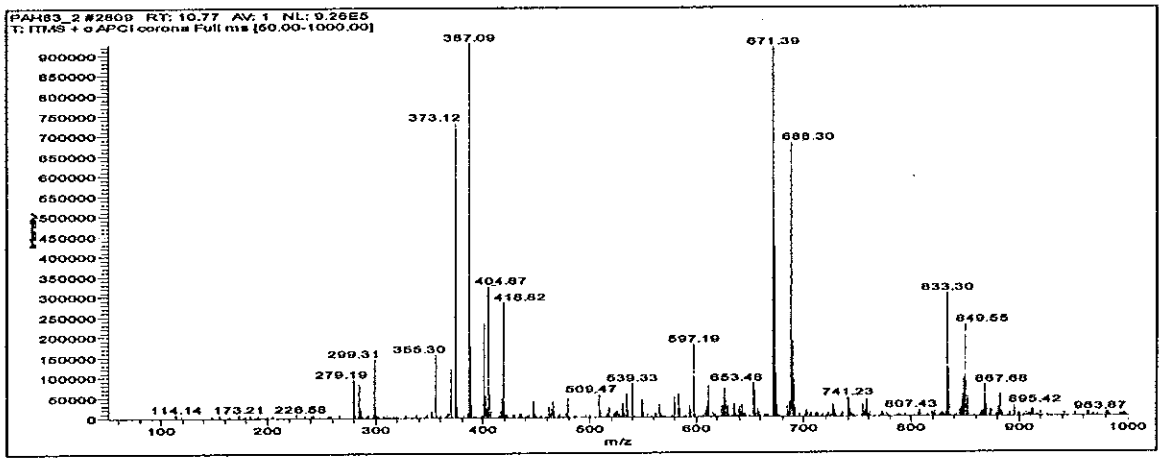

Figure 128 Mass spectrum (MS-APCI) of P-2

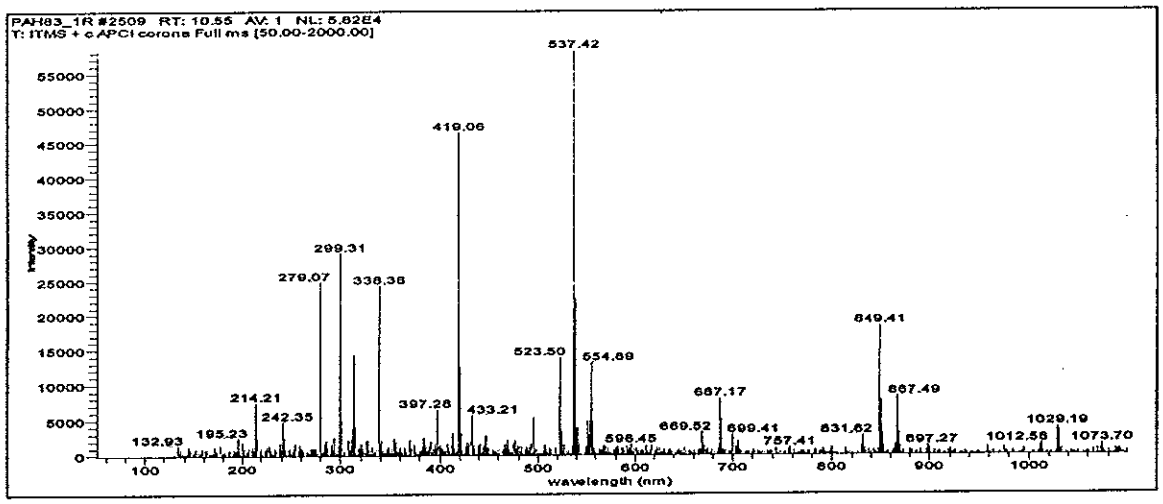

Figure 129 Mass spectrum (MS-APCI) of P-1

VITAE

Name Mr. Sarot Cheenpracha

Student ID 4723010

Educational Attainment

Degree	Name of Institution	Year of Graduation
B.Sc. (Chemistry)	Prince of Songkla University	2001
M.Sc. (Organic Chemistry)	Prince of Songkla University	2003

Scholarship Awards during Enrolment

Scholarship was awarded by the Thailand Research Fund through the Royal Golden Jubilee Ph.D. Program (Grant No. PHD/0157/2547), the Center for Innovation in Chemistry: Postgraduate Education and Research Program in Chemistry, Prince of Songkla University through Natural Products from Mangrove Plants and Synthetic Materials Research Unit (NSU) and Graduate School.

List of Publications and Proceedings

Publications

1. Cheenpracha, S.; Srisuwan, R.; Karalai, C.; Ponglimanont, C.; Chantrapromma, S.; Chantrapromma, K.; Fun, H.-K.; Anjum, S.; Atta-ur-Rahman 2005. "New diterpenoids from stems and roots of *Caesalpinia crista*". *Tetrahedron*, 61, 8656-8662.
2. Cheenpracha, S.; Karalai, C.; Ponglimanont, C.; Subhadhirasakul S.; Tewtrakul, S. 2006. "Anti-HIV-1 protease activity of compounds from *Boesenbergia pandurata*". *Bioorg. Med. Chem.* 14, 1710-1714.
3. Cheenpracha, S.; Karalai, C.; Ponglimanont, C.; Chantrapromma K.; Laphookhieo, S. 2006. "Cassane-type diterpenes from the seeds of *Caesalpinia crista*". *Helv. Chim. Acta*, 89, 1062-1066.
4. Cheenpracha, S.; Yodsaoue, O.; Karalai, C.; Ponglimanont, C.; Subhadhirasakul, S.; Tewtrakul, S.; Kanjana-opas, A. 2006. "Potential anti-allergic *ent*-kurene diterpenes from the bark of *Suregada multiflora*". *Phytochemistry*, 67, 2630-2634.

Proceedings

1. **Cheenpracha, S.**; Karalai, C.; Ponglimanont, C. "Cassane-type diterpenes from stems of *Caesalpinia crista*". PERCH Conference IV. Jomtein Palm Beach, Pattaya, Chonburi, Thailand. 8-11 May 2005. (Poster)
2. **Cheenpracha, S.**; Srisuwan, R.; Karalai, C.; Ponglimanont, C.; Chantrapromma, S.; Chantrapromma, K.; Fun, H.-K.; Anjum, S.; Atta-ur-Rahman. "New diterpenoids from stems and roots of *Caesalpinia crista*" The 4th PSU Symposium on Graduate Research, Faculty of Science, Prince of Songkla University, Hat-Yai, Songkhla, Thailand. 31 March 2006. (Poster)
3. **Cheenpracha, S.**; Karalai, C.; Ponglimanont, C.; Subhadhirasakul, S.; Tewtrakul, S.; Chantrapromma, K. "Diterpenes and cyclohexylchalcones from *Caesalpinia crista*, *Suregada multiflora*, *Boesenbergia pandurata* and their activities". RGJ Conference VIII. Jomtein Palm Beach, Pattaya, Chonburi, Thailand. 20-22 April 2007. (Oral)